



UNIVERSITAT  
POLITÈCNICA  
DE VALÈNCIA

**Developmental plasticity and transgenerational  
reprogramming following vitrified embryo transfer  
in *Oryctolagus cuniculus***

***Ph.D. Thesis by***

Ximo García Domínguez

***Supervisors***

Francisco Marco Jiménez  
José Salvador Vicente Antón

**València, June 2020**



UNIVERSITAT POLITÈCNICA DE VALÈNCIA

**Developmental plasticity and transgenerational reprogramming following vitrified embryo transfer in *Oryctolagus cuniculus***

A thesis submitted to the Polytechnic University of Valencia in partial fulfilment of the requirements for the degree of Doctor of Philosophy

By

**Ximo García Domínguez**



Sig.

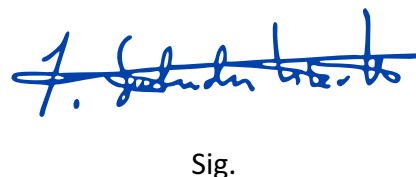
**Thesis Directors**

**Prof. Francisco Marco Jiménez**



Sig.

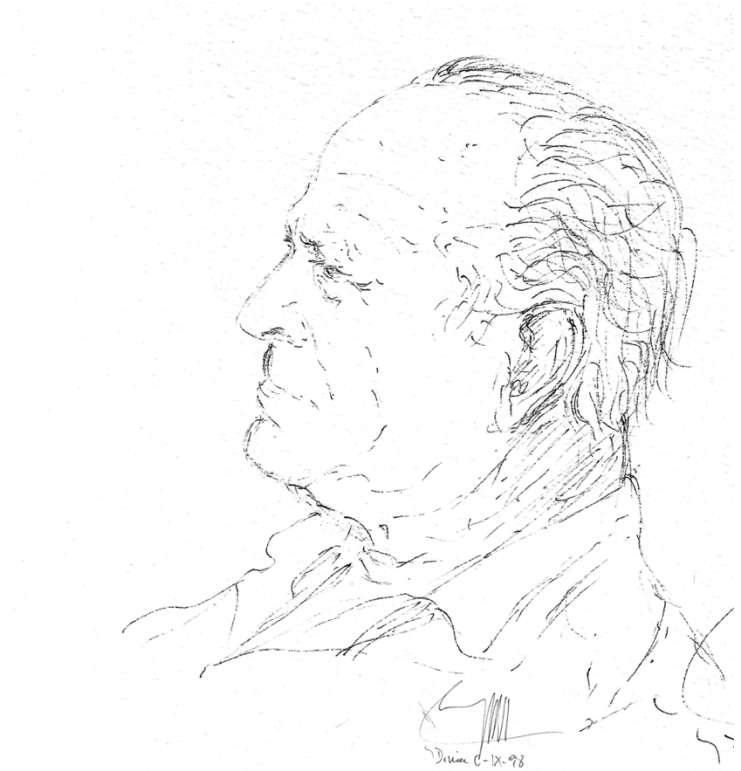
**Prof. José Salvador Vicente Antón**



Sig.







A la memoria de mi abuelo,  
**Juan García Genís**



## **ACKNOWLEDGEMENTS**

## **AGRADECIMIENTOS**

*“Tal vez la gratitud no sea la virtud más importante,  
pero sí es la madre de todas las demás”.*

**Marco Tulio Cicerón**



## AGRADECIMIENTOS

---

Esta parte, desde mi punto de vista, podría ser considerada la más importante de una tesis, y también la más difícil de escribir, puesto que gracias a lo que implica el contenido de estas líneas seguramente haya sido capaz de escribir el resto del documento. El doctorado es un camino que saca, pero al mismo tiempo exige, lo mejor de ti, tanto a nivel profesional como mayoritariamente personal. Por ello, el apoyo y el cariño de todas las personas que han compartido conmigo este tiempo han contribuido, de una manera u otra, a que este documento esté hoy en tus manos. Y es que cuando alguien empieza una tesis doctoral no solo está asumiendo que su vida cambie radicalmente, sino también la de todos aquellos familiares, amigos y compañeros que le acompañan durante el proceso. Por ello, estas líneas van dedicadas a todas esas personas.

Tal vez sea obvio empezar por quienes me dieron la oportunidad de embarcarme en esta aventura: mis directores, **José y Paco**. Los dos me abristeis las puertas del laboratorio de par en par desde el primer día, y sin vuestro tiempo, dedicación y paciencia esto no hubiese sido posible. Tengo la suerte de poder decir que siempre me he sentido valorado, respetado y comprendido, y eso te hace sentir como en casa. Hemos hecho tantas cosas a lo largo de estos años que sería imposible describir en unas pocas líneas cuánto he aprendido con vosotros, tanto en el ámbito de la docencia como en el de la investigación. Gracias por confiar en mí. **José**, creo que es un sentimiento común para todos los que te conocemos el sentir admiración por todo lo que representas. Ha sido una suerte poder aprender de tu visión amplia y crítica. Gracias por ser un buen referente y mirar siempre por mí. **Paco**, todavía recuerdo cuando aceptaste ser el director de mi trabajo final de grado en 2014, en aquella práctica de cultivos. En aquel momento no tenía ni idea de cuánto te tendría que agradecer para siempre. Desde entonces hemos trabajado juntos en muchísimos proyectos, sin importar el día, la hora, el lugar o el motivo, y siempre me has hecho sentir a la altura. Gracias, no solo por contar conmigo para todo lo que ha estado en tu mano, sino también por dejarme aportar todo lo que ha estado en la mía. Gracias por tu forma de ser tan cercana, y por hacerlo todo tan fácil, incluso dejando que se me olvide que tú eres el jefe. A día de hoy siento que no he perdido el tiempo, y tú eres el principal culpable.

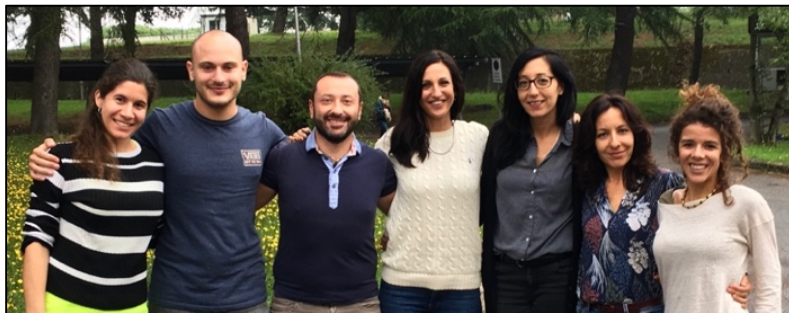
Han sido varios los años de compartir el laboratorio con ciertas personas que han conseguido que aquel lugar sea mucho más que un espacio de trabajo. Por ello, me gustaría darle las gracias al resto del equipo: **David, Carmen, Amparo** y, de una forma especial, **Luis**. Tampoco puedo olvidarme de **Carlos**, por ayudarme en toda la gestión de los animales de la granja, pese a no haberle puesto las cosas fáciles... La ayuda de todos vosotros ha sido fundamental para que todos los experimentos fuesen por el buen camino. Al final, el trabajo en equipo es la clave del éxito y, con un equipo así, poco queda que desear. Gracias a todos por haber estado dispuestos a echarme una mano

cuando ha hecho falta, y por darme un buen consejo siempre que lo he necesitado. Entre todos habéis conseguido que estos años haya sido fácil saltar de la cama con alegría cada mañana, y que el tiempo haya pasado tan rápido. Siento de corazón que en el 5º hemos formado un gran equipo y una gran familia.



**Luis**, haberte podido conocer ha sido de las mejores cosas que me ha dado la tesis. Tu apoyo ha sido esencial durante todos estos años, sobre todo en mis situaciones límite, tanto profesionales como personales. Gracias por haberme comprendido tanto y siempre, y haberme dado la mano independientemente de la hora, la distancia o el motivo, dentro y fuera del laboratorio. Gracias por haber estado en las malas, pero también en las buenas. Tengo la gran suerte de poder llamarte amigo. Se supone que la tesis te cambia la vida, y gracias a ti no me cabe la menor duda. He aprendido muchísimo de ti y creo que eres un ejemplo a seguir en todos los sentidos.

Me gustaría agradecerle también al Dr. **Gianfranco Diretto** la oportunidad de realizar mi estancia en su laboratorio, y el haber logrado junto a su equipo que mi tiempo en Roma haya quedado como un bonito recuerdo. Gracias por querer formar parte de esta aventura.



También me gustaría dedicarle unas líneas a la Dra. **Irene Cervelló**, a quien, por muchos motivos, le guardo un cariño muy especial. Desde que inicié el trabajo final de máster con ella no hemos dejado de trabajar juntos. Gracias por permitirme entrar en tu equipo y haber escuchado y confiado en mis propuestas desde el principio. Gracias por haber contado conmigo para tantas cosas (¡y muy gordas!). El hecho de que siempre me hayas considerado a la altura es algo que te agradeceré siempre.

No podía olvidarme de dedicarle unas palabras a una persona que, aunque haya llegado hace poco a mi vida, le ha sobrado el tiempo para hacerse de querer. Gracias MD. **Lidia Jilcovi** por cuidarme tanto durante este tiempo, sobretodo en momentos muy delicados. La salud es lo más preciado que tenemos, y contigo no me cabe duda de que puedo estar muy tranquilo. Gracias por ser tan buena persona y querer tanto tu trabajo, algún día espero ser como tú.

Y aunque muchas veces nos olvidamos, fuera de la tesis, también hay vida... Dicen que los amigos son la familia que elegimos, y yo los elegiría mil veces más. Gracias a todos los compañeros del Departamento de Ciencia Animal: **Cris, Agos, Samuel, Víctor, Marina, Germán...** Por haber hecho los días más llevaderos, haberme escuchado en momentos de crisis existencial y haber montado esos fantásticos asados de granja. ¡Vamos, guerreros! Y aunque parezca mentira, antes de la tesis, también había vida... A muchos les tengo que agradecer que se hayan armado de valor para poder hacerse un hueco en mi día a día y querer saber constantemente de mí. Sin duda el éxito profesional depende en gran medida del bienestar personal y, para ello, que muchos hayáis compartido conmigo este camino, y todas sus piedras, ha sido algo fundamental. Por ello, hay ciertos nombres que no pueden faltar en esta tesis, ya que, en parte, se la debo a ellos: **Rebeca, Andrea, Manu, Elena, Raúl, Irene, Laia, Gabriel, Alexandra, Alba, Sara, Majo, Rubén, Silvia, Graci, Dani, Miquel, Jesús...** Gracias por haber estado dispuestos a tanto y haberme escuchado cuando lo he necesitado (que no ha sido pocas veces). Vosotros me habéis enseñado el verdadero valor de la amistad, y demostrado que ésta no entiende ni de tiempo ni de distancias. Gracias por no fallar nunca.

Y si he dejado a mi familia para el final es simplemente porque es lo más difícil, ya que por mucho que escriba jamás podré reflejar cuánto les tengo que agradecer, no solo en estos últimos años, sino en toda mi vida. A mis abuelos, **Juan y Pepica, Ramón y Carmen**, antes que nada, me gustaría pedirles perdón por no haberles dedicado todo el tiempo que se merecían durante estos años. Gracias por haberme enseñado a valorar las cosas, a ver la vida con perspectiva y a creer en mí. Dicen que uno recoge lo que siembra, y yo no puedo quererlos más: gracias por quererme tanto. Quisiera



dedicarle unas palabras en especial a mi abuela **Pepica**, quien siempre me ha enseñado que el saber no ocupa lugar. Estoy convencido de que, si la época te lo hubiese permitido, habrías llegado muy lejos, pues así lo has demostrado a lo largo de tus

actuales 94 años. Sé que a mi abuelo **Juan** le habría encantado vivir conmigo este momento: siempre ha estado muy orgulloso de mí, y a mí me gustaba que lo estuviese. Le echo mucho de menos y es algo que durará para siempre. Y aunque no podré leer la tesis con él, a él le dedico este trabajo.

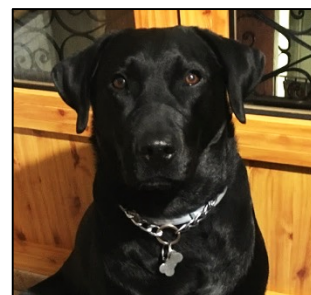
Finalmente, quisiera atribuirles el mérito de esta tesis a mi madre, **Mari Luz**, y a mi padre, **Ximo**, ya que a ellos se lo debo todo en esta vida. Gracias por enseñarme siempre el camino correcto y haberme apoyado siempre en todas mis decisiones y sus



consecuencias, menos en una. Todavía recuerdo cuando me fui a València a estudiar Biotecnología y pensé en abandonar a las pocas semanas. Jamás estaré lo suficientemente agradecido de que tú, mamá, no me lo consintieses, y de que tú, papá, la apoyases, ya que no fue nada fácil. Gracias por trabajar tanto y haberos privado de ciertas cosas para que a mí no me haya faltado de nada: siempre habéis considerado mis estudios y mi felicidad como una prioridad. A lo largo de mi vida habéis dejado que yo decida el camino, y

vosotros os habéis encargado de allanarlo, fuese cual fuese y costase lo que costase. Si algún día soy padre espero poder darles a mis hijos todo lo que vosotros habéis dado por mí, porque más es imposible. Nadie os avisó de dónde os metáis cuando me tuvisteis, y, pese a lo difícil que os lo he puesto, habéis sido los padres entregados, comprensivos y cariñosos que un hijo necesita. Con vosotros a mi lado no me da miedo nada. Por ello, aunque no siempre os lo demuestro como os merecéis, os quiero y os necesito para seguir alcanzando mis metas. En definitiva, gracias por ser perfectos.

Me gustaría terminar este apartado dedicándole unas palabras a una criatura que llegó a mi vida cuando yo empezaba la tesis, **Cora**. Gracias por ser la única que no se ha movido de mi lado durante días y noches de trabajo. Gracias por saber cuándo debes “molestar” y obligarme a desconectar y descansar. Es increíble cómo alguien tan diferente a ti es capaz de abrirse un hueco en la familia y hacerte sentir tan completo.



**¡Gracias a todos por formar parte de esto!**







**Developmental plasticity and transgenerational reprogramming  
following vitrified embryo transfer in *Oryctolagus cuniculus***

**ABSTRACT**



## ABSTRACT

---

During the embryonic preimplantation period, major epigenetic reprogramming occurs, but this phenomenon is sensitive to the environmental conditions. Assisted Reproductive Technologies (ARTs) involve the furthest change from the natural environment by failing to mimic optimal maternal conditions, and thereby entail consequences for late development. The general aim of this thesis was to study the long-term and transgenerational effects of the in vitro stressors occurring during an embryo vitrification and transfer procedure on the rabbit model.

In particular, the aim of Chapter I was to evaluate the potential of the rabbit as a model for this study. First of all, we describe in detail two effective protocols to transfer and vitrify rabbit embryos with high efficiency. After that, we prove that transferring early or compact morula leads to rates of survival at birth >70% in fresh and >55% after vitrification. The ease of performing both embryo cryopreservation and embryo transfer procedures, the high numbers of descendants that we are able to obtain and the short life cycle of the rabbit encouraged and facilitated the following studies.

Chapter II was designed to perform a follow-up study on the short and long-term effects of embryo transfer and embryo vitrification techniques per se on New Zealand rabbits. In addition, we compared the effects of two vitrification devices (cryotop vs ministraw), which provide different cooling-warming rates. The prenatal embryo survival, offspring growth, its adult phenotype, health status, reproductive performance, and lactation performance were the studied traits. Prenatal survival rates were lower for fresh-transferred (FT) and vitrified-transferred (VT) embryos compared with a naturally-conceived (NC) group. Compared to NC offspring, FT animals showed a reduced growth rate that led to lower body weight at adulthood. Postnatal deviations were higher for the VT offspring, which exhibited higher birth weight, low growth rate and were smaller than FT and NC animals at adulthood. These results demonstrated an individual effect of each technique per se, which are also cumulative. Both embryo transfer and vitrification techniques also affect milk yield and nutritional composition in the adult females. Between both cryodevices, we noted that cryotop exerted a positive effect on foetal survival, but incurred higher phenotypic deviations postnatally than the straw device, so the choice of vitrification device should not be underestimated. Despite these phenotypic changes, all progenies were healthy and fertile. Therefore, this was our first approximation demonstrating the high developmental plasticity provided by the mammalian embryo under different in vitro stressors.

Once it was demonstrated that each technique involved in the transfer of cryopreserved embryos had an effect per se, the aim of Chapter III was to evaluate the entire vitrified embryo transfer procedure (VET) effects on development of both males and females separately, using Californian rabbits. Again, we detected that VT animals have modifications of the birth weight and growth pattern, but males were more affected than females. At adulthood, males were subjected to a *post mortem* autopsy to examine the organ weights. Compared to NC animals, those VT were smaller and showed a significantly lower liver and heart weight. After that, a comparative proteomic analysis of liver tissue was conducted to investigate molecular cues underlying this phenotype. Functional analysis of the differentially expressed proteins showed changes in relation to oxidative phosphorylation and dysregulations in the zinc and lipid metabolism. These results supported that VET is not a neutral procedure. However, a blood analysis (haematological and biochemical) revealed that health status was comparable between VT and NC animals.

In Chapter IV, VT and NC animal cohorts established in the previous chapter were mated over two subsequent generations within each group without any embryonic manipulation. In this way, a three generation (F1, F2 and F3) model was constituted in order to assess the transgenerational effects of the VET. As previously, postnatal development of both VT and NC progenies were followed and males were compared in each generation. After mating, fertility was evaluated and animals were subjected to a *post mortem* autopsy to examine the organ weights. The results showed that direct (F1) effects of the VET were also intergenerational (F2) and transgenerational (F3), as VT progenies have a lower growth velocity that incurred lower adult body weight in each generation. Alterations in the liver and heart weights were inherited by F2, but only liver changes persisted until F3. After that, a comparative molecular (transcriptomic and metabolomics) study was performed in the liver tissue, comparing VT and NC animals in each generation. RNA-seq data revealed 642 differentially expressed transcripts between F1 animals, of which 133 were inherited by F2 and 120 by F3. Accordingly, 151, 190 and 159 differentially accumulated metabolites were detected in the F1, F2 and F3, respectively. Functional analysis suggested alterations in the zinc and unsaturated fatty acid metabolism across the generations, which incur alterations in a complex molecular network that can be correlated with the VT phenotype. Nonetheless, similarities in the fertility between VT males and their NC counterparts in each generation denote that VET did not seem to impair the health status in the VT animals.

Finally, during Chapter V, our purpose was to complete our previous knowledge of the transgenerational molecular changes occurring after a VET in liver tissue. We performed a multi-omics approach based on a deeper metabolomic approach and a proteomic study, to verify the previous molecular changes. In addition, the epigenomic status was interrogated as a potential mechanism explaining the canalisation of embryo stress until

adulthood and subsequent generations. Both metabolomic and proteomic analyses validated and expanded our previous molecular study (chapter IV), showing global alteration in the hepatic metabolism of VT animals, mainly related to lipid metabolism (e.g. polyunsaturated fatty acids, steroids, steroid hormones, ...). The overall results denoted that metabolic disorders participated in a complex network of physiological pathways that collectively could support physiological differences between VT and NC animals. Broad methylation changes were detected in the hepatic epigenome, involving genes related with lipid metabolism and apoptosis. These data demonstrated molecular transgenerational inheritance induced by VET in ancestors' embryos. Even so, once again, the health status of VT animals appears similar to that in NC animals.

Overall, the results of this thesis enabled us to confirm that embryo VET incur long-term consequences for the phenotype and the molecular physiology of the resultant offspring. For years, it has been believed that, although VET can be lethal to some embryos, it does not affect survivors, for which it is regarded as neutral. Through this thesis, it has been demonstrated for the first time that embryo VET induces a developmental reprogramming that persists until adulthood and in subsequent generations. Epigenetic mechanisms are believed to mediate this developmental plasticity and its transgenerational inheritance, as our results also support. Therefore, different fields that are nourished by the embryo cryopreservation and transfer technologies, such as human medicine or animal production, should evaluate how these effects can affect the efficiency or the achievement of their objectives.





**Developmental plasticity and transgenerational reprogramming  
following vitrified embryo transfer in *Oryctolagus cuniculus***

**RESUMEN**



## RESUMEN

---

Durante el período preimplantacional, se produce una amplia reprogramación epigenética en el embrión. Sin embargo, este fenómeno es sensible a las condiciones ambientales. En este contexto, las tecnologías de reproducción asistida (ARTs) suponen un cambio drástico en el entorno natural del embrión, ya que éstas no consiguen imitar las condiciones maternas óptimas. De esta manera, la aplicación de las ARTs conlleva consecuencias para el desarrollo posterior del organismo. El objetivo general de esta tesis fue estudiar los efectos a largo plazo y transgeneracionales del estrés provocado por las condiciones *in vitro* durante un procedimiento de vitrificación y transferencia de embriones, utilizando el conejo como modelo animal.

En particular, el objetivo del Capítulo I fue evaluar el potencial del conejo como modelo para este estudio. En primer lugar, se describen en detalle dos protocolos altamente efectivos para transferir y vitrificar embriones de conejo. Utilizando ambas técnicas, se demuestra que la transferencia de mórulas temprana o compactas nos permite obtener tasas de supervivencia al nacimiento superiores al 70% en fresco y al 55% tras la vitrificación. La facilidad con la que se pueden realizar los procedimientos de criopreservación y transferencia de embriones, el elevado número de descendientes que podemos obtener y el corto ciclo de vida del conejo, fueron claves para fomentar y facilitar los siguientes estudios.

El Capítulo II fue diseñado para llevar a cabo un seguimiento, a corto y largo plazo, de los efectos producidos por la transferencia de embriones y la técnica de vitrificación embrionaria *per se*, empleando conejos neozelandeses. Además, se compararon los efectos de dos dispositivos de vitrificación distintos (el cryotop y la ministraw), los cuales proporcionan diferentes velocidades de enfriamiento y calentamiento. Los parámetros que se estudiaron fueron la supervivencia prenatal del embrión, el crecimiento de la descendencia, su fenotipo adulto, su estado de salud, su rendimiento reproductivo y su rendimiento en la lactancia. Las tasas de supervivencia prenatal fueron menores tanto para los embriones transferidos en fresco (FT), como para los transferidos tras su vitrificación (VT), en comparación con aquellos concebidos de forma natural (NC). En comparación con la descendencia NC, los animales FT mostraron una menor tasa de crecimiento que condujo a un menor peso corporal en la edad adulta. Las desviaciones postnatales fueron más altas para la descendencia VT y, aunque ésta mostró un mayor peso al nacer, su tasa de crecimiento y peso corporal adulto fue menor en comparación con los animales FT y NC. Estos resultados demostraron que cada técnica aplicada durante la transferencia de embriones vitrificados tiene un efecto individual *per se*, los cuales, además, son acumulativos. De igual manera, tanto la transferencia de embriones como las técnicas de vitrificación afectaron negativamente el rendimiento de lactación y la composición nutricional de la leche de las hembras adultas. Curiosamente, aunque

el cryotop ejerció un efecto positivo sobre la supervivencia embrionaria, condujo a mayores desviaciones fenotípicas postnatales en comparación con la minitraw. En base a estos resultados, la elección del dispositivo de vitrificación no debe ser considerada una acción trivial. Sin embargo, a pesar de estos cambios fenotípicos, todas las progenies fueron sanas y fértiles. Por lo tanto, en este primer estudio, queda reflejada la gran plasticidad que ofrece el embrión de los mamíferos en su desarrollo ante diferentes factores estresantes *in vitro*.

Una vez quedó demostrado que cada técnica involucrada en la transferencia de embriones criopreservados tiene un efecto *per se*, el objetivo del Capítulo III fue evaluar los efectos del procedimiento completo de transferencia de embriones vitrificados (VET) en el desarrollo de machos y hembras por separado. Para ello, se utilizaron conejos de origen californiano. Nuevamente, detectamos que los animales VT presentaron alteraciones tanto del peso al nacer como en el patrón de crecimiento. Sin embargo, observamos que los machos se vieron más afectados que las hembras. En la edad adulta, los machos fueron sometidos a una autopsia *post mortem* y sus órganos fueron pesados. Comparados con los animales NC, los VT mostraron un peso menor, además de una reducción significativa del peso del hígado y el corazón. Tras ello, se realizó un análisis comparativo del proteoma hepático, tratando de elucidar las marcas moleculares subyacentes a este fenotipo. El análisis funcional de las proteínas diferencialmente expresadas demostró cambios relacionados con la fosforilación oxidativa, el metabolismo del zinc, y el metabolismo lipídico. Estos resultados sugieren que el VET no es un procedimiento neutral. Sin embargo, el análisis sanguíneo (hematológico y bioquímico) reveló que el estado de salud entre los animales VT y NC era comparable.

En el Capítulo IV, las cohortes de animales VT y NC establecidas en el capítulo anterior, se aparearon durante dos generaciones consecutivas, dentro de cada grupo experimental, y sin ninguna manipulación embrionaria. De esta forma, se constituyó un modelo de tres generaciones (F1, F2 y F3) para evaluar los efectos transgeneracionales del VET. En cada generación, se estudió y comparó el desarrollo postnatal de los machos VT y NC. Tras su apareamiento, en cada generación, se realizó un estudio para evaluar la fertilidad de los machos. Posteriormente éstos animales fueron sometidos a una autopsia *post mortem* para examinar los pesos de sus órganos. Los resultados mostraron que los efectos directos (F1) del VET presentaron un carácter intergeneracional (F2) y transgeneracional (F3), puesto que las progenies VT presentaron una menor velocidad de crecimiento y un menor peso corporal adulto comparados con los animales NC coetáneos. Las alteraciones en el hígado y el corazón fueron transmitidas a la F2, pero solo los cambios hepáticos persistieron hasta la F3. Tras ello, se realizó un estudio molecular (transcriptómico y metabolómico) comparativo del tejido hepático entre los animales VT y NC de cada generación. Los datos del RNA-seq revelaron 642 transcritos diferencialmente expresados en la F1, de los cuales 133 fueron heredados por la F2 y

120 por la F3. Concordantemente, 151, 190 y 159 metabolitos diferencialmente acumulados fueron detectados en la generación F1, F2 and F3, respectivamente. El análisis funcional de los datos moleculares demostró alteraciones en el metabolismo del zinc y los ácidos grasos insaturados a lo largo de las tres generaciones. Estos cambios pueden generar alteraciones en una red molecular compleja que puede correlacionarse con el fenotipo mostrado por los animales VT. Sin embargo, la fertilidad fue similar entre los machos VT y NC de cada generación, siendo éste un buen indicador de que el VET no pareció afectar el estado de salud de los animales VT.

Finalmente, a lo largo del Capítulo V, nuestro propósito fue completar nuestro conocimiento previo acerca de los cambios moleculares transgeneracionales que ocurren después del VET en el tejido hepático. Para ello, se realizó una aproximación multi-ómica, y se llevó a cabo un estudio más profundo a nivel metabolómico y un análisis proteómico para validar las consecuencias subyacentes a los cambios moleculares previamente detectados. Además, se realizó un análisis del epigenoma hepático, entendido como posible mecanismo de canalización del estrés embrionario hasta la edad adulta y las generaciones posteriores. Tanto el estudio metabolómico como el proteómico validaron y ampliaron el estudio molecular del capítulo anterior, demostrando alteraciones globales en el metabolismo hepático de los animales VT, principalmente relacionado con alteraciones del metabolismo lipídico (ácidos grasos poliinsaturados, esteroides, hormonas esteroideas...). En general, los resultados indicaron que los trastornos metabólicos participaron en una red compleja de vías fisiológicas que colectivamente podrían apoyar las diferencias observadas entre los animales VT y NC. Además, se detectaron grandes cambios de metilación en el epigenoma hepático, involucrando genes relacionados con el metabolismo lipídico y la apoptosis. De esta forma, se demuestra una herencia transgeneracional de las marcas moleculares inducidas por el VET en los antepasados. Sin embargo, una vez más, en base al estudio sanguíneo (hematológico y bioquímico) el estado de salud de los animales VT fue similar al de los NC.

Así pues, los resultados de esta tesis nos permiten confirmar que la aplicación de un VET en los embriones tempranos tiene consecuencias a largo plazo sobre el fenotipo y la fisiología molecular de la descendencia resultante. Durante años, se ha creído que, aunque el VET puede ser letal, éste no causaba ningún efecto en los embriones que sobrevivían al proceso, por lo que se consideraba una técnica neutral. A lo largo de esta tesis se ha demostrado, por primera vez, que el VET induce una reprogramación embrionaria del desarrollo que persiste hasta la edad adulta y en las generaciones posteriores. Se cree que los mecanismos epigenéticos median esta plasticidad del desarrollo y su herencia transgeneracional, un hecho también avalado por nuestros resultados. Por lo tanto, los diferentes campos que actualmente se nutren de la criopreservación y transferencia de embriones, como la medicina y la producción

animal, deberían evaluar cómo estos procedimientos pueden afectar a la eficiencia o la consecución de sus objetivos.

**Developmental plasticity and transgenerational reprogramming  
following vitrified embryo transfer in *Oryctolagus cuniculus***

**RESUM**





Durant el període preimplantacional, es produïx una àmplia reprogramació epigenètica en l'embrió. No obstant això, este fenomen és sensible a les condicions ambientals. En este context, les tecnologies de reproducció assistida (ARTs) suposen un canvi dràstic en l'entorn natural de l'embrió, ja que estes no aconsegueixen imitar les condicions maternes òptimes. Per tant, l'aplicació de les ARTs té conseqüències en el posterior desenvolupament de l'organisme. L'objectiu general d'aquesta tesi va ser estudiar els efectes a llarg termini i transgeneracionals de l'estrés provocat per les condicions *in vitro* durant un procediment de vitrificació i transferència d'embrions, utilitzant el conill com a model animal.

En particular, l'objectiu del Capítol I va ser avaluar el potencial del conill com a model per a aquest estudi. En primer lloc, es descriuen en detall dos protocols altament efectius per a transferir i vitrificar embrions de conill. Utilitzant ambdues tècniques, es demostra que la transferència de mòrules, primerenques o compactes, ens permet obtindre taxes de supervivència al naixement superiors al 70% en fresc i al 55% després de la vitrificació. La facilitat amb què es poden realitzar els procediments de criopreservació i transferència d'embrions, l'elevat nombre de descendents que podem obtindre i el curt cicle de vida del conill, van ser claus per a fomentar i facilitar els següents estudis.

El Capítol II va ser dissenyat per a dur a terme un seguiment, a curt i llarg termini, dels efectes produïts per la transferència d'embrions i la tècnica de vitrificació embrionària *per se*, emprant conills neozelandesos. A més, es comparen els efectes de dos dispositius de vitrificació diferents (el cryotop i la ministraw), els quals proporcionen diferents velocitats de refredament i calfament. Els paràmetres que es van estudiar van ser la supervivència prenatal de l'embrió, el creixement de la descendència, el seu fenotip adult, el seu estat de salut, el seu rendiment reproductiu i el seu rendiment en la lactància. Les taxes de supervivència prenatal van ser menors tant per als embrions transferits en fresc (FT), com per als transferits després de la seua vitrificació (VT), en comparació amb aquells concebuts de forma natural (NC). En comparació amb la descendència NC, els animals FT van mostrar una menor taxa de creixement que va conduir a un menor pes corporal en l'edat adulta. Les desviacions post-natals van ser més altes per a la descendència VT i, encara que aquesta va mostrar un major pes al nàixer, la seua taxa de creixement i pes corporal adult va ser menor en comparació amb els animals FT i NC. Aquests resultats van demostrar que cada tècnica aplicada durant la transferència d'embrions vitrificats té un efecte individual *per se*, els quals, a més, són acumulatius. De la mateixa manera, tant la transferència d'embrions com les tècniques de vitrificació van afectar negativament el rendiment de lactació i la composició nutricional de la llet de les femelles adultes. Curiosament, encara que el cryotop va

exercir un efecte positiu sobre la supervivència embrionària, va conduir a majors desviacions fenotípiques post-natals en comparació amb la minisraw. Basant-se en aquests resultats, l'elecció del dispositiu de vitrificació no ha de ser considerada una acció trivial. No obstant això, a pesar d'aquests canvis fenotípics, totes les progènies van ser sanes i fèrtils. Per tant, en aquest primer estudi, queda reflectida la gran plasticitat que ofereix l'embrió dels mamífers en el seu desenvolupament davant dels diferents factors estressants *in vitro*.

Una vegada va quedar demostrat que cada tècnica involucrada en la transferència d'embrions criopreservats té un efecte *per se*, l'objectiu del Capítol III va ser avaluar els efectes del procediment complet de transferència d'embrions vitrificats (VET) en el desenvolupament dels mascles i femelles per separat. Per a això, es van utilitzar conills d'origen californià. Novament, detectem que els animals VT van presentar alteracions tant del pes al nàixer com en el patró de creixement. No obstant això, observem que els mascles es van veure més afectats que les femelles. En l'edat adulta, els mascles van ser sotmesos a una autòpsia *post mortem* i els seus òrgans van ser pesats. Comparats amb els animals NC, els VT van mostrar un pes menor, a més d'una reducció significativa del pes del fetge i el cor. Després d'això, es va realitzar un anàlisi comparatiu del proteoma hepàtic, tractant d'elucidar les marques moleculars subjacents a aquest fenotip. L'anàlisi funcional de les proteïnes diferencialment expressades va demostrar canvis relacionats amb la fosforilació oxidativa, el metabolisme del zinc, i el metabolisme lipídic. Aquests resultats suggereixen que el VET no és un procediment neutral. No obstant això, l'anàlisi sanguini (hematològic i bioquímic) va revelar que l'estat de salut entre els animals VT i NC era comparable.

En el Capítol IV, les cohorts d'animals VT i NC establides en el capítol anterior, es van aparellar durant dos generacions consecutives, dins de cada grup experimental, i sense cap manipulació embrionària. D'esta manera, es va constituir un model de tres generacions (F1, F2 i F3) per a avaluar els efectes transgeneracionals del VET. En cada generació, es va estudiar i comparar el desenvolupament post-natal dels mascles VT i NC. Després del seu aparellament, en cada generació, es va realitzar un estudi per a avaluar la fertilitat dels mascles. Posteriorment estos animals van ser sotmesos a una autòpsia *post mortem* per a examinar el pes dels seus òrgans. Els resultats van mostrar que els efectes directes (F1) del VET van presentar un caràcter intergeneracional (F2) i transgeneracional (F3), ja que les progènies VT van presentar una menor velocitat de creixement i un menor pes corporal adult comparats amb els animals NC coetanis. Les alteracions en el fetge i el cor van ser transmeses a la F2, però només els canvis hepàtics van persistir fins a la F3. Després d'això, es va realitzar un estudi molecular (transcriptòmic y metabòlic) comparatiu del teixit hepàtic entre els animals VT i NC de cada generació. Les dades del RNA-seq van revelar 642 transcrits diferencialment expressats en la F1, dels quals 133 van ser heretats per la F2 i 120 per la F3.

Concordantment, es van detectar 151, 190 i 159 metabòlits diferencialment acumulats en les generacions F1, F2 i F3, respectivament. L'anàlisi funcional de les dades moleculars va demostrar alteracions en el metabolisme del zinc i dels àcids grassos insaturats al llarg de les tres generacions. Estos canvis poden generar alteracions en una xarxa molecular complexa que pot correlacionar-se amb el fenotip mostrat pels animals VT. No obstant això, la fertilitat va ser semblant entre els mascles VT i NC de cada generació, sent este un bon indicador de que el VET no pareix afectar l'estat de salut dels animals VT.

Finalment, al llarg del Capítol V, el nostre propòsit va ser completar el nostre coneixement previ sobre els canvis moleculars transgeneracionals que ocorren després del VET en el teixit hepàtic. Per a això, vam realitzar una aproximació multi-òmica, i es va dur a terme un estudi més profund a nivell metabolòmic y un anàlisi proteòmic per a validar les conseqüències subjacents als canvis moleculars prèviament detectats. A més, es va realitzar una anàlisi de l'epigenoma hepàtic, entés com a possible mecanisme de canalització de l'estrés embrionari fins a l'edat adulta i les generacions posteriors. Tant l'estudi metabolòmic com el proteòmic van validar i ampliar l'estudi molecular del capítol anterior, demostrant alteracions globals en el metabolisme hepàtic dels animals VT, principalment relacionat amb alteracions del metabolisme lipídic (àcids grassos poliinsaturats, esteroides, hormones asteroïdees...). En general, els resultats van indicar que els trastorns metabòlics poden participar en una xarxa complexa de vies fisiològiques que col·lectivament podrien recolzar les diferències observades entre els animals VT i NC. A més, es van detectar grans canvis de metilació en l'epigenoma hepàtic, involucrant gens relacionats amb el metabolisme lipídic i l'apoptosi. D'esta manera, es demostra una herència transgeneracional de les marques moleculars induïdes pel VET en els avantpassats. No obstant això, una vegada més, basant-se en l'estudi sanguini (hematològic i bioquímic) l'estat de salut dels animals VT va ser semblant al dels NC.

Així, els resultats d'esta tesi ens permeten confirmar que l'aplicació d'un VET en els embrions primerencs té conseqüències a llarg termini sobre el fenotip i la fisiologia molecular de la descendència resultant. Durant anys, s'ha cregut que, encara que el VET pot ser letal, este no causava cap efecte en els embrions que sobreviuen al procés, per la qual cosa es considerava una tècnica neutral. Al llarg d'aquesta tesi s'ha demostrat, per primera vegada, que el VET induïx una reprogramació embrionària del desenvolupament que persisteix fins a l'edat adulta i en les generacions posteriors. Es creu que els mecanismes epigenètics medien aquesta plasticitat del desenvolupament i la seua herència transgeneracional, un fet també avalat pels nostres resultats. Per tant, els diferents camps que actualment es nodreixen de la criopreservació i transferència d'embrions, com la medicina i la producció animal, haurien d'avaluar com aquests procediments poden afectar l'eficiència o la consecució dels seus objectius.



**Developmental plasticity and transgenerational reprogramming  
following vitrified embryo transfer in *Oryctolagus cuniculus***

## **ABBREVIATIONS**



## ABBREVIATIONS

---

### -A-

**ABN** Percentage of abnormal forms  
**ACN** Acetonitrile  
**ALH** Amplitude of Lateral Head displacement  
**APCI** Atmospheric Pressure Chemical Ionisation  
**ARA** Arachidonic Acid  
**ART** Artificial Reproduction Technology  
**ATP** Adenosine Triphosphate

### -B-

**BCF** Beat Cross Frequency  
**BM** Base Medium  
**BP** Biological Process

### -C-

**CC** Cellular Component  
**COH** Controlled Ovarian Hyperstimulation  
**CON** Spermatic Concentration

### -D-

**DAMs** Differentially Accumulated Metabolites  
**DDA** Data-Dependent Acquisition  
**DEPs** Differentially Expressed Proteins  
**DETs** Differentially Expressed Transcripts  
**DMGs** Differentially Methylated Genes  
**DMR** Differentially Methylated Region  
**DMSO** Dimethyl Sulfoxide  
**DOHaD** Developmental Origins of Health and Disease  
**DPBS** Dulbecco's Phosphate-Buffered Saline

### -E-

**EC** Embryo Cryopreservation  
**EDTA** Ethylenediaminetetraacetic acid  
**EG** Ethylene Glycol  
**ESHRE** European Society of Human Reproduction and Embryology  
**ESI** Electrospray Ionisation  
**ET** Embryo Transfer

**-F-**

**F1** F1 Generation  
**F2** F2 Generation  
**F3** F3 Generation  
**FA** Fatty Acid  
**FAc** Formic Acid  
**FC** Fold Change  
**FDR** False Discovery Rate  
**FT** Fresh-Transferred

**-G-**

**GCC** Germ Cells Cryopreservation  
**GLM** General Linear Model  
**GO** Gene Ontology  
**GSH** Glutathione

**-H-**

**HM** Heat Map  
**HPLC** High Performance Liquid Chromatography  
**HRMS** High Resolution Mass Spectrometry

**-I-**

**ICSI** Intracytoplasmic Sperm Injection  
**IVC** *In Vitro* Culture  
**IVF** *In Vitro* Fertilisation  
**IVM** *In Vitro* Maturation

**-K-**

**KEGG** Kyoto Encyclopaedia of Genes and Genomes

**-L-**

**LA** Linoleic Acid  
**LC** Liquid Chromatography  
**LCPUFA** Long-Chain Polyunsaturated Fatty Acid  
**LIN** Linearity Coefficient (VSL/VCL × 100)

**-M-**



**MF** Molecular Function  
**MGCs** Mature Germ Cells  
**MOT** Percentage of sperm motility  
**mRNA** Messenger Ribonucleic Acid  
**MS** Mass Spectrometry  
**MT** Metallothioneins

**-N-**

**NADH** Nicotinamide Adenine Dinucleotide  
**NAR** Percentage of normal apical ridge  
**NC** Naturally-Conceived

**-O-**

**OXPHO** Oxidative Phosphorylation

**-P-**

**P450** Cytochrome P450  
**PCA** Principal Component Analysis  
**PGCs** Primordial Germ Cells  
**PGD** Preimplantation Genetic Diagnosis  
**PRO** Percentage of progressive motility

**-R-**

**RNA-Seq** RNA Sequencing  
**ROS** Reactive Oxygen Species

**-S-**

**SCC** Somatic Cell Count  
**SN** Supernatant  
**Spz** Spermatozoa;  
**STR** Straightness Coefficient  
**SWATH** Sequential Window Acquisition of all Theoretical Fragment Ion Spectra

**-T-**

**TFA** Trifluoroacetic Acid  
**TSE** Total Sperm Per Ejaculate

**-U-**

**UPV** Universidad Politècnica de Valencia

**-V-**

**VAP** Average Path Velocity  
**VCL** Curvilinear Velocity  
**VET** Vitrified Embryo Transfer Procedure  
**VIA** Percentage of viable sperm  
**VSL** Straight-Line Velocity  
**VT** Vitrified-Transferred  
**VTc** Vitrified-Transferred in Cryotop  
**VTs** Vitrified-Transferred in Straw

**-W-**

**WOB** Wobble Coefficient ( $VSL/VAP \times 100$ )

**-Z-**

**Zn** Zinc





**Developmental plasticity and transgenerational reprogramming  
following vitrified embryo transfer in *Oryctolagus cuniculus***

## **INDEX OF CONTENTS**



<b>1. GENERAL INTRODUCTION .....</b>	<b>3</b>
1.1. UBIQUITOUS PHENOTYPIC PLASTICITY .....	3
1.1.1. <i>Developmental programming</i> .....	3
1.1.2. <i>Transgenerational developmental programming</i> .....	3
1.1.3. <i>Epigenetic mechanisms</i> .....	4
1.2. CRITICAL WINDOW OF THE PREIMPLANTATION PERIOD .....	5
1.3. CONSEQUENCES OF INTERCEDING PREIMPLANTATION DEVELOPMENT .....	5
1.3.1. <i>“Vulnerability”</i> .....	5
1.3.2. <i>“Opportunity”</i> .....	6
1.3.3. <i>The advent of assisted reproduction technologies (ARTs)</i> .....	6
1.4. IMPLICATIONS FOR EMBRYO CRYOPRESERVATION .....	8
1.5. REFERENCES .....	9
<b>2. OBJECTIVES .....</b>	<b>17</b>
<b>3. CHAPTER I. MINIMALLY INVASIVE EMBRYO TRANSFER AND EMBRYO VITRIFICATION AT THE OPTIMAL EMBRYO STAGE IN THE RABBIT MODEL.....</b>	<b>21</b>
3.1. INTRODUCTION .....	23
3.2. PROTOCOL .....	25
3.2.1. <i>Embryo transfer</i> .....	25
3.2.2. <i>Embryo vitrification and warming</i> .....	29
3.3. REPRESENTATIVE RESULTS .....	31
3.4. DISCUSSION .....	34
3.5. CONCLUSION .....	36
3.6. REFERENCES .....	36
<b>4. CHAPTER II. DEVELOPMENTAL PLASTICITY IN RESPONSE TO EMBRYO CRYOPRESERVATION: THE IMPORTANCE OF THE VITRIFICATION DEVICE IN RABBITS .....</b>	<b>43</b>
4.1. INTRODUCTION .....	45
4.2. MATERIALS AND METHODS .....	46
4.2.1. <i>Animals and ethical statements</i> .....	46
4.2.2. <i>Experimental design</i> .....	46
4.2.3. <i>Embryo vitrification</i> .....	48
4.2.4. <i>In vitro culture</i> .....	48
4.2.5. <i>Embryo transfer</i> .....	48
4.2.6. <i>Prenatal development</i> .....	49
4.2.7. <i>Postnatal growth performance and body weight study</i> .....	49

4.2.8. Determination peripheral blood parameters.....	49
4.2.9. Male reproductive performance.....	50
4.2.10. Female reproductive performance .....	51
4.2.11. Lactation performance: milk yield, milk composition and nutritional potential.....	51
4.2.12. Statistical analysis of phenotypic data .....	52
4.3. RESULTS .....	52
4.3.1. Effect of embryo vitrification on the embryonic in vitro development .....	52
4.3.2. Prenatal survival: rates of implantation, foetal losses and offspring .....	53
4.3.3. Postnatal growth performance and body weight.....	53
4.3.4. Healthy status: Peripheral blood parameters.....	55
4.3.5. Reproductive performances.....	55
4.3.6. Lactation performance .....	55
4.4. DISCUSSION .....	59
4.5. CONCLUSION .....	62
4.6. REFERENCES .....	62

## **5. CHAPTER III. LONG-TERM PHENOTYPIC AND PROTEOMIC CHANGES FOLLOWING VITRIFIED EMBRYO TRANSFER IN THE RABBIT MODEL..... 69**

5.1. INTRODUCTION .....	71
5.2. MATERIALS AND METHODS .....	72
5.2.1 Animals and ethical statements .....	72
5.2.2. Vitrified embryo transfer procedure.....	73
5.2.3. Experimental design .....	73
5.2.4. Growth performance during postnatal development.....	75
5.2.5. Body weight and organ phenotypic comparison .....	75
5.2.6. Determination of peripheral blood parameters .....	75
5.2.7. Statistical analysis of phenotypic data .....	76
5.2.8. Comparative proteomic analysis .....	76
5.3. RESULTS .....	79
5.3.1. Postnatal growth and body weight .....	79
5.3.2. Body weight and organ phenotype at adulthood.....	80
5.3.3. Peripheral blood parameters (healthy status).....	81
5.3.4. Comparative study of the liver proteome.....	81
5.4. DISCUSSION .....	82
5.5. CONCLUSION .....	86
5.6. REFERENCES .....	86



<b>6. CHAPTER IV. LONG-TERM AND TRANSGENERATIONAL PHENOTYPIC, TRANSCRIPTIONAL AND METABOLIC EFFECTS IN RABBIT MALES BORN FOLLOWING VITRIFIED EMBRYO TRANSFER.....</b>	<b>95</b>
6.1. INTRODUCTION .....	97
6.2. MATERIALS AND METHODS .....	98
6.2.1 <i>Animals and ethical statements</i> .....	98
6.2.2. <i>Experimental design</i> .....	98
6.2.3. <i>Vitrified embryo transfer procedure</i> .....	100
6.2.4. <i>Growth, body weight and organ weight study</i> .....	101
6.2.5. <i>Semen collection and sperm evaluation</i> .....	101
6.2.6. <i>Fertility rate and number of liveborn</i> .....	102
6.2.7. <i>Statistical analyses</i> .....	102
6.2.8. <i>Transcriptomic analysis of the liver</i> .....	103
6.2.9. <i>Semi-polar and non-polar analysis of the liver metabolome</i> .....	104
6.3. RESULTS .....	105
6.3.1. <i>Establishment of the two experimental progenies (VT vs NC) across the three generations (F1, F2, F3)</i> .....	105
6.3.2. <i>Growth performance, body weight and organ phenotype study</i> .....	106
6.3.3. <i>Sperm and fertility rate assessment</i> .....	109
6.3.4. <i>Comparative study of the liver transcriptome</i> .....	109
6.3.5. <i>Comparative study of the liver metabolome</i> .....	111
6.4. DISCUSSION .....	113
6.5. CONCLUSION .....	118
6.6. REFERENCES .....	119
<b>7. CHAPTER V. TRANSGENERATIONAL EFFECTS FOLLOWING VITRIFIED EMBRYO TRANSFER IN RABBITS: A MULTI-OMIC APPROACH.....</b>	<b>129</b>
7.1. INTRODUCTION .....	131
7.2. MATERIALS AND METHODS .....	132
7.2.1 <i>Animals and ethical statements</i> .....	132
7.2.2. <i>Experimental design</i> .....	133
7.2.3. <i>Determination of peripheral blood parameters</i> .....	134
7.2.4. <i>Sample collection for molecular study</i> .....	135
7.2.5. <i>Semi-polar and non-polar analysis of the liver metabolome</i> .....	135
7.2.6. <i>Comparative proteomic analysis</i> .....	137
7.2.7. <i>Genome-wide DNA methylation profiling by MBD-Seq</i> .....	138
7.3. RESULTS .....	139
7.3.1. <i>Peripheral blood parameters (healthy status)</i> .....	139
7.3.2. <i>Comparative study of the liver metabolome</i> .....	140
7.3.3. <i>Comparative study of the liver proteome</i> .....	142
7.3.4. <i>Comparative study of the liver epigenome</i> .....	144

7.4. DISCUSSION .....	146
7.5. CONCLUSION .....	148
7.6. REFERENCES .....	149
<b>8. GENERAL DISCUSSION .....</b>	<b>157</b>
8.1. DISCUSSION AND FUTURE PROSPECTS .....	157
8.2. REFERENCES .....	163
<b>9. CONCLUSIONS .....</b>	<b>171</b>
<b>10. ANNEX I. SUPPLEMENTARY INFORMATION - CHAPTER III.....</b>	<b>175</b>
<b>11. ANNEX II. SUPPLEMENTARY INFORMATION - CHAPTER IV .....</b>	<b>183</b>
<b>12. ANNEX III. SUPPLEMENTARY INFORMATION - CHAPTER V .....</b>	<b>247</b>

## INDEX OF FIGURES

---

<b>Figure 1.1.</b> <i>In vivo vs In vitro</i> environmental differences during the periconceptual period.....	7
<b>Figure 1.2.</b> Epigenetic genome reprogramming during gamete and early embryo development.....	8
<b>Figure 3.1.</b> Laparoscopic embryo transfer assisted by laparoscopy (External view).....	28
<b>Figure 3.2.</b> Laparoscopic embryo transfer assisted by laparoscopy (Internal view). ....	29
<b>Figure 3.3.</b> Schematization of correctly loaded straw.....	31
<b>Figure 3.4.</b> Rabbit embryos.....	32
<b>Figure 4.1.</b> Experimental design.....	47
<b>Figure 4.2.</b> Bodyweight development: comparing differences between animals naturally-conceived (NC) and those born after fresh embryo transfer (FT), vitrified embryo transfer using a ministraw (VTs), and vitrified embryo transfer using cryotop (VTc) .....	54
<b>Figure 4.3.</b> Growth curves: comparing differences between animals naturally-conceived (NC) and those born after fresh embryo transfer (FT), vitrified embryo transfer using a ministraw (VTs), and vitrified embryo transfer using cryotop (VTc) .....	54
<b>Figure 4.4.</b> Peripheral blood analysis (haematological and biochemical): comparing differences between animals naturally-conceived (NC) and those born after fresh embryo transfer (FT), vitrified embryo transfer using a ministraw (VTs), and vitrified embryo transfer using cryotop (VTc). .....	56
<b>Figure 5.1.</b> Experimental design.....	74
<b>Figure 5.2.</b> Growth curves and differences in body weight between animals derived from vitrified-transferred embryos (VT) and those naturally conceived (NC).....	79
<b>Figure 5.3.</b> Molecular analysis of liver samples obtained from adult males derived from vitrified-transferred embryos (VT) and naturally-conceived animals (NC). .....	82
<b>Figure 6.1.</b> Experimental design.....	99

**Figure 6.2.** Scatterplots showing the phenotypic raw data distributions of naturally-conceived (NC) and vitrified-transferred (VT) progenies during three generations (F1, F2, F3). .....107

**Figure 6.3.** Differences in phenotypic traits between naturally-conceived (NC) and vitrified-transferred (VT) progenies during three generations (F1, F2, F3).....108

**Figure 6.4.** Molecular analysis of the liver samples collected from adult males derived from vitrified-transferred embryos (VT) and naturally-conceived (NC), which was compared in each generation (F1, F2, F3).....113

**Figure 7.1.** Experimental design.....133

**Figure 7.2.** Metabolite profile changes in the liver of F3 animals after vitrified embryo transfer procedure. ....141

**Figure 7.3.** Protein profile changes in the liver of F3 animals after vitrified embryo transfer procedure.....143

**Figure 7.4.** Genome-wide methylation changes in the liver of F3 animals after vitrified embryo transfer procedure.....145

## INDEX OF TABLES

---

<b>Table 3.1.</b> Efficiency of fresh rabbit embryo transfer ( <i>in vivo</i> derived) by laparoscopy.	33
<b>Table 3.2.</b> Viability of non-compacted vs compact vitrified morula. ....	33
<b>Table 4.1.</b> Prenatal survival. Rates of implantation, foetal losses and offspring in natural-conceived, fresh embryo transfer, vitrified embryo transfer using ministraw, and vitrified embryo transfer using cryotop.....	53
<b>Table 4.2.</b> <i>Male reproductive performance: comparing differences between naturally-conceived males and those born after fresh embryo transfer, vitrified embryo transfer using ministraw, and vitrified embryo transfer using cryotop. ....</i>	57
<b>Table 4.3.</b> <i>Female reproductive and lactation performance: comparing differences between naturally-conceived females and those born after fresh embryo transfer, vitrified embryo transfer using ministraw, and vitrified embryo transfer using cryotop. ....</i>	58
<b>Table 5.1.</b> Body weight and dissection data of adult males derived from vitrified-transferred embryos and those naturally conceived. ....	80
<b>Table 5.2.</b> Haematological and biochemical comparison between peripheral blood of animals derived from a vitrified embryo transfer procedure (vitrified-transferred) and those naturally conceived (naturally conceived). ....	81
<b>Table 6.1.</b> Efficiency in the establishment of the naturally-conceived and vitrified-transferred progenies across three generations (F1, F2, F3). ....	105
<b>Table 6.2.</b> Ejaculates/sperm parameters and motility assessment of males from the vitrified-transferred progeny (VT) compared to those naturally conceived (NC). ....	110
<b>Table 7.1.</b> Haematological and biochemical comparison, assessing the transgenerational effect of the vitrified embryo transfer procedure.....	140



# **GENERAL INTRODUCTION**

X. Garcia-Dominguez

Institute for Animal Science and Technology (ICTA), Laboratory of Reproductive Biotechnology,  
Universitat Politècnica de València, 46022 Valencia, Spain





# 1. GENERAL INTRODUCTION

---

## 1.1. UBIQUITOUS PHENOTYPIC PLASTICITY

### 1.1.1. Developmental programming

When oocyte and sperm fuse, the newly formed genetic code provides a blueprint for the developmental trajectory of the new individual. Nevertheless, diverse phenotypes may arise from a single genotype depending on the environmental conditions under which life takes place. This phenomenon is broadly referred to as “phenotypic plasticity” and is a ubiquitous aspect of organisms [1,2]. If the phenotype varies as an immediate response to variation in external stimuli, we talk about “contextual plasticity” [3]. In contrast, “developmental plasticity” describes situations where a specific environmental exposure during early development leads to a lasting alteration in phenotype [2,4].

On this basis, in 1990 David Barker published his theory of foetal programming in “The Fetal and Infant Origins of Adult Disease”, which today is recognised under the term “Developmental Origins of Health and Disease (DOHaD) theory”. The DOHaD theory proposed a link between periconceptual, foetal and early infant phases of life and the long-term development of health disorders, which might be transgenerational [5]. However, the underlying mechanism of these changes had yet to be determined.

### 1.1.2. Transgenerational developmental programming

Plasticity in developmental programming has evolved to provide the organism with the best chances of survival and reproductive success under changing environments [6]. The existence of ‘transgenerational’ effects is a key element of developmental programming, whereby an early-life exposure may affect the later life health and development, not only of the F1 generation, but also of future generations (F2 and beyond). The transmission of developmentally programmed phenotypes across generations has been observed in both human and animal models [7,8]. In evolutionary terms, the acceptance of transgenerational effects as an integral part of developmental programming is related to a potential beneficial purpose, allowing organisms pregnancy-by-pregnancy the rapid adjustment of phenotype to changing environments [8,9]. However, inherited effects of parental environments may be maladaptive if progeny individuals encounter later dissimilar environmental conditions [9,10]. In

addition, exposure to an adverse early-life environment leads to long-term health problems that can be recapitulated in subsequent generations [8,11,12].

### 1.1.3. Epigenetic mechanisms

Epigenetic marks regulating cell-, tissue-, and developmental stage-specific gene expression are mitotically inherited in somatic cells and may be altered in response to internal and external stimuli. The idea that environment-induced epigenetic changes in mammals could be inherited through the germline, independent of genetic mechanisms, has stimulated much debate [13]. Today, developmental plasticity responses are closely linked to epigenetic mechanisms that allow flexible, dynamic and heritable cell reprogramming [14,15]. Metastability of the epigenome explains why development is both plastic and canalised. Metastable epialleles are variably expressed in genetically identical individuals due to epigenetic modifications established during early life by environmental influences [16,17]. In this sense, epigenetic marks act as a signal relaying information about an organism's early-life environment to its future self, improving fit between future environment and phenotype [2].

It has been proposed that epigenetic marks could be transmitted through the germline and persist in subsequent generations, providing the molecular basis for the inheritance of acquired traits [17]. This does not alter the basic Darwinian evolutionary paradigm, but simply provides a neo-Lamarckian component, this time with the help of epigenetics [14,17]. Therefore, many authors have argued in favour of an epigenetic basis for transgenerational programming [7]. Although it has been well documented in plants, nematodes and fruit flies, the occurrence of transgenerational epigenetic inheritance in mammals remains controversial [17]. This is because, in general, epigenetic marks are cleared and re-established each generation by the waves of epigenetic reprogramming that take place in germ cell development and early embryogenesis. This mechanism allows the acquisition of totipotency and could serve to prevent the transmission of responses to environmental insults that individuals have encountered during their life [17,18]. However, examples of transgenerational epigenetic inheritance induced by parental genotype, physiology or environment have been increasingly numerous in model animals [19,20], demonstrating that some loci appear to escape epigenetic reprogramming. Nonetheless, few of the well-established transgenerational effects are adaptive [19,20], so the heritability of these changes has been the focus of attention for several diseases [12].

## 1.2. CRITICAL WINDOW OF THE PREIMPLANTATION PERIOD

The window of developmental plasticity covers preimplantation development, which is a critical period of elegantly orchestrated molecular events that begins after fertilisation and is extended until the uterine epithelium is invaded by the hatched blastocyst [21]. Initially, sperm and oocyte genomes are silent as a consequence of an hypermethylated DNA. However, upon fertilisation, extensive epigenetic reprogramming takes place, whereby the two highly differentiated gametes come together and reorganise their cellular and molecular signatures, by global DNA demethylation, to establish a transcriptionally activated, totipotent zygote [22,23]. Proper embryo genome activation is essential for development because it coordinates cell division and cell differentiation, which ensures adequate cell fate determination and ultimately, organogenesis [23,24]. However, these delicate mechanisms need to be supported by the maternal physiology across the oviduct and uterine epithelia, which release crucial key growth factors, hormones, nutrients and cytokines that ensure optimal reprogramming [25-27]. Therefore, stressors impacting the preimplantation period during gestation may transform optimal conditions of the maternal environment into suboptimal ones, which can be a cause of atypical embryo programming that conflicts later in life [28,29].

## 1.3. CONSEQUENCES OF INTERCEDING PREIMPLANTATION DEVELOPMENT

Current literature clearly shows that disturbing optimal preimplantation development has consequences on the epigenomes and therefore in the subsequent developmental programme [30]. There may be two triggers for this reprogramming, which respond to the concept of “vulnerability” and “opportunity”.

### 1.3.1. “Vulnerability”

As previously described, a large-scale reorganisation of the epigenome takes place during the preimplantation period on the few cells involved. This epigenetic rearrangement makes early embryos particularly vulnerable to developmental disturbances [21,30]. In this sense, many examples of embryo programming are likely to be the result of a direct perturbation of the normal preimplantation epigenetic reprogramming. Some environmental chemicals, such as polycyclic aromatic hydrocarbons, solvents, endocrine disruptors and some heavy metals are highlighted as potential elements implicated in the development of long-term health problems in the offspring following maternal and subsequent *in utero* exposure [31,32]. The underlying cause is the interaction of these elements with the biological mechanisms involved in

epigenome remodelling, which can cause errors (epimutations). Although some of these epimutations appear to be corrected by normal subsequent reprogramming, others are not corrected and so can be inherited over several generations.

### 1.3.2. “Opportunity”

Unlike the previous point, it has been also accepted that some reshapes in the developmental trajectory can be viewed as true biological processes, conserved during evolution and driven by the developmental plasticity to optimise offspring phenotypes in response to extrinsic environmental cues [30,33]. Probably the clearest examples come from studies evaluating maternal malnutrition during pregnancy, in which preimplantation embryos undergo molecular and metabolic adaptations to cope with nutrient deficits or excesses during episodes of undernutrition and overnutrition [34]. However, if there is a mismatch between the environment in which the organism develops and that in which it emerges, adaptive embryo responses during the preimplantation may become maladaptive in the long-term and cause disease [29,34]. As an example, a higher survival rate was reported for rats when their diet matched that consumed by their respective dam during gestation, but survival decreased if rat diet differed [35]. Thus, offspring development can be influenced by suboptimal preimplantation conditions (developmental plasticity), whose legacy appear to be propagated to subsequent generations [35].

### 1.3.3. The advent of assisted reproduction technologies (ARTs)

Based on the previous literature, we now accept that intrauterine environment affects the epigenetic restructuring of the genome in the early embryo, changing its gene expression, the adult phenotype and propensity for disease [12,30]. In addition, these disturbances can persist long after the sensing event has occurred, and some of them might be transgenerational inherited. Direct evidence comes from assisted reproductive treatments in which mature gametes and the preimplantation embryo are exposed to precisely timed *in vitro* manipulations.

The advent of ART in mammals involves an extraordinary change in the environment where the beginning of a new organism takes place, requiring the *in vitro* handling of gametes and embryos in a synthetic culture environment deprived of the dynamic conditions offered by the maternal tract [27,36,37]. In addition, ARTs introduce a range of environmental exposures that deviates extensively from the *in vivo* conception, including mechanical manipulation, light exposure, fluctuations in temperature and oxygen concentration, pH deviations, and *in vitro* culture under non-standardised

culture mediums in which the embryo-maternal signalling are absent (Figure 1.1) [27,38]. Therefore, safety concerns regarding ART are as old as ARTs themselves [39,40].

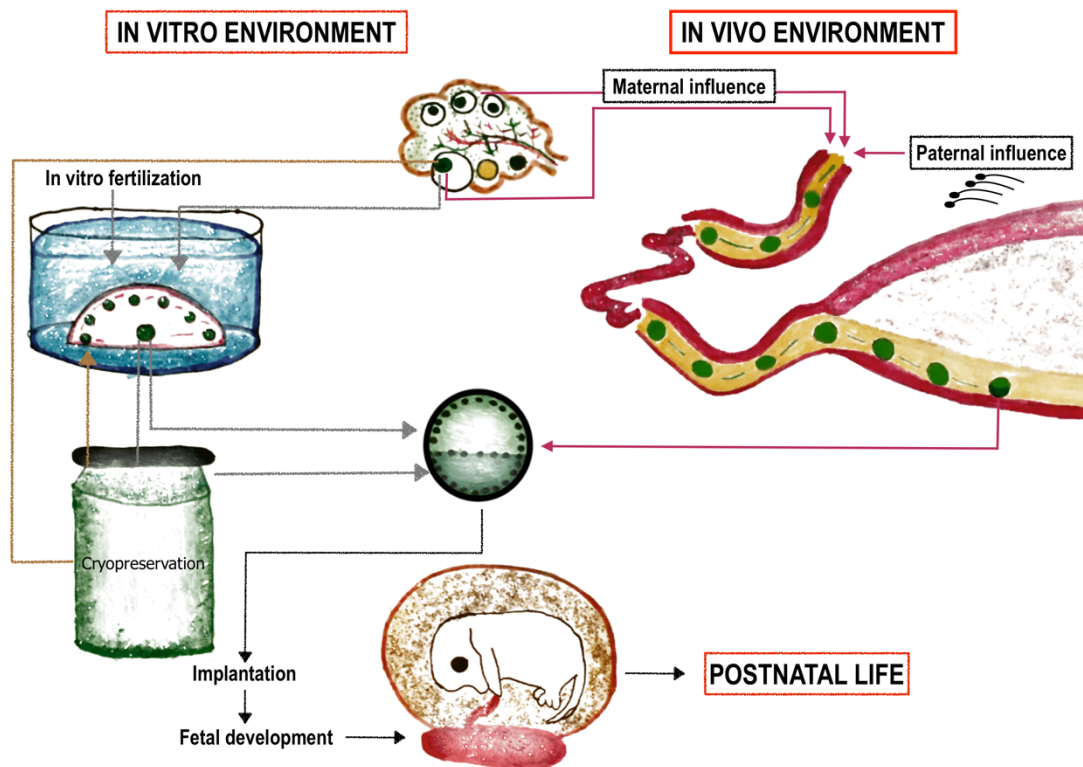


**Figure 1.1.** *In vivo* vs *In vitro* environmental differences during the periconceptional period. (The work of Clara Marco Marín to perform this figure is acknowledged).

In accordance with the DOHaD theory, today it is known that the environmental conditions during ARTs could lead to specific changes in DNA methylation dynamics with consequences for later life [40]. To date, ART has been linked, both in human and model species studies, with adverse obstetric and perinatal outcomes, an increased risk of birth defects, cancers, growth and development disorders, immunological and neurological disturbances, and increased risk of chronic ageing-related diseases such as obesity, type 2 diabetes and cardiovascular disease [30,37,41,42]. Both “vulnerability” and “opportunity” are put forward as underlying causes whereby ARTs incurs developmental reshapes into later life. The former is because developmental time points at which ARTs are implemented are typified by epigenetic rearrangement (Figure 1.2), so extreme environmental perturbations could cause errors that affect the programming of cell states [21,33]. The latter is attributed to the high degree of developmental plasticity exhibited by the mammalian embryo in responding to suboptimal *in vitro* conditions, which incur adaptive responses that can conflict in later stages [43].

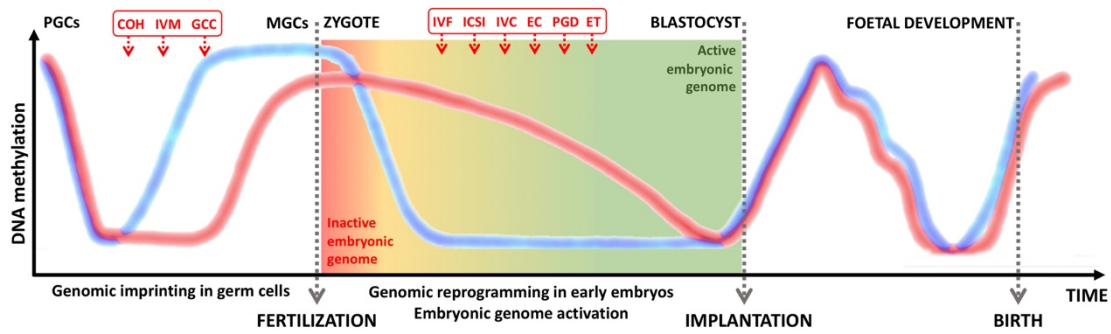


**Figure 1.2.** Epigenetic genome reprogramming during gamete and early embryo development. The scheme shows how maternal (red) and paternal (blue) genomes are epigenetically reprogrammed during gametogenesis (from primordial germ cells, PGCs; to mature germ cells, MGCs), early embryonic and *in utero* development. These are sensitive periods that may be affected by different assisted reproductive technologies, such as controlled ovarian hyperstimulation (COH), gamete *in vitro* maturation (IVM), germ cells cryopreservation (GCC), *in vitro* fertilisation (IVF), intracytoplasmic sperm injection (ICSI), *in vitro* culture (IVC), embryo cryopreservation (EC), preimplantation genetic diagnosis (PGD) and embryo transfer (ET). Adapted from Zacchini *et al.* [40].

#### 1.4. IMPLICATIONS FOR EMBRYO CRYOPRESERVATION

The discovery in 1949 of the cryoprotective properties of glycerol for mammalian spermatozoa [44] emphasised the advantages of preserving the germplasm at ultra-low temperatures. This approach constituted one way of maximising the availability of reproductive material independently of time and geographic location [45]. However, with sperm cryopreservation, only the haploid genotype is conserved and, if the original genetic background is required, appropriate oocytes would also have to be available in the future [46]. This management disadvantage was overcome in 1971 with the reporting of successful mammalian embryo cryopreservation by two independent groups [47,48], which allowed them to preserve the entire genotype. Over the past four decades, this procedure has been adapted and embryos of more than 25 mammalian species have been successfully cryopreserved, achieving live offspring after embryo thawing and transfer [49]. Slow freezing was the original approach used but, in 1985, vitrification was introduced as a simple and cheap way to cryopreserve mammalian embryos in the absence of ice [50]. Today, biobanking is a rapidly growing industry, covering diverse fields such as human medicine, livestock production and animal model research [49,51]. To this end, embryo cryopreservation has become a routine, having been used to freeze millions of embryos of mice and cattle, and many hundreds of thousands of human embryos [49]. In addition, substantial efforts are taking place to extend the success of embryo cryopreservation to wildlife conservation, especially for endangered species [52]. However, to fulfil the purposes of a cryobank, the stored embryos must result in healthy offspring, with the expected phenotype and able to reproduce [53,54]. Successful embryo cryopreservation without post-thawing adverse effect after long-term storage has been reported in mice (11 years [55]), rabbits (15

years [56]), pigs (3 years [57]), sheep (13 years [58]), bovine (15 years [59]) and humans (20 years [54]). However, long-term follow-up data on these offspring are scarce, as although cryopreservation can be lethal to some embryos, it is not considered to have any delayed effects in survivors [60]. This is because the only criteria used to qualify the resultant progeny as “normal” were the lack of malformation at birth and the capacity to fertilise [60].

Our own Department of Animal Science set up a genetic resource bank in 1991 to assist the Universidad Politécnica de Valencia (UPV) in the development and management of a genetic improvement programme for meat rabbits. The aim was to maintain and preserving breeds from pathogens or catastrophe, minimising the impact of genetic drift and facilitating diffusion [61,62]. However, over the years we noted that embryo cryopreservation changed the gene expression of preimplantation embryos, decreased placenta weight and disturbed its physiology, increased foetal losses throughout gestation, reduced early foetal growth, impacted on offspring phenotype at birth and in the long term, and influenced reproductive features hereditarily [63-70]. We know that developing embryos can be differentially affected and adapted depending on the timing, type and degree of environmental exposure, with more severe stress precipitating more deviant responses in the cells that subsequently form tissues and organs [38,43]. Revitalisation of the whole organism from cryopreserved embryos requires embryo exposure to: (i) toxic cryoprotectant solutions, (ii) non-physiologic ultra-low temperatures, and (iii) other ARTs such as embryo transfer [71]. Increasing evidence suggests that cryopreservation may be associated with deviations from the physiological epigenetic marks with putative long-term effects [45,72], which are supported by our own research background.

## 1.5. REFERENCES

- [1]. Murren CJ, Auld JR, Callahan H, Ghalambor CK, Handelsman CA, Heskell MA, *et al.* Constraints on the evolution of phenotypic plasticity: limits and costs of phenotype and plasticity. *Heredity (Edinb)*. 2015;115:293-301.
- [2]. Laubach ZM, Perng W, Dolinoy DC, Faulk CD, Holekamp KE, Getty T. Epigenetics and the maintenance of developmental plasticity: extending the signalling theory framework. *Biol Rev Camb Philos Soc*. 2018;93:1323-1338.
- [3]. Stamps JA. Individual differences in behavioural plasticities. *Biol Rev Camb Philos Soc*. 2016;91:534-67.
- [4]. Nettle D, Bateson M. Adaptive developmental plasticity: what is it, how can we recognize it and when can it evolve? *Proc Biol Sci*. 2015;282:20151005.
- [5]. Lacagnina S. The Developmental Origins of Health and Disease (DOHaD). *Am J Lifestyle Med*. 2019;14:47-50.

- [6]. Hochberg Z, Feil R, Constancia M, Fraga M, Junien C, Carel JC, *et al.* Child health, developmental plasticity, and epigenetic programming. *Endocr Rev.* 2011;32:159-224.
- [7]. Aiken CE, Ozanne SE. Transgenerational developmental programming. *Hum Reprod Update.* 2014;20:63-75.
- [8]. Aiken CE, Tarry-Adkins JL, Ozanne SE. Transgenerational Developmental Programming of Ovarian Reserve. *Sci Rep.* 2015;5:16175.
- [9]. Donelan SC, Hellmann JK, Bell AM, Luttbeg B, Orrock JL, Sheriff MJ, *et al.* Transgenerational Plasticity in Human-Altered Environments. *Trends Ecol Evol.* 2020;35:115-124.
- [10]. Baker BH, Sultan SE, Lopez-Ichikawa M, Waterman R. Transgenerational effects of parental light environment on progeny competitive performance and lifetime fitness. *Philos Trans R Soc Lond B Biol Sci.* 2019;374:20180182.
- [11]. Zhu Z, Cao F, Li X. Epigenetic Programming and Fetal Metabolic Programming. *Front Endocrinol (Lausanne).* 2019;10:764.
- [12]. Carpinello OJ, DeCherney AH, Hill MJ. Developmental Origins of Health and Disease: The History of the Barker Hypothesis and Assisted Reproductive Technology. *Semin Reprod Med.* 2018;36:177-182.
- [13]. Martos SN, Tang WY, Wang Z. Elusive inheritance: Transgenerational effects and epigenetic inheritance in human environmental disease. *Prog Biophys Mol Biol.* 2015;118:44-54.
- [14]. Skinner MK. Role of epigenetics in developmental biology and transgenerational inheritance. *Birth Defects Res C Embryo Today.* 2011;93:51-5.
- [15]. Prudhomme J, Morey C. Epigenesis and plasticity of mouse trophoblast stem cells. *Cell Mol Life Sci.* 2016;73:757-74.
- [16]. Dolinoy DC, Das R, Weidman JR, Jirtle RL. Metastable epialleles, imprinting, and the fetal origins of adult diseases. *Pediatr Res.* 2007;61:30R-37R.
- [17]. Horsthemke B. A critical view on transgenerational epigenetic inheritance in humans. *Nat Commun.* 2018;9:2973.
- [18]. Legoff L, D'Cruz SC, Tevosian S, Primig M, Smagulova F. Transgenerational Inheritance of Environmentally Induced Epigenetic Alterations during Mammalian Development. *Cells.* 2019;8.pii: E1559.
- [19]. Siklenka K, Erkek S, Godmann M, Lambrot R, McGraw S, Lafleur C, *et al.* Disruption of histone methylation in developing sperm impairs offspring health transgenerationally. *Science.* 2015;350:aab2006.
- [20]. Perez MF, Lehner B. Intergenerational and transgenerational epigenetic inheritance in animals. *Nat Cell Biol.* 2019;21:143-151.
- [21]. Feuer S, Rinaudo P. Preimplantation stress and development. *Birth Defects Res C Embryo Today.* 2012;96:299-314.
- [22]. Fraser R, Lin CJ. Epigenetic reprogramming of the zygote in mice and men: on your marks, get set, go! *Reproduction.* 2016;152:R211-R222.



- [23]. Jukam D, Shariati SAM, Skotheim JM. Zygotic Genome Activation in Vertebrates. *Dev Cell*. 2017;42:316-332.
- [24]. Boland MJ, Nazor KL, Loring JF. Epigenetic regulation of pluripotency and differentiation. *Circ Res*. 2014;115:311-24.
- [25]. Zheng LL, Tan XW, Cui XZ, Yuan HJ, Li H, Jiao GZ, *et al*. Preimplantation maternal stress impairs embryo development by inducing oviductal apoptosis with activation of the Fas system. *Mol Hum Reprod*. 2016;22:778-790.
- [26]. Tríbulo P, Siqueira LGB, Oliveira LJ, Scheffler T, Hansen PJ. Identification of potential embryokines in the bovine reproductive tract. *J Dairy Sci*. 2018;101:690-704.
- [27]. Ramos-Ibeas P, Heras S, Gómez-Redondo I, Planells B, Fernández-González R, Pericuesta E, *et al*. Embryo responses to stress induced by assisted reproductive technologies. *Mol Reprod Dev*. 2019;86:1292-1306.
- [28]. Burkuš J, Kačmarová M, Kubandová J, Kokošová N, Fabianová K, *et al*. Stress exposure during the preimplantation period affects blastocyst lineages and offspring development. *J Reprod Dev*. 2015;61:325-31.
- [29]. Fleming TP, Eckert JJ, Denisenko O. The Role of Maternal Nutrition During the Periconceptual Period and Its Effect on Offspring Phenotype. *Adv Exp Med Biol*. 2017;1014:87-105.
- [30]. Fleming TP, Watkins AJ, Velazquez MA, Mathers JC, Prentice AM, Stephenson J, *et al*. Origins of lifetime health around the time of conception: causes and consequences. *Lancet*. 2018;391:1842-1852.
- [31]. Waring RH, Harris RM, Mitchell SC. In utero exposure to carcinogens: Epigenetics, developmental disruption and consequences in later life. *Maturitas*. 2016;86:59-63.
- [32]. Onuzulu CD, Rotimi OA, Rotimi SO. Epigenetic modifications associated with in utero exposure to endocrine disrupting chemicals BPA, DDT and Pb. *Rev Environ Health*. 2019;34:309-325.
- [33]. Fleming TP, Velazquez MA, Eckert JJ. Embryos, DOHaD and David Barker. *J Dev Orig Health Dis*. 2015;6:377-83.
- [34]. Velazquez MA. Impact of maternal malnutrition during the periconceptual period on mammalian preimplantation embryo development. *Domest. Anim. Endocrinol*. 2015;51:27-45.
- [35]. Parlee SD, MacDougald OA. Maternal nutrition and risk of obesity in offspring: the Trojan horse of developmental plasticity. *Biochim Biophys Acta*. 2014;1842:495-506.
- [36]. Ventura-Juncá P, Irrázaval I, Rolle AJ, Gutiérrez JI, Moreno RD, Santos MJ. In vitro fertilization (IVF) in mammals: epigenetic and developmental alterations. Scientific and bioethical implications for IVF in humans. *Biol Res*. 2015;48:68.
- [37]. Vrooman LA, Bartolomei MS. Can assisted reproductive technologies cause adult-onset disease? Evidence from human and mouse. *Reprod Toxicol*. 2017;68:72-84.

- [38]. Feuer SK, Rinaudo PF. Physiological, metabolic and transcriptional postnatal phenotypes of in vitro fertilization (IVF) in the mouse. *J Dev Orig Health Dis.* 2017;8:403-410.
- [39]. Cohen ME. The brave new baby and the law: fashioning remedies for the victims of in vitro fertilization. *Am. J. Law Med.* 1978;4:319-336.
- [40]. Zacchini F, Sampino S, Stankiewicz AM, Haaf T, Ptak GE. Assessing the epigenetic risks of assisted reproductive technologies: a way forward. *Int J Dev Biol.* 2019;63:217-222.
- [41]. Chen M, Heilbronn LK. The health outcomes of human offspring conceived by assisted reproductive technologies (ART). *J Dev Orig Health Dis.* 2017;8:388-402.
- [42]. Duranthon V, Chavatte-Palmer P. Long term effects of ART: What do animals tell us? *Mol Reprod Dev.* 2018;85:348-368.
- [43]. Roseboom TJ. Developmental plasticity and its relevance to assisted human reproduction. *Hum Reprod.* 2018;33:546-552.
- [44]. Polge C, Smith AU, Parkes AS. Revival of spermatozoa after vitrification and dehydration at low temperature. *Nature* 1949;164:666.
- [45]. Morrell JM, Mayer I. Reproduction biotechnologies in germplasm banking of livestock species: a review. *Zygote.* 2017;25:545-557.
- [46]. Glenister PH, Thornton CE. Cryoconservation--archiving for the future. *Mamm Genome.* 2000;11:565-71.
- [47]. Whittingham DG. Survival of mouse embryos after freezing and thawing. *Nature* 1971;233:125-6.
- [48]. Wilmut I. The effect of cooling rate, warming rate, cryoprotective agent, and stage of development on survival of mouse embryos. *Life Sci* 1972;11:1071-9.
- [49]. Leibo SP, Sztejn JM. Cryopreservation of mammalian embryos: Derivation of a method. *Cryobiology.* 2019;86:1-9.
- [50]. Rall WF, Fahy GM. Ice-free cryopreservation of mouse embryos at -196°C by vitrification. *Nature* 1985;313:573-5.
- [51]. Saragusty J, Loi P. Exploring dry storage as an alternative biobanking strategy inspired by Nature. *Theriogenology.* 2019;126:17-27.
- [52]. Hildebrandt TB, Hermes R, Colleoni S, Diecke S, Holtze S, Renfree MB, *et al.* Embryos and embryonic stem cells from the white rhinoceros. *Nat Commun.* 2018;9:2589.
- [53]. Rall WF, Schmidt PM, Lin X, Brown SS, Ward AC, Hansen CT. Factors affecting the efficiency of embryo cryopreservation and rederivation of rat and mouse models. *ILAR J.* 2000;41:221-7.
- [54]. Dowling-Lacey D, Mayer JF, Jones E, Bocca S, Stadtmauer L, Oehninger S. Live birth from a frozen-thawed pronuclear stage embryo almost 20 years after its cryopreservation. *Fertil Steril.* 2011;95:1120.e1-3.
- [55]. Glenister PH, Lyon MF. Long-term storage of eight-cell mouse embryos at - 196 degrees C. *J In Vitro Fert Embryo Transf.* 1986;3:20-27.

- [56]. Lavara R, Baselga M, Vicente JS. Does storage time in LN2 influence survival and pregnancy outcome of vitrified rabbit embryos? *Theriogenology*. 2011;76:652–7.
- [57]. Sánchez-Osorio J, Cuello C, Gil MA, Parrilla I, Almiñana C, Caballero I, *et al*. In vitro postwarming viability of vitrified porcine embryos: Effect of cryostorage length. *Theriogenology*. 2010;74:486-490.
- [58]. Fogarty NM, Maxwell WM, Eppleston J, Evans G. The viability of transferred sheep embryos after long-term cryopreservation. *Reprod Fertil Dev*. 2000;12:31-7.
- [59]. Fang Y, Zeng S, Fu X, Jia B, Li S, An X, *et al*. Developmental competence in vitro and in vivo of bovine IVF blastocyst after 15 years of vitrification. *Cryo Lett*. 2014;35:232-238.
- [60]. Auroux M. Long-term effects in progeny of paternal environment and of gamete/embryo cryopreservation. *Hum Reprod Update*. 2000;6:550–563.
- [61]. Leibo SP. Cryobiology: preservation of mammalian embryos. *Basic Life Sci*. 1986;37:251-272.
- [62]. Marco-Jiménez F, Baselga M, Vicente JS. Successful re-establishment of a rabbit population from embryos vitrified 15 years ago: The importance of biobanks in livestock conservation. *PLoS One*. 2018;13:e0199234.
- [63]. Mocé ML, Blasco A, Santacreu MA. In vivo development of vitrified rabbit embryos: effects on prenatal survival and placental development. *Theriogenology*. 2010;73:704–710.
- [64]. Saenz-de-Juano MD, Marco-Jiménez F, Peñaranda DS, Joly T, Vicente JS. Effects of slow freezing procedure on late blastocyst gene expression and survival rate in rabbit. *Biol Reprod*. 2012;87:91.
- [65]. Saenz-de-Juano MD, Marco-Jimenez F, Schmaltz-Panneau B, Jimenez-Trigos E, Viudes-de-Castro MP, *et al*. Vitrification alters rabbit foetal placenta at transcriptomic and proteomic level. *Reproduction*. 2014;147:789-801.
- [66]. Saenz-de-Juano MD, Peñaranda DS, Marco-Jiménez F, Vicente JS. Does vitrification alter the methylation pattern of OCT4 promoter in rabbit late blastocyst? *Cryobiology*. 2014;69:178-80.
- [67]. Saenz-de-Juano MD, Vicente JS, Hollung K, Marco-Jiménez F. Effect of Embryo Vitrification on Rabbit Foetal Placenta Proteome during Pregnancy. *PLoS One*. 2015;10:e0125157.
- [68]. Vicente JS, Saenz-de-Juano MD, Jiménez-Trigos E, Viudes-de-Castro MP, Peñaranda DS, Marco-Jiménez F. Rabbit morula vitrification reduces early foetal growth and increases losses throughout gestation. *Cryobiology*. 2013;67:321-6.
- [69]. Lavara R, Baselga M, Marco-Jiménez F, Vicente JS. Embryo vitrification in rabbits: Consequences for progeny growth. *Theriogenology*. 2015;84:674-80.
- [70]. Lavara R, Baselga M, Marco-Jiménez F, Vicente JS. Long-term and transgenerational effects of cryopreservation on rabbit embryos. *Theriogenology*. 2014;81:988-92.

- [71]. Sparks AE. Human embryo cryopreservation-methods, timing, and other considerations for optimizing an embryo cryopreservation program. *Semin Reprod Med.* 2015;33:128-44.
- [72]. Chatterjee A, Saha D, Niemann H, Gryshkov O, Glasmacher B, Hofmann N. Effects of cryopreservation on the epigenetic profile of cells. *Cryobiology.* 2017;74:1-7.

# **OBJECTIVES**

X. Garcia-Dominguez

Institute for Animal Science and Technology (ICTA), Laboratory of Reproductive Biotechnology,  
Universitat Politècnica de València, 46022 Valencia, Spain



## 2. OBJECTIVES

---

The general aim of this thesis was to study the long-term effects of the *in vitro* embryo manipulations during a vitrified embryo transfer procedure, and their transgenerational inheritance, on the rabbit model.

This aim was itemised into the following specific objectives:

- Evaluation and characterisation of the embryo transfer and vitrification effects on the phenotype, health status and reproductive performance in the resulting offspring.
- Study of the hepatic molecular signatures to determine the possible underlying mechanisms related to the previous phenotypic characterisation.
- Determine the possible inheritance of the effects induced by the vitrified embryo transfer procedure on the long-term phenotype and molecular (transcriptional and metabolic) physiology.
- Perform a multi-omic (metabolomic, proteomic and epigenomic) approach in order to complete the molecular framework related with the transgenerational phenotype induced by the vitrified embryo transfer procedure.





## CHAPTER I

# MINIMALLY INVASIVE EMBRYO TRANSFER AND EMBRYO VITRIFICATION AT THE OPTIMAL EMBRYO STAGE IN THE RABBIT MODEL

X. Garcia-Dominguez<sup>1</sup>, F. Marco-Jiménez<sup>1</sup>, M.P. Viudes-de-Castro<sup>2</sup>, J.S. Vicente<sup>1</sup>

<sup>1</sup>Institute for Animal Science and Technology (ICTA), Laboratory of Reproductive Biotechnology, Universitat Politècnica de València, 46022 Valencia, Spain

<sup>2</sup>Animal Technology and Research Center (CITA),  
Instituto Valenciano de Investigaciones Agrarias (IVIA), 12400 Segorbe, Castellón, Spain

*Journal of Visualised Experiments*, 2019; 147: e58055



### ABSTRACT

Assisted reproductive techniques (ART), such as *in vitro* embryo culture or embryo cryopreservation, affect natural development patterns with perinatal and postnatal consequences. To ensure the innocuousness of ART applications, studies in animal models are necessary. In addition, as a last step, embryo development studies require evaluation of their capacity to develop full-term healthy offspring. Here, embryo transfer to the uterus is indispensable to perform any ART-related experiment.

The rabbit has been used as a model organism to study mammalian reproduction for over a century. In addition to its phylogenetic proximity to the human species and its small size and low maintenance cost, it has important reproductive characteristics such as induced ovulation, a chronology of early embryonic development similar to humans and a short gestation that allow us to study the consequences of ART application easily. Moreover, ART (such as intracytoplasmic sperm injection, embryo culture, or cryopreservation) are applied with suitable efficiency in this species.

Using the laparoscopic embryo transfer technique and the cryopreservation protocol presented in this article, we describe (i) how to transfer embryos through an easy, minimally invasive technique and (ii) an effective protocol for long-term storage of rabbit embryos to provide time- flexible logistical capacities and the ability to transport the sample. The outcomes obtained after transferring rabbit embryos at different developmental stages indicate that morula is the ideal stage for rabbit embryo recovery and transfer. Thus, an oviductal embryo transfer is required, justifying the surgical procedure. Furthermore, rabbit morulae are successfully vitrified and laparoscopically transferred, proving the effectiveness of the described techniques.

### VIDEO LINK

The video component of this article can be found at <https://www.jove.com/video/58055/>



### 3.1. INTRODUCTION

With the aims of bypassing human infertility or improving dissemination of livestock of high genetic value and preserving animal genetic resources, a set of techniques collectively termed assisted reproduction technologies, such as superovulation, *in vitro* fertilisation, embryo culture, or cryopreservation, were developed [1,2]. Currently, hormonal treatments are given to stimulate the ovaries and produce a large number of antral ovarian follicles [1]. Oocytes collected from these follicles can be matured, fertilised, and developed *in vitro* until they are either cryopreserved or transferred to surrogate mothers [3]. However, during these treatments, gametes and zygotes are exposed to a series of non-physiological processes that could require embryo adaptation to survive in these conditions [4,5]. This adaptation is possible due to early embryo plasticity, which allows embryo changes in gene expression and developmental programming [6]. However, these modifications can influence the subsequent stages of embryo development until adulthood, and it is now widely accepted that methods, timing, cryopreservation procedure or culture conditions show different outcomes on embryo fate [7,8]. Therefore, to elucidate the specific induced effects of ARTs, the use of well-characterised animal models is inevitable.

The first documented live birth resulting from transfer of mammalian embryos took place in 1890 [9]. Today, embryo transfer (ET) to a surrogate female is a crucial step in studying the ART-induced effects during preimplantation or subsequent embryo development stages [10]. ET techniques depend on the size and anatomical structure of each animal. In the case of large-sized animal models, it has been possible to perform ET by transcervical nonsurgical ET techniques, but in smaller-size species catheterisation of the cervix is more complex and surgical techniques are frequently used [11]. However, surgical ET can cause haemorrhaging that could impair implantation and embryo development, as blood can invade the uterine lumen, causing embryo death [10]. Transcervical nonsurgical ET techniques are still applied in humans, baboons, bovine, pigs and mice [12-17], but surgical ETs are still being used in species such as goats, sheep or other animals which present additional difficulties [10,18-21], such as rabbits (two independent cervixes) or mice (small size). Nonetheless, surgical transfer methods tend to have gradually been replaced by less invasive methods. Endoscopy was used to transfer embryos, for example, in rabbits, pigs and small ruminants [18-20]. These minimally invasive endoscopy methods can be used to transfer embryos into the ampulla via the infundibulum, which is essential in rabbits and has demonstrated beneficial effects in some species [20]. This is based on the importance of the correct dialogue between embryo and mother during early embryo stages in the oviduct. Thus, the embryo remodelling that takes place in rabbits during embryo migration through the oviduct is essential to achieve embryos able to implant [22,23].

Larger-size animal models, such as bovine, are interesting because the biochemical and preimplantation features are similar to those in human species [24]. However, large animals are too expensive to use in preliminary trials, and rodents are considered an ideal model (76% model organisms are rodents) for laboratory research [25]. Nevertheless, the rabbit model provides some advantages over rodents in reproductive studies, as some reproductive biological processes exhibited by humans are more similar in rabbits than those in mice. Human and rabbits present a similar chronological embryonic genome activation, gastrulation and hemochorial placenta structure. In addition, using rabbits it is possible to know the exact timing of fertilisation and pregnancy stages due to their induced ovulation [25]. Rabbit life cycles are short, completing gestation in 31 days and reaching puberty at about 4-5 months; the animal is easy to handle due to its docile and non-aggressive behaviour, and its upkeep is very economical compared to the expense of larger animals. Moreover, it is crucial to mention that rabbits have a duplex uterus with two independent cervixes [11,25]. This places the rabbit in a preferential position, as embryos from the different experimental groups can be transferred into the same animal, but into a different uterine horn. This allows us to compare both experimental effects, reducing the maternal factor from the results.

Today, nonsurgical ET methods are not in use in rabbit. Some studies carried out in the late 90s using a transcervical ET technique resulted in low delivery rates ranging from 5.5% to 20.0% [11,26] versus 50-65% by surgical methods, among them the laparoscopy procedure described by Besenfelder and Brem [18]. The low success rates of these nonsurgical ET methods in rabbits coincide with the lack of the necessary embryo remodelling in the oviduct, which is avoided in transcervical ET. Here, we describe an effective minimally invasive laparoscopic ET procedure using rabbits as a model organism. This technique provides a model for further reproductive research in large animals and humans.

Because rabbits have a particularly narrow time window for embryo implantation, ET in this species requires a high degree of synchrony between the developmental stage of the embryo at ET and the physiological status of the recipient [27]. In some cases, after a reproductive treatment that slows embryo development (e.g. *in vitro* culture) or alters the endometrial receptivity (e.g. superovulation treatments), there is no synchrony between the embryo and the maternal uterus. These situations can negatively affect ET outcomes. To respond in these contexts, we describe an effective rabbit morula vitrification protocol that allows us to pause, organise and resume the experiments. This process is logistically desirable for reproductive studies and gives us the capacity for long-term storage of embryos, allowing their transport. The laparoscopic procedure and cryopreservation strategies allow better planning of studies with fewer animals. Thus, our methodology offers hygienic and economic advantages and conforms to the concept

of the 3Rs (replacement, reduction and refinement) of animal research with the stated goal of improving human treatment of experimental animals. Thus, with these methods, rabbits constitute an ideal model organism for *in vivo* reproductive assays.

## 3.2. PROTOCOL

All experimental procedures used in this study were performed in accordance with Directive 2010/63/EU EEC for animal experiments and reviewed and approved by the Ethical Committee for Experimentation with Animals of the Universitat Politècnica de València, Spain (code: 2015/VSC/PEA/00170). An authorisation certificate issued by the Valencian governmental administration to experiment on animals is held by XGD (code: 2815), FMJ (code: 2273), MPVC (code: 0593) and JSV (code: 0690).

### 3.2.1. Embryo transfer

#### 1. Preparation of recipient females

- 1.1. Use only sexually mature females (> 4.5 months old).
- 1.2. One week before ET, adapt females to a 16 h light/8 h dark regime to initiate follicular growth and enhanced female receptivity.
- 1.3. Select the recipient females, observing the turgidity and colour of the vulva. If the vulva is turgid and reddish, the female is receptive.
- 1.4. Induce pseudopregnancy (ovulation) by a single intramuscular injection of 1 µg of buserelin acetate (synthetic analogue of Gonadotropin-releasing hormone) regardless of body weight. Note: Normally, 0.8 µg is a suitable dose for ovulation induction in medium-size rabbits (4-5 kg), so 1 µg generally guarantees the ovulation.
- 1.5. Induce ovulation as many days beforehand as the age of the embryos to be transferred (for example, 70-72 h before fresh morula ET).

#### 2. Anaesthesia and analgesia

- 2.1. Weigh the rabbit and load the following anaesthetics and analgesics. In a 1 mL syringe with a 30G needle: load xylazine (5mg/kg) and buprenorphine hydrochloride (0.03 mg/kg). In another 1 mL syringe with a 23G pericranial needle, load ketamine hydrochloride (35 mg/kg).
- 2.2. Hold the rabbit and inject the xylazine-buprenorphine mixture intramuscularly.
- 2.3. Insert the pericranial needle with ketamine in the marginal ear vein, slowly introducing all the syringe contents intravenously.

- 2.4. Fix the needle and leave it inserted throughout the remaining steps to administer more anaesthesia if necessary.
  - 2.5. Leave the rabbit in the cage (clean and without any other animals) on a warm stage.
  - 2.6. Once unconscious, apply eye ointment to avoid dryness of the eye and check for the absence of the palpebral reflex. Note: This protocol provides a surgical anaesthesia plane for a minimum of 30 min. If a longer time is required, inject additional dosages with half of the amount of ketamine hydrochloride described in 2.1 after 30 min.
  - 2.7. Monitor the depth of anaesthesia by checking the pedal reflex and breathing movement. Changes in the breathing pattern to an irregular and faster rate indicate loss of the proper plane of anaesthesia.
  - 2.8. Monitor the colour of the mucous membranes (eyes, lips, etc.), respiratory rate (30-60 breaths per minute), heart rate (120-325 beats per minute) and rectal temperature (38-39.6 °C).
  - 2.9. Eight hours before transfer, withhold food from animals to avoid the greater gut size and activity until the ET process is finished. Leave free access to water.
3. Embryo preparation
- 3.1. Warm the embryo manipulation media to 25 °C: Base Medium (BM), consisting of Dulbecco's Phosphate-Buffered Saline (DPBS) supplemented with 0.2% (w/v) of Bovine Serum Albumin.
  - 3.2. Working under a stereomicroscope, rinse fresh or warmed embryos with BM.
  - 3.3. Using sterile gloves, attach an appropriately configured 17G epidural catheter to a 1 mL syringe.
  - 3.4. Aspirate 1 cm of BM into the catheter, followed by a small air bubble.
  - 3.5. Aspirate 5-7 embryos in a volume of 10 µL of BM, followed by another small air bubble.
  - 3.6. Finish loading the catheter by aspirating 1 cm of BM.
4. Embryo transfer
- 4.1. Consider the use of sterile gloves, gown and mask to ensure an aseptic environment.
  - 4.2. Sterilise surgical instruments, clean the surfaces where surgery will be performed, and wipe them with 70° ethanol.
  - 4.3. Perform anaesthesia as previously detailed, checking for loss of reflexes.
  - 4.4. Shave the fur from the ventral abdomen with an electric razor.



- 4.5. Prepare the ventral abdomen aseptically. Clean the surgical area and remove any remaining hair. Wash the surgical area with a chlorhexidine gluconate soap. Sanitise the area with chlorhexidine solution and ethanol 96<sup>o</sup> (3 times).
- 4.6. Place the animal on a warm surgical table, in Trendelenburg's position (head down at 45°) to ensure that the stomach and intestines are cranially located. Consider the evacuation of the bladder if it is turgid. If any viscera are damaged in the process, the animal may die. It is therefore important to have them properly located (Figure 3.1).
- 4.7. Cover the area using a sterile towel, with a hole (fenestration) exposing the shaved area, to separate the surgical site from any potential contaminating areas.
- 4.8. Insert one endoscopic trocar 5 cm into the abdominal cavity, 2 cm caudal to the xiphoid process, and insufflate through it the peritoneal cavity with a pressure-regulating mechanical insufflator. Note: The intra-abdominal pressure should be 8-12 mmHg with CO<sub>2</sub> (Figure 3.1A).
- 4.9. Insert the endoscope camera through the endoscopic trocar (Figure 3.1B). Note: Identify the reproductive tract, determining the status and position of the infundibulum and ampulla before ET to facilitate the next steps.
- 4.10. Insert the 17G epidural needle into the inguinal region between 2-3 cm from the infundibulum (Figure 3.1B).
- 4.11. Identify the entrance of the infundibulum (Figure 3.2A,B).
- 4.12. Insert the loaded catheter (step 3.6) through the epidural needle into the abdomen (Figure 3.1C).
- 4.13. Locate the oviduct and insert 1-2 cm of the epidural catheter through the infundibulum in the ampulla (Figure 3.2A-C). Do not progress very far into the oviduct to prevent damage and haemorrhage.
- 4.14. Release the embryos into the oviduct by gently pressing the plunger of the syringe coupled to the catheter (Figure 3.2D-F). Both air bubbles must exit the catheter.
- 4.15. Remove the catheter just after the embryos have been released.
- 4.16. Rinse the catheter, aspirating and releasing manipulating medium to check the absence of the embryos and confirm their successful transfer.
- 4.17. Repeat steps 4.11 to 4.16 in the other side of the uterus, if desired.
- 4.18. Remove the epidural needle and endoscope camera.
- 4.19. Release CO<sub>2</sub> through the endoscopic trocar. If excess gas remains in the abdomen of the animal, it will have pain and discomfort.
- 4.20. Remove the endoscopic trocar from the abdominal cavity. Remove the surgical towel.
- 4.21. Discontinue anaesthesia.
- 4.22. Clean the incision made by the trocar with chlorhexidine solution. Close the incision made by the trocar with a micronised aluminium and a plastic dressing.

## 5. Postoperative care

- 5.1. Treat the animals with antibiotics: 10 mg/kg of enrofloxacin, subcutaneously, every 24 h for 5 days.
- 5.2. Administer analgesics: buprenorphine hydrochloride (0.03 mg/kg), intramuscularly, each 12 h for 3 days; Meloxicam (0.2 mg/kg), subcutaneously, every 24 h for 3 days.
- 5.3. Monitor the animals for at least 30 min after surgery (depending on the animal and the dose of anaesthesia used) making sure they recover their physiological conditions.
- 5.4. Identify the recipient (e.g. ear tattoo) and house animals individually in a clean cage with the appropriate environmental condition.

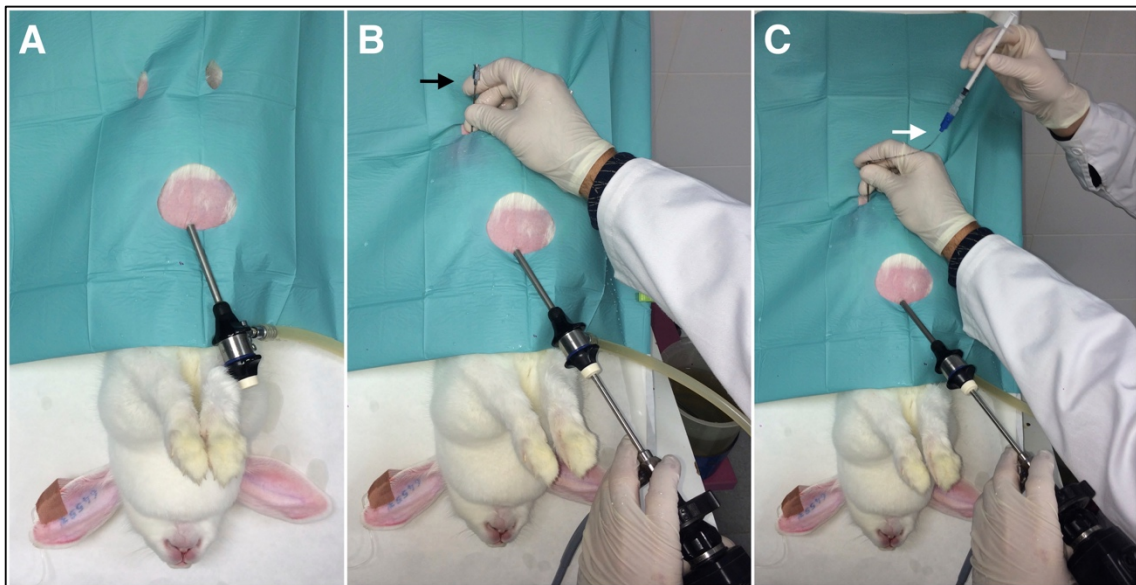


**Figure 3.1.** Laparoscopic embryo transfer assisted by laparoscopy (External view). [A] Insertion of the endoscopic trocar (one port). [B] Insertion of the endoscopic camera and the epidural needle (black arrow). [C] Insertion of the embryo transfer catheter (white arrow) through the epidural needle.

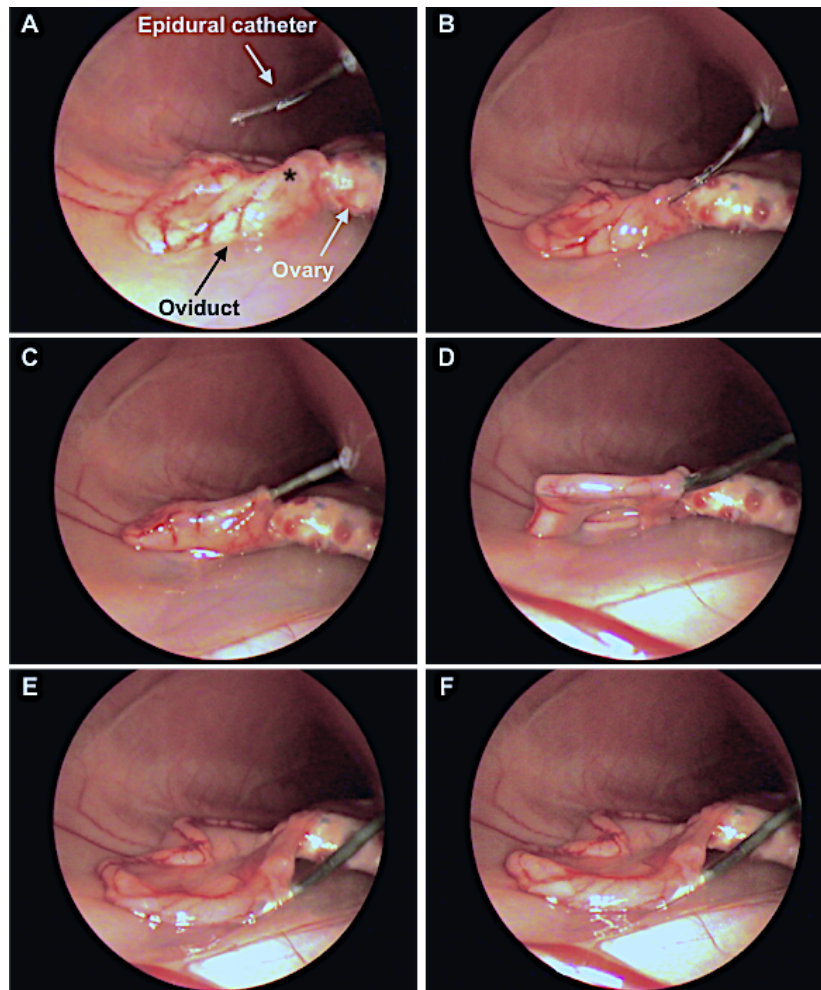


**Figure 3.2.** Laparoscopic embryo transfer assisted by laparoscopy (Internal view). [A] Insertion of the catheter through the epidural needle into the abdominal zone. Asterisk indicates the infundibulum. [B,C,D] The catheter loaded with the embryos is inserted into ampulla region across the infundibulum. [E,F] Release of the embryos, confirmed by the visualisation of a swollen oviduct. This figure has been adapted from Marco-Jiménez *et al.* [38].

### 3.2.2. Embryo vitrification and warming

1. Perform all the manipulations at room temperature (around 22 °C) to reduce the vitrification solution toxicity at warmer temperatures. Note: Embryos can be moved using 0.1-2  $\mu\text{L}$  automatic pipette in this protocol, but other similar devices to move the embryos dragging the minimum volume can be suitable.
2. Vitrify the embryos in a two-step addition procedure:
  - 2.1. Place the embryos for 2 minutes in equilibrating solution consisting of 10% (v/v) ethylene glycol and 10% (v/v) dimethyl sulfoxide dissolved in BM.

- 2.2. Move the embryos (from step 2.1) for 1 minute into vitrification solution consisting of 20% (v/v) ethylene glycol and 20% (v/v) dimethyl sulfoxide dissolved in BM.
3. Load the embryos into a 125  $\mu$ L plastic ministraw (which contains one closed end with a cotton plug and one open extreme). The process is schematised in Figure 3.3.
  - 3.1. Couple the closed end of 125  $\mu$ L ministraw with the appropriate microdispenser (e.g. Captroll III<sup>®</sup>).
  - 3.2. Aspirate BM until 1/3 of the straw length, following by a small air bubble.
  - 3.3. Aspirate the embryos in a volume of 40  $\mu$ L of vitrification solution, followed by another small air bubble.
  - 3.4. Aspirate BM until the first liquid fraction (step 3.2) reaches the cotton.
  - 3.5. Close the open end with a straw plug.
4. Perform step 2.2 while step 3 is being done to ensure that no more than one-minute elapses, which would be toxic to embryos.
5. Plunge the ministraw directly into liquid nitrogen to achieve vitrification.
6. Store the ministraw in a dewar for liquid nitrogen for the desired time.
7. Thaw the embryos in a single step.
  - 7.1. Place the ministraw horizontally 10 cm from liquid nitrogen vapour for 20-30 s.
  - 7.2. When the crystallisation process begins inside the ministraw, immerse the ministraw in a water bath at 25 °C for 10-15 s.
  - 7.3. Remove the ministraw plug and cut the cotton plug.
  - 7.4. With a coupled microdispenser, expel all the ministraw content into a plate containing 0.33 M sucrose solution at 25 °C in BM for 5 minutes. Note: This step must be done quickly in order to reduce embryo exposure to the vitrification solution.
  - 7.5. Move the embryos to a new plate containing BM solution for another 5 min.
  - 7.6. Consider only non-damaged embryos (with intact mucin coat and zona pellucida) to continue with the ET. Note: Take into account that in vitrified-warmed embryos, asynchronous transfers (e.g. 60-62 h in morula transfers) may improve the results by allowing a resynchronisation between the embryo and the maternal endometrium.

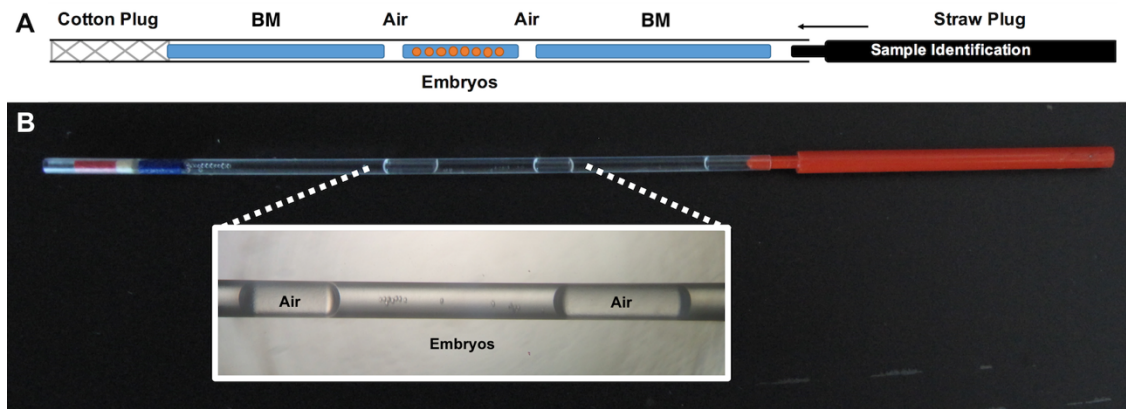


**Figure 3.3.** Schematization of correctly loaded straw. [A] BM refers to the embryo manipulating media employed during vitrification. Embryos must be loaded in vitrification solution. [B] Macroscopic appearance of the loaded straw with a magnified detail of the embryo position. This large- volume device allows us to vitrify large number of embryos, unlike minimum volume devices. Furthermore, the handling of this device is easier compared with minimum volume devices, while the results are similar in rabbits [41].

### 3.3. REPRESENTATIVE RESULTS

Minimally invasive laparoscopic transfer of fresh or vitrified embryos places the rabbit among the best model animals for reproductive studies. Table 3.1 shows the results of fresh ET at different developmental stages (Figure 3.4) of transferred embryos. The survival rate at birth (percentage of embryos resulting in a pup) proved the efficacy of the laparoscopic technique described in this paper. The higher values were achieved when the ET was performed with embryos in the morula stage, either early or compact morulae. Based on these results, we performed a second experiment to demonstrate the survival rate after vitrification of these embryos. Thus, in Table 3.2 we show the results obtained after transferring vitrified rabbit morulae recovered at the same time, differentiating between those embryos that had reached a good degree of compaction or not. The survival rate at birth was different between the different embryo stages, being higher in compacted morulae. Therefore, laparoscopic embryo transfer is a reliable technique to transfer fresh and vitrified embryos in rabbits.



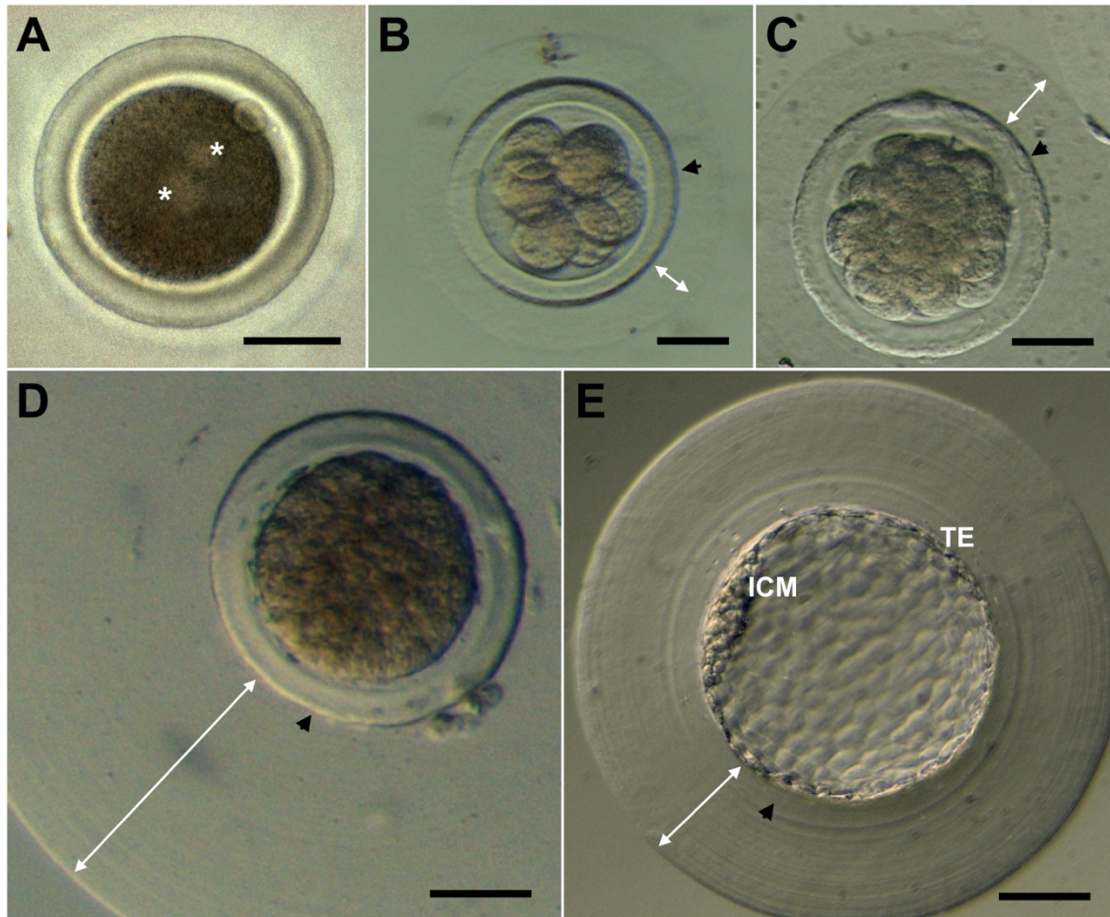


**Figure 3.4.** Rabbit embryos. [A] Pronuclear. [B] Eight cells. [C] Early morula. [D] Compact morula. [E] Blastocyst. Asterisk indicates the two pronuclei. Black arrows indicate the zona pellucida. White arrows indicate the mucin coat, which normally varies between embryos. ICM: Inner Cell Mass. TE: Trophectoderm. Scale bar: 50  $\mu$ m.

**Table 3.1.** Efficiency of fresh rabbit embryo transfer (*in vivo* derived) by laparoscopy.

Developmental stage <sup>1</sup>	Embryos	Recipients	Place of transfer	Pregnancy rate (%)	Implantation rate (%)	Survival rate at birth (%) <sup>2</sup>
Pronuclear	78	7	Oviduct	7 (100)	50 (64.0) <sup>b</sup>	34 (43.6) <sup>b</sup>
Eight cells	81	7	Oviduct	7 (100)	60 (74.1) <sup>b</sup>	53 (65.4) <sup>a</sup>
Early morula	81	7	Oviduct	7 (100)	80 (98.8) <sup>a</sup>	60 (74.1) <sup>a</sup>
Compact morula	80	7	Oviduct	7 (100)	80 (100) <sup>a</sup>	58 (72.5) <sup>a</sup>
Blastocyst	80	7	Uterus	7 (100)	73 (91.3) <sup>a</sup>	38 (47.5) <sup>b</sup>

<sup>1</sup>Different embryos were recovered at 18-20h (pronuclear), 36-38h (8 cells), 60-62 h (early morula), 70-72 h (compact morula) and 80-82 h (blastocyst) after mating. Compact (>32 cells) and non-compact morulae (≈32 cells) can be found at 70-72 h, but only compact morulae were transferred. <sup>2</sup>Survival rate at birth from recipient pregnant does. <sup>a,b</sup> Values with different superscripts in the same column are statistically different (p<0.001).

**Table 3.2.** Viability of non-compact vs compact vitrified morula.

Developmental stage	Transferred embryos	Recipients	Pregnancy rate (%)	Survival rate at birth (%) <sup>1</sup>
Non-compact	135	10	9 (90)	62 (45.9) <sup>b</sup>
Compacted	150	10	10 (100.0)	98 (65.3) <sup>a</sup>
<b>TOTAL</b>	<b>285</b>	<b>20</b>	<b>19 (95)</b>	<b>160 (56.1)</b>

<sup>1</sup>Survival rate at birth from recipient pregnant does. Embryos were recovered at the same time (70-72 h) and were distinguished into compact (>32 cells) and non-compact morulae (≈32 cells), being transferred into asynchronous foster mothers. <sup>a,b</sup> Values with different superscripts are statistically different (p<0.001).

### 3.4. DISCUSSION

Since the first documented live birth case from transferred embryos [9], this technique and the rabbit species have become crucial in reproductive studies. Besides, embryo research studies involving gamete or embryo manipulation, production, cryopreservation, etc. require as a last step the evaluation of embryo capacity to generate healthy full-term offspring. Therefore, embryo transfer technique is indispensable [13,28]. Over the years, the surgical methods initially employed to transfer embryos into the maternal uterus have gradually been replaced by less invasive methods in the vast majority of species [13-15,21,27,29,30]. However, in rabbits, intraoviductal ET in early embryo stages or *in vitro* produced embryos becomes unavoidable to ensure a similar result to natural conditions. In rabbits, intraoviductal mucin coat is a crucial factor allowing embryo implantation, as it takes place after the remodelling of the embryonic coatings during blastocyst expansion in the uterine horns. However, mucin coat deposition is limited to the oviduct for 3 days following ovulation, and the molecular mechanisms of coat material deposition are largely unknown [31]. For these reasons, it is known that *in vitro*-developed blastocysts did not survive when transferred to the uterus [32-34], and embryos with a damaged mucin coat have a lower survival rate [35]. Likewise, groups that reported a transcervical embryo transfer in rabbits resulted in very low liveborn rates [11,26]. Here, we present a minimally invasive technique, adapted from Besenfelder and Brem [18], to transfer embryos with successful birth rates. According to the results in Table 3.1, the morula stage in rabbit embryos was the best embryonic stage to achieve a high survival rate at birth. One possible explanation is the greater sensitivity to manipulation of the earliest stages. Interestingly, the success rate increases as the embryonic stage progresses, possibly due to the greater exposure of the embryo to oviductal secretions prior to its recovery. But when embryos reach the blastocyst stage and are place-concordant transferred to the uterus, the values decrease drastically. Not excluding what has been said, a possible explanation could be that the embryos transferred into the oviduct can restore the possible damage generated in the mucin layer during embryo manipulation. Therefore, blastocysts transferred into the uterus would be deprived of this mechanism, which could compromise their implantation capacity.

The technique is performed using a single-port instrument (5 mm endoscope trocar), with slight, brief manipulation. Therefore, the 5-mm endoscope trocar incision does not require suture. Laparoscopic technique benefits include decreased postoperative pain, quicker return to normal activity, and fewer postoperative complications. In addition, endoscopic procedures induce fewer abdominal adhesions and allow a better immune response by the recipient compared with open surgery [21,36,37]. Accumulating evidence from our lab has demonstrated the effectiveness of this ET procedure in the rabbit model. Thus, in the last five years a total of 3,909 embryos (1,335 fresh and 2,574



vitrified embryos) were transferred through the procedure described in the present manuscript. As a result of this technique, the offspring rates of fresh and vitrified transfer embryos were 62.9% and 42.5%, respectively [38-47]. Many studies are all based on this technique: Marco-Jiménez *et al.* [38-41], Vicente *et al.* [42], Viudes-de-Castro *et al.* [43], Saenz-de-Juano *et al.* [44,45,47], Lavara *et al.* [46].

Practical recommendations for carrying out this technique are described below. In embryo culture experiments, it is also advisable to use a new catheter for embryo transfer instead of the one used to move the embryos between the culture media and manipulation media. This avoids transfer of mineral oil and ensures an optimal flow. During ET it is important to minimise handling of the reproductive tract, as excessive manipulation of the oviduct could result in adhesions. If the oviduct is twisted, employ the epidural syringe to try to position it correctly, not the catheter, as it contains the embryos and the mechanical manipulation could cause their loss. Once the catheter passes through the oviduct, it slides easily. If it does not, the catheter may have deviated. Once inside the oviduct, if the media does not flow, move the catheter out slightly and try to reinsert it again. If it still does not flow, the catheter is clogged. Remove it from the oviduct and release the content into a dish with a clean medium. Then, reload the embryos into another catheter and try to reinsert it into the oviduct again. Delivery usually takes places 28-30 days after morula transfer.

In addition, there is evidence indicating that the embryo developmental stage can be more advanced than the uterine environment in pseudopregnant females, but not the opposite. Specifically, embryos have the ability to wait for the favourable womb environment, but the womb environment cannot wait for the embryos at the right stage for implantation [10]. With regard to vitrified embryos, after a short/long-term storage it is possible to synchronise the developmental stage of the embryo with the corresponding favourable womb environment. Furthermore, if the embryo donor is also the embryo recipient, the detrimental effects of superovulation on the endometrium can be bypassed by using the vitrification technique and transferring the embryos in a subsequent cycle [48]. In rabbits, vitrified embryos transferred into oviducts of recipients induced to ovulate 60-62 h beforehand (asynchrony) is a highly efficient technique [44,49]. Related with this, it has been suggested that the oviductal embryo transition during 10-12 h could explain the beneficial effects in the restoration of cell physiology and replacement of dead cells, and probably repair the damage induced in mucin coat during embryo manipulation. Besides, vitrified embryos present a delay in development, as they have been metabolically suspended during the storage. Therefore, transfer of cryopreserved embryos into asynchronous recipients allows the embryo to reactivate its metabolic activity and thus the embryo stage of development is synchronised with the womb environment. Instead, if cryopreserved embryos are transferred into synchronic receptors, the unmatched crosstalk between the mother

and the embryo hinders the onset of a successful pregnancy. In rabbit, the highest survival rate has been obtained after intraoviductal transfer of cryopreserved morulae [49]. Our data are consistent with this report, although the morula stage exhibits different survival rates following cryopreservation depending on their degree of compaction at 70-72 h (Table 3.2). Here, compacted morulae showed higher survival rates at birth in comparison to non-compacted morulae, which was in concordance with previous reports showing that every stage of development had its own mechanism relative to the permeation of cryoprotectants and the extent of dehydration during the addition of the cryopreservation solution [50]. Underlying these techniques, we have demonstrated that a combination of vitrification and intraoviductal embryo transfer is a successful strategy to re-establish rabbit populations after 15 years of storage in liquid nitrogen, without adverse effect on their post-thaw survival and live birth [51].

The following details should be taken into account to successfully perform this technique. It is important to bear in mind that the increasing density of the consecutive mediums used for vitrification (DPBS, equilibration solution, vitrification solution) could induce embryo contraction due to progressive embryo dehydration. However, its normal appearance is recovered when the embryo is equilibrated with the medium. Furthermore, when the embryo is moved between increasing density media, it tends to move to the surface of the media due to density movements. To avoid embryo loss and ensure the time of vitrification, it is recommendable to perform the vitrification in small drops of the media that will keep the embryo in place.

### **3.5. CONCLUSION**

In conclusion, here we describe both an ET technique and an embryo vitrification method that facilitate future studies which use rabbits as a model. Based on the close phylogenetic distance between rabbits and humans, the use of this model could provide results easily transferable to human clinical medicine. In addition, our method offers some hygienic and economic advantages, conforming to the concept of the 3 Rs of animal welfare (replacement, reduction and refinement), while maintaining the goal of improving humane treatment of experimental animals.

### **3.6. REFERENCES**

- [1]. Chen M, Heilbronn LK. The health outcomes of human offspring conceived by assisted reproductive technologies (ART). *J Dev Orig Health Dis.* 2017;8:388-402.
- [2]. Lavara R, Baselga M, Marco-Jiménez F, Vicente JS. Embryo vitrification in rabbits: Consequences for progeny growth. *Theriogenology.* 2015;84:674-80.

- [3]. Sirard MA. The influence of in vitro fertilization and embryo culture on the embryo epigenetic constituents and the possible consequences in the bovine model. *J Dev Orig Health Dis.* 2017;8:411–417.
- [4]. Feuer SK, Rinaudo PF. Physiological, metabolic and transcriptional postnatal phenotypes of in vitro fertilization (IVF) in the mouse. *J Dev Orig Health Dis.* 2017;8:403-410.
- [5]. Jiang Z, Wang Y, Lin J, Xu J, Ding G, Huang H. Genetic and epigenetic risks of assisted reproduction. *Best Pract Res Clin Obstet Gynaecol.* 2017;44:90-104.
- [6]. Fleming TP, Velazquez MA, Eckert JJ. Embryos, DOHaD and David Barker. *J Dev Orig Health Dis.* 2015;6:377-83.
- [7]. Sparks AE. Human embryo cryopreservation-methods, timing, and other considerations for optimizing an embryo cryopreservation program. *Semin Reprod Med.* 2015;33:128-44.
- [8]. Swain JE. Optimal human embryo culture. *Semin Reprod Med.* 2015;33:103-117.
- [9]. Heape W. Preliminary note on the transplantation and growth of mammalian ova within a uterine foster-mother. *Proc. R. Soc. Lond.* 1890;48:457-458.
- [10]. Bermejo-Alvarez P, Park KE, Telugu BP. Utero-tubal embryo transfer and vasectomy in the mouse model. *J Vis Exp.* 2014;84:e51214.
- [11]. Kidder JD, Roberts PJ, Simkin ME, Foote RH, Richmond ME. Nonsurgical collection and nonsurgical transfer of preimplantation embryos in the domestic rabbit (*Oryctolagus cuniculus*) and domestic ferret (*Mustela putorius furo*). *J Reprod Fertil.* 1999;116:235-242.
- [12]. Tiras B, Cenksoy PO. Practice of embryo transfer: recommendations during and after. *Semin Reprod Med.* 2014;32:291–296.
- [13]. Cui L, Zhang Z, Sun F, Duan X, Wang M, Di K, et al. Transcervical embryo transfer in mice. *J Am Assoc Lab Anim Sci.* 2014;53:228-31.
- [14]. Moreno-Moya JM, Ramírez L, Vilella F, Martínez S, Quiñonero A, Noguera I, et al. Complete method to obtain, culture, and transfer mouse blastocysts nonsurgically to study implantation and development. *Fertil Steril.* 2014;101:e13.
- [15]. Hasler JF. Forty years of embryo transfer in cattle: a review focusing on the journal *Theriogenology*, the growth of the industry in North America, and personal reminiscences. *Theriogenology.* 2014;81:152–169.
- [16]. Bauer C. The baboon (*Papio* sp.) as a model for female reproduction studies. *Contraception.* 2015;92:120–123.
- [17]. Martinez EA, Martinez CA, Nohalez A, Sanchez-Osorio J, Vazquez JM, Roca J, et al. Nonsurgical deep uterine transfer of vitrified, in vivo-derived, porcine embryos is as effective as the default surgical approach. *Sci Rep.* 2015;5:10587.
- [18]. Besenfelder U, Brem G. Laparoscopic embryo transfer in rabbits. *J Reprod Fertil.* 1993;99:53–56.

- [19]. Besenfelder U, Mödl J, Müller M, Brem G. Endoscopic embryo collection and embryo transfer into the oviduct and the uterus of pigs. *Theriogenology*. 1997;47:1051–1060.
- [20]. Besenfelder U, Havlicek V, Kuzmany A, Brem G. Endoscopic approaches to manage in vitro and in vivo embryo development: use of the bovine oviduct. *Theriogenology*. 2010;73:768–776.
- [21]. Fonseca JF, Souza-Fabjan JM, Oliveira ME, Leite CR, Nascimento-Penido PM, Brandão FZ, et al. Nonsurgical embryo recovery and transfer in sheep and goats. *Theriogenology*. 2016;86:144-51.
- [22]. Denker HW. Structural dynamics and function of early embryonic coats. *Cells Tissues Organs*. 2000;166:180–207.
- [23]. Marco-Jiménez F, López-Bejar M. Detection of glycosylated proteins in rabbit oviductal isthmus and uterine endometrium during early embryo development. *Reprod Domest Anim*. 2013;48:967–973.
- [24]. Ménézo YJ, Hérubel F. Mouse and bovine models for human IVF. *Reprod Biomed Online*. 2002;4:170–175.
- [25]. Fischer B, Chavatte-Palmer P, Viebahn C, Navarrete Santos A, Duranthon V. Rabbit as a reproductive model for human health. *Reproduction*. 2012;144:1–10.
- [26]. Besenfelder U, Strouhal C, Brem G. A method for endoscopic embryo collection and transfer in the rabbit. *Zentralbl Veterinarmed A*. 1998;45:577–579.
- [27]. Daniel N, Renard JP. Embryo transfer in rabbits. *Cold Spring Harb Protoc*. 2010;2010:pdb.prot5357.
- [28]. Saenz-de-Juano MD, Marco-Jimenez F, Schmaltz-Panneau B, Jimenez-Trigos E, Viudes-de-Castro MP, et al. Vitrification alters rabbit foetal placenta at transcriptomic and proteomic level. *Reproduction*. 2014;147:789-801.
- [29]. Green M, Bass S, Spear B. A device for the simple and rapid transcervical transfer of mouse embryos eliminates the need for surgery and potential post-operative complications. *Biotechniques*. 2009;47:919–924.
- [30]. Duan X, Li Y, Di K, Huang Y, Li X. A nonsurgical embryo transfer technique in mice. 2016;32:440–446.
- [31]. Denker HW, Gerdes HJ. The dynamic structure of rabbit blastocyst coverings. I. Transformation during regular preimplantation development. *Anat Embryol (Berl)*. 1979;157:15–34.
- [32]. Seidel GE, Bowen RA, Kane MT. In vitro fertilization, culture, and transfer of rabbit ova. *Fertil Steril*. 1976;27:861–870.
- [33]. Binkerd, P.E., Anderson, J.B. Transfer of cultured rabbit embryos. *Gamete Res*. 1979;2:65
- [34]. Murakami H, Imai H. Successful implantation of in vitro cultured rabbit embryos after uterine transfer: a role for mucin. *Mol Reprod Dev*. 1996;43:167–170.

- [35]. Techakumphu, M., Wintenberger-Torrès, S., Sevellec, C., Ménéz, Y. Survival of rabbit embryos after culture or culture/freezing. *Anim. Reprod. Sci.* 1987;13:221-228.
- [36]. Gitzelmann CA, Mendoza-Sagaon M, Talamini MA, Ahmad SA, Pegoli W Jr, Paidas CN. Cell-mediated immune response is better preserved by laparoscopy than laparotomy. *Surgery.* 2000;127:65-71.
- [37]. Huang SG, Li YP, Zhang Q, Redmond HP, Wang JH, Wang J. Laparotomy and laparoscopy diversely affect macrophage-associated antimicrobial activity in a murine model. *BMC Immunol.* 2013;14:27.
- [38]. Marco-Jiménez F, Jiménez-Trigos E, Almela-Miralles V, Vicente JS. Development of Cheaper Embryo Vitrification Device Using the Minimum Volume Method. *PLoS One.* 2016;11:e0148661.
- [39]. Marco-Jimenez F, Jimenez-Trigos E, Lavara R, Vicente JS. Generation of live offspring from vitrified embryos with synthetic polymers SuperCool X-1000 and SuperCool Z-1000. *Cryo Letters.* 2014;35:286–292.
- [40]. Marco-Jimenez F, Jimenez-Trigos E, Lavara R, Vicente JS. Use of cyclodextrins to increase cytoplasmic cholesterol in rabbit embryos and their impact on live kits derived from vitrified embryos. *Cryo Letters.* 2014;35:320–326.
- [41]. Marco-Jiménez F, Lavara R, Jiménez-Trigos E, Vicente JS. In vivo development of vitrified rabbit embryos: effects of vitrification device, recipient genotype, and asynchrony. *Theriogenology.* 2013;79:1124–1129.
- [42]. Vicente JS, Saenz-de-Juano MD, Jiménez-Trigos E, Viudes-de-Castro MP, Peñaranda DS, Marco-Jiménez F. Rabbit morula vitrification reduces early foetal growth and increases losses throughout gestation. *Cryobiology.* 2013;67:321–326.
- [43]. Viudes-de-Castro MP, Marco-Jiménez F, Cedano-Castro JI, Vicente JS. Effect of corifollitropin alfa supplemented with or without LH on ovarian stimulation and embryo viability in rabbit. *Theriogenology.* 2017;98:68–74.
- [44]. Saenz-de-Juano MD, Marco-Jimenez F, Schmaltz-Panneau B, Jimenez-Trigos E, Viudes-de-Castro MP, et al. Vitrification alters rabbit foetal placenta at transcriptomic and proteomic level. *Reproduction.* 2014;147:789-801.
- [45]. Saenz-de-Juano MD, Marco-Jimenez F, Viudes-de-Castro MP, Lavara R, Vicente JS. Direct comparison of the effects of slow freezing and vitrification on late blastocyst gene expression, development, implantation and offspring of rabbit morulae. *Reprod Domest Anim.* 2014;49:505–511.
- [46]. Lavara R, Baselga M, Marco-Jiménez F, Vicente JS. Long-term and transgenerational effects of cryopreservation on rabbit embryos. *Theriogenology.* 2014;81:988-92.
- [47]. Saenz-de-Juano MD, Marco-Jiménez F, Vicente JS. Embryo transfer manipulation cause gene expression variation in blastocysts that disrupt implantation and offspring rates at birth in rabbit. *Eur J Obstet Gynecol Reprod Biol.* 2016;207:50–55.

- [48]. Roque M, Valle M, Kostolias A, Sampaio M, Geber S. Freeze-all cycle in reproductive medicine: current perspectives. *JBRA Assist Reprod.* 2017;21:49–53.
- [49]. Tsunoda Y, Soma T, Sugie T. Effect of post-ovulatory age of recipient on survival of frozen-thawed rabbit morulae. *J Reprod Fertil.* 1982;65:483–487.
- [50]. Vanderzwalmen P, Bertin G, Debauche Ch, Standaert V, van Roosendaal E, Vandervorst M, et al. Births after vitrification at morula and blastocyst stages: effect of artificial reduction of the blastocoelic cavity before vitrification. *Hum Reprod.* 2002;17:744-51.
- [51]. Lavara R, Baselga M, Vicente JS. Does storage time in LN2 influence survival and pregnancy outcome of vitrified rabbit embryos? *Theriogenology.* 2011;76:652–7.

### **ACKNOWLEDGEMENTS**

This work was supported by funds from the Ministry of Economy and Competitiveness of Spain (AGL2017-85162-C2-1-R) and Generalitat Valenciana Research Programme (PrometeoII 2014/036). Ximo Garcia-Dominguez was supported by a research grant from the Ministry of Economy and Competitiveness (BES-2015-072429). The authors would like to thank Neil Macowan Language Services for revising the English version of the manuscript.

## CHAPTER II

# **DEVELOPMENTAL PLASTICITY IN RESPONSE TO EMBRYO CRYOPRESERVATION: THE IMPORTANCE OF THE VITRIFICATION DEVICE IN RABBITS**

X. Garcia-Dominguez, J.S. Vicente, F. Marco-Jiménez

Institute for Animal Science and Technology (ICTA), Laboratory of Reproductive Biotechnology,  
Universitat Politècnica de València, 46022 Valencia, Spain

*Animals*, 2020; 10: 804





### ABSTRACT

Assisted reproductive technologies affect natural development patterns with perinatal and postnatal consequences. In this study, we evaluated the effect of embryo vitrification using two different devices on adulthood phenotype in rabbits. *In vitro* development, prenatal embryo survival, body weight, growth performance, haematological and biochemical peripheral blood analysis, reproductive performance, and lactation performance traits were compared between the experimental groups. They derived from naturally-conceived embryos (NC), fresh-transferred embryos (FT), vitrified-transferred embryos using mini-straw (VTs), or vitrified-transferred embryos using cryotop (VTc). Straw-vitrified embryos exhibited lower *in vitro* developmental rates and *in vivo* survival rates following embryo transfer compared to its cryotop-vitrified counterparts. Moreover, the VTs group exhibited higher foetal losses than VTc, FT, and NC groups. Independently of the vitrification device, vitrified-transferred (VT) offspring showed a skewed sex ratio in favour of males, and an increased birth bodyweight. In contrast, postnatal daily growth was diminished in all ART (i.e., FT and VT) animals. In adulthood, significant differences in body weight between all groups was founded—all ART progenies weighed less than NC animals and, within ART, VT animals weighed less than FT. For VT groups, weight at adulthood was higher for the VTs group compared with the VTc group. Peripheral blood parameters ranged between common values. Moreover, no differences were found in the fertility rates between experimental groups. Furthermore, similar pregnancy rates, litter sizes, and the number of liveborns were observed, regardless of the experimental group. However, decreased milk yield occurred for VTc and FT animals compared to VTs and NC animals. A similar trend was observed for the milk composition of dry matter and fat. Concordantly, reduced body weight was found for suckling kits in the VTc and FT groups compared to VTs and NC animals. Our findings reveal that developmental changes after the embryo vitrification procedure could be associated with an exhibition of the embryonic developmental plasticity. Moreover, to our best knowledge, this study reports the first evidence demonstrating that the vitrification device used is not a trivial decision, providing valuable information about how the cooling–warming rates during vitrification can be partly responsible of the postnatal phenotypic variations.



## 4.1. INTRODUCTION

Despite advances in assisted reproductive technologies (ART), *in vitro* conditions fail to mimic the optimal physiological dynamism within the reproductive tract [1,2]. In this sense, embryonic plasticity allows embryos to develop responses to ensure their short-term survival in sub-optimal environments [3], which could increase the risk of developmental deviations and disease later in life [4]. Therefore, although ART progenies seem healthy, there is increasing awareness of potential long-term consequences of ART, raising the importance of discerning whether ART leaves a subtle legacy in ART offspring [5].

In humans, it is difficult to determine associations between treatment and outcome, as lifestyle or demographic and clinical factors such as patient infertility can act as potential confounders that bias results [6,7]. Thus, controversially, ART has been linked with adverse obstetric and perinatal outcomes, as well as increased risk of congenital disabilities, cancers, and growth and development disorders [7]. Furthermore, emerging evidence suggests that ART may also predispose individuals to an increased risk of chronic ageing-related diseases such as obesity, type 2 diabetes, and cardiovascular disease. However, recently, the largest studies assessing ART consequences found no alarming evidence in the long-term health outcomes of adults [8,9]. Using fertile and healthy animal models, confounding factors were avoided, thus providing adequate experimental groups to reveal the effects of ART *per se*. Hence, these studies demonstrated both individual and cumulative effects of each ART procedure on foetal and postnatal phenotypes [10–12].

According to the last report from the European Society of Human Reproduction and Embryology (ESHRE), the steepest increase in treatment numbers was observed in cryopreserved embryo transfer (+13.6%), placing this technique as the second most commonly used in fertility treatments [13]. Unlike most ART trying to mimic the physiological conditions, cryopreservation requires embryo exposure to non-physiologic low temperatures and toxic cryoprotectant solutions to avoid ice-induced injuries [14]. In this context, progenies born after embryo cryopreservation could have an increased risk for many worrisome diseases in comparison to other ARTs [15,16]. In recent years, many laboratories worldwide have completely replaced slow freezing by vitrification because of its improved cryosurvival outcomes [17]. The breakthrough in the field of vitrification came when sample volume was reduced to a level that permitted lowering of the cryoprotectant concentration by maximising cooling and warming rates [18,19]. For this purpose, numerous devices have been described in the literature that minimise the volume of the vitrification solution to allow better heat transfer [18,19]. However, despite all of this effort to reduce embryo damage and increase their survival, consistent long-term follow-up data on the resultant offspring are non-existent. Here, we

developed an experimental model approach to evaluate the effects of the embryo cryopreservation procedure, including two clinical vitrification devices, in relation to adulthood phenotype in rabbits.

## 4.2. MATERIALS AND METHODS

All chemicals, unless otherwise stated, were reagent-grade and purchased from Sigma-Aldrich Química S.A. (Alcobendas, Madrid, Spain).

### 4.2.1. Animals and ethical statements

New Zealand rabbits belonging to the Universitat Politècnica de València were used throughout the experiment. The animal study protocol was reviewed and approved by the “Universitat Politècnica de València” Committee prior to initiation of the study (code: 2015/VSC/PEA/00061). All experiments were performed in accordance with relevant guidelines and regulations set forth by Directive 2010/63/EU EEC. Animal experiments were conducted at the accredited animal care facility (code: ES462500001091). An authorisation certificate issued by the Valencian governmental administration to experiment on animals is held by XGD (code: 2815), FMJ (code: 2273) and JSV (code: 0690).

### 4.2.2. Experimental design

Figure 4.1 illustrates the experimental design conceived to elucidate the accumulative effects of the successive ART used in the embryo cryopreservation–transfer procedure. Accordingly, using a naturally conceived (NC) population as control group, offspring derived from fresh-transferred (FT) embryos were compared to those derived from vitrified-transferred (VT) embryos. Furthermore, VT progeny were obtained using two common clinical vitrification devices, ministraw (VTs) and cryotop (VTc), to evaluate the influences of the cooling–warming rates provided by large vitrification volumes versus the minimum volume strategy. With this aim, a total of 22 donor females were superovulated using 3 µg of corifollitropin alpha in four sessions (4–6 females per session). After 3 days, females were inseminated with semen of unrelated males with proved fertility and induced to ovulate with an intramuscular injection of 1 µg of buserelin acetate (Hoechst Marion Roussel, Madrid, Spain). Three days post-insemination, a total of 598 embryos catalogued as normal (presenting homogenous cellular mass, mucin coat, and spherical zona pellucida) were recovered *post mortem*. All embryos were pooled for later distribution in the different parts of the study, thus

reducing the effect of embryo donors. Of the total, 226 and 214 embryos were subjected to vitrification/warming processes using ministraw and cryotop as devices, respectively. After warming, only undamaged embryos (presenting homogenous cellular mass, mucin coat, and spherical zona pellucida) were kept, noting 221 (97.8% survival rate) and 211 (98.6% survival rate) embryos vitrified in ministraw and cryotop, respectively. Then, to test the effect of each device on the embryo developmental potential, 134 ministraw-vitrified and 110 cryotop-vitrified embryos were cultured *in vitro* for 48 h, evaluating their capability to reach the hatching/hatched blastocyst stage. Sixty-two fresh embryos were used as control. Of the remaining embryos, 87 ministraw-vitrified, 101 cryotop-vitrified, and 96 fresh embryos were transferred into foster mothers (14–16 per foster mother). At birth, progenies constituted VTs, VTc, and FT groups, respectively. In addition, the NC population was established from six females inseminated the same day as the previous ones, allowing them to give birth without any ART manipulation.

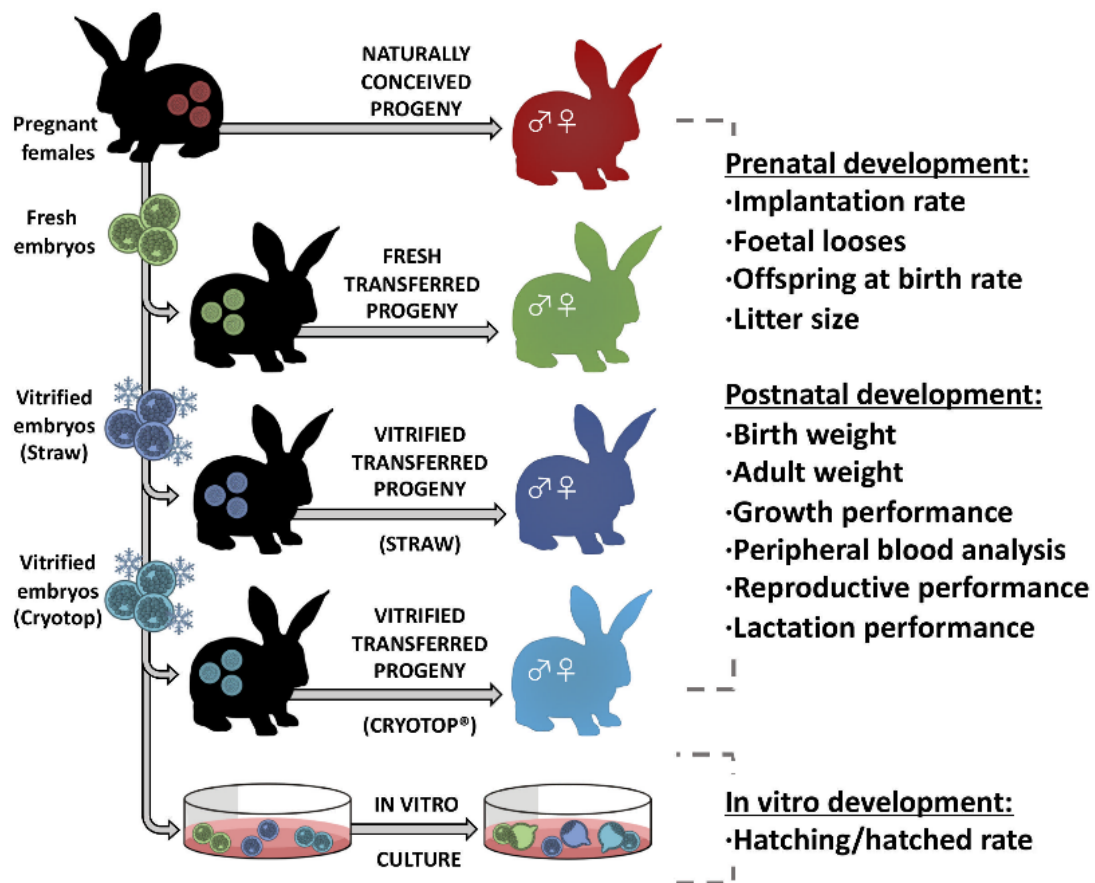


**Figure 4.1.** Experimental design. Using a naturally-conceived population as control group, features of offspring derived from fresh-transferred embryos were compared to those derived from vitrified-transferred embryos through two common vitrification devices (ministraw and cryotop). In addition, we compare the *in vitro* developmental potential of vitrified embryos using fresh ones as controls.

Twelve days after ovulation induction, foster females were examined by laparoscopy to determine the embryo implantation rate and to assess the foetal losses. On the day of

birth, litter size per parity was annotated and compared between the experimental groups (NC, FT, VTs, VTc). After this, the four progenies were sexed and microchipped for tracking individually from birth until adulthood, comparing their growth performance. After weaning (fourth week), animals were caged collectively (eight rabbits per cage) until the ninth week. Then, animals were individually kept in separate cages (flat deck indoor cages: 75 × 50 × 40 cm). Once in adulthood (20 weeks old), the health status was assessed on the haematological and biochemical peripheral blood parameters. Male and female reproductive performance was also evaluated. Specifically, seminal traits, litter size, and lactation performance (milk yield and its composition) were assessed.

#### **4.2.3. Embryo vitrification**

Vitrification was achieved in two steps according to previous studies [20–22]. Briefly, in the first step, embryos were placed for 2 min in a solution consisting of 10% (v/v) dimethyl sulfoxide (DMSO) and 10% (v/v) ethylene glycol (EG). In the second step, embryos were suspended for 1 min in a solution of 20% DMSO and 20% EG. Next, embryos suspended in vitrification medium were loaded into 0.125 mL French ministraws (IMV Technologies, L'Aigle, France) or into cryotop (< 1 µL of vitrification medium; Kitazato Corp., Shizuoka, Japan). Then, both cryodevices were plunged directly into liquid nitrogen to achieve vitrification. For warming, embryos were placed in 2 mL of 0.33 M sucrose at 25 °C to remove cryoprotectants, and washed 5 min later.

#### **4.2.4. *In vitro* culture**

A total of 244 vitrified embryos (134 in ministraw and 110 in cryotop) and 62 fresh embryos were cultured through 3 experimental sessions during 48 h in medium TCM199 supplemented with 10% (v/v) foetal bovine serum and 1% (v/v) antibiotics (penicillin G sodium 300,000 IU/L, penicillin G procaine 700,000 IU/L, and dihydrostreptomycin sulphate 1250 mg/L; Divasa Farmavic, Barcelona, Spain). Culture conditions were 38.5°C and 5% CO<sub>2</sub> in humidified atmosphere. The *in vitro* development ability until hatching/hatched blastocyst stage was recorded to calculate the developmental rate (total embryos developed/total embryos cultured).

#### **4.2.5. Embryo transfer**

Warmed or fresh embryos were laparoscopically transferred into the oviduct of asynchronous foster mothers [22], following the protocol described by Besenfelder and Brem et al. [23]. Briefly, foster mothers were anaesthetised with xylazine (5mg/kg;

Rompun; Bayern AG, Leverkusen, Germany) intramuscularly and ketamine hydrochloride (35 mg/kg; Imalgene 1000; Merial S.A, Lyon, France) intravenously, and placed in Trendelenburg's position. Then, embryos were loaded in a 17G epidural catheter, which was inserted through a 17G epidural needle into the inguinal region. Finally, while the process was monitored by single-port laparoscopy, the catheter was introduced into the oviduct through the infundibulum to release the embryos. Using this procedure, between 14 and 16 embryos were transferred in each foster mother. Both embryo vitrification and transfer processes used in this experiment were described in detail in Garcia-Dominguez et al. [22].

#### 4.2.6. Prenatal development

Twelve days after ovulation induction, foster mothers were anaesthetised as previously and examined by laparoscopy to assess the rate of transferred embryos that implanted (implantation rate). After birth, foetal loss rate and offspring rate were calculated, taking into account the relationship between litter size and the number of implanted embryos, and litter size and number of transferred embryos per female, respectively. In the NC group, the number of *corpora lutea* (number of oocytes released) was taken into account for estimation of available embryos. At birth, litter size and sex ratio (males:females) were recorded and compared between each progeny (NC, FT, VTs, VTc).

#### 4.2.7. Postnatal growth performance and body weight study

Body weights were annotated from birth to adulthood. Body weight differences between each progeny (NC, FT, VTs, VTc) were assessed at birth, 9th week (prepubertal age), and 20th week (adulthood). Growth curves were also estimated by nonlinear regression using the Gompertz equation, well suited for rabbits [24]:  $y = a \exp[-b \exp(-kt)]$ . In addition, growth rate was estimated as the average weight gain between the fourth and ninth week, a period when the rabbit growth is exponential.

#### 4.2.8. Determination peripheral blood parameters

In adulthood, 20 (10 of each sex) individual blood samples from each experimental group (NC, FT, VTs, VTc) were obtained from the central ear artery. From each animal, two blood samples were taken. The first one was dispensed into an EDTA-coated tube (Deltalab S.L., Barcelona, Spain), and the other into a serum-separator tube (Deltalab S.L., Barcelona, Spain). Blood count was performed from EDTA tubes, 10 minutes after collection at the most, by using an automated veterinary haematology analyser MS 4e

automatic cell counter (MeletSchloesing Laboratories, France) according to the manufacturer's instructions. The blood parameters recorded were white blood cells, lymphocytes, monocytes, granulocytes, red blood cells, haematocrit, and haemoglobin. From the second tube, biochemical analysis of the serum glucose, cholesterol, albumin, total bilirubin, and bile acids were performed. Briefly, after blood coagulation, samples were immediately centrifuged at  $3000 \times g$  for 10 minutes and serum was stored at  $-20^{\circ}\text{C}$  until analysis. Then, glucose, cholesterol, albumin, and total bilirubin levels were analysed by enzymatic colorimetric methods, whereas bile acids were estimated by photometry. All the methodologies were performed in an automatic chemistry analyser model Spin 200E (Spinreact, Girona, Spain), following the manufacturer's instructions. All samples were processed in duplicate.

#### 4.2.9. Male reproductive performance

Seminal traits, fertility rate, and litter size were studied. From each experimental group, 10 males began the training period with an artificial vagina at 18 weeks of age, collecting one ejaculate per week. Experimental evaluation of the males began at six months of age. One ejaculate per male was collected weekly, and ejaculates from males of the same experimental group were pooled in each session. Three  $20 \mu\text{L}$  aliquots of each pool were taken. The first and second aliquots were diluted at a ratio of 1:20 with Tris-citrate-glucose extender (250 mM tris-hydroxymethylaminomethane, 83 mM citric acid, 50 mM glucose, pH 6.8–7.0, 300 mOsm/kg). The first sample was assessed for individual sperm motility and motion parameters using the Integrated Semen Analysis System version 1.0.17 (ISAS; Projectes i Serveis R + D). The system was set to record images at 25 frames/s. Then,  $10 \mu\text{L}$  of the sample was placed in a  $10 \mu\text{m}$  deep Makler counting chamber. Sperm motility was assessed at  $\times 200$  magnification at  $37^{\circ}\text{C}$  using a negative phase contrast microscope. For each sample, 4 microscopic fields were analysed and a minimum of 200 sperm evaluated. The following sperm activity variables were assessed: sperm motility (%), progressive motility (%), curvilinear velocity (VCL,  $\mu\text{m s}^{-1}$ ), straight-line velocity (VSL,  $\mu\text{m s}^{-1}$ ), average path velocity (VAP,  $\mu\text{m s}^{-1}$ ), linearity coefficient (LIN; calculated as  $(\text{VSL}/\text{VCL}) \times 100$ , %), straightness coefficient (STR), wobble coefficient (WOB;  $\text{VSL}/\text{VAP} \times 100$ ), amplitude of lateral head displacement (ALH,  $\mu\text{m}$ ), and beat cross-frequency (BCF, Hz). The second sample was assessed for the percentage of live spermatozoa (viability, VIA) using the LIVE/DEAD sperm viability kit (Molecular Probes), which consists essentially of two DNA-binding fluorescent stains—a membrane-permeant stain, SYBR-14, and a conventional dead-cell stain, propidium iodide. The third sample was diluted at a ratio of 1:20 with 0.5% of glutaraldehyde solution in phosphate-buffered saline and observed by phase contrast at  $\times 400$  magnification to calculate the concentration, in a Thoma-Zeiss counting cell chamber, and evaluate both the



percentages of intact apical ridge and abnormal sperm (on the basis of morphological abnormalities of head, neck, mid-piece, and tail).

For fertility assessment, seminal pools of each experimental group adjusted to  $40 \times 10^6$  spermatozoa/mL were used to perform 296 inseminations (72 NC, 77 FT, 71 VTs, and 76 VTc) in New Zealand crossbred females. Each female was inseminated with a seminal dose of 0.5 ml ( $20 \times 10^6$  spermatozoa). At insemination time, females were injected intramuscularly with 1  $\mu$ g of buserelin acetate (Hoechst Marion Roussel, Madrid, Spain) to induce ovulation. Only receptive does (red colour of vulvar lips) were inseminated, using a standard curved plastic pipette (Imporvet, Barcelona, Spain). The number of does that gave birth by number of inseminations (fertility rate) were recorded. At parturition day, the litter sizes per parity were annotated.

#### **4.2.10. Female reproductive performance**

Pregnancy rate, litter size, and number of liveborns were evaluated. For pregnancy rate assessment, seminal pools of control males were adjusted to  $20 \times 10^6$  spermatozoa per dose. A total of 66 receptive adult females (16 NC, 12 FT, 20 VTs, and 18 VTc) were inseminated as described above. The number of does that became pregnant by number of inseminations (pregnancy rate) was recorded. At parturition day, the litter size per parity and the number of liveborns were annotated.

#### **4.2.11. Lactation performance: milk yield, milk composition and nutritional potential**

After females had given birth, lactation performance was assessed on 41 females (10 NC, 10 FT, 11 VTs, and 10 VTc). Litters were equated to 10 kits, replacing those that died during the experiment. The milk yield was assessed on the second and third week of lactation to cover the point of maximum production. Taking advantage of the fact that rabbit pups are nursed only for about 3 min once every 24 h, milk yield was assessed using the weight-suckle-weight method [25]. First, the litters were maintained in the closed nest at 18:00. After that, the litters and the mothers were weighed before suckling at 8:00 the following day. At this time, the mothers were allowed to enter the nest and be suckled by their litters. Finally, each mother and her litter were re-weighed after suckling within 10 min. The difference in weight of each dam and its litter before and after suckling were annotated. The average of these differences was recorded as the daily milk yield of the female.

The milk composition was analysed 2 days after the milk yield evaluation in each week. Again, the litters were kept in the closed nest at 18:00. At 8:00 on the following day, the

mammary glands were shaved and disinfected with ethanol. Then, mothers were injected intramuscularly with 10 U.I. of oxytocin (Oxytocin Pituitaria Calier, Alvet Escartí S.L., Guadassuar, Valencia, Spain) to promote mammary gland contraction and milk let-down. After that, at least 15 mL of milk was collected in sterile tubes from each female by alternating manual milking between the mammary glands. Milk composition (dry matter, fat, crude protein, and lactose) was determined by mid-infrared spectroscopy using a MilkoScan FT120 (Foss Electric A/S, Hillerød, Denmark). Manual chemical methods were used to adjust the calibration lines of the equipment: desiccation (dry matter), SOXHLET (fat), and KJELDAHL (protein). Lactose content was calculated by difference with the other components. The somatic cell count (SCC) was analysed with a Fossomatic 5000 (Foss Electric A/S, Hillerød, Denmark). To test the nutritional milk value, suckling kits' weaning weight (4 weeks of age) was recorded.

#### **4.2.12. Statistical analysis of phenotypic data**

Differences in binomial traits (rates of development, pregnancy, implantation, foetal losses, offspring, fertility, and sex ratio) were assessed using a probit link model with binomial error distribution, including the experimental group (NC vs. FT vs. VTs vs. VTc) and embryo transfer session (four levels) as fixed effects, and foster mother as a random effect. Meanwhile, a general linear model (GLM) was fitted for the quantitative traits (body weights, growth rate, seminal parameters, litter size, number of liveborns, milk yield, milk composition, and milk SCC) analysis including the experimental group and embryo transfer session as a fixed effect, and foster mother as a random effect, as was done previously. For body weight analysis, sex was included as fixed effect, and litter size was used as covariate, although it remained non-significant from the ninth week of age. For milk yield and its composition, the week of extraction was used as fixed effect with two levels (second and third), and female body weight was used as the covariate for milk yield correction. A *p*-value of less than 0.05 was considered indicative of a statistically significant difference. The data are presented as least square mean  $\pm$  standard error of the mean. All statistical analyses were performed with SPSS 21.0 software package (SPSS Inc., Chicago, Illinois, USA, 2002).

### **4.3. RESULTS**

#### **4.3.1. Effect of embryo vitrification on the embryonic *in vitro* development**

After 48 h of *in vitro* culture, the *in vitro* development rate of embryos vitrified in ministraw was significantly lower compared to those vitrified in cryotop and fresh embryos ( $0.79 \pm 0.027$  vs.  $0.88 \pm 0.028$  and  $0.94 \pm 0.031$ , for ministraw vs cryotop and

fresh, respectively,  $p < 0.05$ ). There were no significant differences between cryotop and fresh groups.

### 4.3.2. Prenatal survival: rates of implantation, foetal losses and offspring

Lower implantation rate was recorded for ART progenies (FT, VTs and VTc) compared to NC progeny (Table 4.1). However, compared to the FT group, a lower implantation rate was noted for VTs than for VTc embryos. Likewise, the rate of foetal losses was higher for the VTs embryos than for all the other groups (Table 4.1). A higher offspring rate was recorded for NC group than for ART animals, of which, compared to FT group, this rate was lower for VTs than for VTc embryos (Table 4.1). At birth, similar litter sizes were recorded between NC and FT groups, but both VT progenies showed lower values. Therefore, overall results indicate that more reduced survival rate was obtained for ART embryos. However, whereas similar trends were observed between VTc and FT embryos, those VTs showed lower prenatal survival. Female embryos could be more sensitive than males to the vitrification process because the sex ratio of VT progenies was altered in favour of males compared with the NC group. Finally, 73 NC, 71 FT, 45 VTs and 65 VTc animals constituted the four experimental groups.

**Table 4.1.** Prenatal survival. Rates of implantation, foetal losses and offspring in natural-conceived, fresh embryo transfer, vitrified embryo transfer using ministraw, and vitrified embryo transfer using cryotop.

TRAITS	Naturally-conceived	Fresh-transferred	Vitrified-transferred	
			Ministraw	Cryotop
Embryos (n)	85 <sup>†</sup>	96	87	101
Foster mothers	6	6	6	7
Implantation rate	0.95 ± 0.021 <sup>a</sup>	0.88 ± 0.034 <sup>b</sup>	0.67 ± 0.051 <sup>c</sup>	0.78 ± 0.041 <sup>b,c</sup>
Foetal losses rate	0.10 ± 0.033 <sup>b</sup>	0.15 ± 0.039 <sup>b</sup>	0.31 ± 0.061 <sup>a</sup>	0.17 ± 0.042 <sup>b</sup>
Offspring rate	0.86 ± 0.038 <sup>a</sup>	0.74 ± 0.045 <sup>b</sup>	0.52 ± 0.054 <sup>c</sup>	0.65 ± 0.048 <sup>b,c</sup>
Litter size	12.2 ± 0.83 <sup>a</sup>	11.8 ± 0.83 <sup>a</sup>	7.5 ± 0.83 <sup>b</sup>	9.3 ± 0.77 <sup>b</sup>
Sex ratio (♂:♀)	0.75:1 <sup>b</sup>	1.08:1 <sup>a,b</sup>	1.33:1 <sup>a</sup>	1.5:1 <sup>a</sup>
Total born (n)	73	71	45	65

n: Number; <sup>†</sup>Estimated from the ovulation rate. Data are expressed as mean ± standard error of means. <sup>a,b</sup> Values within a row with different superscripts differ ( $p < 0.05$ ).

### 4.3.3. Postnatal growth performance and body weight

Even after using litter size as covariate, it was noted that embryo vitrification increased the birth weight, independently of the vitrification device used during the process (Figure 4.2,  $p < 0.05$ ). No effects on birth weight were found in the FT group. All ART progenies showed significantly reduced body weight at adulthood compared to the NC

group, VT animals being smaller than those in FT. Adult body weight was also sensitive to the embryo vitrification methodology, of which the higher cooling-warming rates supplied by the cryotop incurred lower body weight at adulthood, with VTs remaining higher than VTc ones (Figure 4.2). No sexual dimorphism was observed and no interaction between treatment and sex were found.

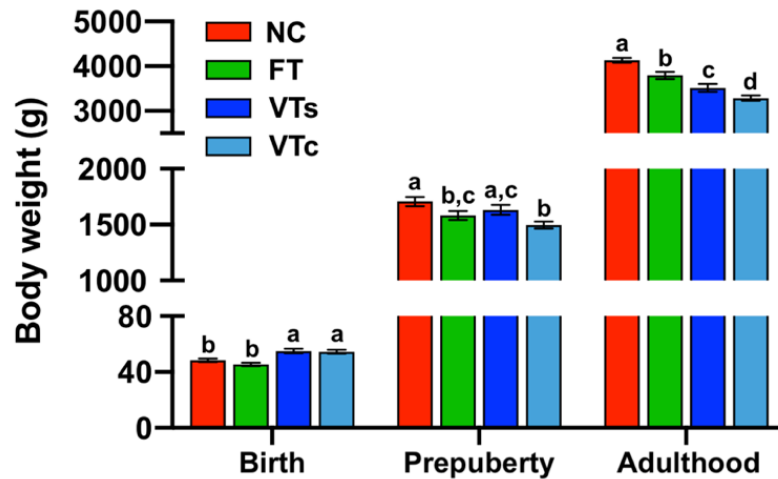


**Figure 4.2.** Bodyweight development: comparing differences between animals naturally-conceived (NC) and those born after fresh embryo transfer (FT), vitrified embryo transfer using a ministraw (VTs), and vitrified embryo transfer using cryotop (VTc).

Gompertz growth curves showed a fit with a mean r-squared value of  $0.99 \pm 0.007$ , describing a trend in which the growth decreases as embryonic manipulation increases (Figure 4.3).

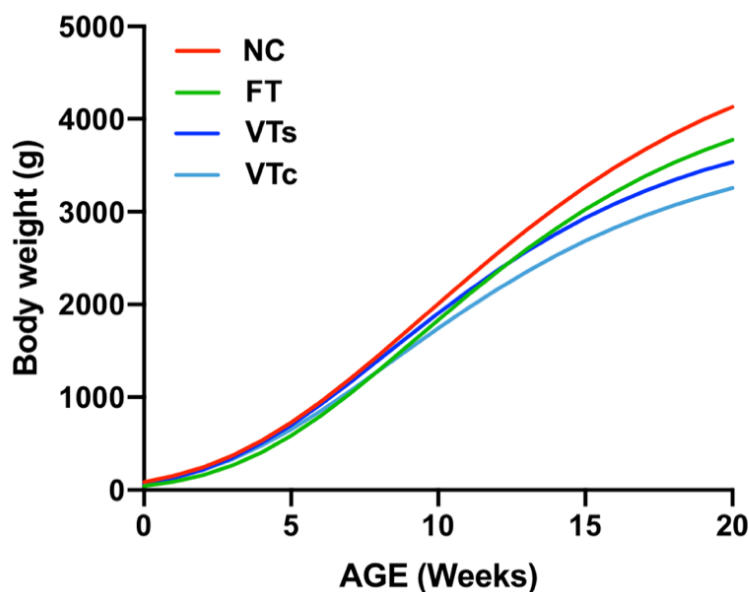


**Figure 4.3.** Growth curves: comparing differences between animals naturally-conceived (NC) and those born after fresh embryo transfer (FT), vitrified embryo transfer using a ministraw (VTs), and vitrified embryo transfer using cryotop (VTc).

As estimated by the Gompertz equation (a parameter), this trend was also patent in late adulthood ( $4073.0 \pm 98.80$  g,  $3792.1 \pm 92.18$  g,  $4489.4 \pm 98.64$  g and  $5123.1 \pm 97.74$  g for VTs, VTc, FT and NC groups, respectively, Figure 4.3). In addition, estimating the growth rate in a period of exponential growth (4th to 9th week), it was demonstrated that postnatal growth rate was reduced in all ART groups ( $31.0 \pm 1.4$  g/day,  $29.2 \pm 1.01$  g/day and  $32.7 \pm 1.1$  g/day for VTs, VTc and FT, respectively) compared to the NC ( $36.2 \pm 1.3$  g/day) progeny ( $p < 0.05$ ). Among ART progenies, lower growth rate was recorded for VTc animals compared to FT group, and that of the VTs was intermediate. Therefore, differences in growth rates agreed with the differences recorded for adult body weights. Overall results indicated that both embryo transfer and vitrification processes have an impact on the offspring growth performance *per se*, with more strong effects after using high cooling-warming rates than for lower ones.

#### 4.3.4. Healthy status: Peripheral blood parameters

From the haematological and biochemical point of view, both ART (FT, VTs and VTc) and NC progenies seemed healthy, as peripheral blood parameters ranged between normal values in all the experimental groups (Figure 4.4).

#### 4.3.5. Reproductive performances

Regarding male reproductive performance, significant variations in the seminal concentration, progressive motility, viable sperm, straight-line velocity, linearity coefficient, wobble coefficient and amplitude of lateral head displacement were found among the experimental progenies (Table 4.2). However, similar fertility rates and litter size recorded among the experimental groups (Table 4.2) indicated that, independently of their origin, males produced sperm of sufficient quality. Therefore, slight changes in the seminal traits were biologically irrelevant. Likewise, regarding female reproductive performance, no differences were obtained either in the pregnancy rate, litter size or the number of liveborn (Table 4.3). Therefore, reproductive performance was adequate independently of the experimental group and sex.

#### 4.3.6. Lactation performance

The results for lactation performance are shown in Table 4.3. Compared to NC animals, lower milk yield was observed in FT and VTc females. In contrast, VTs females showed a milk yield comparable to the NC females. A similar trend was observed for the milk composition analysis: whereas dry matter and fat levels were comparable between NC and VTs milk, these values were lower in the milk of FT and VTc females. Protein content

was higher in VTs milk than for the other groups. On the other hand, lactose content was higher in VTc milk than for the other groups. The somatic cell count showed higher levels in VTc than in VTs and NC milk, being similar to the FT group. The nutritional potential of the milk was tested based on the weaning weight of the suckling kits. Concordantly, lower weaning weights were recorded for the FT and VTc groups, compared to the NC and VTs groups ( $512.0 \pm 10.11$  g and  $531.4 \pm 9.58$  g vs  $576.9 \pm 9.46$  and  $561.4 \pm 8.42$  g, for FT and VTc vs NC and VTs respectively,  $p < 0.05$ ).

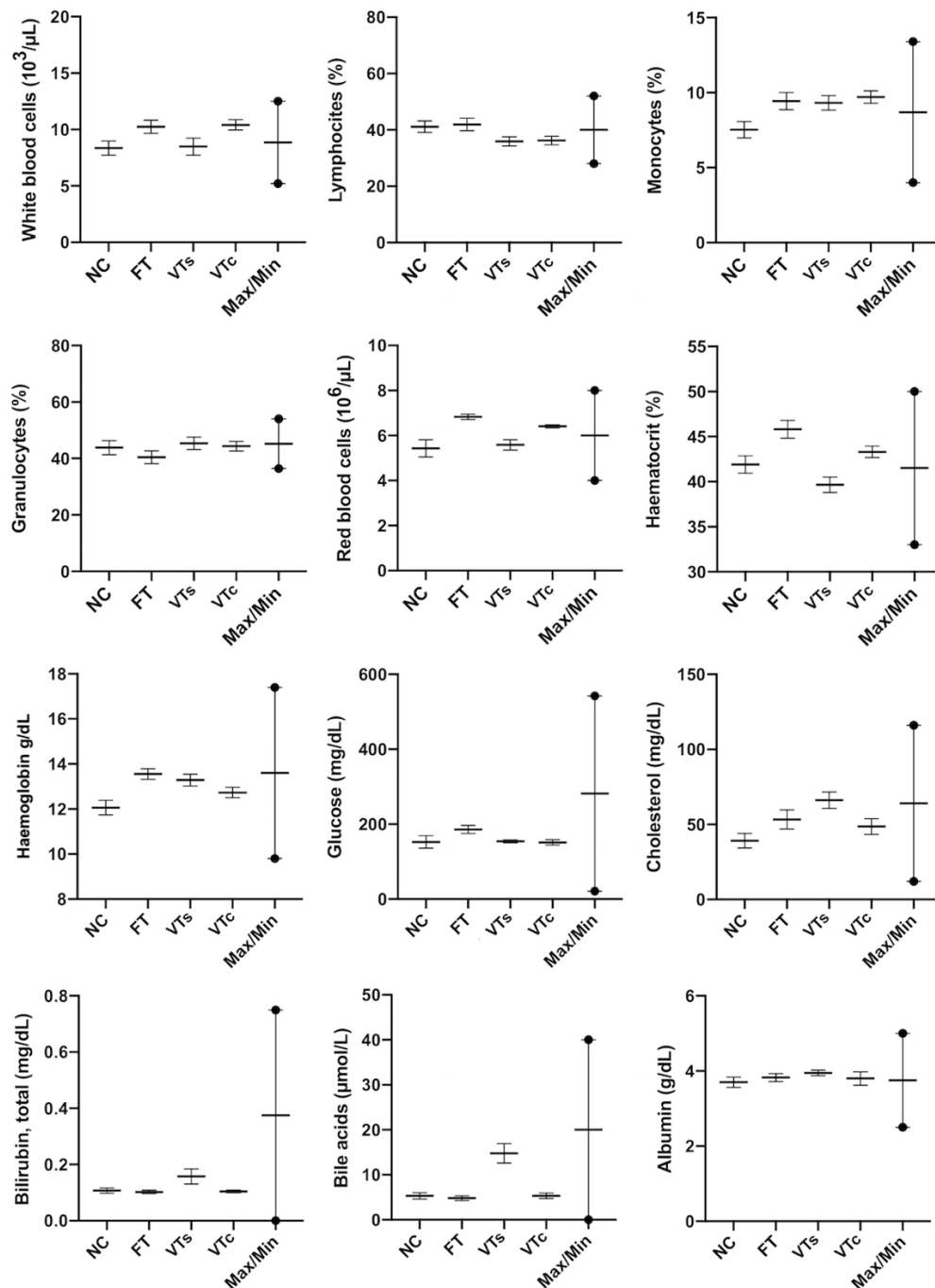


**Figure 4.4.** Peripheral blood analysis (haematological and biochemical): comparing differences between animals naturally-conceived (NC) and those born after fresh embryo transfer (FT), vitrified embryo transfer using a ministraw (VTs), and vitrified embryo transfer using cryotop (VTc).

**Table 4.2.** Male reproductive performance: comparing differences between naturally-conceived males and those born after fresh embryo transfer, vitrified embryo transfer using ministraw, and vitrified embryo transfer using cryotop.

TRAITS	Naturally-conceived	Fresh-transferred	Vitrified-transferred (ministraw)	Vitrified-transferred (cryotop)
	13	15	12	10
<b>Semen parameters</b>				
<b>CON</b> ( $10^6$ spz/ml)	253.8 ± 31.7 <sup>1a,b</sup>	317.8 ± 28.58 <sup>a</sup>	217.3 ± 34.47 <sup>b</sup>	248.5 ± 34.47 <sup>a,b</sup>
<b>MOT</b> (%)	88.6 ± 2.46	87.4 ± 2.37	90.3 ± 2.56	83.8 ± 2.95
<b>PRO</b> (%)	50.4 ± 2.87 <sup>a,b</sup>	43.1 ± 2.77 <sup>b</sup>	53.1 ± 2.98 <sup>a</sup>	42.1 ± 3.45 <sup>b</sup>
<b>VIA</b> (%)	90.5 ± 1.60 <sup>a</sup>	87.4 ± 1.55 <sup>a,b</sup>	84.8 ± 1.87 <sup>b</sup>	89.6 ± 1.87 <sup>a,b</sup>
<b>NAR</b> (%)	95.1 ± 0.86	94.7 ± 0.80	93.1 ± 0.94	95.3 ± 1.04
<b>ABN</b> (%)	19.6 ± 2.01	19.1 ± 1.88	17.9 ± 2.19	17.1 ± 2.01
<b>VCL</b> ( $\mu\text{m s}^{-1}$ )	98.5 ± 3.38	103.9 ± 3.11	100.3 ± 3.23	106.9 ± 3.96
<b>VSL</b> ( $\mu\text{m s}^{-1}$ )	48.8 ± 2.18 <sup>a</sup>	42.5 ± 2.09 <sup>b</sup>	49.1 ± 2.18 <sup>a</sup>	43.4 ± 2.67 <sup>a,b</sup>
<b>VAP</b> ( $\mu\text{m s}^{-1}$ )	69.9 ± 2.25	66.1 ± 2.17	70.2 ± 2.25	67.9 ± 2.76
<b>LIN</b> (%)	48.5 ± 2.19 <sup>a</sup>	41.2 ± 2.11 <sup>b</sup>	49.1 ± 2.19 <sup>a</sup>	40.6 ± 2.68 <sup>b</sup>
<b>STR</b> (%)	69.1 ± 2.22	63.8 ± 2.04	68.1 ± 2.12	64.9 ± 2.59
<b>WOB</b> (%)	68.8 ± 1.67 <sup>a,b</sup>	64.1 ± 1.54 <sup>c</sup>	69.8 ± 1.60 <sup>a</sup>	64.4 ± 1.96 <sup>c,b</sup>
<b>ALH</b> ( $\mu\text{m}$ )	2.3 ± 0.12 <sup>a,b</sup>	2.3 ± 0.12 <sup>a,b</sup>	2.0 ± 0.12 <sup>b</sup>	2.5 ± 0.15 <sup>a</sup>
<b>BCF</b> (Hz)	9.8 ± 0.49	9.8 ± 0.47	9.9 ± 0.49	9.7 ± 0.69
<b>Fertility rate</b>	0.97 ± 0.019	0.94 ± 0.028	0.93 ± 0.030	0.92 ± 0.031
<b>Litter size</b>	12.1 ± 0.38	11.7 ± 0.40	11.9 ± 0.43	12.3 ± 0.41

n: Number; **CON**: Spermatic concentration; **TSE**: Total sperm per ejaculate; **spz**: Spermatozoa; **MOT**: Percentage of sperm motility; **PRO**: Percentage of progressive motility; **VIA**: Percentage of viable sperm; **NAR**: Percentage of normal apical ridge; **ABN**: Percentage of abnormal forms; **VCL**: Curvilinear velocity; **VSL**: Straight-line velocity; **VAP**: Average path velocity; **LIN**: Linearity coefficient (VSL/VCL × 100); **STR**: Straightness coefficient; **WOB**: Wobble coefficient (VSL/VAP × 100); **ALH**: Amplitude of lateral head displacement; **BCF**: Beat cross frequency. Data are expressed as least-square means ± standard error of means. <sup>a,b</sup> Values within a row with different superscripts differ (p<0.05)

**Table 4.3.** Female reproductive and lactation performance: comparing differences between naturally-conceived females and those born after fresh embryo transfer, vitrified embryo transfer using ministraw, and vitrified embryo transfer using cryotop.

TRAIT	Naturally-conceived	Fresh-transferred	Vitrified-transferred (ministraw)	Vitrified-transferred (cryotop)
<b>Inseminated females</b>	16	12	20	18
<b>Pregnant females</b>	16	11	20	17
<b>Reproductive performance</b>				
<b>Litter size</b>	10.5 ± 0.65	9.1 ± 0.69	10.2 ± 0.62	9.1 ± 0.65
<b>Liveborn</b>	8.5 ± 0.68	8.9 ± 0.85	8.6 ± 0.60	8.5 ± 0.66
<b>Lactation performance</b>				
<b>Milk yield (g/day)</b>	261.9 ± 12.21 <sup>a</sup>	206.5 ± 13.44 <sup>b</sup>	255.2 ± 10.98 <sup>a</sup>	219.6 ± 11.26 <sup>b</sup>
<b>Dry matter (%)</b>	36.3 ± 0.56 <sup>a</sup>	33.5 ± 0.59 <sup>b</sup>	36.0 ± 0.54 <sup>a</sup>	33.94 ± 0.56 <sup>b</sup>
<b>Fat (%)</b>	21.6 ± 0.51 <sup>a</sup>	18.5 ± 0.53 <sup>b</sup>	20.5 ± 0.48 <sup>a</sup>	18.3 ± 0.51 <sup>b</sup>
<b>Protein (%)</b>	10.9 ± 0.17 <sup>b</sup>	11.0 ± 0.18 <sup>a,b</sup>	11.5 ± 0.17 <sup>a</sup>	11.2 ± 0.18 <sup>a,b</sup>
<b>Lactose (%)</b>	2.5 ± 0.08 <sup>b</sup>	2.4 ± 0.08 <sup>b</sup>	2.5 ± 0.08 <sup>b</sup>	2.8 ± 0.08 <sup>a</sup>
<b>Somatic cells (10<sup>3</sup>/mL)</b>	371.9 ± 101.09 <sup>b</sup>	557.3 ± 113.92 <sup>a,b</sup>	408.1 ± 98.77 <sup>b</sup>	725.3 ± 101.09 <sup>a</sup>

Data are expressed as least-square means ± standard error of means. <sup>a,b</sup> Values within a row with different superscripts differ (p<0.05)



#### 4.4. DISCUSSION

Here, we describe how embryo manipulation techniques incur phenotypic changes throughout life. First, we provide long-term follow-up data of the ART cumulative effect during a vitrified embryo transfer procedure. Accurately, we unravel those effects related to the cryopreservation *per se* and those associated with the embryo manipulation during the transfer procedure. Second, we report that the vitrification device effected distinct differences in the *in vitro* and *in vivo* (prenatal and postnatal) development trajectory. Third, ART animals seemed healthy due to haematological and biochemical parameters and similar reproductive performance. Therefore, we support the idea that developmental changes exhibited by ART progenies are due to an embryo developmental plasticity response.

It is well known that cells can respond to any adverse environmental condition that perturbs cellular homeostasis. Previous studies have suggested that stress during preimplantation embryo stage precipitates deviant postnatal phenotypes [10–12]. Overall, to be cryopreserved, embryos require exposure to an environment in which they have no intrinsic ability to survive, which exposes them to risk of a variety of types of damage or “cryoinjury” during exposure to lethal temperature [14]. Cryopreservation could thus be considered one of the most invasive ART routinely used [26]. In this article, we tested the effects of two vitrification devices on embryonic development. Our results showed similar *in vitro* developmental rates between fresh and cryotop-vitrified embryos, but a lower rate for straw-vitrified embryos. Cryotop allows extremely faster cooling and warming rates in comparison with the straw devices [27,28]. Moreover, in agreement with our findings, it has been described that increasing the cooling rate improves survival rates [18,19]. Similarly, other studies based on minimum volume vitrification assays have demonstrated improved survival rates [29]. This trend was confirmed across gestation, where higher foetal losses were recorded for VTs embryos, in line with previous results [30]. A plausible explanation is that higher cryodamage induced by straw vitrification could incur in improper foetal placenta development, probably due to preferential confinement of damaged cells to the trophoctoderm [31]. Remarkably, it has been described that ART impact the biological processes of placental growth, development, morphology, and function [32]. Thus, female embryos seemed more sensitive to the vitrification conditions, as skewed sex ratio towards male gender was detected at birth. This phenomenon has been well established among ART births, which has been related with abnormal inactivation in one of the two X chromosomes in females and a higher rate of irregular placentation that incurs higher mortality for female embryos [33–36]. However, in the field of embryo cryopreservation, information is limited and controversial, and changes in the sex ratio have been attributed to the grading criteria used, instead of to the cryopreservation procedure *per se* [37–39]. Thus,

to our best knowledge, this is the first study to demonstrate in a randomised model that embryo vitrification could imbalance the offspring sex ratio in favour of males.

Further evidence for the cryopreservation impact comes from postnatal phenotypic observations. In this article, we have shown that animals born after embryo cryopreservation exhibit higher birth weight and poor growth performance independently of the tested device. Higher birth weight has been observed following embryo cryopreservation in different mammalian species, including humans [31,40,41]. Concordantly, it has been described that ART increases the risk of some foetal overgrowth syndromes, such as large offspring syndrome in bovines and Beckwith–Wiedemann syndrome in humans, both associated with epigenetic changes [42–45]. In this sense, epigenetic studies point toward differential methylation of critical genes for growth that may be responsible for the increased incidence of body weight disorders following ART [46]. In addition, epigenetic variations in ART births can remain in adulthood [26]. In this sense, in agreement with previous findings [10–12,47], we reported that embryo manipulation incurred a cumulative effect, leading to growth and adult body weight deviations, with more severe preimplantation stress precipitating more deviant phenotypes. These phenotypic modifications meet the concerns of ART practitioners, especially those regarding birth weight, growth trajectories, and developmental defects [10]. Today, it is well established that superovulation can also alter the epigenetic status of the resultant embryos and thereby incur long-term effects for the offspring [48]. Moreover, when different stressors exist, these can act synergistically inducing more adversarial effects. However, it is difficult to distinguish between the adverse effects caused by superovulation or by the subsequent ART, because current protocols require superovulation as an initial step. Thus, in most studies, all adverse effects are considered together as part of the ART protocol [11]. Nevertheless, ART animals are seemingly healthy, supported by the haematological and biochemical analyses of the peripheral blood, which are within the normal physiological range of variability. Furthermore, it is widely known that critical health conditions may impair the reproductive system [49]. Although potential effects of ART over reproductive traits have been described [50,51], here, reassuringly, no differences in reproductive performance were noticed between ART and NC progenies.

Throughout this study, it was demonstrated that although cryotop has a positive effect on the *in vitro* and *in vivo* embryo survival, postnatal growth performance was severely impaired, ultimately leading to lower body weight at adulthood. A plausible explanation for this difference is that preimplantation embryos can develop a stress-dependent response when faced with different cooling–warming rates during vitrification. On the other hand, some studies suggested that embryo cryopreservation may act as selection pressure, filtering-out ART-sensitive embryos that not sustain the stresses associated with vitrification and warming processes [52–54]. In this sense, and in concordance with

the higher mortality exhibited by the VTs embryos, it is well established that straw devices provoke slower cooling–warming rates, and thus more troublesome conditions for embryo survival than cryotop devices [18,19,27–29]. Therefore, straw could produce a more powerful selection pressure that ultimately selects ART-resistant embryos, originating an offspring with less deviant developmental trajectories. However, to further characterise the effect of embryo cryopreservation procedure and methodology, we analysed lactation performance through milk yield and milk composition in NC, FT, VTc, and VTs females. Herein, we find evidence that does derived from FT and VTc embryos had lower lactation performance compared with the NC group. In contrast, milk yield and composition of VTs does were not affected, remaining similar to the NC group. Increased SCC levels in VTc and FT milk suggest poorer breast health condition and milk quality in these groups [55]. Thus, overall results indicated that a more reduced lactation performance was exhibited by FT and VTc does compared to the NC group, leaving that of the VTs unaltered. To determine whether milk yield deficiency could affect body weight in suckling kits, we determined the bodyweight at four weeks of age (weaning). Consistently, the bodyweight of the suckling kits was severely impaired in FT and VTc females compared to NC and VTs females. Litter size in which rabbit does were raised before weaning did not influence their later milk yield [25]. However, reshapes in both prenatal and postnatal trajectories can influence mammary gland development in a manner that will determine milk yields during subsequent lactations [25,56]. In agreement with our findings, a recent study on *in vitro* embryo production showed significant changes in growth and reductions in the milk yield and fat and protein production in bovine [57]. Nevertheless, the underlying mechanisms associating embryo manipulation and milk yield or composition remains to be explored. We hypothesise that, as skewed sex ratio reflects, embryo “cryoselection” might act especially on female embryos, which could favour the inheritance of determinant alleles [58] that can be related with the proper lactation performance manifested by VTs females. As the breast milk is of fundamental importance for the short- and long-term survival of suckling new-borns, following the ART-conceived offspring could be necessary, as the effects of altered breastfeeding can be combined with a transgenerational inheritance of the ART-induced phenotypes [59,60]. Until the recent past, it was unclear whether embryo manipulation could alter health and development throughout the course of life, because for many years good fertility and the absence of malformations were the only criteria used to qualify the resulting progeny as “normal” [61]. Hence, as the long-term effects have not been considered for a long time, the information available is scarce. Although we cannot assure that embryo transfer and vitrification manipulation might cause epigenetic modifications, our results unequivocally described an example of the plasticity of early development.

## 4.5. CONCLUSION

Together, findings from our animal model approach showed significant phenotypic changes in the adult rabbit after embryo vitrification. Hence, our study provides evidence of long-term phenotypic changes after embryo manipulation, supporting that stress during early embryo development precipitates deviant postnatal phenotypes. Moreover, to our best knowledge, this study reports the first piece of evidence demonstrating that the vitrification device used is not a trivial decision, providing valuable information about how the cooling-warming rates during vitrification can be partly responsible of postnatal phenotypic variations. In this sense, our results highlight ART as a possible trigger of the embryonic developmental plasticity manifestation in mammalian species. Although ART progenies seem healthy, further studies reaching senescence age and involving several species are needed to accumulate robust information about ART to guarantee the safety of reproductive technologies.

## 4.6. REFERENCES

- [1]. Ng KYB, Mingels R, Morgan H, Macklon N, Cheong Y. In vivo oxygen, temperature and pH dynamics in the female reproductive tract and their importance in human conception: a systematic review. *Hum Reprod Update* 2018;24:15-34.
- [2]. García-Martínez S, Sánchez Hurtado MA, Gutiérrez H, Sánchez Margallo FM, Romar R, Latorre R, *et al.* Mimicking physiological O<sub>2</sub> tension in the female reproductive tract improves assisted reproduction outcomes in pig. *Mol Hum Reprod* 2018;24:260-270.
- [3]. Roseboom TJ. Developmental plasticity and its relevance to assisted human reproduction. *Hum Reprod* 2018;33:546-552.
- [4]. Vrooman LA, Bartolomei MS. Can assisted reproductive technologies cause adult-onset disease? Evidence from human and mouse. *Reprod Toxicol* 2017;68:72-84.
- [5]. Servick K. Unsettled questions trail IVF's success. *Science* 2014;345: 744-6.
- [6]. Skelly AC, Dettori JR, Brodt ED. Assessing bias: the importance of considering confounding. *Evid Based Spine Care J* 2012;3:9-12.
- [7]. Chen M, Heilbronn LK. The health outcomes of human offspring conceived by assisted reproductive technologies (ART). *J Dev Orig Health Dis* 2017;8:388-402.
- [8]. Halliday J, Lewis S, Kennedy J, Burgner DP, Juonala M, Hammarberg K, *et al.* Health of adults aged 22 to 35 years conceived by assisted reproductive technology. *Fertil Steril* 2019;112:130-139.
- [9]. Juonala M, Lewis S, McLachlan R, Hammarberg K, Kennedy J, Saffery R, *et al.* American Heart Association ideal cardiovascular health score and subclinical atherosclerosis in 22-35-year-old adults conceived with and without assisted reproductive technologies. *Hum Reprod* 2020;35:232-239.

- [10]. Duranthon V, Chavatte-Palmer P. Long term effects of ART: What do animals tell us?. *Mol Reprod Dev* 2018;85:348-368.
- [11]. Ramos-Ibeas P, Heras S, Gómez-Redondo I, Planells B, Fernández-González R, Pericuesta E, *et al.* Embryo responses to stress induced by assisted reproductive technologies. *Mol Reprod Dev* 2019;86:1292-1306.
- [12]. Feuer SK, Rinaudo PF. Physiological, metabolic and transcriptional postnatal phenotypes of in vitro fertilisation (IVF) in the mouse. *J Dev Orig Health Dis* 2017;8:403-410.
- [13]. De Geyter C, Calhaz-Jorge C, Kupka MS, Wyns C, Mocanu E, Motrenko T, *et al.* ART in Europe, 2015: results generated from European registries by ESHRE. *Hum Reprod Open* 2020;2020:hoz038.
- [14]. Sparks AE. Human embryo cryopreservation-methods, timing, and other considerations for optimizing an embryo cryopreservation program. *Semin Reprod Med* 2015;33:128-44.
- [15]. Hargreave M, Jensen A, Hansen MK, Dehlendorff C, Winther JF, Schmiegelow K, *et al.* Association Between Fertility Treatment and Cancer Risk in Children. *JAMA* 2019;322:2203-2210.
- [16]. Norrman E, Petzold M, Clausen TD, Henningsen AK, Opdahl S, Pinborg A, *et al.* Type 1 diabetes in children born after assisted reproductive technology: a register-based national cohort study. *Hum Reprod* 2020;35:221-231.
- [17]. Rienzi L, Gracia C, Maggiulli R, LaBarbera AR, Kaser DJ, Ubaldi FM, *et al.* Oocyte, embryo and blastocyst cryopreservation in ART: systematic review and meta-analysis comparing slow-freezing versus vitrification to produce evidence for the development of global guidance. *Hum Reprod Update* 2017;23:139-155.
- [18]. Arav A. Cryopreservation of oocytes and embryos. *Theriogenology* 2014;81:96-102.
- [19]. Saragusty J, Arav A. Current progress in oocyte and embryo cryopreservation by slow freezing and vitrification. *Reproduction* 2011;141:1-19.
- [20]. Vicente JS, García-Ximénez F. Osmotic and cryoprotective effects of a mixture of DMSO and ethylene glycol on rabbit morulae. *Theriogenology* 1994;42:1205-15.
- [21]. Vicente JS, Viudes-de-Castro MP, García ML. In vivo survival rate of rabbit morulae after vitrification in a medium without serum protein. *Reprod Nutr Dev* 1999;39:657-62.
- [22]. García-Dominguez X, Marco-Jimenez F, Viudes-de-Castro MP, Vicente JS. Minimally invasive embryo transfer and embryo vitrification at the optimal embryo stage in rabbit model. *J Vis Exp.* 2019;147:e58055.
- [23]. Besenfelder U, Brem G. Laparoscopic embryo transfer in rabbits. *J Reprod Fertil* 1993;99:53-6.
- [24]. Blasco A, Gómez E. A note of growth curves of rabbit lines selected on growth rate or litter size. *Anim Prod* 1993;57:332-334.

- [25]. Maertens L, Lebas F, Szendrő Z. Rabbit milk: a review of quantity, quality and non-dietary affecting factors. *World Rabbit Science* 2006;14:205–230.
- [26]. Novakovic B, Lewis S, Halliday J, Kennedy J, Burgner DP, Czajko A, *et al.* Assisted reproductive technologies are associated with limited epigenetic variation at birth that largely resolves by adulthood. *Nat Commun* 2019;10:3922.
- [27]. Seki S, Mazur P. The Dominance of Warming Rate Over Cooling Rate in the Survival of Mouse Oocytes Subjected to a Vitrification Procedure. *Cryobiology* 2009;59:75–82.
- [28]. Mazur P, Seki S. Survival of mouse oocytes after being cooled in a vitrification solution to  $-196^{\circ}\text{C}$  at  $95^{\circ}$  to  $70,000^{\circ}\text{C}/\text{min}$  and warmed at  $610^{\circ}$  to  $118,000^{\circ}\text{C}/\text{min}$ : A new paradigm for cryopreservation by vitrification. *Cryobiology* 2011;62:1–7.
- [29]. Zhang X, Catalano PN, Gurkan UA, Khimji I, Demirci U. Emerging technologies in medical applications of minimum volume vitrification. *Nanomedicine (Lond)* 2011;6:1115-29.
- [30]. Marco-Jiménez F, Lavara R, Jiménez-Trigos E, Vicente JS. In vivo development of vitrified rabbit embryos: effects of vitrification device, recipient genotype, and asynchrony. *Theriogenology* 2013;79:1124-9.
- [31]. Saenz-de-Juano MD, Marco-Jimenez F, Schmaltz-Panneau B, Jimenez-Trigos E, Viudes-de-Castro MP, Peñaranda DS, *et al.* Vitrification alters rabbit foetal placenta at transcriptomic and proteomic level. *Reproduction* 2014;147:789-801.
- [32]. Riesche L, Bartolomei MS. Assisted Reproductive Technologies and the Placenta: Clinical, Morphological, and Molecular Outcomes. *Semin Reprod Med* 2018;36:240-248.
- [33]. Tan K, Wang Z, Zhang Z, An L, Tian J. IVF affects embryonic development in a sex-biased manner in mice. *Reproduction* 2016;151:443–453.
- [34]. Tan K, An L, Miao K, Ren L, Hou Z, Tao L, *et al.* Impaired imprinted X chromosome inactivation is responsible for the skewed sex ratio following in vitro fertilization. *Proc. Natl. Acad. Sci. U. S. A.* 2016;113:3197–3202.
- [35]. Maalouf WE, Mincheva MN, Campbell BK, Hardy ICW. Effects of assisted reproductive technologies on human sex ratio at birth. *Fertil. Steril.* 2014;101:1321–1325.
- [36]. Supramaniam PR, Mittal M, Ohuma EO, Lim LN, McVeigh E, Granne I, *et al.* Secondary sex ratio in assisted reproduction: An analysis of 1 376 454 treatment cycles performed in the UK. *Hum. Reprod. Open.* 2019;2019:hoz020.
- [37]. Lin PY, Huang FJ, Kung FT, Wang LJ, Chang SY, Lan KC. Comparison of the offspring sex ratio between fresh and vitrification-thawed blastocyst transfer. *Fertil. Steril.* 2009;92:1764–1766.
- [38]. Chen M, Du J, Zhao J, Lv H, Wang Y, Chen X, *et al.* The sex ratio of singleton and twin delivery offspring in assisted reproductive technology in China. *Sci. Rep.* 2017;7:e7754.

- [39]. Leme LO, Carvalho JO, Franco MM, Dode MAN. Effect of sex on cryotolerance of bovine embryos produced in vitro. *Theriogenology* 2020;141:219–227.
- [40]. Spijkers S, Lens JW, Schats R, Lambalk CB. Fresh and Frozen-Thawed Embryo Transfer Compared to Natural Conception: Differences in Perinatal Outcome. *Gynecol Obstet Invest* 2017;82:538-546.
- [41]. Chen L, Ni X, Xu Z, Fang J, Zhang N, Li D. Effect of frozen and fresh embryo transfers on the birthweight of live-born twins. *Eur J Obstet Gynecol Reprod Biol* 2020;246:50-54.
- [42]. Uk A, Collardeau-Frachon S, Scavion Q, Michon L, Amar E. Assisted Reproductive Technologies and imprinting disorders: Results of a study from a French congenital malformations registry. *Eur J Med Genet* 2018;61:518-23.
- [43]. Li Y, Donnelly CG, Rivera RM. Overgrowth Syndrome. *Vet Clin North Am Food Anim Pract* 2019;35:265-276.
- [44]. Chen Z, Hagen DE, Elsik CG, Ji T, Morris CJ, Moon LE, *et al.* Characterization of global loss of imprinting in fetal overgrowth syndrome induced by assisted reproduction. *Proc Natl Acad Sci U S A* 2015;112:4618-23.
- [45]. Mussa A, Molinatto C, Cerrato F, Palumbo O, Carella M, Baldassarre G, *et al.* Assisted Reproductive Techniques and Risk of Beckwith-Wiedemann Syndrome. *Pediatrics* 2017;140:e20164311.
- [46]. Van Heertum K, Weinerman R. Neonatal outcomes following fresh as compared to frozen/thawed embryo transfer in in vitro fertilisation. *Birth Defects Res* 2018;110:625-629.
- [47]. Feuer SK, Liu X, Donjacour A, Lin W, Simbulan RK, Giritharan G, *et al.* Use of a mouse in vitro fertilisation model to understand the developmental origins of health and disease hypothesis. *Endocrinology*. 2014 May;155:1956-69.
- [48]. Marshall KL, Rivera RM. The effects of superovulation and reproductive aging on the epigenome of the oocyte and embryo. *Mol. Reprod. Dev.* 2018;85:90-105.
- [49]. Baker HW. Reproductive effects of nontesticular illness. *Endocrinol Metab Clin North Am* 1998;27:831-50.
- [50]. Calle A, Miranda A, Fernandez-Gonzalez R, Pericuesta E, Laguna R, Gutierrez-Adan A. Male mice produced by in vitro culture have reduced fertility and transmit organomegaly and glucose intolerance to their male offspring. *Biol Reprod* 2012;87:34.
- [51]. Belva F, Bonduelle M, Roelants M, Michielsen D, Van Steirteghem A, Verheyen G, *et al.* Semen quality of young adult ICSI offspring: the first results. *Hum Reprod* 2016;31:2811-2820.
- [52]. Vidal M, Vellvé K, González-Comadran M, Robles A, Prat M, Torné M, *et al.* Perinatal outcomes in children born after fresh or frozen embryo transfer: A Catalan cohort study based on 14,262 newborns. *Fertil. Steril.* 2017;107:940-947.

- [53]. Sallem A, Santulli P, Barraud-Lange V, Le Foll N, Ferreux L, Maignien C, *et al.* Extended culture of poor-quality supernumerary embryos improves ART outcomes. *J. Assist. Reprod. Genet.* 2018;35:311-319.
- [54]. Marsico TV, de Camargo J, Valente RS, Sudano MJ. Embryo competence and cryosurvival: Molecular and cellular features. *Anim. Reprod.* 2019;16:423-439.
- [55]. Mehdid A, Martí-De Olives A, Fernández N, Rodríguez M, Peris C. Effect of stress on somatic cell count and milk yield and composition in goats. *Res Vet Sci* 2019;125:61-70.
- [56]. Sinclair KD, Rutherford KM, Wallace JM, Brameld JM, Stöger R, Alberio R, *et al.* Epigenetics and developmental programming of welfare and production traits in farm animals. *Reprod Fertil Dev* 2016. doi: 10.1071/RD16102.
- [57]. Siqueira LGB, Dikmen S, Ortega MS, Hansen PJ. Postnatal phenotype of dairy cows is altered by in vitro embryo production using reverse X-sorted semen. *J Dairy Sci* 2017;100:5899-5908.
- [58]. Mahsoudi B, Li A, O'Neill C. Assessment of the Long-Term and Transgenerational Consequences of Perturbing Preimplantation Embryo Development in Mice. *Biol. Reprod.* 2007;77:889-896.
- [59]. Del Ciampo LA, Del Ciampo IRL. Breastfeeding and the benefits of lactation for women's health. *Rev. Bras. Ginecol. e Obstet.* 2018;40:354–359.
- [60]. Calle A, Fernandez-Gonzalez R, Ramos-Ibeas P, Laguna-Barraza R, Perez-Cerezales S, Bermejo-Alvarez P, *et al.* Long-term and transgenerational effects of in vitro culture on mouse embryos. *Theriogenology* 2012;77:785–793.
- [61]. Auroux M. Long-term effects in progeny of paternal environment and of gamete/embryo cryopreservation. *Hum Reprod Update* 2000;6:550-63.

## ACKNOWLEDGEMENTS

This work was supported by funds from the Ministry of Economy and Competitiveness of Spain (AGL2014-53405-C2-1-P and AGL2017-85162-C2-1-R) and Generalitat Valenciana Research Programme (PrometeoII 2014/036). Ximo García-Dominguez was supported by a research grant from the Ministry of Economy and Competitiveness (BES-2015-072429). The authors would like to thank Neil Macowan Language Services for revising the English version of the manuscript.



## CHAPTER III

# **LONG-TERM PHENOTYPIC AND PROTEOMIC CHANGES FOLLOWING VITRIFIED EMBRYO TRANSFER IN THE RABBIT MODEL**

X. Garcia-Dominguez, F. Marco-Jiménez, D.S. Peñaranda, J.S. Vicente

Institute for Animal Science and Technology (ICTA), Laboratory of Reproductive Biotechnology,  
Universitat Politècnica de València, 46022 Valencia, Spain

*Animals*, 2020; 10: 1043



### ABSTRACT

Nowadays, assisted reproductive technologies (ARTs) are considered valuable contributors to our past, but a future without their use is inconceivable. However, in recent years, several studies have evidenced a potential impact of ART on long-term development in mammal species. To date, the long-term follow-up data are still limited. So far, studies have mainly focused on *in vitro* fertilisation or *in vitro* culture, with information from gametes/embryos cryopreservation field being practically missing. Herein, we report an approach to determine whether a vitrified embryo transfer procedure would have long-term consequences on the offspring. Using the rabbit as a model, we compared animals derived from vitrified-transferred embryos versus those naturally conceived, studying the growth performance, plus the weight throughout life, and the internal organs/tissues phenotype. The healthy status was assessed over the haematological and biochemical parameters in peripheral blood. Additionally, a comparative proteomic analysis was conducted in the liver tissue to investigate molecular cues related to vitrified embryo transfer in an adult tissue. After vitrified embryo transfer, birth weight was increased, and the growth performance was diminished in a sex-specific manner. In addition, vitrified-transferred animals showed significantly lower body, liver and heart weights in adulthood. Molecular analyses revealed that vitrified embryo transfer triggers reprogramming of the liver proteome. Functional analysis of the differentially expressed proteins showed changes in relation to oxidative phosphorylation and dysregulations in the zinc and lipid metabolism, which has been reported as possible causes of a disturbed growth pattern. Therefore, we conclude that vitrified embryo transfer is not a neutral procedure, and it incurs long-term effects in the offspring both at phenotypic and molecular levels. These results described a striking example of the developmental plasticity exhibited by the mammalian embryo.



## 5.1. INTRODUCTION

Since their implementation, assisted reproductive technologies (ARTs) have made major contributions to human health, livestock production and environmental management in the past and will continue to do so in future [1,2]. However, from the outset there has been concern about the influence of these technologies in embryo and postnatal development. This is the basis of the Developmental Origins of Health and Disease (DOHaD) theory, which posits that environmental stresses during development can increase the risk of disease later in life [3]. At the center of the DOHaD theory is the concept of developmental plasticity, which implies that the biological pathways governing prenatal development are not fixed [3,4]. Therefore, in response to environmental signals, this developmental plasticity allows phenotypic changes in developing embryos to be better suited to the environment in which they will be born. Nevertheless, extreme stressors, such as ART conditions, can force developing embryos to carry out a strong reshaping of their developmental trajectories to guarantee their short-term survival [3–5]. However, this reprogramming in embryonic cells that subsequently forms tissues and organ systems may influence an individual's susceptibility to alterations in growth, development and health [3,6–13]. Controversially, ART has been linked in humans with adverse obstetric and perinatal outcomes, birth defects, cancers, growth disorders, obesity and chronic ageing-related diseases [10]. But, in human studies, it is difficult to discriminate whether these effects are caused by ARTs or originate from either genetic abnormalities or risk factors intrinsic to infertile patients with low-quality gametes [9,10]. Thus, animal models using fertile and healthy animals, which avoid these confounding factors and provide adequate control groups, are essential to reveal the effects of ART *per se*. Through this approach, several evidences of long-lasting ART consequences have been reported in properly designed animal models [3,7–9,14–16], although the vast majority of these results has been evidenced in the mouse model. The renaissance of the laboratory rabbit as a reproductive model for human health is closely related to the growing evidence of periconceptual metabolic programming and its determining effects on offspring and adult health [17]. Moreover, many molecular/physiological events during human embryo development are more similar to those in rabbits than in mice, placing the rabbit as a pertinent animal model choice to study the impact of a disturbed periconceptual environment during ART and obtain results that are feasibly transferable to the clinic.

Until now, the vast majority of research has focused on improving birth rates after ART, and only a few groups are trying to discern whether these techniques leave a subtle legacy in offspring [18]. According to the last report from the European Society of Human Reproduction and Embryology (ESHRE), one of the steepest increases in treatment numbers was observed in the transfer of cryopreserved embryo (+13.6%), placing this technique as the second most commonly used in fertility treatments [19].

This indispensable tool in infertility laboratories maximizes the efficacy of ovarian stimulation cycles by allowing storage of the excess embryos and their later use, as well as enabling fertility preservation [20]. However, while the vast majority of studies mentioned above evaluated the effects of techniques that try to imitate physiological conditions, such as *in vitro* fertilisation (IVF) or *in vitro* culture (IVC), cryopreservation procedures involve gamete/embryo exposure to potentially toxic cryoprotectant solutions and sub-zero temperatures [20]. Our recent study has demonstrated that each technique involved in a vitrified embryo transfer procedure (i.e., embryo vitrification-warming and embryo transfer) has an additive effect over the short- and long-term offspring development [15]. Then, negative synergies can exist when more than one stressor is present, with more severe preimplantation stress precipitating more deviant phenotypes [7–9,15]. Thereby, in most studies, all negative effects are considered jointly as part of the ART protocol. In this context, arguably the most pressing question in the DOHaD field is identifying how the molecular changes occurring secondary to ART exposures alter the growth and metabolic trajectories across the life course, to better know their biological relevance. Based on several omics approaches, ART practitioners are increasingly trying to elucidate the molecular mechanisms whereby these developmental changes arise after embryo manipulation (reviewed in [7,21]). Therefore, here we develop a rabbit model to assess the synergic effects of whole *in vitro* manipulations during a vitrified embryo transfer procedure, as clinical operation, studying both its phenotypic and molecular long-term effects.

## 5.2. MATERIALS AND METHODS

All chemicals, unless otherwise stated, were reagent-grade and purchased from Sigma-Aldrich Química S.A. (Alcobendas, Madrid, Spain).

### 5.2.1 Animals and ethical statements

Californian breed rabbits were used throughout the experiment [42]. All experiments complied with the Directive 2010/63/EU EEC and institutional guidelines of the Universitat Politècnica de València Ethical Committee. All animals were bred and euthanised in an approved animal facility (code: ES462500001091). Experimental protocols were conducted under the supervision of the animal welfare committee in charge of this animal facility (code: 2018/VSC/PEA/0116). An authorisation certificate issued by the Valencian governmental administration for experimentation on animals is held by XGD (code: 2815), FMJ (code: 2273) and JSV (code: 0690).

### 5.2.2. Vitrified embryo transfer procedure

Embryo vitrification and warming steps were adapted from the highly efficient protocol developed previously to cryopreserve rabbit embryos by vitrification [23,24]. This protocol allows the survival of >80% of the warmed embryos, having generated thousands of descendants in our laboratory since its implementation [24]. Briefly, vitrification was achieved in two steps. In the first step, embryos were placed for 2 min in a solution consisting of 10% (v/v) dimethyl sulfoxide (DMSO) and 10% (v/v) ethylene glycol (EG). In the second step, embryos were suspended for 1 min in a solution of 20% DMSO and 20% EG. Then, embryos suspended in vitrification medium were loaded into 0.125 mL plastic straws (French sterile ministraw; IMV Technologies, L'Aigle, France), which were sealed and plunged directly into liquid nitrogen to achieve vitrification. For warming, embryos were placed in 2 mL of 0.33 M sucrose at 25 °C to remove cryoprotectants and washed 5 min later. After warming, embryos were bilaterally transferred into the oviducts of pseudopregnant foster mothers by laparoscopy (10–14 embryos per female), following the protocol described by Besenfelder and Brem [25]. Ovulation was induced with an intramuscular dose of 1 µg of buserelin acetate (Suprefact, Hoechst Marion Roussel S.A, Madrid, Spain) 68–72 h before transfer. Briefly, foster mothers were anaesthetized with xylazine (5 mg/kg; Rompun; Bayern AG, Leverkusen, Germany) intramuscularly and ketamine hydrochloride (35 mg/kg; Imalgene 1000; Merial S.A, Lyon, France) intravenously and placed in Trendelenburg's position. Then, embryos were loaded in a 17G epidural catheter, which was inserted through a 17G epidural needle into the inguinal region. Finally, monitoring the process by single-port laparoscopy, the catheter was introduced in the oviduct through the infundibulum to release the embryos. Both embryo vitrification and transfer processes used in this experiment were described in detail recently [24].

### 5.2.3. Experimental design

Figure 5.1 illustrates the experimental design. Two experimental groups were developed and compared to study the effects of the entire vitrified embryo transfer (VET) operation: one from vitrified embryos transferred to the foster mothers (vitrified-transferred group: VT) and the other without any embryo manipulations (naturally conceived group: NC). Non-consanguineous healthy adult males and females with proven fertility were used to constitute both experimental groups. A total of 27 females were inseminated with the semen of unrelated males. Ovulation was induced with an intramuscular injection of 1 µg of buserelin acetate (Suprefact, Hoechst Marion Roussel S.A, Madrid, Spain). After three days, embryos from 13 females were recovered, vitrified-warmed and transferred into 13 foster mothers. Finally, a total of 158 vitrified-warmed embryos were transferred (95.3% survival rate after warming), generating 69

VT animals at birth (average litter size of  $5.3 \pm 0.64$ ). Meanwhile, the NC group was generated using the remaining 14 females, which were maintained without any embryonic manipulation until the day of parturition.

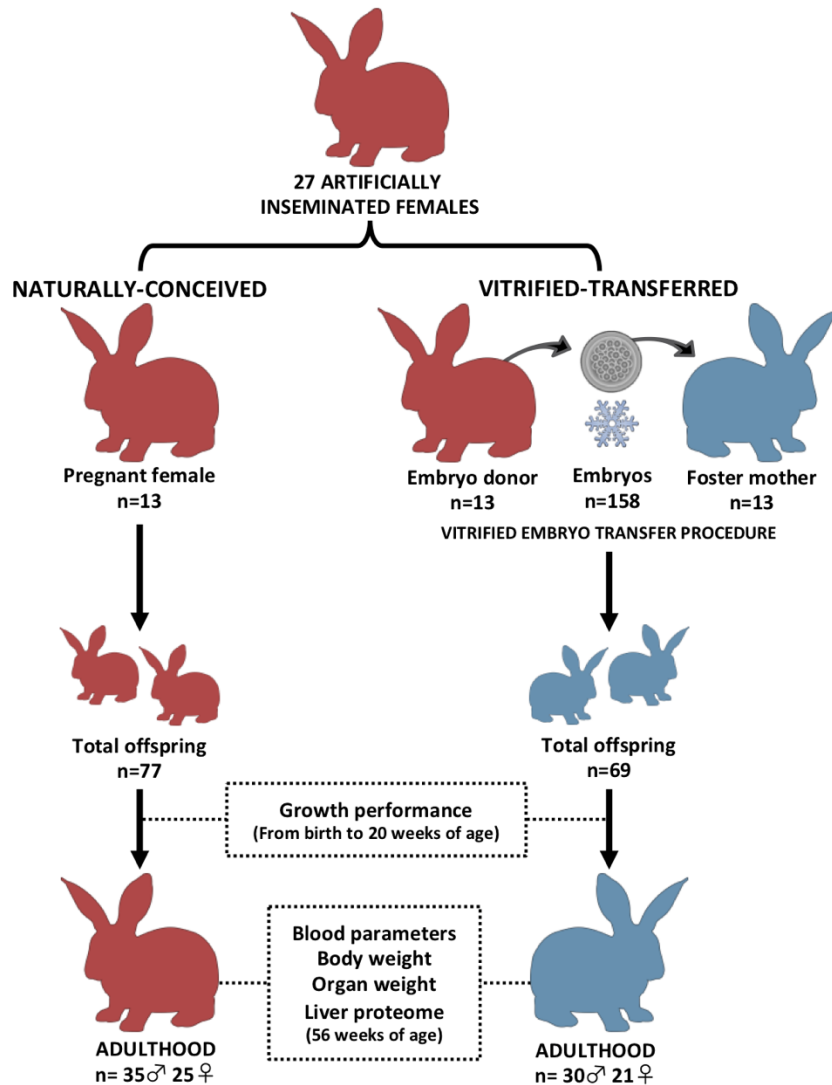


**Figure 5.1.** Experimental design. Two experimental progenies were developed and compared during development and in adulthood. Vitrified-transferred population arises from vitrified embryos; meanwhile naturally-conceived population was generated without embryo manipulations.

A total of 77 NC animals were obtained at birth (average litter size of  $5.5 \pm 0.62$ ). The average litter sizes are in line with previous studies using this rabbit line [26]. On the day of birth, offspring were weighed, sexed and microchipped. Until nine weeks of age, animals were randomly distributed and caged collectively (eight rabbits per cage), and then were individually kept in separate cages (flat deck indoor cages:  $75 \times 50 \times 40$  cm). Until adulthood (20 weeks of age), both sexes were followed to determine the effects of the VET over the postnatal growth. In late adulthood (56 weeks of age), several organs were obtained and weighed from male animals (organ weight study). Females were



excluded from this study, since they were mated once they reach the adult stage to obtain the F2 generation (see the next chapter). In addition, the use of males allows the reduction of confounding factors, as females are intrinsically more variable than males due to their cyclical reproductive hormones [27]. Liver tissue samples were also collected due to the liver's crucial role in growth and organ development from the foetal stage [28,29]. Then, a more in-depth study was done on this tissue, studying its proteomic signature to find molecular cues related to the phenotypic variations after VET.

#### **5.2.4. Growth performance during postnatal development**

A total of 65 males (30 from VT and 35 from NC group) and 46 females (21 from VT and 25 from NC group) were weighed weekly from 1 to 20 weeks of age. In each week, the body weight differences between the experimental groups were evaluated.

#### **5.2.5. Body weight and organ phenotypic comparison**

Males were euthanised by barbiturate overdose (125 mg/kg) injected intravenously at week 56 (late adulthood), when the growth plate was closed. Then, the body weight, organ (liver, lungs, heart, kidneys, adrenal glands, spleen and gonads) weights and fat tissue (perirenal and scapular) weight were determined.

#### **5.2.6. Determination of peripheral blood parameters**

Before euthanasia, 40 individual blood samples (20 from VT and 20 from NC animals) were taken from the central ear artery. Animals were selected randomly, keeping 1–2 animals of each litter (parity) within each experimental group. From each animal, two blood samples were taken. The first was dispensed into an EDTA-coated tube (Deltalab S.L., Barcelona, Spain) and the other into a serum-separator tube (Deltalab S.L., Barcelona, Spain). Blood count was performed from EDTA tubes at most 10 min after the collection using an automated veterinary haematology analyser MS 4e automated cell counter (MeletSchloesing Laboratories, Osny, France) according to the manufacturer's instructions. The blood parameters recorded were as follows: white blood cells, lymphocytes, monocytes, granulocytes, red blood cells, haemoglobin and haematocrit. From the second tube, biochemical analyses of the serum glucose, cholesterol, albumin, total bilirubin and bile acids were performed as hepatic metabolic indicators. Briefly, samples were immediately centrifuged at 3000× g for 10 min, and serum was stored at –20 °C until analysis. Then, glucose, cholesterol, albumin and total

bilirubin levels were analysed by enzymatic colorimetric methods, while bile acids were measured by photometry. All the methodologies were performed in an automatic chemistry analyser model Spin 200E (Spinreact, Girona, Spain), following the manufacturer's instructions. All samples were processed in duplicate.

### 5.2.7. Statistical analysis of phenotypic data

A general linear model (GLM) was fitted for the analysis of body weight in each week, organ weights and peripheral blood parameters, including the experimental group as fixed effect, and the biological and foster mother as random effects. Litter size was used as covariate for body weight correction since birth until adulthood, although it remained non-significant from the third week of age. In the case of organ weights, data were corrected using body weight as a covariate. The growth rate was estimated by nonlinear regression using the Gompertz curve equation, well suited for rabbits [15,30]:  $y = a \exp(-b \exp(-kt))$ , where  $y$  is the observed body weight of one individual at a specific age ( $t$ ). The rest of the parameters ( $a$ ,  $b$  and  $k$ ) of the Gompertz function have a biological interpretation,  $k$  being the parameter related to the rate of maturing (growth rate). The growth curves were plotted using the estimated parameters. Data were expressed as least-squares means  $\pm$  standard error of means. Differences of  $p < 0.05$  were considered significant. All statistical analyses were performed with SPSS 21.0 software package (SPSS Inc., Chicago, Illinois, USA).

### 5.2.8. Comparative proteomic analysis

A total of 8 individual samples (4 VT and 4 NC) were taken from adult rabbit males (selected randomly from different litters), retrieving some liver biopsies from the same organ (one individual, one sample). The uniformity of the liver tissue (four major cell types, of which hepatocytes constitute  $\approx 70\%$  of the total liver cell population) facilitates the sampling and data interpretation [31]. The samples were immediately washed with a phosphate-buffered saline solution to remove blood remnants and were directly flash-frozen in liquid nitrogen and stored at  $-80\text{ }^{\circ}\text{C}$  for the proteomic study. The proteome analyses were performed in the Proteomics Unit of the University of Valencia, Valencia, Spain (member of the PRB2-ISCIII ProteoRed Proteomics Platform). Proteins from liver biopsy were extracted in Lysis buffer (7M Urea, 2M thiourea, 4% CHAPS, 30 mM Tris pH 8.5) using 2D Grinding Kit (GE Healthcare, Chicago, IL, USA). Samples were quantified by an RC\_DC kit (BioRad, Hercules, CA, USA) according to the manufacturer's instructions.

First, we conducted a data-dependent acquisition (DDA) analysis to study the complete proteome by building up a spectral library using in-gel digestion and LC-MS/MS. The

complete proteome was analysed from a pool obtained by mixing aliquots with an equivalent amount of all the samples (100 µg in total) to build the spectral library from a 1D SDS PAGE gel. The carrier of the gel corresponding to the library was cut into three pieces, which were then digested with sequencing grade trypsin (Promega), as described elsewhere [32]. Gel slides were digested at 37 °C using 500 ng of trypsin. The digestion was stopped with 10% trifluoroacetic acid (TFA), and the supernatant (SN) was removed. Then, the library gel slides were dehydrated with pure acetonitrile (ACN). The new peptide solutions were combined with the corresponding SN. The peptide mixtures were dried in a speed vacuum and resuspended in 100 µL 2% ACN (v/v); 0.1% TFA (v/v). Five microliters of the digested fragments was loaded into a trap column (3 µm particle size C18-CL, 350 µm diameter × 0.5 mm long; Eksigent Technologies) and desalted with 0.1% TFA (v/v) at 3 µL/min for 5 min. The peptides were loaded into an analytical column (LC Column, 3 µm C18-CL, 75 µm × 12 cm, Nikkyo), and equilibrated in 5% ACN 0.1% formic acid (FAc) (v/v). Peptide elution was carried out with a linear gradient of 5 to 35% B for 90 min (A: 0.1% FAc (v/v); B: ACN, 0.1% FAc (v/v)) at a flow rate of 300 nL/min. Peptides were analysed in a mass spectrometer nanoESI qTOF (5600 TripleTOF, ABSCIEX, Alcobendas, Madrid, Spain). The tripleTOF was operated in information-dependent acquisition mode, in which a 250 ms TOF MS scan from 350 to 1250 m/z was performed, followed by 150 ms product ion scans from 350 to 1500 m/z on the 25 most intense 2–5 charged ions. The rolling collision energy equations were set for all ions as for 2+ ions according to the following equations:  $|CE| = (\text{slope}) \times (m/z) + (\text{intercept})$ .

After that, analysis of individual samples was carried out by LC-SWATH-MS acquisition. To determine quantitative differences in liver protein composition among our experimental rabbit progenies, the SWATH analysis of individual liver samples was performed. Thus, 20 µg of total protein extracted from each sample was loaded in the 1D SDS PAGE, and the carrier corresponding to each sample was digested with sequencing-grade trypsin (Promega), as described elsewhere [32], using 500 ng of trypsin for each sample, and digestion was set to 37 °C. The trypsin digestion was stopped with 10% TFA (v/v), the SN was removed and the library gel slides were dehydrated with pure ACN. The new peptide solutions were combined with the corresponding SN. The peptide mixtures were dried in a speed vacuum and resuspended in 25 µL of 2% ACN (v/v); 0.1% TFA (v/v). Five microliters of each sample was loaded into a trap column (3 µm particles size 18-CL, 350 µm diameter × 0.5 mm long; Eksigent Technologies) and desalted with 0.1% TFA (v/v) at 3 µL/min for 5 min. The peptides were loaded into an analytical column (LC Column, 3 µm C18-CL, 75 µm × 12 cm, Nikkyo), equilibrated in 5% ACN (v/v) 0.1% FAc (v/v). Peptide elution was carried out with a linear gradient of 5 to 35% B in 120 min (A: 0.1% FAc (v/v); B: ACN, 0.1% FAc (v/v)) at a flow rate of 300 nL/min. The tripleTOF was operated in SWATH mode, in which a 0.050 s TOF MS scan from 350 to 1250 m/z was performed, followed by 0.080 s product ion scans from 350 to 1250 m/z (3.05 s/cycle). The SWATH windows used were as follows: 15 Da

window widths from 450 to 1000 Da, 37 windows. Collision energy was set to optimum energy for a 2+ ion, and the mass spectrometer was always operated in high-sensitivity mode.

For protein identification, validation and quantification, data were analysed as follows. After library LC-MS/MS, the SCIEX.wiff data-files were processed using ProteinPilot v5.0 search engine (AB SCIEX, Alcobendas, Madrid, Spain). The Paragon algorithm (5.0.2.0, 5174) of ProteinPilot was used to search against the Uniprot Mammalia protein sequence database (1,376,814 proteins searched) with the following parameters: trypsin specificity, cys-alkylation, without taxonomy restriction, and the search effort set to through and false discovery rate (FDR) correction for proteins [33]. To avoid using the same spectral evidence in more than one protein, the identified proteins were grouped based on MS/MS spectra by the Protein-Pilot Pro Group™ Algorithm, regardless of the peptide sequence assigned. The protein within each group that could explain the most spectral data with confidence was depicted as the primary protein of the group. The resulting Protein-Pilot group file was loaded into PeakView® (v2.1, AB SCIEX, Alcobendas, Madrid, Spain), and peaks from SWATH runs were extracted with a peptide confidence threshold of 95% confidence and a FDR less than 1%. The number of peptides per protein was set at 50, and six transitions per peptide were necessary to quantify one peptide. Modified peptides were excluded. After peptide detection, peptides were aligned among different samples using peptides detected at high confidence from the library. The extracted ion chromatograms were integrated, and the areas were used to calculate the total protein quantity. The mass spectrometry proteomics data were deposited with the ProteomeXchange Consortium via the PRIDE [34] partner repository with the dataset identifiers PXD016677 (SWATH data) and PXD016874 (Spectral Library data).

The quantitative data obtained by PeakView® were analysed using MarkerView® (v1.2, AB SCIEX). Normalization of the calculated areas was done by summing total areas. A t-test was used to identify the differentially expressed proteins (DEPs) among the two experimental groups (VT and NC). Proteins were considered differentially expressed with an adjusted p-value  $\leq 0.05$ . Rabbit (*Oryctolagus cuniculus*) identifiers were obtained using the Blast tool from UniProt, keeping the output with the high-identity score. Principal component analysis (PCA) and Heat-Map (HM) clustering were performed using ClustVis (<https://biit.cs.ut.ee/clustvis/>). Functional descriptive pie charts of DEPs were obtained from the Panther web tool (<http://pantherdb.org/>) using *Homo sapiens* as a reference and the human orthologous gene names (obtained from Biomart-Ensembl web tool: <https://www.ensembl.org/info/data/biomart/index.html>) as input data. Functional annotation of DEPs, enrichment analysis of their associated “Gene Ontology” (GO) terms and “Kyoto Encyclopedia of Genes and Genomes” (KEGG) pathways analysis were computed using the free available bioinformatics software

DAVID Functional Annotation Tool (<https://david.ncicrf.gov/home.jsp>; version 6.8), considering a P-value (modified Fisher's exact test, EASE score) of less than 0.05.

## 5.3. RESULTS

### 5.3.1. Postnatal growth and body weight

At parturition, animals from the vitrified-transferred (VT) group showed higher birth weight than those from the naturally conceived (NC) group. There was no interaction between treatment and sex. Mean birth weights were  $67.8 \pm 1.46$  and  $60.5 \pm 1.72$  g for VT and NC males, respectively ( $p < 0.05$ ), using the covariate litter size ( $6.9 \pm 0.38$ , significant effect at  $p < 0.05$ ). In the case of females, the mean birth weights were  $63.3 \pm 1.71$  and  $58.1 \pm 1.45$  g for VT and NC groups, respectively ( $p < 0.05$ ), using the covariate litter size ( $6.7 \pm 0.28$ , significant effect at  $p < 0.05$ ). However, VT animals showed reduced growth until adulthood compared to those NC (Figure 5.2).

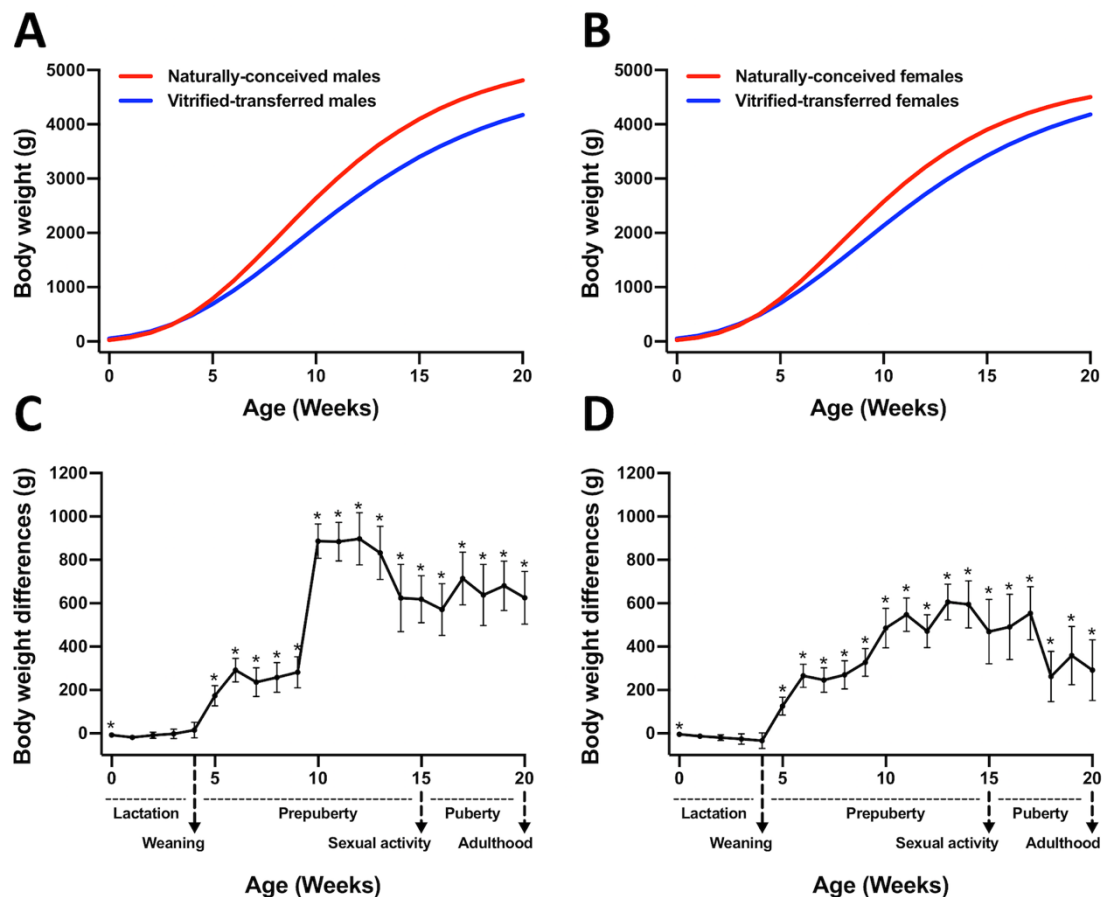


**Figure 5.2.** Growth curves and differences in body weight between animals derived from vitrified-transferred embryos (VT) and those naturally conceived (NC). Growth curves were fitted using the Gompertz equation for [A] males (NC vs VT) and [B] females (NC vs VT). Differences in body weight for [C] males and [D] females were computed as NC-VT. Asterisks denote significant differences in body weight.

Hence, the parameters governing the Gompertz growth curve established that the growth velocity (*k* parameter) was lower in the VT compared with the NC group, both in males ( $0.16 \pm 0.005$  VT vs  $0.20 \pm 0.007$  NC,  $p < 0.05$ , Figure 5.2A) and females ( $0.17 \pm 0.005$  VT vs  $0.21 \pm 0.004$  NC,  $p < 0.05$ , Figure 5.2B). Therefore, weaned animals showed significant mean weight differences between groups (NC-VT  $\pm$  standard error) from 5 to 9 weeks of age:  $248.0 \pm 20.98$  g for males (Figure 5.2C) and  $246.8 \pm 56.11$  g for females (Figure 5.2D). From this age, the mean weight differences between groups still increased until adulthood (from 10 to 20 weeks of age), being  $724.6 \pm 117.54$  g for males (Figure 5.2C) and  $466.4 \pm 113.64$  g for females (Figure 5.2D).

### 5.3.2. Body weight and organ phenotype at adulthood

At 56 weeks of age, VT males showed lower (7.0%) body weight compared to its NC counterparts (Table 5.1). No differences were observed in the body composition in terms of fat tissue amount (Table 5.1). Moreover, the VT group showed lower liver (9.1%) and heart (13%) weights, even after data were corrected by body weight (Table 5.1). No significant weight differences were observed for the rest of the analysed organs.

**Table 5.1.** Body weight and dissection data of adult males derived from vitrified-transferred embryos and those naturally conceived.

TRAITS	Naturally conceived (n=35)	Vitrified-transferred (n=30)
<b>Body Weight (Kg)</b>	$5.7 \pm 0.10^a$	$5.3 \pm 0.11^b$
<b>Perirenal fat (g)</b>	$173.7 \pm 11.09$	$184.2 \pm 12.13$
<b>Scapular fat (g)</b>	$58.9 \pm 5.32$	$66.1 \pm 5.99$
<b>Kidneys (g)</b>	$22.7 \pm 0.45$	$22.3 \pm 0.42$
<b>Liver (g)</b>	$102.1 \pm 2.51^a$	$92.8 \pm 2.37^b$
<b>Spleen (g)</b>	$1.4 \pm 0.08$	$1.3 \pm 0.07$
<b>Lungs (g)</b>	$25.6 \pm 1.20$	$26.7 \pm 1.13$
<b>Heart (g)</b>	$13.1 \pm 0.40^a$	$11.4 \pm 0.42^b$
<b>Gonads (g)</b>	$6.2 \pm 0.36$	$6.9 \pm 0.34$
<b>Adrenal Glands (g)</b>	$0.6 \pm 0.04$	$0.7 \pm 0.03$

n represents the number of animals. All organ/tissue weights were corrected using the body weight as a covariate. Data are expressed as least-square means  $\pm$  standard error of means. <sup>a,b</sup> Values in the same row with different superscript are significantly different ( $p < 0.05$ ).

### 5.3.3. Peripheral blood parameters (healthy status)

As shown in Table 5.2, there were no significant differences in the peripheral blood cells profile between NC and VT rabbit males. Attending to the serum biochemical data, higher levels of albumin and lower levels of cholesterol were exhibited by the VT animals ( $p < 0.05$ ). However, these levels ranged between the normal values in rabbits [35,36].

**Table 5.2.** Haematological and biochemical comparison between peripheral blood of animals derived from a vitrified embryo transfer procedure (vitrified-transferred) and those naturally conceived (naturally conceived).

PERIPHERAL BLOOD PARAMETERS	Naturally conceived (n=20)	Vitrified-transferred (n=20)
<b>HAEMATOLOGY</b>		
White blood cells ( $10^3/\text{mm}^3$ )	9.7 ± 0.77	8.7 ± 0.77
Lymphocytes (%)	42.6 ± 3.14	41.8 ± 3.14
Monocytes (%)	4.2 ± 0.844	5.1 ± 0.844
Granulocytes (%)	42.5 ± 2.71	45.9 ± 2.71
Red blood cells ( $10^6/\text{mm}^3$ )	6.0 ± 0.14	6.1 ± 0.14
Haemoglobin (g/dL)	12.5 ± 0.32	12.7 ± 0.32
Haematocrit (%)	42.4 ± 1.27	42.3 ± 1.27
<b>SERUM METABOLITES<sup>†</sup></b>		
Albumin (g/dL)	4.2 ± 0.05 <sup>b</sup>	4.4 ± 0.05 <sup>a</sup>
Bile acids ( $\mu\text{mol/L}$ )	7.2 ± 0.87	6.9 ± 0.87
Cholesterol (mg/dL)	40.1 ± 2.09 <sup>a</sup>	31.7 ± 2.09 <sup>b</sup>
Glucose (mg/dL)	127.7 ± 9.41 <sup>b</sup>	141.4 ± 9.41 <sup>a</sup>
Bilirubin total (mg/dL)	0.1 ± 0.01	0.1 ± 0.01

n represents the number of animals. Data are expressed as least-square means ± standard error of means. <sup>a,b</sup> Values in the same row with different superscript are significantly different ( $p < 0.05$ ). <sup>†</sup> Serum indicators of the hepatic function.

### 5.3.4. Comparative study of the liver proteome

The complete spectral library included 28,685 MS/MS spectra corresponding to 14,737 distinct peptides and 1846 proteins with a FDR  $\leq 1\%$ . With the restrictions used for extraction parameters of the areas, 1491 proteins (FDR  $< 1\%$ ) were quantified in the eight samples. Protein data analysis identified 77 differentially expressed proteins (DEPs) in *Oryctolagus cuniculus* taxonomy. PCA and Heat-Map analysis showed that, despite expected individual variability, samples from each group were clustered together (Figure 5.3).

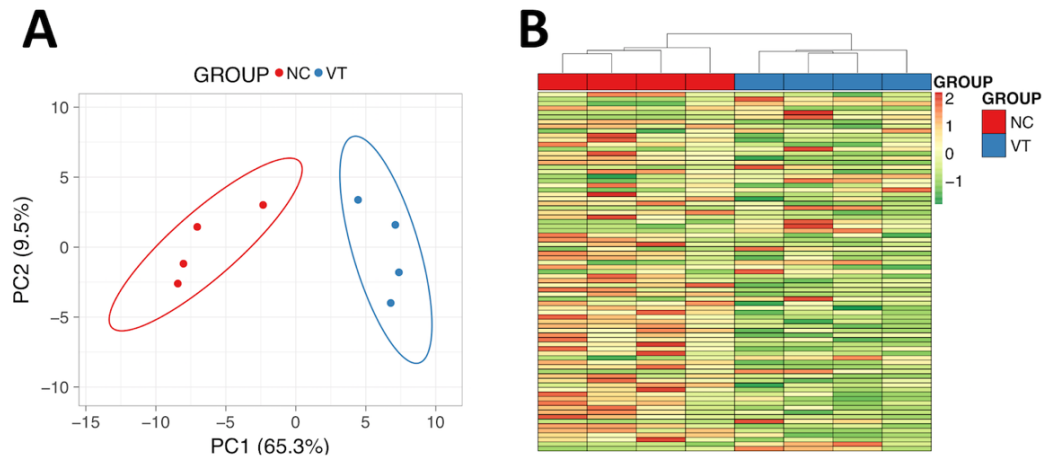


**Figure 5.3.** Molecular analysis of liver samples obtained from adult males derived from vitrified-transferred embryos (VT) and naturally-conceived animals (NC). [A] Principal Component Analysis (PCA) of the proteome. [B] Heat Map clustering of the proteome. Note: The representation of sample variability between the experimental groups was performed, taking into account only the differentially expressed proteins.

From these DEPs, there was a higher number of downregulated (56/77, 72.7%) than upregulated (21/77, 27.3%) in VT samples compared to the NC group. Of the proteins that were significantly different, a total of 66 DEPs were recognised by the DAVID software. Notably, 80% of these DEPs had catalytic/binding activity and 60% are involved in cellular/metabolic process, mainly (76%) in cell and organelles (Annex I, Supplementary Figure S1). Annotation of DEPs and the fold change values obtained are shown in Annex I (Supplementary Table S1). Functional GO term enrichment and KEGG pathway analysis of DEPs were recorded in Annex I (Supplementary Table S2). The most relevant metabolic alteration denoted by the protein profile was that related to the oxidative phosphorylation, suggesting an impaired oxidative metabolism in the mitochondria. Furthermore, hints of dysregulation in the zinc and lipid metabolism were identified.

## 5.4. DISCUSSION

Here, we describe for the first time an integrative study that evaluates and correlates the long-term consequences of the entire vitrified embryo transfer (VET) procedure at the phenotypic and proteomic levels. We observed that individuals born after VET showed a diminished growth rate and lower vital organ weights. Moreover, our findings derived from the hepatic proteomic analysis revealed a significant metabolic reprogramming, leading to changes in the oxidative phosphorylation and dysregulation in the zinc and lipid metabolism. Altogether, our results represent firm evidence of the



developmental plasticity exhibited by mammalian embryos in response to *in vitro* stressors, which results in irreversible phenotypic and developmental variations.

In humans, the first baby born after VET was born only 36 years ago, so the long-term impact of this procedure remains unknown [37]. Here, long-term effects after VET have been demonstrated even though our model is a simplified reality of the usual human process. Today, VET procedures are a primary component of ART cycles [19], and although it can be lethal to some embryos, this technique was considered neutral for survivors for a long time [38]. However, decades ago, some studies began to doubt the innocuousness of this technique [16,38,39]. Recently, we have proven that embryo cryopreservation has an additive effect over those attributable to the *ex vivo* embryo handle during the transfer procedure, both in the short- and long-term offspring development [15]. As *in vitro* embryo handling and transfer are mandatory techniques of the VET clinical service [24], here we compared VT vs. NC animals to comprise the consequences of the whole VET protocol. Supporting this proposal, it has been reported that when different stressors are present, these can act synergistically inducing more adverse effects [7–9,15]. Thereby, in most studies, all adverse effects are commonly considered jointly as part of the ART protocol [9]. First of all, we observed that VT animals exhibited higher body weight at parturition, which was consistent with our previous findings [15,40] and the health outcomes reported in humans [41,42] after VET. Intriguingly, the most dramatic ART effect in cattle and sheep is known as large offspring syndrome, characterised by a large size at birth and increased birth weight [9,43]. Imprinting modifications of some growth-related genes have also been suggested to explain these observed variations [9,30,41,43].

However, although birth deviations are usually re-established through compensatory growth in rabbits [44], VT animals showed a diminished body weight throughout life in comparison with NC animals. Furthermore, we observed that these weight differences were maintained until adulthood, although the body fat was similar between the two experimental groups. Therefore, differences in body weight confirmed a lower growth performance in VT animals, which agreed with previous studies carried out in rabbits undergoing VET [15,30,39]. Concordantly, previous studies have demonstrated that the nature of the preimplantation environment during ART can program development, affecting postnatal growth and phenotype [7,14,45–47]. Notably, although the pattern of postnatal growth alteration in VT animals was similar in both sexes, males duplicated body weight differences between VT and NC compared to the females at the age of 20 weeks. During preimplantation development, male and female embryos may display phenotypic differences that can be attributed to their different sex chromosome complements [48]. This sex asymmetry reflects that preimplantation embryos are already poised to respond differentially to environmental changes in a sex-specific fashion [46,48]. It may explain the frequent sex bias observed in various models of

DOHaD and developmental reprogramming after ART [7,16,46,49]. Based on this evidence, we hold that the postnatal growth trajectory after VET in Californian rabbits is sexually dimorphic, which is in contrast with our previous data derived from New Zealand rabbits [15]. Supporting this, it has been reported that several phenotypes linked to ART are condition-specific and sexually dimorphic, but also strain-specific [7]. Phenotypic variation by strain could be attributed to differences in both genetic code and regulatory mechanisms (e.g., epigenetics), which depends on genetic background. Therefore, the strain is a critical variable in how embryos might differentially respond to similar ART conditions and display different postnatal phenotypes. In this article, we also have shown that animals born after VET exhibit lower liver and heart weights. Alterations in the same organs have been previously described after IVC and VET [30,50,51]. As ART, including embryo cryopreservation [40,52], has been associated with placental alterations, it could be the reason explaining liver disturbances after VET, as decreased materno-fetal nutrition during gestation induces reduced liver mass and perturbed liver function [53]. Besides, liver disturbances could affect the heart, given the strong interaction between both organs' physiologies [54].

The role of the liver in organ growth and development is well documented [28,29]. As the 'omics' sciences are used to describe the flow of biological information in an organism, we examined the hepatic proteomic signature to find out an explanation for the phenotypic differences after VET. Functional analysis revealed five DEPs (*G1SR29*, *G1SEH7*, *G1TZQ6*, *G1TQG1*, *G1SKT4*) involved in oxidative phosphorylation (OXPHO) with an average abundance two times lower in VT animals, suggesting a lower OXPHO activity. As mitochondrial OXPHO is the primary source of ATP to support life and development, OXPHO troubles are found in most diseases related to growth alteration, short stature and dwarfism [55–59], which could explain the diminished growth in VT animals. Concordantly, Feuer et al. [14] also demonstrated that IVF and IVC promoted postnatal growth reduction, correlated with mitochondrial dysfunction and systemic oxidative stress. Evidence of mitochondrial and OXPHO dysfunction has been described in embryos after IVF and cryopreservation [8,60], as well as in adult IVF livers [7]. Here, we provide the first proteomic evidence of OXPHO alterations in adult livers after VET. Besides, we found upregulation in five DEPs (*G1TY06*, *G1TNI4*, *G1T3R4*, *G1T295*, *P04068*) related to the detoxification mechanisms of cytochrome P450, with the first two having glutathione transferase activity. Glutathione transferase activity is one of the main cellular mechanisms to tackle the damage from reactive oxygen species and, together with the P450 enzymes, are involved in the hepatic drug metabolism pathways [61,62]. Then, the upregulation of these proteins could be indicative of high hepatic detoxification requirements in an organism with oxidative metabolic disturbances. We can, therefore, envision a cardinal role for mitochondria in the reprogramming mechanism by which preimplantation stressors induce postnatal alterations, since oxidative stress seems to be ubiquitously present in ART tissues [7].

An in-depth analysis revealed five (*G1TUC2*, *G1TYY5*, *G1TPL7*, *G1U6X6*, *G1SYT7*) downregulated Zn-binding proteins in VT animals. It is known that transcriptional mechanisms are present to reduce gene expression of Zn-binding proteins when zinc is limiting, thus conserving Zn for more essential functions [63]. Therefore, these data suggested a weakened Zn metabolism in VT animals, which could be related with its diminished growth performance. Supporting this, a recent study has reported that serum Zn content was lower in ART children, who were shorter than the naturally conceived counterparts, as Zn is required for healthy growth [64]. In addition, we recorded seven DEPs (*G1SKT4*, *G1U032*, *G1U9R4*, *G1TCQ2*, *G1T3R4*, *G1TSY8*, *G1SZH0*) involved in lipid and fatty acid metabolism. There is evidence demonstrating ART-induction of modifications in the lipid metabolism in embryonic [8], fetal [65] and adult [14,49] stages, suggesting that ART offspring were less efficient in their use of internal lipids for ATP production, probably due to altered mitochondrial function. Particularly, associated functional terms revealed that *G1U9R4* participates in the regulation of the cholesterol biosynthetic process and its metabolism, so its downregulation after VET might explain the lower serum cholesterol levels exhibited by VT animals. This fact agreed with previous studies reporting disturbances of steroid metabolism in the placenta, fetal liver and adult serum and tissues (including liver) after ART [8,14,66,67].

However, despite some phenotypic and physiological changes appearing in VT animals, this progeny appeared healthy, sustained by the peripheral blood results in adulthood. Although some serum markers of hepatic function varied significantly between VT and NC, it remained within the standard values in rabbits. Besides, no striking difference was detected either during the management of both VT and NC animals or during the dissection study. Therefore, as no signs of disease were detected in VT animals, we hold that differences observed in the VT offspring can be partially attributed to a possible selection of cryo-resistant embryos, which originate a subpopulation with intrinsic differences compared to the general population [15]. In addition, it is well accepted that ART incurs environmental stressors during embryo development, triggering embryonic response mechanisms that can result in phenotypic variation later in life. These variations are attributed to the embryonic developmental plasticity [3,4], which refers to the capacity of a genotype to produce different phenotypes in response to environmental changes, contributing to diversity among individuals, populations and species. Reprogramming and developmental plasticity are believed to be mediated by epigenetic changes, which can persist into subsequent generations [6,13]. Therefore, future studies should determine the transgenerational inheritance of the VET effects.

## 5.5. CONCLUSION

In conclusion, *in vitro* embryo manipulation throughout vitrification and transfer procedures causes long-term effects on growth rate, body weight and vital organ weights at adulthood. Furthermore, molecular data obtained from the hepatic tissue are related to these phenotypic changes, paving the way to finding molecular markers and pathways that enhance the knowledge of long-lasting ART effects, their detection and their health relevance. With more novel ARTs waiting on the horizon, this study should represent a significant step towards promoting a paradigm shift in the characterization of long-term consequences of ARTs in adulthood. Taking into account that the long-term effects of ART are specific to each procedure, tissue, sex or species, a systems biology perspective might be the way to elucidate the adaptive mechanisms of embryos during ART procedures.

## 5.6. REFERENCES

- [1]. Crawford GE, Ledger WL. In vitro fertilisation/intracytoplasmic sperm injection beyond 2020. *BJOG An Int J Obstet Gynaecol* 2019;126(2):237–43.
- [2]. Findlay JK, Holland MK, Wong BBM. Reproductive science and the future of the planet. *Reproduction* 2019;158(3):R91–6.
- [3]. Vrooman LA, Bartolomei MS. Can assisted reproductive technologies cause adult-onset disease? Evidence from human and mouse. *Reprod Toxicol* 2017;68:72–84.
- [4]. Roseboom TJ. Developmental plasticity and its relevance to assisted human reproduction. *Hum Reprod* 2018;33:546–52.
- [5]. Fleming TP, Watkins AJ, Velazquez MA, Mathers JC, Prentice AM, Stephenson J, et al. Origins of lifetime health around the time of conception: causes and consequences. *Lancet* 2018;391(10132):1842–52.
- [6]. Feuer S, Rinaudo P. From Embryos to Adults: A DOHaD Perspective on In Vitro Fertilization and Other Assisted Reproductive Technologies. *Healthcare* 2016;4:E51.
- [7]. Feuer SK, Rinaudo PF. Physiological, metabolic and transcriptional postnatal phenotypes of in vitro fertilization (IVF) in the mouse. *J Dev Orig Health Dis* 2017;8:403–10.
- [8]. Duranthon V, Chavatte-Palmer P. Long term effects of ART: What do animals tell us? *Mol Reprod Dev* 2018;85:348–68.
- [9]. Ramos-Ibeas P, Heras S, Gómez-Redondo I, Planells B, Fernández-González R, Pericuesta E, et al. Embryo responses to stress induced by assisted reproductive technologies. *Mol Reprod Dev* 2019;86:1292–306.
- [10]. Chen M, Heilbronn LK. The health outcomes of human offspring conceived by assisted reproductive technologies (ART). *J Dev Orig Health Dis* 2017;8:388–402.

- [11]. Novakovic B, Lewis S, Halliday J, Kennedy J, Burgner DP, Czajko A, et al. Assisted reproductive technologies are associated with limited epigenetic variation at birth that largely resolves by adulthood. *Nat Commun* 2019;10(1):3922.
- [12]. Belva F, Bonduelle M, Roelants M, Michielsen D, Van Steirteghem A, Verheyen G, et al. Semen quality of young adult ICSI offspring: The first results. *Hum Reprod* 2016;31:2811–20.
- [13]. Calle A, Fernandez-Gonzalez R, Ramos-Ibeas P, Laguna-Barraza R, Perez-Cerezales S, Bermejo-Alvarez P, et al. Long-term and transgenerational effects of in vitro culture on mouse embryos. *Theriogenology* 2012;77:785–93.
- [14]. Feuer SK, Liu X, Donjacour A, Lin W, Simbulan RK, Giritharan G, et al. Use of a mouse in vitro fertilization model to understand the developmental origins of health and disease hypothesis. *Endocrinology* 2014;155:1956–69.
- [15]. Garcia-Dominguez X, Vicente JS, Marco-Jiménez F. Developmental Plasticity in Response to Embryo Cryopreservation: The Importance of the Vitrification Device in Rabbits. *Animals* 2020;10(5):804.
- [16]. Dulioust E, Toyama K, Busnel MC, Moutier R, Carlier M, Marchaland C, et al. Long-term effects of embryo freezing in mice. *Proc Natl Acad Sci U S A* 1995;92:589–93.
- [17]. Fischer B, Chavatte-Palmer P, Viebahn C, Santos AN, Duranthon V. Rabbit as a reproductive model for human health. *Reproduction* 2012;144(1):1–10.
- [18]. Servick K. Unsettled questions trail IVF's success. *Science (80- )* 2014;345:744–6.
- [19]. De Geyter C, Calhaz-Jorge C, Kupka MS, Wyns C, Mocanu E, Motrenko T, et al. ART in Europe, 2015: results generated from European registries by ESHRE. *Hum Reprod Open* 2020;2020:hoz038.
- [20]. Sparks AET. Human embryo cryopreservation-methods, timing, and other considerations for optimizing an embryo cryopreservation program. *Semin Reprod Med* 2015;33:128–44.
- [21]. Feuer SK, Liu X, Donjacour A, Simbulan R, Maltepe E, Rinaudo PF. Transcriptional signatures throughout development: the effects of mouse embryo manipulation in vitro. *Reproduction* 2017;153(1):107–122.
- [22]. Estany J, Camacho J, Baselga M, Blasco A. Selection response of growth rate in rabbits for meat production. *Genet Sel Evol* 1992;24:527–37.
- [23]. Vicente JS, Viudes-De-Castro MP, García ML. In vivo survival rate of rabbit morulae after vitrification in a medium without serum protein. *Reprod Nutr Dev* 1999;39(5–6):657–62.
- [24]. Garcia-Dominguez X, Marco-Jimenez F, Viudes-de-Castro MP, Vicente JS. Minimally invasive embryo transfer and embryo vitrification at the optimal embryo stage in rabbit model. *J Vis Exp* 2019;147:e58055.
- [25]. Besenfelder U, Brem G. Laparoscopic embryo transfer in rabbits. *J Reprod Fertil* 1993;99:53–6.

- [26]. Vicente JS, Llobat L, Viudes-de-Castro MP, Lavara R, Baselga M, Marco-Jiménez F. Gestational losses in a rabbit line selected for growth rate. *Theriogenology* 2012;77:81–8.
- [27]. Zucker I, Beery AK. Males still dominate animal studies. *Nature* 2010;465:690.
- [28]. Kineman RD, del Rio-Moreno M, Sarmiento-Cabral A. 40 years of IGF1: Understanding the tissue-specific roles of IGF1/IGF1R in regulating metabolism using the Cre/loxP system. *J Mol Endocrinol* 2018;61:T187–98.
- [29]. Adamek A, Kasprzak A. Insulin-like growth factor (IGF) system in liver diseases. *Int J Mol Sci* 2018;19:E1308.
- [30]. Lavara R, Baselga M, Marco-Jiménez F, Vicente JS. Embryo vitrification in rabbits: Consequences for progeny growth. *Theriogenology* 2015;84:674–80.
- [31]. Ding C, Li Y, Guo F, Jiang Y, Ying W, Li D, et al. A cell-type-resolved liver proteome. *Mol Cell Proteomics* 2016;15(10):3190–202.
- [32]. Shevchenko A, Wilm M, Vorm O, Mann M. Mass spectrometric sequencing of proteins from silver-stained polyacrylamide gels. *Anal Chem* 1996;68(5):850–8.
- [33]. Shilov I V., Seymour SL, Patel AA, Loboda A, Tang WH, Keating SP, et al. The paragon algorithm, a next generation search engine that uses sequence temperature values sequence temperature values and feature probabilities to identify peptides from tandem mass spectra. *Mol Cell Proteomics* 2007;6(9):1638–55.
- [34]. Perez-Riverol Y, Csordas A, Bai J, Bernal-Llinares M, Hewapathirana S, Kundu DJ, et al. The PRIDE database and related tools and resources in 2019: Improving support for quantification data. *Nucleic Acids Res* 2019;47:D442–50.
- [35]. Moore DM, Zimmerman K, Smith SA. Hematological Assessment in Pet Rabbits: Blood Sample Collection and Blood Cell Identification. *Clin Lab Med* 2015;35(3):617–27.
- [36]. Fiorello C V, Divers SJ. Rabbits. In: Carpenter JW (James W, editor. *Exotic Animal Formulary*. Elsevier Inc.; 2013. p. 546–95.
- [37]. Kamel RM. Assisted reproductive technology after the birth of Louise Brown. *J Reprod Infertil* 2013;14(3):96–109.
- [38]. Auroux M, Cerutti I, Ducot B, Loeuillet A. Is embryo-cryopreservation really neutral? A new long-term effect of embryo freezing in mice: Protection of adults from induced cancer according to strain and sex. *Reprod Toxicol* 2004;18:813–8.
- [39]. Cifre J, Baselga M, Gómez EA, De La Luz GM. Effect of embryo cryopreservation techniques on reproductive and growth traits in rabbits. *Anim Res* 1999;48:15–24.
- [40]. Saenz-De-Juano MD, Marco-Jimenez F, Schmaltz-Panneau B, Jimenez-Trigos E, Viudes-De-Castro MP, Penaranda DS, et al. Vitrification alters rabbit foetal placenta at transcriptomic and proteomic level. *Reproduction* 2014;147:789–801.
- [41]. Spijkers S, Lens JW, Schats R, Lambalk CB. Fresh and Frozen-Thawed Embryo Transfer Compared to Natural Conception: Differences in Perinatal Outcome. *Gynecol Obstet Invest* 2017;82:538–46.

- [42]. Hann M, Roberts SA, D'Souza SW, Clayton P, Macklon N, Brison DR. The growth of assisted reproductive treatment-conceived children from birth to 5 years: A national cohort study. *BMC Med* 2018;16(1):224.
- [43]. Chen Z, Robbins KM, Wells KD, Rivera RM. Large offspring syndrome: A bovine model for the human loss-of-imprinting overgrowth syndrome Beckwith-Wiedemann. *Epigenetics* 2013;8(6):591–601.
- [44]. Gidenne T, Combes S, Feugier A, Jehl N, Arveux P, Boisot P, et al. Feed restriction strategy in the growing rabbit. 2. Impact on digestive health, growth and carcass characteristics. *Animal* 2009;3(4):509–15.
- [45]. Velazquez MA, Sheth B, Smith SJ, Eckert JJ, Osmond C, Fleming TP. Insulin and branched-chain amino acid depletion during mouse preimplantation embryo culture programmes body weight gain and raised blood pressure during early postnatal life. *Biochim Biophys Acta - Mol Basis Dis* 2018;1864(2):590–600.
- [46]. Donjacour A, Liu X, Lin W, Simbulan R, Rinaudo PF. In Vitro Fertilization Affects Growth and Glucose Metabolism in a Sex-Specific Manner in an Outbred Mouse Model. *Biol Reprod* 2014;90(4):80.
- [47]. Mahsoudi B, Li A, O'Neill C. Assessment of the Long-Term and Transgenerational Consequences of Perturbing Preimplantation Embryo Development in Mice. *Biol Reprod* 2007;77:889–96.
- [48]. Bermejo-Alvarez P, Rizos D, Lonergan P, Gutierrez-Adan A. Transcriptional sexual dimorphism during preimplantation embryo development and its consequences for developmental competence and adult health and disease. *Reproduction* 2011;141(5):563–70.
- [49]. Feuer SK, Donjacour A, Simbulan RK, Lin W, Liu X, Maltepe E, et al. Sexually dimorphic effect of In Vitro Fertilization (IVF) on adult mouse fat and liver metabolomes. *Endocrinology* 2014;155:4554–67.
- [50]. Fernández-Gonzalez R, Moreira P, Bilbao A, Jiménez A, Pérez-Crespo M, Ramírez MA, et al. Long-term effect of in vitro culture of mouse embryos with serum on mRNA expression of imprinting genes, development, and behavior. *Proc Natl Acad Sci U S A* 2004;101:5880–5.
- [51]. Calle A, Miranda A, Fernandez-Gonzalez R, Pericuesta E, Laguna R, Gutierrez-Adan A. Male Mice Produced by In Vitro Culture Have Reduced Fertility and Transmit Organomegaly and Glucose Intolerance to Their Male Offspring. *Biol Reprod* 2012;87:1–9.
- [52]. Riesche L, Bartolomei MS. Assisted Reproductive Technologies and the Placenta: Clinical, Morphological, and Molecular Outcomes. *Semin Reprod Med* 2018;36:240–8.
- [53]. Hyatt MA, Budge H, Symonds ME. Early developmental influences on hepatic organogenesis. *Organogenesis* 2008;4:170–5.
- [54]. Møller S, Bernardi M. Interactions of the heart and the liver. *Eur Heart J* 2013;34:2804–11.

- [55]. Peterside IE, Selak MA, Simmons RA. Impaired oxidative phosphorylation in hepatic mitochondria in growth-retarded rats. *Am J Physiol - Endocrinol Metab* 2003;285(6 48-6):E1258–66.
- [56]. Von Kleist-Retzow JC, Cormier-Daire V, Viot G, Goldenberg A, Mardach B, Amiel J, et al. Antenatal manifestations of mitochondrial respiratory chain deficiency. *J Pediatr* 2003;143(2):208–12.
- [57]. Hüttemann M, Lee I, Samavati L, Yu H, Doan JW. Regulation of mitochondrial oxidative phosphorylation through cell signaling. *Biochim Biophys Acta - Mol Cell Res* 2007;1773(12):1701–20.
- [58]. Gibson K, Halliday JL, Kirby DM, Yapfitee J, Thorburn DR, Boneh A. Mitochondrial oxidative phosphorylation disorders presenting in neonates: Clinical manifestations and enzymatic and molecular diagnoses. *Pediatrics* 2008;122(5):1003–8.
- [59]. Abu-Libdeh B, Douiev L, Amro S, Shahrour M, Ta-Shma A, Miller C, et al. Mutation in the COX4I1 gene is associated with short stature, poor weight gain and increased chromosomal breaks, simulating Fanconi anemia. *Eur J Hum Genet* 2017;25(10):1142–11146.
- [60]. Hara T, Kin A, Aoki S, Nakamura S, Shirasuna K, Kuwayama T, et al. Resveratrol enhances the clearance of mitochondrial damage by vitrification and improves the development of vitrifiedwarmed bovine embryos. *PLoS One* 2018;13(10):e0204571.
- [61]. Singh A, Prasad KN, Singh AK, Singh SK, Gupta KK, Paliwal VK, et al. Human Glutathione S-Transferase Enzyme Gene Polymorphisms and Their Association With Neurocysticercosis. *Mol Neurobiol* 2017;54(4):2843–51.
- [62]. Almazroo OA, Miah MK, Venkataramanan R. Drug Metabolism in the Liver. *Clin Liver Dis* 2017;21(1):1–20.
- [63]. Bird AJ. Cellular sensing and transport of metal ions: Implications in micronutrient homeostasis. *J Nutr Biochem* 2015;26:1103–15.
- [64]. Xia X ru, Jiang SW, Zhang Y, Hu Y fang, Yi H gang, Liu J, et al. Serum levels of trace elements in children born after assisted reproductive technology. *Clin Chim Acta* 2019;495:664–9.
- [65]. Li B, Xiao X, Chen S, Huang J, Ma Y, Tang N, et al. Changes of Phospholipids in Fetal Liver of Mice Conceived by In Vitro Fertilization1. *Biol Reprod* 2016;94(5):105.
- [66]. Guo XY, Liu XM, Jin L, Wang TT, Ullah K, Sheng JZ, et al. Cardiovascular and metabolic profiles of offspring conceived by assisted reproductive technologies: a systematic review and meta-analysis. *Fertil Steril* 2017;107:622–31.
- [67]. Miles HL, Hofman PL, Peek J, Harris M, Wilson D, Robinson EM, et al. In vitro fertilization improves childhood growth and metabolism. *J Clin Endocrinol Metab* 2007;92(9):3441–5.



## **ACKNOWLEDGEMENTS**

This work was supported by funds from the Ministry of Economy and Competitiveness of Spain (AGL2017-85162-C2-1-R and AGL2014-53405-C2-1-P). Ximo Garcia-Dominguez was supported by a research grant from the Ministry of Economy and Competitiveness (BES-2015-072429). The authors would like to thank Oreto Antunez and Luz Valero, from the Proteomics Unit of the University of Valencia for his help during the proteomic study, and Neil Macowan Language Services for revising the English version of the manuscript.



## CHAPTER IV

# **LONG-TERM AND TRANSGENERATIONAL PHENOTYPIC, TRANSCRIPTIONAL AND METABOLIC EFFECTS IN RABBIT MALES BORN FOLLOWING VITRIFIED EMBRYO TRANSFER**

X. Garcia-Dominguez<sup>1</sup>, F. Marco-Jiménez<sup>1</sup>, D.S. Peñaranda<sup>1</sup>,  
G. Diretto<sup>2</sup>, V. García-Carpintero<sup>3</sup>, J. Cañizares<sup>3</sup>, J.S. Vicente<sup>1</sup>

<sup>1</sup>Institute for Animal Science and Technology (ICTA), Laboratory of Reproductive Biotechnology, Universitat Politècnica de València, 46022 Valencia, Spain

<sup>2</sup>National Agency for New Technologies, Energy and Sustainable Economic Development (ENEA), Casaccia Research Centre, 00123 Rome, Italy

<sup>3</sup>Institute for the Conservation and Breeding of Agricultural Biodiversity (COMAV-UPV), Universitat Politècnica de València, 46022 Valencia, Spain

**Accepted in *Scientific Reports***

(June 12, 2020)



### ABSTRACT

The advent of assisted reproductive technologies (ART) in mammals involved an extraordinary change in the environment where the beginning of a new organism takes place. Under *in vitro* conditions, in which ART is currently being performed, it likely fails to mimic optimal *in vivo* conditions. This suboptimal environment could mediate in the natural developmental trajectory of the embryo, inducing lasting effects until later life stages that may be inherited by subsequent generations (transgenerational effects). Therefore, we evaluated the potential transgenerational effects of embryo exposure to the vitrified embryo transfer procedure in a rabbit model on the offspring phenotype, molecular physiology of the liver (transcriptome and metabolome) and reproductive performance during three generations (F1, F2 and F3).

The results showed that, compared to naturally-conceived animals (NC group), progeny generated after embryo exposure to the cryopreservation-transfer procedure (VT group) exhibited lower body growth, which incurred lower adult body weight in the F1 (direct effects), F2 (intergenerational effects) and F3 (transgenerational effects) generations. Furthermore, VT animals showed intergenerational effects on heart weight and transgenerational effects on liver weight. The RNA-seq data of liver tissue revealed 642 differentially expressed transcripts (DETs) in VT animals from the F1 generation. Of those, 133 were inherited from the F2 and 120 from the F3 generation. Accordingly, 151, 190 and 159 differentially accumulated metabolites (DAMs) were detected from the F1, F2 and F3, respectively. Moreover, targeted metabolomics analysis demonstrated that transgenerational effects were mostly presented in the non-polar fraction. Functional analysis of molecular data suggests weakened zinc and fatty acid metabolism across the generations, associated with alterations in a complex molecular network affecting global hepatic metabolism that could be associated with the phenotype of VT animals. However, these VT animals showed proper reproductive performance, which verified a functional health status. In conclusion, our results establish the long-term transgenerational effects following a vitrified embryo transfer procedure. We showed that the VT phenotype could be the result of the manifestation of embryonic developmental plasticity in response to the stressful conditions during ART procedures.



## 6.1. INTRODUCTION

Since the birth of the first test-tube baby in 1978, the use of assisted reproductive technologies (ARTs) has increased notably. Globally, ART use has doubled over the last decade, with a progressive rise in banking cycles in which all embryos are frozen for future ART cycles [1]. However, ART fails to mimic the optimal *in vivo* conditions due to the lack of knowledge regarding the dynamic regulation across the maternal womb [2,3]. Nowadays, it is well accepted that in responding to environmental cues the embryo demonstrates a high degree of developmental plasticity, modulating its metabolism, gene expression and phenotype [4]. But although this embryo adaptation is thought to increase short-term survival in suboptimal environments during ART, several studies have associated this embryo developmental deviation with adverse consequences later in life (Developmental Origins of Health and Disease theory), as has been extensively described in humans [5–11]. Furthermore, evidence of similar effects has been reported in animal studies, which avoid confounding factors related to parent infertility or other conditions such as lifestyle that further complicate interpretation of the data [5,11–15].

However, it has been hypothesised that under extreme conditions, embryo reprogramming is likely to be the result of a direct perturbation of the process, rather than an embryo adaptation to suboptimal conditions. The underlying assumption is that depending on the nature of the *in vitro* manipulation, the embryo could be differentially impacted, leading to different phenotype outcomes in later life stages [4,5,11–15]. Embryo cryopreservation requires embryo exposure to an environment with toxic chemical agents and extremely low non-physiological temperatures, in which they have no intrinsic ability to survive [16]. So, it has been shown that some developmental changes could emerge following vitrified embryo transfer in the foetus and postnatal life [17–24]. In this context, we have established that each technique required in a vitrified embryo transfer procedure (i.e. embryo vitrification-warming and embryo transfer) produces an additive effect *per se* over the short- and long-term offspring development [24]. In particular, we also showed that the choice of the vitrification device is not a trivial decision, as different cooling-warming rates induced specific developmental responses [24]. However, *in vitro* embryo handling and transfer are fundamental techniques of the clinical operation in a vitrified embryo transfer procedure (VET) [7,11,25]. Then, when different stressors are present, these can act synergistically, inducing more negative effects [13]. To cover this possibility, we recently described a study where the offspring born from cryopreserved-transferred embryos were compared with those conceived naturally [26]. This study was the first demonstrating that VET incur long-term phenotypic consequences correlated with molecular signatures. In the era of “omic” technologies, several studies are trying to elucidate the molecular mechanisms whereby these phenotypic and physiologic

changes occur after embryo manipulation [14,15]. Epigenetic alterations, derived from a disturbed embryo reprogramming due to *in vitro* suboptimal conditions, have been proposed as causes of some long-term and heritable ART effects [5,27–30].

Historically, fertility researchers have been trying to improve the success of ART based on the birth rate increase, but only a few are trying to discern whether ART leaves a subtle legacy in the offspring [31]. Thus, limited knowledge is available on the long-term effects of ART, and the studies assessing its heritability are almost non-existent. Therefore, to our best knowledge, there is a lack of knowledge about how an embryo VET may change the offspring features, and how these effects can be transmitted through the germline and persevere in subsequent generations. Taking all these data into account, the aim in this work is to determine whether embryo exposure to a VET can alter offspring features and molecular signatures across three generations (transgenerational effects).

## **6.2. MATERIALS AND METHODS**

All chemicals, unless otherwise stated, were reagent-grade and purchased from Sigma-Aldrich Química SA (Alcobendas, Madrid, Spain).

### **6.2.1 Animals and ethical statements**

Californian breed rabbits were used for the experiment [32]. From 27, 20 and 20 parities, 146, 117 and 125 animals were generated in the F1, F2 and F3 generation, respectively. All experiments complied with the Directive 2010/63/EU EEC and institutional guidelines of the Universitat Politècnica de València Ethical Committee. All animals were bred and euthanised in an approved animal facility (code: ES462500001091). Experimental protocols were conducted under the supervision of the animal welfare committee in charge of this animal facility (code: 2015/VSC/PEA/00061). An authorisation certificate issued by the Valencian governmental administration to experiment on animals is held by XGD (code: 2815), FMJ (code: 2273) and JSV (code: 0690).

### **6.2.2. Experimental design**

Two experimental groups were established: one from vitrified embryos transferred to foster mothers (VT progeny) and another generated by natural conception (NC progeny). At birth, animals constituted the F1 generation, in which both VT and NC animals were compared to address the direct effects of the vitrified embryo transfer



procedure (VET). After that, the intergenerational effects were assessed in the F2 generation. Finally, the transgenerational effects were evaluated in the F3 generation, comparing the VT and NC progenies. This is because the direct effect of the VET was present in the embryos which formed the F1 generation and over the germline developing within the embryo that ultimately formed the F2 animals. Therefore, the F3 generation is the first not directly exposed to the VET [33]. Figure 6.1 illustrates the experimental design.

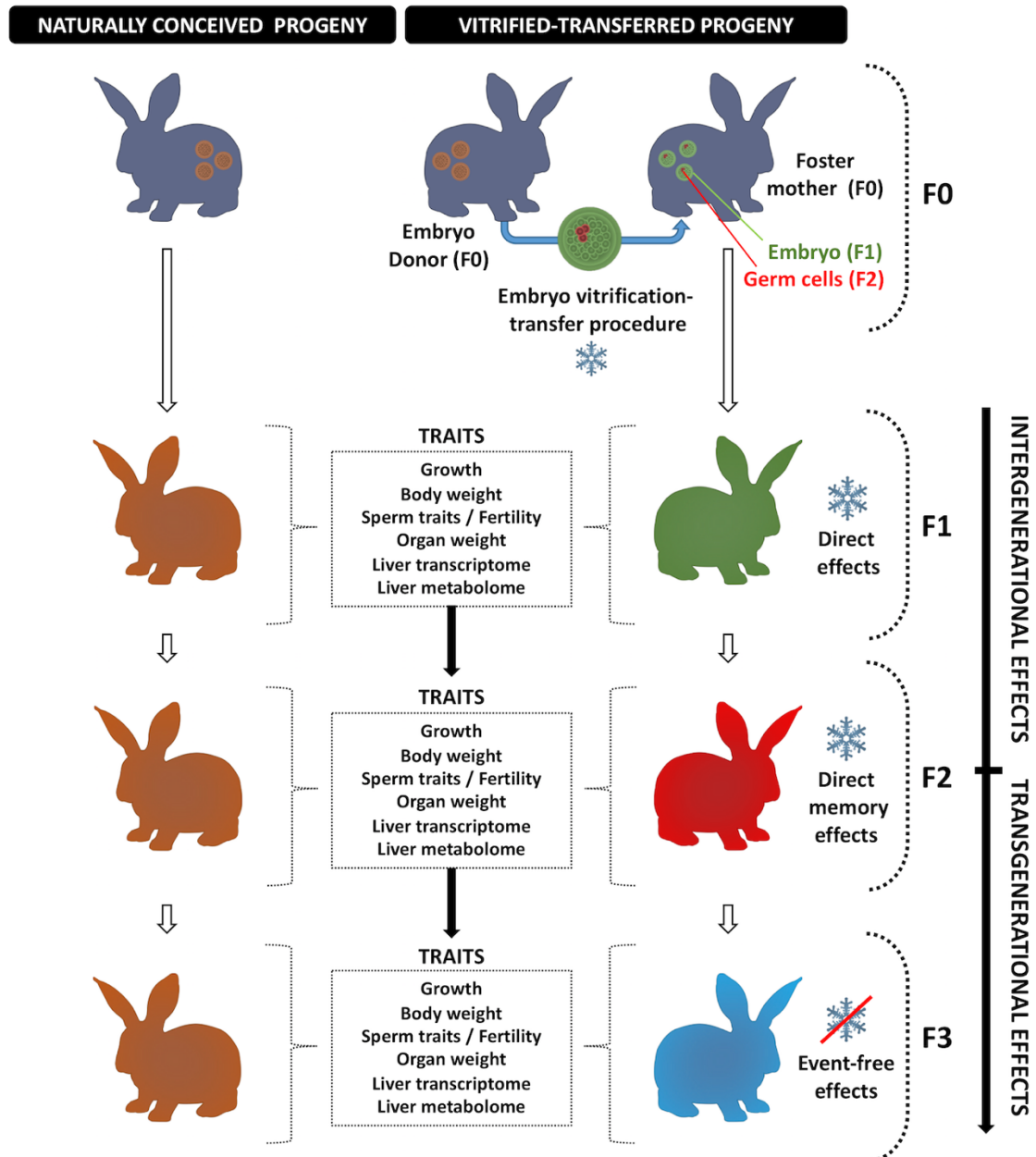


**Figure 6.1.** Experimental design. The experimental progenies were compared in each generation to assess the transgenerational effects of embryo vitrification procedure on body weight across the rabbit development. At adulthood, the seminal and fertility traits were evaluated. After that, animals were euthanised and the organs were weighed. Then, liver samples were collected to perform a molecular (transcriptomic and metabolomic) study.

The NC- and VT-F1 animals belonged from Garcia-Dominguez et al. [26] (chapter III). These animals constituted the founding generation from which F2 and F3 were here obtained. Briefly, a total of 27 females were artificially inseminated and ovulation was induced by an injection of 1 µg of buserelin acetate (Hoechst Marion Roussel, Madrid, Spain). In the VT group, from 13 females, 3-days embryos (late morulae-early blastocyst) were recovered, vitrified-warmed and transferred oviductally to 13 foster mothers (10-14 embryos per female). A total of 158 vitrified-warmed embryos were transferred (95.3% survival rate after warming). Meanwhile, for the NC population, contemporaneous animals were generated at birth from the remaining 14 females initially inseminated. The subsequent generations were generated respecting the experimental groups and following the common management of rabbit reproduction, without embryo vitrification or embryo transfer procedures. To establish the F2 generation, one mature female and one male were randomly selected from each parity produced in the F1 generation and, to reduce inbreeding, mating between animals with common grandparents was avoided. The F3 animals were generated equally from the F2 as described above. In rabbits, it has been demonstrated that an effective preservation of characteristics, such as growth rate and litter size, could be obtained with the offspring of 9 males from different reproductive groups (families), guaranteeing an inbreeding coefficient value of less than 1% per generation [34]. Considering F2 as a transient population towards F3 generation, only those necessary animals were kept until adulthood. On the contrary, as the effects of VET could be more diluted or evasive in the F3 generation, a larger number of F3 animals were maintained until adulthood. Animals of both progenies in each generation were housed in the same conditions throughout the experiment. Weaning took place at week 4. Until 9 weeks of age animals were caged collectively (8 rabbits per cage), and subsequently males were housed individually (flat deck indoor cages; 75×50×40 cm). In order to reduce confounding factors, the phenotypic and molecular analyses were restricted to males, as they are thought to be less variable due to their constant hormone levels [35]. However, F2- and F3-VT animals were obtained by crossing VT males and VT females from the previous VT generation, as inheritable VET effects could be transmitted through both genders.

### **6.2.3. Vitrified embryo transfer procedure**

Embryos were vitrified and warmed according to the highly efficient protocol developed previously to cryopreserve rabbit embryos by vitrification [25,36]. Briefly, vitrification was achieved in two steps. In the first step, embryos were placed for 2 min in a solution consisting of 10% (v/v) dimethyl sulfoxide (DMSO) and 10% (v/v) ethylene glycol (EG). In the second step, embryos were suspended for 1 min in a solution of 20% DMSO and 20% EG. Then, embryos suspended in vitrification medium were loaded into 0.125 mL plastic

straws, which were sealed and plunged directly into liquid nitrogen to achieve vitrification. Embryos were warmed in 2 mL of 0.33 M sucrose solution at 25 °C. After 5 min, the embryos were washed and scored, and only undamaged embryos (presenting homogenous cellular mass, mucin coat and spherical zona pellucida) were catalogued as transferable. Then, embryos were transferred into the oviduct of synchronous foster mothers by laparoscopy, following the protocol described by Besenfelder and Brem [25,37]. Briefly, foster mothers were anaesthetised and placed in Trendelenburg's position. Then, embryos were loaded in a 17G epidural catheter, which was inserted through a 17G epidural needle into the inguinal region. Finally, while the process was monitored by single-port laparoscopy, the catheter was introduced in the oviduct through the infundibulum to release the embryos.

#### **6.2.4. Growth, body weight and organ weight study**

Body weights from both progenies were compared in each generation at three relevant points of rabbit development: 4, 9 and 56 weeks of age, coinciding with the weaning, prepubertal and adulthood stages, respectively. Weights of both progenies (NC and VT) were compared in each generation. Furthermore, weights at 4th and 9th weeks comprise a period when the rabbit growth is exponential. Using these values, the average weight gain (AWG) was calculated to estimate the growth velocity. AWG was computed as [9th week weight – 4th week weight]/35 days. Finally, after the last weight was taken, adult males from both groups (65 F1, 22 F2 and 48 F3) were euthanised by barbiturate overdose (125 mg/kg) and the weights of liver, lungs, heart, kidneys, adrenal glands, spleen and gonads were recorded and compared. Scatterplots showing the phenotypic raw data distributions of both experimental groups before statistical analysis were plotted using GraphPad PRISM (8.3.0).

#### **6.2.5. Semen collection and sperm evaluation**

The procedure was conducted as previously described [38]. Briefly, in each generation, the training period for male rabbits (23 F1, 18 F2, and 28 F3 animals, distributed equitably between VT and NC groups) began with an artificial vagina at 18 weeks of age, collecting one ejaculate per week. At the 6th month of age, males were subjected to experimental evaluation. For 12 weeks, two ejaculates per male were collected weekly, with an interval of 30 min between collections. Ejaculates from the same male each day were pooled, and three 20 µL aliquots were taken. The first and second were diluted 1:20 with Tris-citrate-glucose extender (250 mM tris-hydroxymethylaminomethane, 83 mM citric acid, 50 mM glucose, pH 6.8–7.0, 300 mOsmkg<sup>-1</sup>). The first was assessed for individual sperm motility and motion parameters using the Integrated Semen

Analysis System version 1.0.17 (ISAS; Projectes i Serveis R + D). The system was set to record images at 25 frames/s. Then, 10  $\mu\text{L}$  of the sample was placed in a 10- $\mu\text{m}$  deep Makler counting chamber. Sperm motility was assessed at 37 °C at  $\times 200$  magnification using a negative phase-contrast microscope. For each sample, four microscopic fields were analysed, and a minimum of 200 sperm evaluated. The following sperm activity variables were assessed: sperm motility (%), progressive motility (%), curvilinear velocity (VCL,  $\mu\text{m s}^{-1}$ ), straight-line velocity (VSL,  $\mu\text{m s}^{-1}$ ), average path velocity (VAP,  $\mu\text{m s}^{-1}$ ), linearity coefficient (LIN; calculated as  $(\text{VSL}/\text{VCL}) \times 100$ , %), straightness coefficient (STR), wobble coefficient (WOB;  $\text{VSL}/\text{VAP} \times 100$ ), amplitude of lateral head displacement (ALH,  $\mu\text{m}$ ) and beat cross frequency (BCF, Hz). The second sample was assessed for the percentage of live spermatozoa (viability, VIA) using the LIVE/DEAD sperm viability kit (Molecular Probes), which basically consists of two DNA-binding fluorescent dyes: a membrane-permeant dye, SYBR-14, and a conventional dead-cell dye, propidium iodide. The third sample was also diluted 1:20 with 0.5% of glutaraldehyde solution in phosphate-buffered saline and observed by phase-contrast at  $\times 400$  magnification to calculate the concentration, in a Thoma-Zeiss counting cell chamber, and both the percentages of intact apical ridge and abnormal sperm were evaluated (based on morphological abnormalities of head, neck, mid-piece and tail). A total of 249, 134 and 255 ejaculates were evaluated in the F1, F2 and F3 generation, respectively.

#### **6.2.6. Fertility rate and number of liveborn**

The procedure was conducted as previously described [38]. Briefly, a total of 1260 inseminations (260 F1, 775 F2 and 225 F3, distributed equitably between VT and NC groups) using individual ejaculates adjusted to  $40 \times 10^6$  spermatozoa/mL were carried out. Each female was inseminated with 0.5 mL, which was performed within two hours of semen collection. At insemination time, females were injected intramuscularly with 1  $\mu\text{g}$  of buserelin acetate (Hoechst Marion Roussel, Madrid, Spain) to induce ovulation. Only receptive does (red colour of vulvar lips) were inseminated, using a standard curved plastic pipette (Imporvet, Barcelona, Spain). The number of does that gave birth (fertility rate) by the number of inseminations was recorded. Likewise, the number of liveborn per parity was annotated.

#### **6.2.7. Statistical analyses**

Descriptive statistics of the quantitative traits (litter size, body weight, growth, organ weights, sperm parameters and live born) were estimated with data from all generations (Annex II, Supplementary Table S1). After that, differences due to vitrified embryo transfer procedure on these traits in each generation were estimated using Bayesian inference [39]. This methodology is based on probabilities, providing great flexibility to

construct all kinds of confidence intervals with a chosen probability. In all cases, the progeny origin was included as a treatment with two levels (NC and VT) and the organ weights were corrected by the adult body weight of each animal. Bounded flat priors were used for all unknowns and the marginal posterior distributions were estimated by Gibbs sampling. After some exploratory analyses, results were based on Markov chain Monte Carlo chains consisting of 60,000 iterations, with a burn-in period of 10,000, and saving only 1 of every 10 samples for inferences. Summary statistics from the marginal posterior distributions were calculated directly from the samples saved. Convergence was tested using the Geweke Z criterion and Monte Carlo sampling errors were computed using time-series procedures. In all cases, Monte Carlo SE were small and lack of convergence was not detected by the Geweke test. The parameters obtained from the marginal posterior distributions of the phenotypic differences between experimental groups were the mean of the difference ( $D_{NC-VT}$ ; computed as NC-VT), the probability of the difference being greater than 0 when  $D_{NC-VT} > 0$  or lower than 0 when  $D_{NC-VT} < 0$  ( $P_0$ ), and the highest posterior density region at 95% of probability (HPD<sub>95%</sub>).  $D_{NC-VT}$  estimated the mean of the differences between NC and VT traits,  $P_0$  estimated the probability of  $D_{NC-VT} \neq 0$ , and HPD<sub>95%</sub> estimated the accuracy. Statistical differences were considered if  $|D_{NC-VT}|$  surpassed the relevant value (R; proposed as one-third of the SD of the trait) and  $P_0 > 0.8$  (80%). Statistics analysis were computed with the Rabbit program developed by the Institute for Animal Science and Technology (Valencia, Spain).

Differences due to vitrified embryo transfer procedure on fertility rate were assessed using a probit link model with binomial error distribution, according to a mixed model including the experimental group (NC vs VT) as fixed effect. Differences of  $p < 0.05$  were considered significant. These statistical analyses were performed by the SPSS statistical software package, version 21.0 (SPSS Inc., Chicago, Illinois, USA).

### 6.2.8. Transcriptomic analysis of the liver

After the euthanasia was performed, individual hepatic samples were collected (one individual, one sample). Finally, 23 liver samples were collected from the F1 (5 VT and 4 NC), F2 (3 VT and 3 NC) and F3 (4 VT and 4 NC) generations. Immediately, samples were washed with phosphate-buffered saline (PBS) and stored in RNAlater (Ambion Inc., Huntingdon, UK) at  $-20\text{ }^{\circ}\text{C}$  until the transcriptomic analysis. Total RNA of liver were extracted using Ambion (mirVana) and Qiagen (AllPrep) columns. The RNA quantity and quality were determined on a bioanalyser (Agilent Technologies), keeping samples with RIN values  $> 8$  and with  $> 3\text{ }\mu\text{g}$  of total RNA for sequencing. Then, samples were shipped to the MacroGen company (Seoul, South Korea). Afterwards, the mRNA purification was carried out using Sera-mag Magnetic Oligo (dT) Beads, followed by buffer

fragmentation. Reverse transcription was followed by PCR amplification to prepare the samples to be sequenced, keeping the strand information, in an Illumina HiSeq-4000[D1] sequencer (Illumina, San Diego, USA). Resulting raw sequences are available at the NCBI Sequence Read Archive (BioProject ID: PRJNA483096). Raw read qualities were assessed using FastQC software [40]. Only samples with good quality scores were maintained for the final analysis. Reads were mapped against the reference genome for *Oryctolagus cuniculus*, version 2.0 from Ensembl using HISAT2 [41]. Expression was counted using StringTie [42]. This counting was guided using the genome annotation, and a unified set of transcripts was created for the samples analysed. Then, a Fragments Per Kilobase of transcript per Million (FPKM) table with gene expression for each sample was generated and used to assess the expression profile of each sample by Principal Component Analysis (PCA): Annex II, Supplementary Figure S1. Then, a table with raw counts was generated. This table was used for the differential expression analyses using edgeR [43] integrated into the MeV package [44]. Only differentially expressed transcripts (DETs) with a threshold of a false discovery rate (FDR) of  $\leq 0.05$  were considered for further analyses. For comparison between groups, further filtering of DETs was performed. In those samples that registered a coefficient of variation higher than 50% and a difference between mean and median higher than 1, the gene was maintained if half of the samples of the most expressed condition group had an expression two times higher than the mean of the other group. ClustVis [45] software was used to perform the PCA of DETs. InteractiVenn [46] software was used for Venn diagram construction. Functional annotation of DETs, enrichment analysis of their associated GO terms and KEGG pathways analysis were computed using bioinformatics software: DAVID Functional Annotation Tool 6.8 [47], considering a P-value  $< 0.05$  (modified Fisher's exact test, EASE score).

### 6.2.9. Semi-polar and non-polar analysis of the liver metabolome

Targeted and untargeted liquid chromatography-electrospray ionization-high resolution mass spectrometry (LC-ESI-HRMS) analysis of the semi-polar metabolome were performed as previously described [48–50]. Targeted and untargeted liquid chromatography-atmospheric pressure chemical ionization-high resolution mass spectrometry (LC-APCI-HRMS) analysis of the non-polar metabolome were carried as reported before [51–53]. Untargeted metabolomics was performed using the SIEVE software (ThermoFisher scientific). Briefly, after chromatogram alignment and retrieval of all the detected frames (e.g. ions), differentially accumulated metabolites (DAMs) were detected by a statistical analysis (one-way ANOVA plus Tukey's pairwise comparison) using the SPSS software (SPSS Inc., Chicago, Illinois, USA). Differences of  $p \leq 0.05$  were considered significant. PCA of untargeted metabolomes was performed using the ClustVis [45] software. Targeted metabolite identification was performed by

comparing chromatographic and spectral properties with authentic standards (if available) and reference spectra, in house database, literature data, and on the basis of the  $m/z$  accurate masses, as reported in the Pubchem database (<http://pubchem.ncbi.nlm.nih.gov/>) for monoisotopic mass identification, or on the Metabolomics Fiehn Lab Mass Spectrometry Adduct Calculator (<http://fiehnlab.ucdavis.edu/staff/kind/Metabolomics/MS-Adduct-Calculator/>) in the case of adduction detection. Finally, DAMs were detected as described above. Metabolites were quantified relatively by normalisation on the internal standard (formononetin and DL- $\alpha$ -tocopherol acetate) amounts. For each experimental group, 3 independent biological replicates, consisting of 4 animals each, were analysed in each generation. For each biological replicate, at least one technical replicate was carried out.

## 6.3. RESULTS

### 6.3.1. Establishment of the two experimental progenies (VT vs NC) across the three generations (F1, F2, F3)

After the transfer of 158 vitrified-warmed embryos from 13 donors into 13 foster mothers, 69 VT animals were generated. In addition, 77 NC animals were generated from 14 pregnant females (Table 6.1). The progeny produced by these methodologies (F1) were mated over two subsequent generations without embryo manipulations and respecting each experimental group (VT, NC), producing F2 and F3 animals.

**Table 6.1.** Efficiency in the establishment of the naturally-conceived and vitrified-transferred progenies across three generations (F1, F2, F3).

GENERATION		Naturally conceived	Vitrified-transferred
F1	Founding Parities	14	13
	Litter Size	5.5 $\pm$ 0.62	5.3 $\pm$ 0.64
	Live Births	77	69
	Adult Males	35	30
F2	F1 Parities	10	10
	Litter Size	6.1 $\pm$ 0.76	5.6 $\pm$ 0.76
	Live Births	61	56
	Adult Males	13	9
F3	F2 Parities	10	10
	Litter Size	6.1 $\pm$ 0.89	6.4 $\pm$ 0.89
	Live Births	61	64
	Adult Males	24	24

Mating between individuals with common grandparents was avoided. Thus, 56 VT and 61 NC animals constituted the F2 generation, and 64 VT and 61 NC formed the F3 generation (Table 6.1). There were no differences in litter size between VT and NC

animals in each generation (Table 6.1). Thus, embryo VET did not affect the gross reproductive performance of VT progeny, compared to animals that were generated without embryo manipulations (NC). Descriptive data and statistical details were annotated in Annex II (Supplementary Table S1 and Supplementary Table S2).

### 6.3.2. Growth performance, body weight and organ phenotype study

Comparing the growth (AWG) between VT and NC animals, we noticed that VT progeny exhibited an apparent reduction in growth velocity ( $-8.6 \pm 1.34$  g/day in F1,  $-4.7 \pm 2.31$  g/day in F2 and  $-6.6 \pm 1.39$  g/day in F3). Scatterplots showing the phenotypic raw data distributions of both experimental groups before statistical analysis are shown in Figure 6.2. As expected, the higher effect of the VET over the growth velocity was observed in F1, where VT animals already showed a reduced body weight at the time of weaning ( $-62.2 \pm 37.82$  g, Figure 6.3). However, in prepuberty, the reduction in the body weight was patent in VT animals of all three generations ( $-370.1 \pm 77.42$  g in F1,  $-139.3 \pm 122.76$  g in F2 and  $-287.9 \pm 70.67$  g in F3) compared to the NC group (Figure 6.3). This growth trend was maintained until adulthood, where VT animals showed a lower body weight ( $-437.4 \pm 153.43$  g in F1,  $-249.5 \pm 209.20$  g in F2 and  $-247.9 \pm 194.91$  g in F3) in comparison to the NC group (Figure 6.3).

Moreover, the VT group accumulated high probabilities ( $P_0 \geq 0.80$ ) of phenotypic (weight) changes in some organs during the study, whose variation pattern depends on the organ and generation. However, statistical relevant differences were observed only in the liver and heart (Figure 6.3). The liver showed the highest probability of change throughout generations ( $P_0=0.99$  in F1,  $P_0=1.00$  in F2, and  $P_0=1.00$  in F3), even after data were corrected for body weight (Annex II: Supplementary Table S2). VT progeny exhibited lower liver weight ( $-9.3 \pm 3.56$  g) in F1, which was aggravated ( $-12.7 \pm 3.54$  g) in F2 animals. However, this trend was inverted in the F3 generation ( $16.1 \pm 4.99$  g). Attending to the heart phenotype, VT animals showed a reduced organ weight in the F1 ( $-1.5 \pm 0.73$  g), also aggravated in F2 ( $-3.1 \pm 1.87$  g). However, no differences in the heart weight were observed in F3 between VT and NC animals. As specific cases, increased weight was observed in F2 for the lungs ( $3.7 \pm 3.75$  g) and in F3 for the spleen ( $0.2 \pm 0.10$  g). Descriptive data of the phenotypic traits were annotated in Annex II (Supplementary Table S1), and the statistical details were annotated in Annex II (Supplementary Table S2).



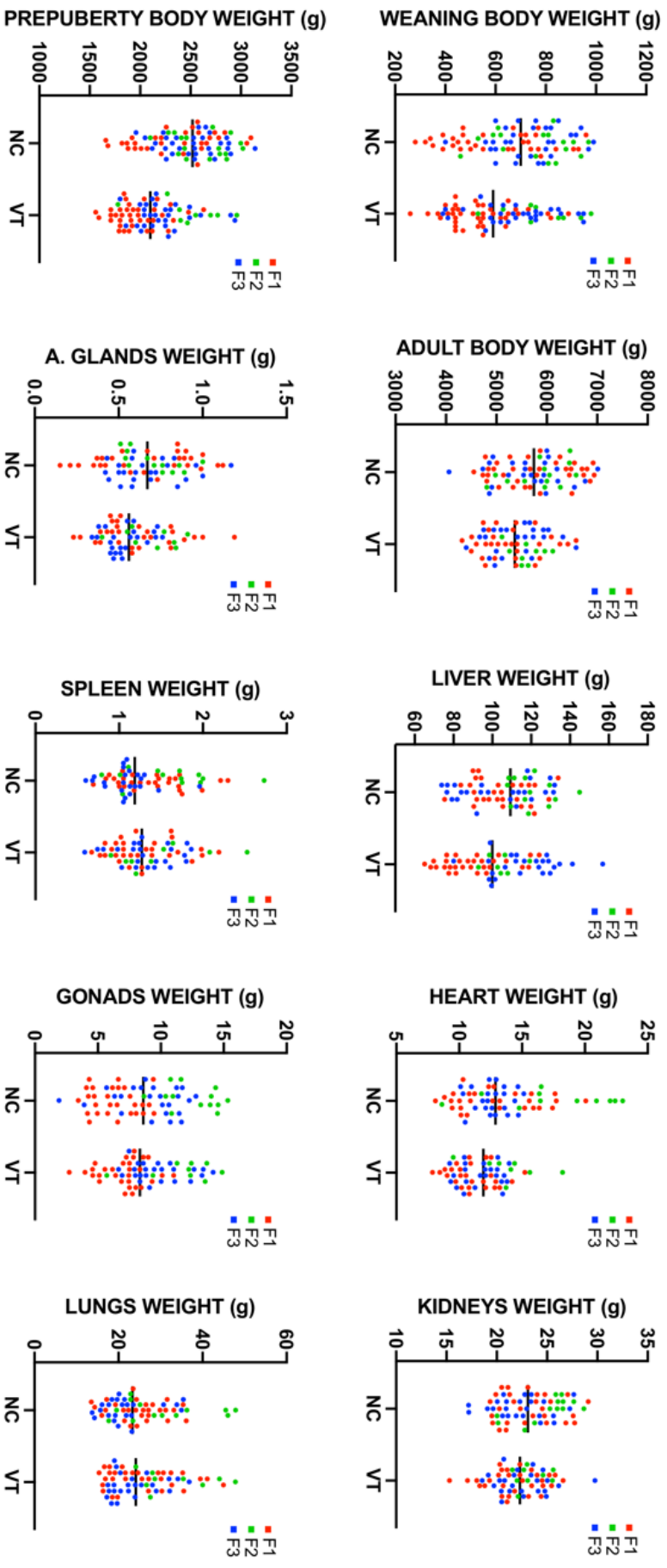


**Figure 6.2.** Scatterplots showing the phenotypic raw data distributions of naturally-conceived (NC) and vitrified-transferred (VT) progenies during three generations (F1, F2, F3).

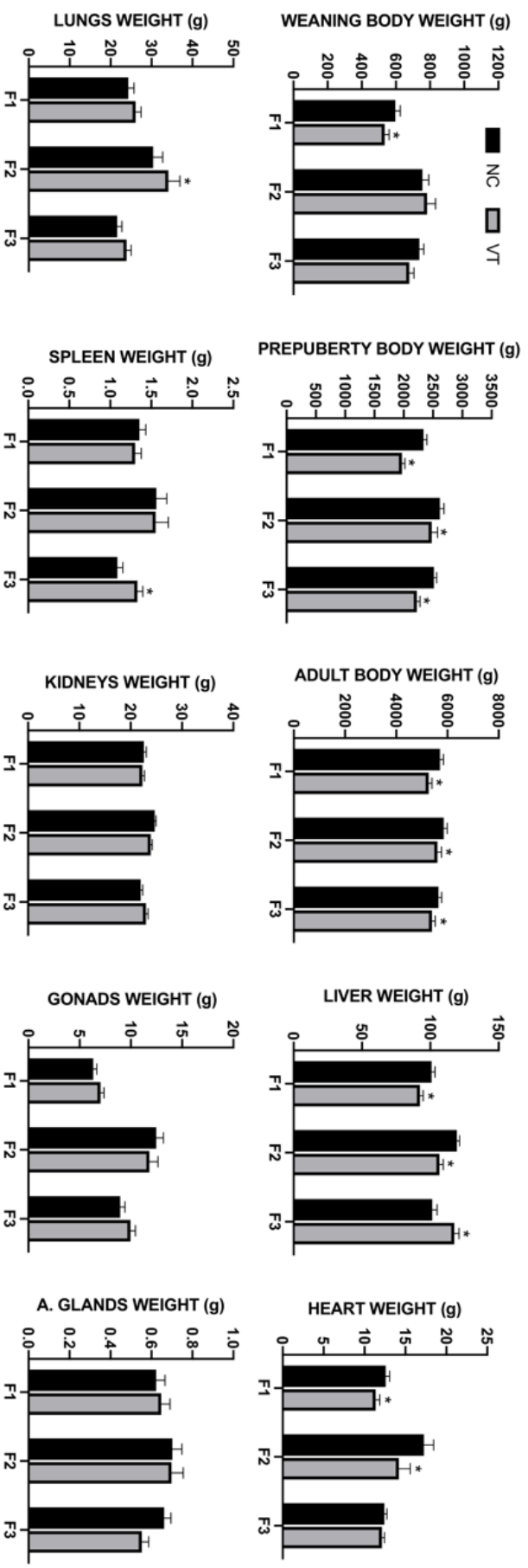


**Figure 6.3.** Differences in phenotypic traits between naturally-conceived (NC) and vitrified-transferred (VT) progenies during three generations (F1, F2, F3). Asterisks denote relevant differences between VT animals and their NC counterparts (Bayesian inference:  $|D_{NCVT}| > R$  and  $P_0 > 0.8$ ).

### 6.3.3. Sperm and fertility rate assessment

Even though no differences in the size of the gonads were observed in any generation, higher ejaculate volumes were produced by VT animals from the F1 and F2 generation. However, an increment in sperm production (TSE) was only observed in F2-VT animals, which also showed lower abnormal sperm percentage (ABN) than their NC counterparts. Attending to the motion parameters, F1-VT animals produced sperm with higher curvilinear velocity (VCL), straight-line velocity (VSL) and average path velocity (VAP). Meanwhile, F3-VT animals showed lower VCL. Results of seminal parameters were annotated in Table 6.2.

Nevertheless, unequivocally, these variations were biologically irrelevant, as no differences were observed in the fertility rate ( $44.1 \pm 1.41\%$ ) in the three generations. Since no experimental group nor generation effect was detected, data were considered together. Besides, we found that VET causes a consistent increase in the number of liveborn in the three generations ( $6.4 \pm 0.30$  VT vs  $4.9 \pm 0.22$  NC). No effect of generation was detected, so data were considered together for the experimental groups. Descriptive data of these traits were annotated in Annex II (Supplementary Table S1), and the statistical details were annotated in Annex II (Supplementary Table S3).

### 6.3.4. Comparative study of the liver transcriptome

In each generation, the transcriptome profiling of adult liver tissue was compared between VT and NC animals. The mean number of raw reads was  $65.1 \pm 23.78$  ( $\pm$ SD) millions, and in each sample, transcripts from 13,313 to 14,414 different genes (from a total of 24,964 annotated transcripts of Oryzun2.0) were detected. PCA plots clustered the samples according to their origin (VT or NC) in the three generations (Figure 6.4A). In the F1 generation, the comparative transcriptomic analysis recorded a differential expression of 642 genes, of which we observed a higher number of downregulated (477/642, 74.3%) than upregulated (165/642, 25.7%) genes in VT samples compared to the NC group. From these DETs, DAVID software recognised 518 genes (Annex II, Supplementary Table S4). After the GO enrichment analysis of these DETs, results showed that 21 biological processes (BP), 16 cellular components (CC) and 9 molecular functions (MF) were significantly affected by the VET. Besides, KEGG analyses revealed 24 disturbed pathways. Functional annotation of the F1 DETs was described in Annex II (Supplementary Table S5). Most importantly, as showed by Venn diagram (Figure 6.4B), of the total DETs annotated in the F1 generation, 133 and 120 DETs were inherited by the F2 and F3 generation, respectively (Annex II, Supplementary Table S6). Functional annotation of these DETs were described in Annex II (Supplementary Table S7 and Supplementary Table S8). On the other hand, comparing the VT and NC progeny in the

**Table 6.2.** Ejaculates/sperm parameters and motility assessment of males from the vitrified-transferred progeny (VT) compared to those naturally conceived (NC).

TRAITS	F1 generation		F2 generation		F3 generation	
	NC	VT	NC	VT	NC	VT
<b>n</b>	76	173	72	62	120	135
<b>SEMEN PARAMETERS</b>						
<b>VOL (ml)</b>	0.69 ± 0.050	0.89 ± 0.033*	0.60 ± 0.033	0.80 ± 0.036*	0.51 ± 0.0211	0.44 ± 0.0202
<b>CON (10<sup>6</sup>)</b>	238.5 ± 15.69	201.7 ± 10.40	181.5 ± 8.45	172.5 ± 9.11	305.6 ± 17.56	307.5 ± 16.79
<b>TSE (10<sup>6</sup> spz)</b>	156.8 ± 15.70	179.1 ± 10.40	92.1 ± 6.92	137.0 ± 7.31*	145.8 ± 8.15	126.5 ± 7.57
<b>MOT (%)</b>	71.9 ± 1.93	76.9 ± 1.28	90.0 ± 0.67	88.5 ± 0.65	52.1 ± 2.61	53.7 ± 2.46
<b>PRO (%)</b>	40.5 ± 1.73	43.0 ± 1.16	55.9 ± 1.30	59.8 ± 1.42	27.5 ± 1.74	29.5 ± 1.64
<b>VIA (%)</b>	74.5 ± 1.13	74.1 ± 0.77	82.6 ± 0.69	83.0 ± 0.75	73.1 ± 1.22	73.2 ± 1.15
<b>NAR (%)</b>	90.3 ± 0.83	90.3 ± 0.55	88.4 ± 0.55	88.2 ± 0.61	92.9 ± 0.56	92.3 ± 0.53
<b>ABN (%)</b>	19.6 ± 0.98	20.7 ± 0.64	18.4 ± 0.60	14.9 ± 0.66*	22.8 ± 0.97	23.1 ± 0.92
<b>MOTION PARAMETERS</b>						
<b>VCL (µm s<sup>-1</sup>)</b>	86.6 ± 2.34	99.8 ± 1.55*	99.8 ± 1.44	96.2 ± 1.53	104.5 ± 2.17	96.4 ± 2.05*
<b>VSL (µm s<sup>-1</sup>)</b>	34.0 ± 1.47	40.4 ± 0.98*	55.9 ± 1.18	55.0 ± 1.28	38.8 ± 1.22	38.3 ± 1.15
<b>VAP (µm s<sup>-1</sup>)</b>	50.0 ± 1.87	59.9 ± 1.23*	74.1 ± 1.31	72.9 ± 1.42	58.3 ± 1.25	55.8 ± 1.40
<b>LIN (%)</b>	40.3 ± 2.15	42.0 ± 1.42	58.7 ± 0.94	57.0 ± 0.98	37.9 ± 1.03	39.9 ± 0.97
<b>STR (%)</b>	68.9 ± 1.07	67.2 ± 0.71	77.1 ± 0.44	75.4 ± 0.46	66.1 ± 0.94	67.6 ± 0.88
<b>WOB (%)</b>	57.2 ± 1.32	59.3 ± 0.87	74.9 ± 0.99	76.0 ± 1.05	56.3 ± 0.95	58.1 ± 0.89
<b>ALH (µm)</b>	2.7 ± 0.55	2.8 ± 0.37	2.7 ± 0.42	2.7 ± 0.44	3.2 ± 0.06	3.0 ± 0.06
<b>BCF (Hz)</b>	10.8 ± 0.18	11.2 ± 0.12	9.9 ± 0.20	9.8 ± 0.22	12.2 ± 0.20	11.8 ± 0.19

**n** is the number of data (measured ejaculates) in each trait; **VOL**: Ejaculate volume; **CON**: Spermatic concentration; **TSE**: Total sperm per ejaculate; **spz**: spermatozoa; **MOT**: Percentage of sperm motility; **PRO**: Percentage of progressive motility; **VIA**: Percentage of viable sperm; **NAR**: percentage of normal apical ridge; **ABN**: Percentage of abnormal forms; **VCL**: Curvilinear velocity; **VSL**: straight-line velocity; **VAP**: average path velocity; **LIN**: linearity coefficient (VSL/VCL × 100); **STR**: straightness coefficient; **WOB**: wobble coefficient (VSL/VAP × 100); **ALH**: amplitude of lateral head displacement; **BCF**: beat cross frequency. Data are expressed as mean ± standard error of means. Asterisks denote relevant differences between VT animals and their NC counterparts (Bayesian inference:  $|D_{NC-VT}| > R$  and  $P_0 > 0.8$ ).

F2 generation, 447 DETs were recorded, of which we observed a higher number of upregulated (261/447, 58.4%) than downregulated (186/447, 41.6%) genes in VT samples compared to the NC group. From these DETs, DAVID recognises 342 genes (Annex II, Supplementary Table S9), whose functional analysis revealed changes in 14 BP, 4 CC, 7 MF and 16 KEGG pathways (Annex II, Supplementary Table S10). Finally, comparing the VT and NC progeny in the F3 generation, 905 DETs were recorded, of which we observed a higher number of downregulated (749/905, 82.8%) than upregulated (156/905, 17.2%) genes in VT samples compared to the NC group. From these DETs, DAVID recognises 670 genes (Annex II, Supplementary Table S11), whose functional analysis revealed changes in 29 BP, 10 CC, 13 MF and 37 KEGG pathways (Annex II, Supplementary Table S12).

Generally, analysis of DETs was conducted comparing the vitrified progenies with their coetaneous NC counterparts in each generation. However, the subset of DETs inherited by F2 and F3 generations were also analysed, observing that many disturbances registered in F1 were carried over to its descendants (F2), this effect being more diluted in F3, as expected. Then, as a consequence of the direct impact of the VET, DETs recorded in F1 revealed negative regulation of growth due to deficient mineral absorption and changes in the arachidonic acid metabolic process attributed to a disturbed unsaturated fatty acids biosynthesis. Functional analysis of DETs listed in F2 and F3 revealed similar dysregulation in the fatty acid biosynthetic process and/or its metabolism, also unveiling hints of mineral absorption alterations. A thorough examination of the 24 common DETs in all three generations highlighted that some of these DETs have mineral ion binding functions, suggesting that dysregulations in the mineral homeostasis were a common feature among VT animals of all three generations. Besides, we detected DETs encoding a glutathione S-transferase and Malic enzyme 1, suggesting alterations in the redox metabolism. Curiously, these common DETs were not always switched in the same direction, suggesting that there are different underlying causes for the changes in molecular patterns in each generation. In contrast, fatty acid-binding protein 4 appeared downregulated in all three generations. Altogether, this information demonstrated that VT livers presented clear evidence of dysregulations in lipid metabolism. In addition, some DETs recorded in each generation denoted alterations in the carbohydrate metabolism, cellular structure and function, as well as immune system responses.

### **6.3.5. Comparative study of the liver metabolome**

In each generation, the metabolome profiling of adult liver tissue was compared between VT and NC animals. First of all, we carried out an untargeted metabolomic analysis to gain a general overview of the metabolic changes in all the comparisons

under study. After subsequent retrieval of all detected ions, we identified 151, 190 and 159 differentially accumulated metabolites (DAMs) in F1, F2 and F3, respectively ( $p < 0.05$ ). The variability among semi-polar and non-polar metabolites was investigated by building PCA diagrams, which clustered the samples according to their VT or NC origin in the three generations (Figure 6.4A). Overall DAMs variation across generations indicated that VT livers showed an up-accumulation of semi-polar metabolites (average fold change of 0.22, 0.36 and 0.82 for F1, F2 and F3 generation, respectively), but a down-accumulation of non-polar ones except for the F2 generation (average fold change of -0.36, 0.19 and -0.67 for F1, F2 and F3 generation, respectively). This fact suggested a high concordance between non-polar DAMs and DETs, as a high proportion of DETs were downregulated in F1 and F3, but upregulated in F2.

To better investigate changes in known liver metabolites, we performed a targeted metabolomic analysis in which we quantified, relatively, 109 metabolites involved in primary (sugars, amino acids, organic acids, lipids, etc.) metabolism. The complete metabolite dataset was reported in Annex II (Supplementary Table S13). Specifically, 50, 41 and 47 DAMs were detected in F1, F2 and F3 generations. Globally, we identified that most of these DAMs belonged to the non-polar fraction of the metabolome in all three generations (37/50 [74.0%], 28/41 [68.3%] and 42/47 [89.4%] in F1, F2 and F3, respectively). In concordance, as shown in Venn diagrams (Figure 6.4B), a high proportion of non-polar DAMs recorded in F1 after VET were also present in generations F2 and F3. In contrast, semi-polar DAMs appeared most discrete in F1 after VET and, although some of them were also present in F2, were mostly restored in F3. Functional clustering of DAMs in each generation revealed direct, intergenerational and transgenerational effects of VET over several metabolic pathways, including glycolysis, gluconeogenesis, citrate cycle, biosynthesis of amino acids, biosynthesis of unsaturated fatty acids and those stemming from the metabolism of arachidonic acid, cholesterol, glycerolipids, glycerophospholipids and sphingolipids. Some of these observations agreed with the transcriptomic study and, in the same manner, DAMs did not always switch in the same direction between generations. Focussing on the common DAMs in all three generations, only 2 (oxalosuccinate and tryptophan) belonged to the semi-polar fraction; meanwhile, 13 belonged to the non-polar fraction. Of the latter, 7 were triglycerides and 6 were related to the unsaturated fatty acids biosynthetic pathway. Among them, we found that arachidonic acid (ARA), and thereby several DAMs for which ARA acts as a precursor (eicosanoids: leukotrienes, prostaglandins and thromboxanes), also displayed dysregulated levels in VT samples.

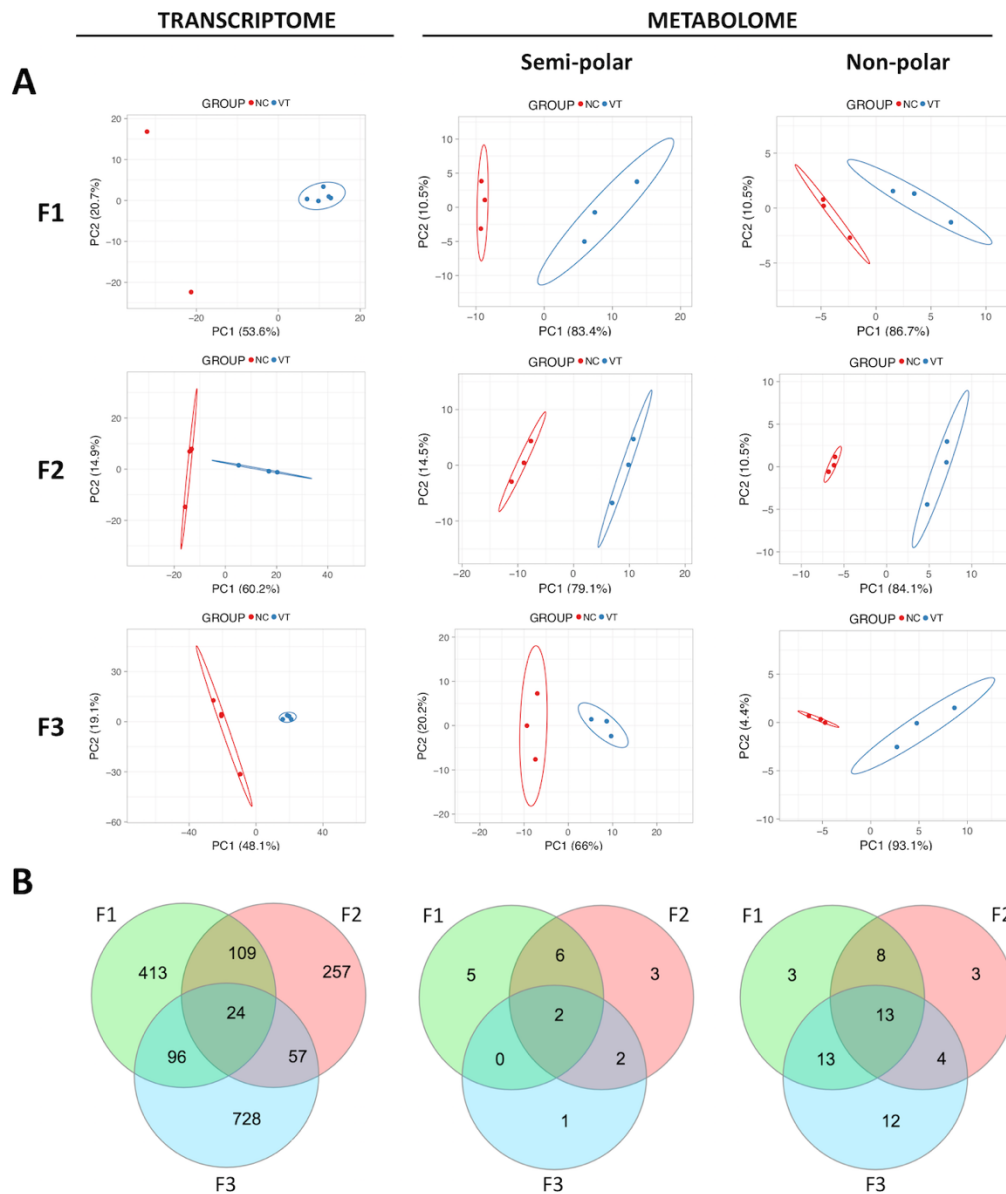


**Figure 6.4.** Molecular analysis of the liver samples collected from adult males derived from vitrified-transferred embryos (VT) and naturally-conceived (NC), which was compared in each generation (F1, F2, F3). **[A]** Principal Component Analysis (PCA) of the transcriptome, semi-polar metabolome and non-polar metabolome. The representation of sample variability between the experimental groups was performed taking into account only the differentially expressed transcripts and differentially accumulated metabolites (untargeted). **[B]** Venn diagram summarising differentially expressed transcripts and targeted metabolites between NC and VT progenies in F1, F2, F3, and those commonly present between generations.

## 6.4. DISCUSSION

Several studies have reported that early embryo manipulation can trigger developmental consequences both in human and animal models [4,7,12–15,24]. Nevertheless, no previous reports have examined the transgenerational effects of the vitrified embryo transfer procedure (VET). Our findings demonstrate, for the first time,

the transgenerational inheritance of changes induced by embryo exposure to VET over the offspring growth performance, adult body weight, phenotype of vital organs and their molecular physiology and metabolism. Deviations in the growth pattern and phenotype have been described by several authors after ART, evidencing that different procedures applied to different genotypes would lead to different outcomes, probably through specific epigenetic modifications [17,24,54–60]. Besides, several studies described ART related organ changes [29,30,55,58,60]. The transgenerational effects occur when alterations in the epigenetic marks, caused by embryo manipulation, persist into subsequent generations despite the extensive reprogramming that takes place both in gametes and in the early embryo [27,28]. This transgenerational epigenetic inheritance has been well documented in plants, nematodes and flies, but its occurrence in mammals, and particularly in humans, remains controversial [61,62]. However, a few disclosed that ART-induced effects could be heritable and persist transgenerationally [29,30,63,64]. In agreement, here we demonstrated that the evidence of transgenerational effects on body and organ weight variations is consistent, but in a tissue-specific manner. In F1, VT animals showed a lower weight in liver and heart, as previously described [26,55]. Concordantly, some authors also reported evidence of liver and heart weights changes after *in vitro* embryo culture, but only the hepatic disturbances showed a transgenerational inheritance [29,60]. Taken together, these data suggest that the liver could be a highly sensitive organ to ART. Indeed, heart affections could be caused by liver disturbances, given the strong interaction between the physiology of both organs [65]. In this context, placental dysfunction described after embryo cryopreservation [20,21] could partly explain this liver disturbance, as decreased maternofetal nutrition during gestation produces both reduced liver mass and perturbed liver function [66]. Intriguingly, weight decrease in the liver and heart was intensified in F2-VT animals. This generation came from gametes originated from primordial germ cells (PGCs) developed in F1 embryos exposed to VET [33]. As PGCs require meticulous epigenetic dynamics for their proper development [67], feasible epigenetic modifications induced in PGCs may be more marked, explaining to some extent the higher organ differences in F2-VT animals. Furthermore, we found an interaction between the experimental group and the generation for liver weight, which was lighter in F1- and F2-VT animals, but more prominent in the F3-VT animals. Notably, we observed organomegaly for lungs and spleen in F2-VT and F3-VT animals respectively, but not in F1. Mahsoudi et al. [30] described similar effects after *in vitro* culture, reporting interactions between generations and treatment for organ weights, and the appearance of some varying phenotypes in F2 that were absent in F1 animals. These authors suggested that different underlying causes for the phenotypic changes emerge in each generation. Indeed, the variability and tissue specificity of the available data indicate that if master regulator genes are present, their cellular framework is elusive [15]. A plausible explanation might be that the epigenetic status in each generation could differ because when an epigenetic change caused by direct experience



is transmitted to the offspring, that same experience becomes an indirect environmental trigger for the ontogenetic development of the new individual [68]. Also, in each generation, an extensive epigenetic reprogramming takes place upon fertilisation to remodel the previously acquired epigenetic marks and produce totipotent zygotic states [28,69]. Therefore, how the molecular mechanisms interact to orchestrate the developmental programme may explain the range of results obtained in each generation. Notably, concordantly with the two waves of epigenetic reprogramming that occurred from F1 to F3, some VET-induced phenotypic differences disappeared or were ameliorated in F3 animals, suggesting a partial restoration of the VET-induced epigenetic disorders. Thus, the long-term effects of VET on body weight had the highest impact on the F1 generation, whereas approximately the half of the effect was observed in F2 and F3. If the advent of ART disrupts this crucial epigenetic rearrangement in F1, it could be that the same mechanism repaired some of the induced deviations two generations later.

Many investigations have also confirmed that ART induces molecular changes in the preimplantation embryo and beyond parturition, where it was associated with some of the ART-induced phenotypes [14,15]. Here, we assessed the transgenerational effects of VET on the gene expression and metabolic profiles in liver tissue, an organ that supports growth and regulates metabolism from the foetal stage [70,71]. We found that transcriptomic and metabolomic PCA analysis data revealed separate clusters between both experimental groups in each generation. Consequently, 642, 447 and 905 DETs, and 151, 190 and 159 DAMs (untargeted data) were detected in F1, F2 and F3, respectively. Among the DETs recorded in F1, we detected a subset related to the “negative regulation of growth” biological process. Besides, 3 of these DETs were among the most downregulated transcripts (average fold change < -4) and encode metallothioneins (MT), small proteins involved in zinc (Zn) trafficking and protective mechanisms against oxidative stress and toxic metals [72]. MT is essential for embryonic liver development, and MT deficiency impairs hepatocyte development and provokes liver deterioration at later stages [73], which could explain the lower hepatic weight at adulthood in VT animals. Notably, MT expression is linked directly to zinc availability [72,74], so downregulation of MT coding genes could suggest lower Zn abundance in VT livers. KEGG analysis reveals that lower Zn levels might be caused due to an impaired Zn absorption in the intestine (“mineral absorption” pathway), as the body zinc is replenished daily through diet [74]. Concordantly, a recent study described that serum Zn levels in children born via ART were significantly decreased [75]. As Zn is required for healthy growth, its deficiency contributes to growth retardation, and thereby Zn-deficient ART children were smaller than those conceived naturally [75]. Therefore, the lower growth performance exhibited by VT rabbits strengthens this study, supporting that Zn deficiencies could be related to the phenotype in question. Interestingly, dysregulations in MT encoding genes were also found in F2 and F3 VT animals.

In addition, downregulation of DETs encoding for Zn-binding proteins was found in the three generations. Transcriptional mechanisms are present to reduce gene expression of Zn-binding proteins when zinc is limiting, thus conserving Zn for more essential functions [76]. Related to this, some of the common DETs in the three generations have mineral ion binding functions, suggesting that mineral homeostasis dysregulation could be a transgenerational-inherited effect of the VET. Furthermore, Zn status may affect fatty acid (FA) metabolism, as it acts as a cofactor in FA desaturases and elongases enzymes, which are essential for the biosynthesis of long-chain poly-unsaturated FA (LCPUFA) and its metabolic regulation [77,78]. In agreement, Wang et al. found a dysregulated profile of these compounds in the livers of ART mice [79]. In the present study, we detected several DAMs in the three generations that are involved in the LCPUFA biosynthetic pathway, which led to a transgenerationally disturbed LCPUFA profile. Besides, among DETs recorded across F1, F2 and F3 generation, several encoded for desaturases or enzymes involved in the LCPUFA metabolism. These findings suggest that LCPUFA biosynthetic and metabolic processes might be impaired by a synergic effect between transcriptional dysregulation in the involved enzymes collectively with their decreased activity due to Zn deficiencies. Several enriched GO and KEGG terms support LCPUFA disturbances, which were validated by the metabolomic data. Among DAMs commonly noted for the three generations, we observed some LCPUFA required for optimal growth and development [80,81]. In addition, it is worth highlighting that common DETs that participate in the “ARA metabolic process” term enrichment were also present in the “negative regulation of growth” term enrichment. It is well established that arachidonic acid (ARA) is decisive for optimal growth and health [81]. ARA and its derivate metabolites, collectively known as eicosanoids, play essential roles for the coordination of cellular differentiation, organogenesis, foetal growth, postnatal growth and development (for review see Hadley et al. [81]). In our study, low ARA levels were noted in F1- and F3-VT livers, whereas in F2-VT ARA content resulted increased. This finding is not contradictory, since it might reflect an impaired conversion of ARA to eicosanoids in F2-VT livers, as some of them were simultaneously down-accumulated. It is worth mentioning that in line with the phenotypic traits, molecular changes also reflected specific patterns in each generation. Of note, we encountered a downregulated fatty acid-binding protein in the three generations, which could be associated with the extended alteration in lipid and lipid-related pathways, since it acts as lipid chaperone, crucial proteins for the lipid metabolism and eicosanoid biosynthesis [82]. Despite further research being required, we hypothesise that deficiencies in the metabolism of Zn and LCPUFA could be related to the transgenerational phenotype exhibited by VT animals. Interestingly, Zn and ARA-derived eicosanoids are crucial components for the immune system responses, and their deficiencies increased susceptibility to infections [75,81]. In our study, functional annotation of DETs throughout generations, validated by the metabolomic data, proposed a general

dysregulation in the immune system. In agreement with this hypothesis, it has been observed that ART offspring suffer more infections, their development being slower [83]. Authors concluded that individuals that must allocate more energy to immunity and tissue repair due to infection are likely to have less energy to allocate to growth and development. On the other hand, another interesting finding of our study was that both LCPUFAs and ARA are fundamental components in the mitochondrial and cellular membranes of the liver and almost all other organs, aiding in the synthesis of phosphatidylcholines [81,84,85]. In agreement, we detected a wide range of down-accumulated phosphatidylcholines in the VT livers along the three generations. Cell membranes are the basis of the organisation of the cell and changing its composition alters its function [81,84,85], which could contribute to the physiological and metabolic differences between VT and NC animals. This event could explain the range of GO term and KEGG routes obtained for DETs and related to cellular structures and functions in each generation, some of which are conserved from F1 to F2 and F3.

Specifically, LCPUFAs and eicosanoids are endogenous ligands for PPARs, a superfamily of nuclear transcription factors responsible for upregulating genes of key mitochondrial enzymes [84]. KEGG analysis revealed disturbances in the “PPAR signalling pathway” for F1- and F2-VT animals, which appeared jointly with some DAMs implicated in oxidative phosphorylation (OXPHO). In agreement with our previous proteomic study, we suggest that animals born after a VET exhibit dysregulation concerning the OXPHO process [26]. These results could explain that VT progeny are susceptible to mitochondrial dysfunctions, which seemed to be restored in F3. In agreement, DAMs related to OXPHO were founded in F1 and F2, but not in F3. Concordantly, Feuer et al. [58] also reported alterations in the postnatal growth trajectory linked to broad changes in metabolic homeostasis, characterised by mitochondrial dysfunction and systemic oxidative stress. As oxidative changes are ubiquitously present in postnatal ART tissues [15], it might explain the presence of common DETs encoding glutathione S-transferase and malic enzyme 1, which participate in a molecular system to maintain redox balance [86,87]. Besides, malic enzyme 1 links the catabolic pathways of glycolysis and citric acid cycle to the anabolic pathways of fatty acid and cholesterol biosynthesis through NADPH, thus having critical roles in mitochondrial energy metabolism and maintenance of homeostasis [87]. Interestingly, several DAMs participating in these metabolic pathways were found in all generations, suggesting that VET triggers a metabolic reprogramming in the liver affecting a wide range of interconnected pathways, including those related with metabolism of carbohydrates and amino acids. As reviewed by Feuer’s group [14,15,57], dysregulations in the metabolism of glucose, amino acids and long-chain FA have been encountered in IVF livers, which were associated with an altered mitochondrial function. Changes in some metabolites have been proposed as potential compensatory effects against those disturbed by ART, but altogether these dysregulations can disrupt optimal energy expenditure and might further contribute to

the postnatal phenotypes associated with ART [15]. Altogether, our findings provide strong evidence of these metabolic peculiarities after VET, which have been reported in IVF mice, and are beginning to be validated in IVF humans [10,88].

Despite all the changes attributed to VET, the VT progeny seemed healthy, as no striking difference was detected either during the management or during the dissection study in either generation, in line with our previously reported study [24]. In addition, the fertilising capacity is a measure of health status of the resultant progeny, also used after ART [30,89]. Related to this, ART has been linked with reduced sperm quality in studies performed in mice and humans [29,90]. Reassuringly, here we observed that although some deviations in seminal parameters were recorded, they were within the normal physiological range of variability [38] and seemed irrelevant, because a similar fertility rate was observed between VT and NC progenies. These results indicated that VET is not reproductive health-related. In addition, we found that the number of liveborn was transgenerationally increased in VT animals, reinforcing our hypothesis postulated years ago that suggested epigenetic mechanisms as the underlying cause [63]. These findings highlight that further research is needed to investigate whether these effects are attributable to a legacy inherited through mother or/and father. Both positive and adverse health effects have been observed after embryo cryopreservation [18] based on a still misunderstood embryonic plasticity, which refers to the capacity of a genotype to produce different phenotypes in response to environmental changes through epigenetic mechanisms [4,28,91]. Recent evidence supports the relevance of the ART stressors on early embryos, triggering a high range of self-reprogramming that can be condition- and strain-specific, sexually dimorphic and may not emerge until later into adulthood [15]. Besides, without being exclusive, we hypothesised that cryopreservation could act as a selection pressure (“cryo-selection”), since not all embryos survive this process, which could favour the inheritance of alleles responsible for this deviant phenotype in VT animals [24]. However, although the rabbit is considered an excellent reproductive model for human health [25], caution is required when extrapolating results from rabbit studies to humans.

## 6.5. CONCLUSION

In summary, to our best knowledge, here we provide the first evidence that long-term effects induced by VET in F1 offspring, both phenotypic and molecular, can be inherited by subsequent generations, triggering both intergenerational (F2) and transgenerational (F3) effects. Our results support and extend the list of studies reporting ART effects, but mainly contribute to the knowledge regarding long-term transgenerational effects, of which evidence remains scarce. This study should serve as a discussion table to conceive

new works that assess the effects on females and another current ART, and thereby determine the most efficient and safest techniques to generate offspring.

## 6.6. REFERENCES

- [1]. Canovas S, Ross PJ, Kelsey G, Coy P. DNA Methylation in Embryo Development: Epigenetic Impact of ART (Assisted Reproductive Technologies). *Bioessays*. 2017;39:1700106.
- [2]. García-Martínez S, Hurtado MAS, Gutiérrez H, Margallo FMS, Romar R, Latorre R, et al. Mimicking physiological O<sub>2</sub> tension in the female reproductive tract improves assisted reproduction outcomes in pig. *Mol Hum Reprod* 2018;24:260–70.
- [3]. Ng KYB, Mingels R, Morgan H, Macklon N, Cheong Y. In vivo oxygen, temperature and pH dynamics in the female reproductive tract and their importance in human conception: A systematic review. *Hum Reprod Update* 2018;24(1):15–34.
- [4]. Roseboom TJ. Developmental plasticity and its relevance to assisted human reproduction. *Hum Reprod* 2018;33:546–52.
- [5]. Feuer S, Rinaudo P. From Embryos to Adults: A DOHaD Perspective on *In Vitro* Fertilization and Other Assisted Reproductive Technologies. *Healthcare* 2016;4:E51.
- [6]. Zandstra H, Brentjens LBPM, Spauwen B, Touwslager RNH, Bons JAP, Mulder AL, et al. Association of culture medium with growth, weight and cardiovascular development of IVF children at the age of 9 years. *Hum Reprod* 2018;33:1645–56.
- [7]. Chen M, Heilbronn LK. The health outcomes of human offspring conceived by assisted reproductive technologies (ART). *J Dev Orig Health Dis* 2017;8:388–402.
- [8]. Chen L, Yang T, Zheng Z, Yu H, Wang H, Qin J. Birth prevalence of congenital malformations in singleton pregnancies resulting from in vitro fertilization/intracytoplasmic sperm injection worldwide: a systematic review and meta-analysis. *Arch Gynecol Obstet* 2018;297:1115–30.
- [9]. Zhang WY, Selamet Tierney ES, Chen AC, Ling AY, Fleischmann RR, Baker VL. Vascular Health of Children Conceived via In Vitro Fertilization. *J Pediatr* 2019;214:47–53.
- [10]. Guo XY, Liu XM, Jin L, Wang TT, Ullah K, Sheng JZ, et al. Cardiovascular and metabolic profiles of offspring conceived by assisted reproductive technologies: a systematic review and meta-analysis. *Fertil Steril* 2017;107:622–31.
- [11]. Vrooman LA, Bartolomei MS. Can assisted reproductive technologies cause adult-onset disease? Evidence from human and mouse. *Reprod Toxicol* 2017;68:72–84.
- [12]. Duranthon V, Chavatte-Palmer P. Long term effects of ART: What do animals tell us? *Mol Reprod Dev* 2018;85:348–68.

- [13]. Ramos-Ibeas P, Heras S, Gómez-Redondo I, Planells B, Fernández-González R, Pericuesta E, et al. Embryo responses to stress induced by assisted reproductive technologies. *Mol Reprod Dev* 2019;86:1292–306.
- [14]. Feuer SK, Liu X, Donjacour A, Simbulan R, Maltepe E, Rinaudo PF. Transcriptional signatures throughout development: the effects of mouse embryo manipulation in vitro. *Reproduction* 2017;153(1):107–122.
- [15]. Feuer SK, Rinaudo PF. Physiological, metabolic and transcriptional postnatal phenotypes of in vitro fertilization (IVF) in the mouse. *J Dev Orig Health Dis* 2017;8:403–10.
- [16]. Sparks AET. Human embryo cryopreservation-methods, timing, and other considerations for optimizing an embryo cryopreservation program. *Semin Reprod Med* 2015;33:128–44.
- [17]. Dulioust E, Toyama K, Busnel MC, Moutier R, Carlier M, Marchaland C, et al. Long-term effects of embryo freezing in mice. *Proc Natl Acad Sci U S A* 1995;92:589–93.
- [18]. Auroux M, Cerutti I, Ducot B, Loeuillet A. Is embryo-cryopreservation really neutral? A new long-term effect of embryo freezing in mice: Protection of adults from induced cancer according to strain and sex. *Reprod Toxicol* 2004;18:813–8.
- [19]. Vicente JS, Saenz-de-Juano MD, Jiménez-Trigos E, Viudes-de-Castro MP, Peñaranda DS, Marco-Jiménez F. Rabbit morula vitrification reduces early foetal growth and increases losses throughout gestation. *Cryobiology* 2013;67:321–6.
- [20]. Saenz-De-Juano MD, Marco-Jimenez F, Schmaltz-Panneau B, Jimenez-Trigos E, Viudes-De-Castro MP, Penaranda DS, et al. Vitrification alters rabbit foetal placenta at transcriptomic and proteomic level. *Reproduction* 2014;147:789–801.
- [21]. Saenz-de-Juano MD, Vicente JS, Hollung K, Marco-Jiménez F. Effect of embryo vitrification on rabbit foetal placenta proteome during pregnancy. *PLoS One* 2015;147:789–801.
- [22]. Berntsen S, Pinborg A. Large for gestational age and macrosomia in singletons born after frozen/thawed embryo transfer (FET) in assisted reproductive technology (ART). *Birth Defects Res* 2018;110:630–43.
- [23]. Maheshwari A, Pandey S, Raja EA, Shetty A, Hamilton M, Bhattacharya S. Is frozen embryo transfer better for mothers and babies? Can cumulative meta-analysis provide a definitive answer? *Hum Reprod Update* 2018;24:35–58.
- [24]. Garcia-Dominguez X, Vicente JS, Marco-Jiménez F. Developmental Plasticity in Response to Embryo Cryopreservation: The Importance of the Vitrification Device in Rabbits. *Animals* 2020;10(5):804.
- [25]. Garcia-Dominguez X, Marco-Jimenez F, Viudes-de-Castro MP, Vicente JS. Minimally invasive embryo transfer and embryo vitrification at the optimal embryo stage in rabbit model. *J Vis Exp* 2019;147:e58055.
- [26]. Garcia-Dominguez X, Marco-Jimenez F, Peñaranda DS, Vicente JS. Long-term phenotypic and proteomic changes following vitrified embryo transfer in the rabbit model. *Animals* 2020;10(6): 1043.

- [27]. Ventura-Juncá P, Irrarázaval I, Rolle AJ, Gutiérrez JI, Moreno RD, Santos MJ. In vitro fertilization (IVF) in mammals: Epigenetic and developmental alterations. Scientific and bioethical implications for IVF in humans. *Biol Res* 2015;48:68.
- [28]. Calle A, Fernandez-Gonzalez R, Ramos-Ibeas P, Laguna-Barraza R, Perez-Cereales S, Bermejo-Alvarez P, et al. Long-term and transgenerational effects of in vitro culture on mouse embryos. *Theriogenology* 2012;77:785–93.
- [29]. Calle A, Miranda A, Fernandez-Gonzalez R, Pericuesta E, Laguna R, Gutierrez-Adan A. Male Mice Produced by In Vitro Culture Have Reduced Fertility and Transmit Organomegaly and Glucose Intolerance to Their Male Offspring1. *Biol Reprod* 2012;87:1–9.
- [30]. Mahsoudi B, Li A, O’Neill C. Assessment of the Long-Term and Transgenerational Consequences of Perturbing Preimplantation Embryo Development in Mice1. *Biol Reprod* 2007;77:889–96.
- [31]. Servick K. Unsettled questions trail IVF’s success. *Science* (80- ) 2014;345:744–6.
- [32]. Estany J, Camacho J, Baselga M, Blasco A. Selection response of growth rate in rabbits for meat production. *Genet Sel Evol* 1992;24:527–37.
- [33]. Skinner MK. What is an epigenetic transgenerational phenotype?. F3 or F2. *Reprod Toxicol* 2008;25:2–6.
- [34]. Vicente JS, Viudes-de-Castro MP, García M de la L, Baselga M. Effect of rabbit line on a program of cryopreserved embryos by vitrification. *Reprod Nutr Dev* 2003;43(2):137–43.
- [35]. Zucker I, Beery AK. Males still dominate animal studies. *Nature* 2010;465:690.
- [36]. Vicente JS, Viudes-De-Castro MP, García ML. In vivo survival rate of rabbit morulae after vitrification in a medium without serum protein. *Reprod Nutr Dev* 1999;39(5–6):657–62.
- [37]. Besenfelder U, Brem G. Laparoscopic embryo transfer in rabbits. *J Reprod Fertil* 1993;99:53–6.
- [38]. Marco-Jiménez F, Vicente JS. Overweight in young males reduce fertility in rabbit model. *PLoS One* 2017;12:e0180679.
- [39]. Blasco A. The use of Bayesian statistics in meat quality analyses: A review. *Meat Sci* 2005;69:115–22.
- [40]. Andrews S. FASTQC A Quality Control tool for High Throughput Sequence Data [Internet]. Babraham Inst. 2015;Available from: <http://www.bioinformatics.babraham.ac.uk/projects/fastqc>
- [41]. Kim D, Langmead B, Salzberg SL. HISAT: A fast spliced aligner with low memory requirements. *Nat Methods* 2015;12:357–60.
- [42]. Perteua M, Perteua GM, Antonescu CM, Chang TC, Mendell JT, Salzberg SL. StringTie enables improved reconstruction of a transcriptome from RNA-seq reads. *Nat Biotechnol* 2015;33:290–5.

- [43]. Robinson MD, McCarthy DJ, Smyth GK. edgeR: A Bioconductor package for differential expression analysis of digital gene expression data. *Bioinformatics* 2009;26:139–40.
- [44]. Wang YE, Kutnetsov L, Partensky A, Farid J, Quackenbush J. WebMeV: A Cloud Platform for Analyzing and Visualizing Cancer Genomic Data. *Cancer Res* 2017;77:e11–4.
- [45]. Metsalu T, Vilo J. ClustVis: A web tool for visualizing clustering of multivariate data using Principal Component Analysis and heatmap. *Nucleic Acids Res* 2015;44:566–70.
- [46]. Heberle H, Meirelles VG, da Silva FR, Telles GP, Minghim R. InteractiVenn: A web-based tool for the analysis of sets through Venn diagrams. *BMC Bioinformatics* 2015;16:169.
- [47]. Huang DW, Sherman BT, Lempicki RA. Systematic and integrative analysis of large gene lists using DAVID bioinformatics resources. *Nat Protoc* 2009;4:44–57.
- [48]. Diretto G, Rubio-Moraga A, Argando A J, Castillo P, Gómez-Gómez L, Ahrazem O. Tissue-specific accumulation of sulfur compounds and saponins in different parts of garlic cloves from purple and white ecotypes. *Molecules* 2017;22(8):E1359.
- [49]. Cappelli G, Giovannini D, Basso AL, Demurtas OC, Diretto G, Santi C, et al. A *Corylus avellana* L. extract enhances human macrophage bactericidal response against *Staphylococcus aureus* by increasing the expression of anti-inflammatory and iron metabolism genes. *J Funct Foods* 2018;45:499–511.
- [50]. Di Meo F, Aversano R, Diretto G, Demurtas OC, Villano C, Cozzolino S, et al. Anti-cancer activity of grape seed semi-polar extracts in human mesothelioma cell lines. *J Funct Foods* 2019;61:103515.
- [51]. Fiore A, Dall’Osto L, Cazzaniga S, Diretto G, Giuliano G, Bassi R. A quadruple mutant of *Arabidopsis* reveals a  $\beta$ -carotene hydroxylation activity for LUT1/CYP97C1 and a regulatory role of xanthophylls on determination of the PSI/PSII ratio. *BMC Plant Biol* 2012;12:50.
- [52]. Rambla JL, Trapero-Mozos A, Diretto G, Moraga AR, Granell A, Gómez LG, et al. Gene-metabolite networks of volatile metabolism in Airen and Tempranillo grape cultivars revealed a distinct mechanism of aroma bouquet production. *Front Plant Sci* 2016;7:1619.
- [53]. Sulli M, Mandolino G, Sturaro M, Onofri C, Diretto G, Parisi B, et al. Molecular and biochemical characterization of a potato collection with contrasting tuber carotenoid content. *PLoS One* 2017;12(9):e0184143.
- [54]. Cifre J, Baselga M, Gómez EA, De La Luz GM. Effect of embryo cryopreservation techniques on reproductive and growth traits in rabbits. *Anim Res* 1999;48:15–24.
- [55]. Lavara R, Baselga M, Marco-Jiménez F, Vicente JS. Embryo vitrification in rabbits: Consequences for progeny growth. *Theriogenology* 2015;84:674–80.
- [56]. Nusbaumer D, Da Cunha LM, Wedekind C. Sperm cryopreservation reduces offspring growth. *Proc R Soc B Biol Sci* 2019;286:20191644.



- [57]. Feuer SK, Donjacour A, Simbulan RK, Lin W, Liu X, Maltepe E, et al. Sexually dimorphic effect of In Vitro Fertilization (IVF) on adult mouse fat and liver metabolomes. *Endocrinology* 2014;155:4554–67.
- [58]. Feuer SK, Liu X, Donjacour A, Lin W, Simbulan RK, Giritharan G, et al. Use of a mouse in vitro fertilization model to understand the developmental origins of health and disease hypothesis. *Endocrinology* 2014;155:1956–69.
- [59]. Velazquez MA, Sheth B, Smith SJ, Eckert JJ, Osmond C, Fleming TP. Insulin and branched-chain amino acid depletion during mouse preimplantation embryo culture programmes body weight gain and raised blood pressure during early postnatal life. *Biochim Biophys Acta - Mol Basis Dis* 2018;1864(2):590–600.
- [60]. Fernández-Gonzalez R, Moreira P, Bilbao A, Jiménez A, Pérez-Crespo M, Ramírez MA, et al. Long-term effect of in vitro culture of mouse embryos with serum on mRNA expression of imprinting genes, development, and behavior. *Proc Natl Acad Sci U S A* 2004;101:5880–5.
- [61]. Horsthemke B. A critical view on transgenerational epigenetic inheritance in humans. *Nat Commun* 2018;9:2973.
- [62]. Perez MF, Lehner B. Intergenerational and transgenerational epigenetic inheritance in animals. *Nat Cell Biol* 2019;21:143–51.
- [63]. Lavara R, Baselga M, Marco-Jiménez F, Vicente JS. Long-term and transgenerational effects of cryopreservation on rabbit embryos. *Theriogenology* 2014;81:988–92.
- [64]. Rexhaj E, Paoloni-Giacobino A, Rimoldi SF, Fuster DG, Anderegg M, Somm E, et al. Mice generated by in vitro fertilization exhibit vascular dysfunction and shortened life span. *J Clin Invest* 2013;123:5052–60.
- [65]. Møller S, Bernardi M. Interactions of the heart and the liver. *Eur Heart J* 2013;34:2804–11.
- [66]. Hyatt MA, Budge H, Symonds ME. Early developmental influences on hepatic organogenesis. *Organogenesis* 2008;4:170–5.
- [67]. Hajkova P. Epigenetic reprogramming in the germline: Towards the ground state of the epigenome. *Philos Trans R Soc B Biol Sci* 2011;366:2266–73.
- [68]. Lacal I, Ventura R. Epigenetic Inheritance: Concepts, Mechanisms and Perspectives. *Front Mol Neurosci* 2018;11:292.
- [69]. Fraser R, Lin CJ. Epigenetic reprogramming of the zygote in mice and men: On your marks, get set, go! *Reproduction* 2016;152:R211–22.
- [70]. Adamek A, Kasprzak A. Insulin-like growth factor (IGF) system in liver diseases. *Int J Mol Sci* 2018;19:E1308.
- [71]. Kineman RD, del Rio-Moreno M, Sarmiento-Cabral A. 40 years of IGF1: Understanding the tissue-specific roles of IGF1/IGF1R in regulating metabolism using the Cre/loxP system. *J Mol Endocrinol* 2018;61:T187–98.
- [72]. Davis SR, Cousins RJ. Metallothionein Expression in Animals: A Physiological Perspective on Function. *J Nutr* 2000;130:1085–8.

- [73]. Günes Ć, Heuchel R, Georgiev O, Müller KH, Lichtlen P, Blüthmann H, et al. Embryonic lethality and liver degeneration in mice lacking the metal-responsive transcriptional activator MTF-1. *EMBO J* 1998;17:2846–54.
- [74]. Kambe T, Tsuji T, Hashimoto A, Itsumura N. The physiological, biochemical, and molecular roles of zinc transporters in zinc homeostasis and metabolism. *Physiol Rev* 2015;95:749–84.
- [75]. Xia X ru, Jiang SW, Zhang Y, Hu Y fang, Yi H gang, Liu J, et al. Serum levels of trace elements in children born after assisted reproductive technology. *Clin Chim Acta* 2019;495:664–9.
- [76]. Bird AJ. Cellular sensing and transport of metal ions: Implications in micronutrient homeostasis. *J Nutr Biochem* 2015;26:1103–15.
- [77]. Meesapyodsuk D, Qiu X. The front-end desaturase: Structure, function, evolution and biotechnological use. *Lipids*. 2012;47(3):227–37.
- [78]. Chimhashu T, Malan L, Baumgartner J, Van Jaarsveld PJ, Galetti V, Moretti D, et al. Sensitivity of fatty acid desaturation and elongation to plasma zinc concentration: A randomised controlled trial in Beninese children. *Br J Nutr* 2018;
- [79]. Wang LY, Le F, Wang N, Li L, Liu XZ, Zheng YM, et al. Alteration of fatty acid metabolism in the liver, adipose tissue, and testis of male mice conceived through assisted reproductive technologies: Fatty acid metabolism in ART mice. *Lipids Health Dis* 2013;12:5.
- [80]. Li J, Yin H, Bibus DM, Byelashov OA. The role of Omega-3 docosapentaenoic acid in pregnancy and early development. *Eur J Lipid Sci Technol* 2016;118(11):1692–701.
- [81]. Hadley KB, Ryan AS, Forsyth S, Gautier S, Salem N. The essentiality of arachidonic acid in infant development. *Nutrients* 2016;8:216.
- [82]. Makowski L, Hotamisligil GS. The role of fatty acid binding proteins in metabolic syndrome and atherosclerosis. *Curr. Opin. Lipidol.* 2005;16(5):543–8.
- [83]. Waynforth D. Effects of conception using assisted reproductive technologies on infant health and development: An evolutionary perspective and analysis using UK millennium cohort data. *Yale J Biol Med* 2018;91:225–35.
- [84]. Sullivan EM, Pennington ER, Green WD, Beck MA, Brown DA, Shaikh SR. Mechanisms by which dietary fatty acids regulate mitochondrial structure-function in health and disease. *Adv Nutr* 2018;9:247–62.
- [85]. Richardson UI, Wurtman RJ. Polyunsaturated fatty acids stimulate phosphatidylcholine synthesis in PC12 cells. *Biochim Biophys Acta - Mol Cell Biol Lipids* 2007;1771(4):558–63.
- [86]. Singh A, Prasad KN, Singh AK, Singh SK, Gupta KK, Paliwal VK, et al. Human Glutathione S-Transferase Enzyme Gene Polymorphisms and Their Association With Neurocysticercosis. *Mol Neurobiol* 2017;54(4):2843–51.

- [87]. Yu HF, Duan CC, Yang ZQ, Wang YS, Yue ZP, Guo B. Malic enzyme 1 is important for uterine decidualization in response to progesterone/cAMP/PKA/HB-EGF pathway. *FASEB J* 2020;34(3):3820–37.
- [88]. Chen M, Wu L, Zhao J, Wu F, Davies MJ, Wittert GA, et al. Altered glucose metabolism in mouse and humans conceived by IVF. *Diabetes* 2014;63(10):3189–98.
- [89]. Auroux M. Long-term effects in progeny of paternal environment and of gamete/embryo cryopreservation. *Hum Reprod Update* 2000;6:550–63.
- [90]. Belva F, Bonduelle M, Roelants M, Michielsen D, Van Steirteghem A, Verheyen G, et al. Semen quality of young adult ICSI offspring: The first results. *Hum Reprod* 2016;31:2811–20.
- [91]. Laubach ZM, Perng W, Dolinoy DC, Faulk CD, Holekamp KE, Getty T. Epigenetics and the maintenance of developmental plasticity: extending the signalling theory framework. *Biol Rev* 2018;93(3):1323–38.

## **ACKNOWLEDGEMENTS**

This work was supported by funds from the Ministry of Economy and Competitiveness of Spain (AGL2014-53405-C2-1-P) and Generalitat Valenciana Research Programme (PrometeoII 2014/036). Ximo García-Dominguez was supported by a research grant from the Ministry of Economy and Competitiveness (BES-2015-072429). The authors would like to thank Neil Macowan Language Services for revising the English version of the manuscript.



## CHAPTER V

# **TRANSGENERATIONAL EFFECTS FOLLOWING VITRIFIED EMBRYO TRANSFER IN RABBITS: A MULTI-OMIC APPROACH**

X. Garcia-Dominguez<sup>1</sup>, G. Diretto<sup>2</sup>, D.S. Peñaranda<sup>1</sup>, S. Frusciante<sup>2</sup>  
V. García-Carpintero<sup>3</sup>, J. Cañizares<sup>3</sup>, F. Marco-Jiménez<sup>1</sup>, J.S. Vicente<sup>1</sup>

<sup>1</sup>Institute for Animal Science and Technology (ICTA), Laboratory of Reproductive Biotechnology, Universitat Politècnica de València, 46022 Valencia, Spain

<sup>2</sup>Italian National Agency for New Technologies, Energy and Sustainable Development (ENEA), Casaccia Research Centre, 00123 Rome, Italy.

<sup>3</sup>Institute for the Conservation and Breeding of Agricultural Biodiversity (COMAV-UPV), Universitat Politècnica de València, 46022 Valencia, Spain



### ABSTRACT

The concept of developmental programming, attributed to embryonic plasticity, suggests transgenerational molecular inheritance in animals. This study aimed to investigate transgenerational inheritance of the effects induced by a vitrified embryo transfer procedure (VET). To this end, studying the F3 generation, progeny from vitrified-transferred embryos (VT animals) were compared with their naturally-conceived counterparts (NC animals). Here, a combined metabolomic, proteomic and epigenomic approach was conducted in the liver tissue. Herein, we report that targeted and untargeted metabolome analysis revealed a global alteration in the hepatic metabolism of VT animals, mainly related to lipid metabolism (e.g. polyunsaturated fatty acids, steroids, steroid hormones...). Proteomic analyses supported the metabolomic results, unveiling changes in VT animals related to the previous metabolites. The overall results denoted that metabolic disorders participated in a complex network of physiological pathways that collectively could support physiological differences between VT and NC animals. Moreover, previous deviations were associated with methylation changes involved in lipid metabolism and apoptosis genes. Remarkably, the health status of VT animals appeared similar to that in NC animals. Our data demonstrated molecular transgenerational inheritance induced by vitrified embryo transfer procedures in ancestors. Further research is needed to validate the significance of these findings.





## 7.1. INTRODUCTION

During the preimplantation period, major epigenetic reprogramming occurs, to provide the developing embryo with an epigenetic profile coherent with pluripotency, from which differentiated cells acquire lineage-specific transcriptional profiles [1]. Nevertheless, modifications in environmental conditions can modify this epigenetic reprogramming in the early embryo, changing its developmental programme [2]. This developmental plasticity is thought to allow advantageous adaptive response mechanisms to be adapted appropriately to the environment in which the embryo will be developed [3]. However, stressful exposures outside its natural range in mammalian embryos that have not evolved appropriate mechanisms may result in non-adaptive responses [4]. This theory, now called developmental origins of health and disease (DOHaD), postulates that suboptimal environment during embryo or foetal development may lead to adjustments in the anatomy, physiology and metabolism of various organ systems and thereby influence disease susceptibility [3,4].

Assisted Reproductive Technologies (ARTs) entail the furthest change from the natural environment, coinciding with a critical window typified by epigenetic rearrangement when extreme environmental perturbations could cause errors that affect the programming of cell states [2,5]. *In vivo*, developing embryos are exposed to dynamic conditions of hormones, nutrients, growth factors and cytokines produced by the female. Meanwhile, embryos developed under *in vitro* conditions are exposed to static and limited nutrients, and in contact with end products of metabolism in polystyrene substrates [6]. Besides, ART includes an environmental exposure that deviates widely from *in vivo* conception, including mechanical manipulation, light exposure, fluctuations in temperature, synthetic culture mediums, gas atmosphere and pH deviations, plus absence of embryo-maternal signalling [6,7]. Therefore, safety concerns regarding ART are a serious object of debate [5,8]. To date, it has been reported that infants conceived by ART have a 3-fold higher incidence of epigenetic disorders than infants conceived naturally [9]. In the same sense, ART conception has been associated with an approximately 2-fold increased risk of congenital disabilities or perinatal mortality [10]. Furthermore, emerging evidence of short and medium-term studies suggests that ART treatment may also predispose individuals to an increased risk of growth deviations or chronic ageing-related diseases [11]. Knowledge regarding the long-term consequences of ART procedures remains quite modest in humans, as most of the ART children are still young [6,12]. Furthermore, due to continuous changes in ART practice, and to numerous confounding factors that may be associated with health complications (e.g. parental age, male or female infertility, social status, lifestyle, etc.) it is challenging to provide exhaustive answers from clinical outcomes [5]. Thus, published data are circumstantial, limited, and occasionally contradictory [10]. Till now, research data coming from model species avoided confounding factors to meet the concerns of ART practitioners,

especially those regarding birth weight and growth trajectories, metabolic health, cardiovascular troubles and epigenetic alterations [13]. However, both human and model species studies have provided a notable increase of information reinforcing the hypothesis that most of these ART-related health marks may be attributable to epigenetic variation induced during the periconceptional period [2,5,10,14]. The molecular mechanisms whereby it occurs have yet to be elucidated. It is known that any embryo manipulation led to a specific and unique molecular signature in developing embryos and adult tissues, showing a tissue-specific impact of *in vitro* stressors on gene expression [7,15]. However, the underlying molecular networks behind ART phenotypes require additional studies. Moreover, there is another controversial question regarding ‘transgenerational epigenetic inheritance’, whereby acquired marks may affect not only the F1 generation but also are inherited by future generations through the germline (concepts reviewed in [16,17]). This event has been thoroughly documented in plants, nematodes and fruit flies but, although some shreds of evidence have been reported in ART animals, its occurrence in mammals and particularly in humans remains enigmatic [2,17]. Recently, Garcia-Dominguez et al. reported in a rabbit model that embryo manipulations during a vitrified embryo transfer (VET) procedure incur both long-term and transgenerational phenotypic and molecular alterations for the offspring [18–20]. In the current study, we applied a multi-omic approach (metabolomic, proteomic and epigenomic) to better understand the molecular framework related to these transgenerational effects in adult animals, comparing the molecular signatures of the liver tissue of animals born from vitrified-transferred (VT) embryos and those animals naturally-conceived (NC).

## 7.2. MATERIALS AND METHODS

All chemicals, unless otherwise stated, were reagent-grade and purchased from Sigma-Aldrich Química S.A. (Alcobendas, Madrid, Spain).

### 7.2.1 Animals and ethical statements

Californian rabbits were used for the experiment [21]. All experiments complied with the Directive 2010/63/EU EEC and institutional guidelines of the Universitat Politècnica de València Ethical Committee. All animals were bred and euthanised in an approved animal facility (code: ES462500001091). Experimental protocols were conducted under the supervision of the animal welfare committee in charge of this animal facility (code: 2015/VSC/PEA/00061). An authorisation certificate issued by the Valencian governmental administration to experiment on animals is held by XGD (code: 2815), FMJ (code: 2273) and JSV (code: 0690).

## 7.2.2. Experimental design

Figure 7.1 illustrates the experimental design. The direct effect of VET was present in the embryos which formed the F1 generation and over the germline developing within these embryos, which ultimately originated the F2 generation. Then, the F3 generation is the first not directly exposed to the VET procedure [22]. Therefore, to study transgenerational inheritance of the effects induced after VET in the parental genome, it is necessary to obtain the F3 generation. With this aim, two experimental progenies were established as described before [19,20].

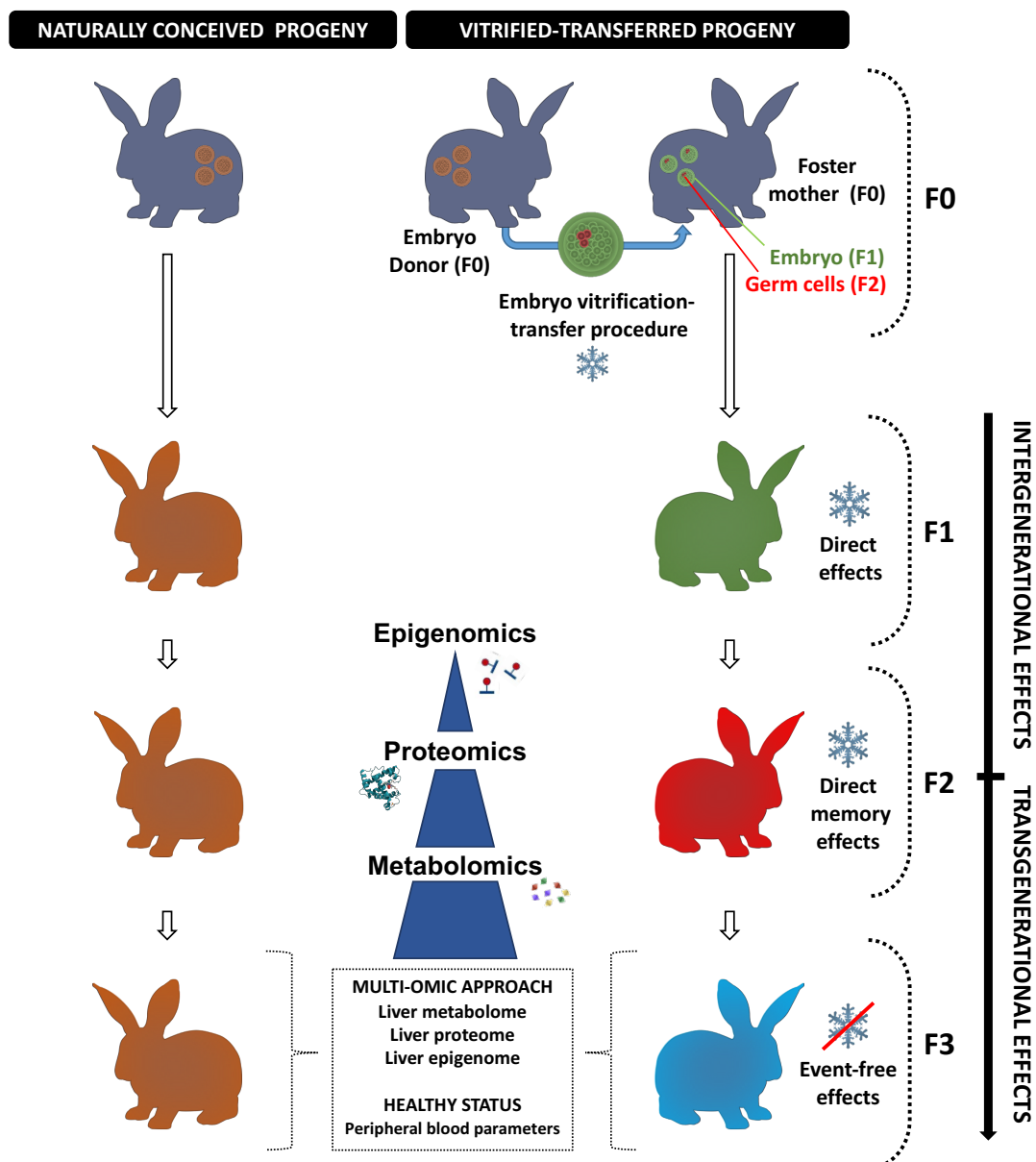


**Figure 7.1.** Experimental design. Two experimental progenies were developed, one from vitrified-transferred embryos and other by natural conception. F3 animals were compared to assess the transgenerational molecular inheritance of the effects induced by embryo vitrification in the ancestors' embryos.

Briefly, one was generated from 158 vitrified embryos derived from 13 donors, which were transferred into 13 foster mothers (VT progeny). The other was constituted as a control progeny by naturally-conceived animals (NC progeny), from 14 females inseminated contemporaneously with the previous donors. Embryo cryopreservation and transfer procedures have been described in detail previously [23]. At birth, 77 NC and 69 VT animals of the F1 generation were obtained. Both progenies were mated over two subsequent generations within each experimental group without any embryonic manipulation. To reduce the inbreeding, mating between animals with common grandparents was avoided. Hence, 61 NC and 56 VT animals were obtained for the F2 generation, and 61 NC and 64 VT animals constituted the F3 generation. Animals of both progenies in each generation were housed in the same conditions throughout the experiment. After weaning at 4th week, animals were caged collectively (8 rabbits per cage) until the 9th week. After that, animals were housed individually (flat deck indoor cages; 75×50×40 cm). In order to reduce confounding factors, the analysis was restricted to males, as they are thought to be less variable due to their constant hormone levels [24]. Once F3 progenies (NC and VT) reach the adult stage (56th week), haematological and biochemical analyses on peripheral blood were addressed to evaluate and compare its health status. After that, a comparative metabolomic, proteomic and epigenomic study was carried out between NC and VT animals of the F3 generation.

### **7.2.3. Determination of peripheral blood parameters**

Before the euthanasia, 20 individual blood samples (10 from VT and 10 from NC animals) were obtained from the central ear artery. Animals were selected randomly, keeping one animal of each litter (parity) within each experimental group. From each animal, two blood samples were taken. The first was dispensed into an EDTA-coated tube (Deltalab S.L., Barcelona, Spain), and the other into a serum-separator tube (Deltalab S.L., Barcelona, Spain). Blood count was performed from EDTA-tubes at most 10 min after collection, using an automated veterinary haematology analyser MS 4e automated cell counter (MeletSchloesing Laboratories, France) according to the manufacturer's instructions. The blood parameters recorded were: white blood cells, lymphocytes, monocytes, granulocytes, red blood cells, haemoglobin and haematocrit. From the second tube, biochemical analysis of the serum glucose, cholesterol, albumin, total bilirubin and bile acids were performed, as hepatic metabolic indicators. Briefly, samples were immediately centrifuged at 3000 x g for 10 min, and serum was stored at -20 °C until analysis. Then, glucose, cholesterol, albumin and total bilirubin levels were analysed by enzymatic colorimetric methods, while bile acids were measured by photometry. All the methodologies were performed in an automatic chemistry analyser model Spin 200E (Spinreact, Girona, Spain), following the manufacturer's instruction. All

samples were processed in duplicate. A general linear model (GLM) was fitted for the statistical analysis of the peripheral blood parameters, including as fixed effect the experimental group with two levels (VT and NC). Data were expressed as least-squares means  $\pm$  standard error of means. Differences of p-value  $\leq 0.05$  were considered significant. All statistical analyses were performed with SPSS 21.0 software package (SPSS Inc., Chicago, Illinois, USA).

#### **7.2.4. Sample collection for molecular study**

The uniformity of the liver tissue (four major cell types, of which hepatocytes constitute  $\approx 70\%$  of the total liver cell population) facilitates the sampling [25]. Then, individual liver samples were randomly taken from each animal (one rabbit, one sample). After that, samples were washed with phosphate-buffered saline solution and each individual sample was divided into three parts. Two of them were directly flash-frozen in liquid nitrogen and stored at  $-80^{\circ}\text{C}$  for the metabolomic and proteomic study. The other was stored in RNA-later (Ambion Inc., Huntingdon, UK) at  $-20^{\circ}\text{C}$  for the epigenomic analysis. Each sample for the metabolomic approach were generated mixing tissues from 4 different animals (pools). Thus, 12 pooled samples (6 VT and 6 NC) were used for the metabolomic study. Meanwhile, for proteome and epigenome interrogation, individualised samples were used, which came from the same individuals used for our previous transcriptomic approach [20]. Then, 8 individual samples (4 VT and 4 NC) were used in the proteome and epigenome analysis.

#### **7.2.5. Semi-polar and non-polar analysis of the liver metabolome**

Targeted and untargeted liquid chromatography-electrospray ionization-high resolution mass spectrometry (LC-ESI-HRMS) analysis of the semi-polar metabolome were performed as previously described [26–28]. Semi-polar metabolites were extracted from 10 mg of lyophilised, homogeneously ground hepatic tissue with 0.75 ml of cold 75% (v/v) methanol, 0.1% (v/v) formic acid, spiked with 10  $\mu\text{g/ml}$  formononetin as internal standard. After shaking for 40 min at 20 Hz using a Mixer Mill 300 (Qiagen), samples were centrifuged for 15 min at 20,000g at  $4^{\circ}\text{C}$ . Then, 0.6 ml of supernatant were removed and transferred to HPLC tubes. For each experimental group, 6 independent biological replicates, consisting of 4 animals each, were analysed. For each biological replicate, at least one technical replicate was carried out. Liquid chromatography (LC) was carried out using a Phenomenex C18 Luna column ( $100 \times 2.0$  mm,  $2.5 \mu\text{m}$ ) and the mobile phase was composed by water-0.1% formic acid (A) and acetonitrile-0.1% formic acid (B). The gradient was: 95%A:5%B (1 min), a linear gradient

to 25%A:75%B over 40 min, 2 min isocratic, before going back to the initial LC conditions in 18 min.

Targeted and untargeted liquid chromatography-atmospheric pressure chemical ionization-high resolution mass spectrometry (LC-APCI-HRMS) analysis of the non-polar metabolome were carried as reported before [29–31]. Non-polar metabolites were extracted from 5 mg of lyophilised, homogeneously ground liver tissue was extracted using 1 ml of 25% (v/v) methanol, 50% (v/v) chloroform, 25% (v/v) 50 mM-Tris-HCl, spiked with 50 µg/ml DL- $\alpha$ -tocopherol acetate as internal standard. After centrifugation, the organic hypophase was kept and the aqueous phase re-extracted with the same volume previously used of chloroform spiked with the internal standard. The pooled organic extracts were dried with a Speed Vac concentrator, and the residue was resuspended in ethyl acetate (100 µL). For each experimental group, 6 independent biological replicates, consisting of 4 animals each, were analysed; for each biological replicate, at least one technical replicate was carried out. LC separations were performed using a C30 reverse-phase column (100 × 3.0 mm; 3 µm, YMC Europe). The solvent systems were methanol (A); 75% methanol (v/v), 25% water (v/v) and 0.2% ammonium acetate (B); tert-butyl-methyl ether (C). The gradient elution was as follows: 0 to 6 min 95% A, 5% B, and 0% C; 1 min 80% A, 5% B, and 15% C; 5 min 80% A, 5% B, and 15% C; 20 min 30% A, 5% B, and 65% C; 22 min 30% A, 5% B, and 65% C; 18 min 95% A, 5% B, and 0% C.

Five microlitres of each sample were injected and a flow of 0.25 and 0.8 ml/min was used throughout the LC semi-polar and non-polar runs, respectively. Mass spectrometry analysis was performed using a quadrupole-Orbitrap Q-exactive system (ThermoFisher scientific, USA), operating in positive/negative heated electrospray ionisation (HESI) or atmospheric pressure chemical ionisation (APCI) coupled to an Ultimate HPLC-DAD system (Thermo Fisher Scientific, Waltham, MA). For semi-polar metabolite analysis, mass spectrometer parameters were as follows: capillary and vaporiser temperatures 30°C and 270°C, respectively, discharge current 4.0 KV, probe heater temperature at 370°C, S-lens RF level at 50 V. The acquisition was carried out in the 110/1600 m/z scan range, with the following parameters: resolution 70,000, microscan 1, AGC target 1e6, and maximum injection time 50. Full scan MS with data-dependent MS/MS fragmentation was used for metabolite identification. For non-polar analysis, APCI parameters were as follows: nitrogen was used as sheath and auxiliary gas, set to 20 and 10 units, respectively. The vaporiser temperature was 300°C, the capillary temperature was 250°C, the discharge current was set to 5.5 µA, and S-lens RF level was set at 50. All solvents used were LC-MS grade quality (CHROMASOLV® from Sigma-Aldrich). Metabolites were quantified in a relative way by normalisation on the internal standard (formononetin and DL- $\alpha$ -tocopherol acetate) amounts.

Untargeted metabolomics was performed using the SIEVE software (ThermoFisher Scientific). Briefly, after chromatogram alignment and retrieval of all the detected frames (e.g., ions), differentially accumulated metabolites (DAMs) were detected by a statistical analysis (one-way ANOVA plus Tukey's pairwise comparison) using the SPSS software (SPSS Inc., Chicago, Illinois, USA), considering an adjusted  $p$ -value  $\leq 0.05$ . Principal component analysis (PCA) and Heat-Maps (HM) hierarchical clustering of untargeted metabolomes was performed using the ClustVis online software (<https://biit.cs.ut.ee/clustvis/>). Targeted metabolite identification was performed by comparing chromatographic and spectral properties with authentic standards (if available) and reference spectra, in house database, literature data, and on the basis of the  $m/z$  accurate masses, as reported in the Pubchem database (<http://pubchem.ncbi.nlm.nih.gov/>) for monoisotopic mass identification, or on the Metabolomics Fiehn Lab Mass Spectrometry Adduct Calculator (<http://fiehnlab.ucdavis.edu/staff/kind/Metabolomics/MS-Adduct-Calculator/>) in the case of adduction detection. Finally, DAMs were detected as previously.

#### **7.2.6. Comparative proteomic analysis**

The proteome analyses were performed in the Proteomics Unit of the University of Valencia, Valencia, Spain (member of the PRB2-ISCIII ProteoRed Proteomics Platform). The analysis of the hepatic proteome was performed as previously described [19]. First, we conducted a data-dependent acquisition (DDA) analysis to study the complete proteome by building up a spectral library using in-gel digestion and LC-MS/MS. Then, a sequential window acquisition of all theoretical fragment ion spectra mass spectrometry (LC-SWATH-MS) analysis was performed to determine quantitative differences in liver protein composition among our experimental rabbit progenies.

For protein identification, validation and quantification, data were analysed as follows. After library LC-MS/MS, the SCIEX.wiff data-files were processed using ProteinPilot v5.0 search engine (AB SCIEX, Alcobendas, Madrid, Spain). The Paragon algorithm (5.0.2.0, 5174) of ProteinPilot was used to search against the Uniprot Mammalia protein sequence database (1,376,814 proteins searched) with the following parameters: trypsin specificity, cysteine-alkylation, without taxonomy restriction, and the search effort set to thorough and false discovery rate (FDR) correction for proteins [32]. To avoid using the same spectral evidence in more than one protein, the identified proteins were grouped based on MS/MS spectra by the Protein-Pilot Pro Group™ Algorithm, regardless of the peptide sequence assigned. The protein within each group that could explain the most spectral data with confidence was depicted as the primary protein of the group. The resulting Protein-Pilot group file was loaded into PeakView® (v2.1, AB SCIEX, Alcobendas, Madrid, Spain), and peaks from SWATH runs were extracted with a

peptide confidence threshold of 95% confidence and a FDR less than 1%. The number of peptides per protein was set at 50, and six transitions per peptide were necessary to quantify one peptide. Modified peptides were excluded. After peptide detection, peptides were aligned among different samples using peptides detected at high confidence from the library. The extracted ion chromatograms were integrated, and the areas were used to calculate the total protein quantity. The mass spectrometry proteomics data were deposited with the ProteomeXchange Consortium via the PRIDE [33] partner repository with the dataset identifiers: PXD017972 (SWATH data) and PXD016874 (Spectral Library data).

The quantitative data obtained by PeakView® were analysed using MarkerView® (v1.2, AB SCIEX, Alcobendas, Madrid, Spain). Normalization of the calculated areas was done by summing total areas. A t-test was used to identify the differentially expressed proteins (DEPs) among the two experimental groups (VT and NC). Proteins were considered differentially expressed with an adjusted p-value  $\leq 0.05$ . Rabbit (*Oryctolagus cuniculus*) identifiers were obtained using the Blast tool from UniProt, keeping the output with the high-identity score. Principal component analysis (PCA) and Heat-Map (HM) clustering was performed using ClustVis (<https://biit.cs.ut.ee/clustvis/>). Functional descriptive pie charts of DEPs were obtained from the Panther web tool (<http://pantherdb.org/>) using *Homo sapiens* as a reference and the human orthologous gene names (obtained from Biomart-Ensembl web tool: <https://www.ensembl.org/info/data/biomart/index.html>) as input data. Functional annotation of DEPs, enrichment analysis of their associated “Gene Ontology” (GO) terms and “Kyoto Encyclopedia of Genes and Genomes” (KEGG) pathways analysis were computed using the free available bioinformatics software DAVID Functional Annotation Tool (<https://david.ncifcrf.gov/home.jsp>; version 6.8), considering a P-value (modified Fisher’s exact test, EASE score) of less than 0.05. In addition, DEPs were sent to the Search Tool for the Retrieval of Interacting Genes/Proteins (STRING; <https://string-db.org/>; version 11.0) to build a functional protein association network.

### **7.2.7. Genome-wide DNA methylation profiling by MBD-Seq**

A double extraction of total DNA and RNA of liver were extracted using Ambion (mirVana) and Qiagen (AllPrep) columns following the protocol of Peña-Llopis and Brugarolas [34]. RNA samples were those used previously in our transcriptomic study [20], meanwhile DNA samples were used here to perform the epigenetic approach. DNA integrity were checked using 1% agarose electrophoresis. Then, the MBD-seq service was provided by Macrogen Inc. (Seoul, Republic of Korea).



Methylated DNA was obtained using the MethylMiner Methylated DNA Enrichment kit (Invitrogen, Carlsbad, CA, USA) according to the manufacturer's instructions. Briefly, fragmentation of 1 µg of genomic DNA was performed using adaptive focused acoustic technology (AFA; Covaris) and captured by MBD proteins. The methylated DNA was eluted in high-salt elution buffer. DNA in each eluted fraction was precipitated using glycogen, sodium acetate, and ethanol, and resuspended in DNase-free water. The eluted DNA was used to generate libraries following the standard protocols of TruSeq Nano DNA Library Prep kit (Illumina). The eluted DNA was repaired, an A was ligated to the 3' end, and TruSeq adapters were ligated to the fragments. Once ligation was assessed, the adapter-ligated product was PCR amplified. The final purified product was quantified using qPCR according to the qPCR Quantification Protocol and qualified using Agilent Technologies 4200 TapeStation (Agilent technologies). We sequenced using the HiSeq™ 2500 platform (Illumina).

Reads were mapped using bwa-mem [35] against *Oryctolagus cuniculus* genome assembly OryCun2.0.87 from ENSEMBL (<https://www.ensembl.org/index.html>). Only reads mapped against the genome with a mapq value of 57 or higher were kept using SAMtools [36]. For each sample, Reads Per Kilobase Million (RPKM) was calculated using MEDIPS [37], this values were joined into a table and used for assessing how similar were the samples inside his own experimental group by PCA visualization. The differentially methylated region (DMR) windows were calculated using Bioconductor package MEDIPS [37], using as arguments a window size of 250bp, removing the excess of stacked reads in a given position with  $\text{uniq} = 1e-3$  and using as DMR detection method edgeR. DMR windows with an adjusted p-value  $< 0.005$  were selected for further analyses. BED files were created from OryCun2.0.87 assembly's annotation for 2kbp adjacent gene regions, exon regions and intron regions with in-house scripts. Also, BED files for DMR results were created, merging adjacent windows. In order to check for DMR's potential effects on gene expression, these BED files were compare to seek for genes with DMR associated to them with BEDTools [38]. Once differentially methylated genes (DMGs) were identified, its functional annotation was performed using DAVID Functional Annotation Tool as above.

## 7.3. RESULTS

### 7.3.1. Peripheral blood parameters (healthy status)

As shown in Table 7.1, no significant difference was found in the haematological profile (white blood cells, red blood cells, haemoglobin and haematocrit) between VT and NC animals. Attending to the serum biochemical data, lower levels of cholesterol and higher

levels of glucose were exhibited by the VT animals ( $p < 0.05$ ). However, all parameters ranged between the normal values in rabbits [39].

**Table 7.1.** Haematological and biochemical comparison, assessing the transgenerational effect of the vitrified embryo transfer procedure.

PERIPHERAL BLOOD PARAMETERS	Naturally conceived (n=10)	Vitrified-transferred (n=10)
<b>HAEMATOLOGY</b>		
White blood cells ( $10^3/\text{mm}^3$ )	9.1 ± 1.71	7.4 ± 1.71
Lymphocytes (%)	40.1 ± 2.75	36.0 ± 2.75
Monocytes (%)	7.3 ± 0.72	6.4 ± 0.72
Granulocytes (%)	46.7 ± 2.83	49.3 ± 2.83
Red blood cells ( $10^6/\text{mm}^3$ )	6.1 ± 0.27	6.3 ± 0.27
Haemoglobin (g/dL)	12.6 ± 0.63	13.1 ± 0.63
Haematocrit (%)	43.8 ± 2.26	44.0 ± 2.26
<b>SERUM METABOLITES<sup>†</sup></b>		
Albumin (g/dL)	4.4 ± 0.91	4.5 ± 0.91
Bile acids ( $\mu\text{mol/L}$ )	6.9 ± 1.08	7.1 ± 1.08
Cholesterol (mg/dL)	32.2 ± 1.94 <sup>a</sup>	25.6 ± 1.94 <sup>b</sup>
Glucose (mg/dL)	103.3 ± 10.39 <sup>b</sup>	138.7 ± 10.39 <sup>a</sup>
Bilirubin total (mg/dL)	0.1 ± 0.02	0.1 ± 0.02

n represents the number of animals. Data are expressed as least-square means ± standard error of means. <sup>a,b</sup> Values in the same row with different superscript are significantly different ( $p < 0.05$ ). <sup>†</sup> Serum indicators of the hepatic function.

### 7.3.2. Comparative study of the liver metabolome

First of all, we carried out an untargeted metabolomic analysis to gain a general overview of the metabolic changes occurring between the hepatic tissue of VT and NC animals. In total, 443 metabolites were quantified, of which 290 (65.5%) and 153 (34.5%) belonged from the semi-polar and non-polar fraction, respectively (Figure 7.2A). Specifically, of the total quantified metabolites, 211 (47.6%) were detected as DAMs, of which 160 (75.8%) and 51 (24.2%) belonged from the semi-polar and non-polar fraction, respectively (Figure 7.2A). The variability among these DAMs was investigated by building PCA diagrams, which clustered the samples according to their origin (NC or VT) both for the semi-polar (Figure 7.2B) and non-polar (Figure 7.2C) metabolites. HM clustering graphics showed an overall up-accumulation of the semi-polar DAMs (Figure 7.2D) in VT livers compared to the NC group, whereas those non-polar were generally down-accumulated (Figure 7.2E).

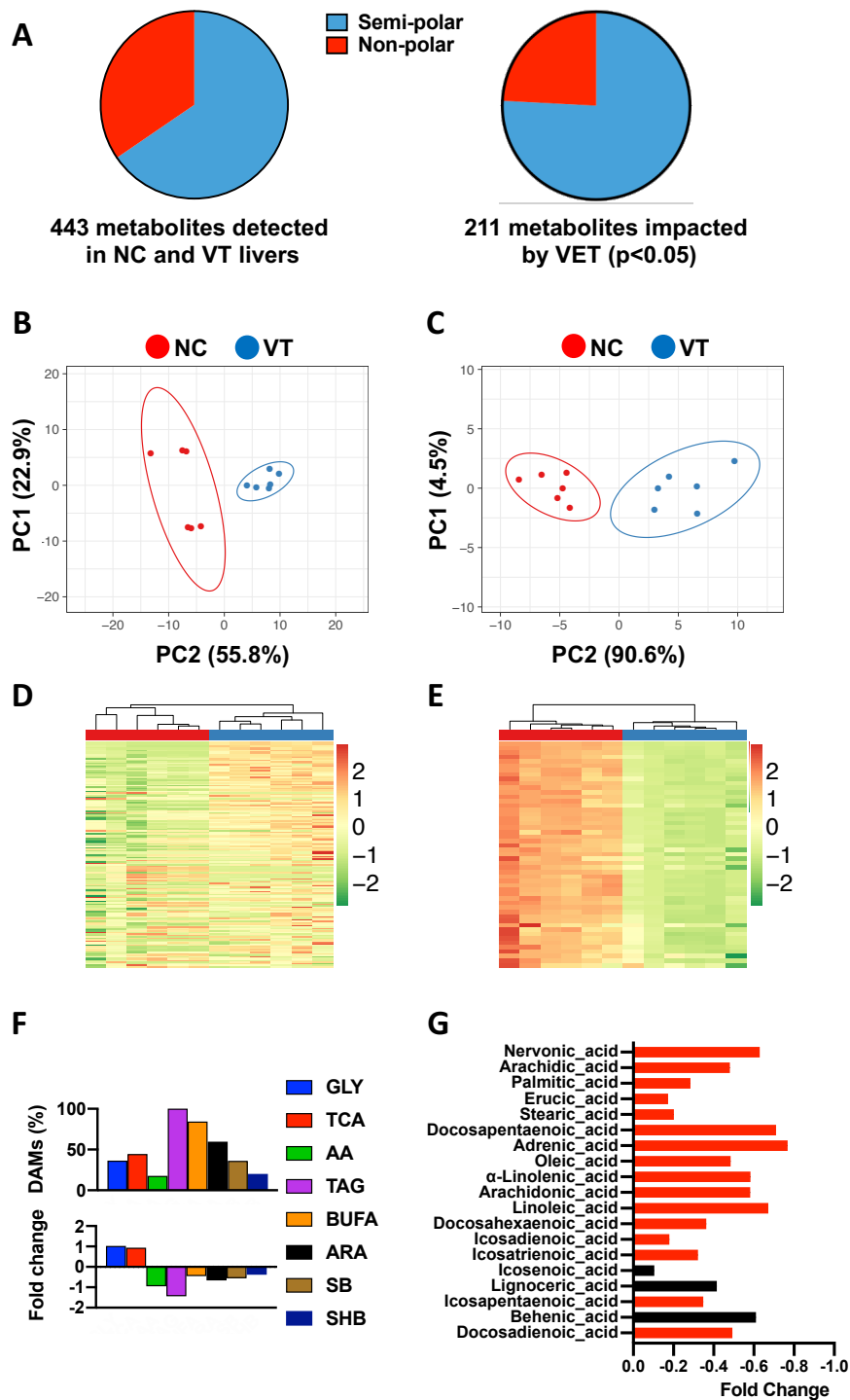


**Figure 7.2.** Metabolite profile changes in the liver of F3 animals after vitrified embryo transfer procedure. Samples between vitrified-transferred (VT) and naturally-conceived (NC) group were compared. [A] Categorical distribution of the 443 metabolites detected by the untargeted analysis and the 211 differentially accumulated metabolites (DAMs) in VT rabbits. [B] Principal Component Analysis (PCA) of the untargeted semi-polar DAMs. [C] PCA of the untargeted non-polar DAMs. [D] Heat Map (HM) clustering of the untargeted semi-polar DAMs. [E] HM clustering of the untargeted non-polar DAMs. [F] Percentage of DAMs, and its fold change, belonging to some metabolic pathways; GLY: Glycolysis-gluconeogenesis; TCA: Citric acid cycle; AA: Biosynthesis of amino acids; TAG: Triglycerides; BUFA: Biosynthesis of unsaturated fatty acids; ARA: Arachidonic acid metabolism; SB: Steroid biosynthesis; SHB: Steroid hormone biosynthesis. [G] DAMs related to the biosynthesis of unsaturated fatty acids pathway. Red bars denote statistical differences.

To better investigate changes in known liver metabolites, we performed a targeted metabolomic analysis in which we quantified, relatively, 153 metabolites. The complete metabolite dataset and its fold change are reported in Annex III (Supplementary Table S1). In total, 72 DAMs were identified in the targeted analysis (Annex III, Supplementary Table S1), of which 65 (90.3%) were down-accumulated in VT samples compared to NC ones. Functional clustering of these metabolites revealed transgenerational effects of VET over several metabolic pathways, including glycolysis-gluconeogenesis, citrate cycle, biosynthesis of amino acids, biosynthesis of unsaturated fatty acids, biosynthesis of steroids and steroid hormones, glycerolipid metabolism and arachidonic acid metabolism (Figure 7.2F). As shown, targeted analysis revealed higher relative affection of the non-polar metabolic pathways compared to the semi-polar ones (Figure 7.2F). Particularly, significant down-accumulation was detected in 16 (84.2%) of the metabolites involved in the unsaturated fatty acids biosynthesis (Figure 7.2G). Of note, VT livers exhibited lower levels of linoleic and arachidonic acids, which act as precursors of a wide range of lipophilic compounds, being some of them also dysregulated (Annex III, Supplementary Table S1). Otherwise, general down-accumulation were detected in 9 (36%) of the interrogated metabolites for the steroid biosynthetic pathway and, as expected, lower levels were detected downstream in some steroid hormones, including testosterone (Annex III, Supplementary Table S1).

### 7.3.3. Comparative study of the liver proteome

The complete spectral library included 28,685 of MS/MS spectra, corresponding to 14,737 distinct peptides and 1,846 proteins with a FDR  $\leq$  1%. With the restrictions used for extraction parameters of the areas, 1,491 proteins (FDR <1%) were quantified in the 8 samples. In comparing the proteomes between the VT and NC livers, 97 DEPs were identified in mammalian taxonomy, of which 96 found their homologous identification in rabbit (*Oryctolagus cuniculus*) taxonomy. PCA (Figure 7.3A) and HM (Figure 7.3B) analysis showed that, despite expected individual variability, samples from each group were clustered together. From these DEPs, there was 52.1% downregulated (50/96) and 47.9% upregulated (46/96) in VT samples compared to NC ones. Pie charts representing the DEPs distribution according to their biological process (Figure 7.3C), molecular function (Figure 7.3D) and cellular component (Figure 7.3E) showed that most DEPs have catalytic and binding activity, are involved in cellular and metabolic process, and are located in cell and organelles.

Of the proteins that were significantly different, a total of 71 DEPs were recognised by the DAVID software, whose annotation and fold change has been described in Annex III (Supplementary Table S2). Functional GO term enrichment and KEGG pathway analysis of DEPs were recorded in Annex III (Supplementary Table S3).

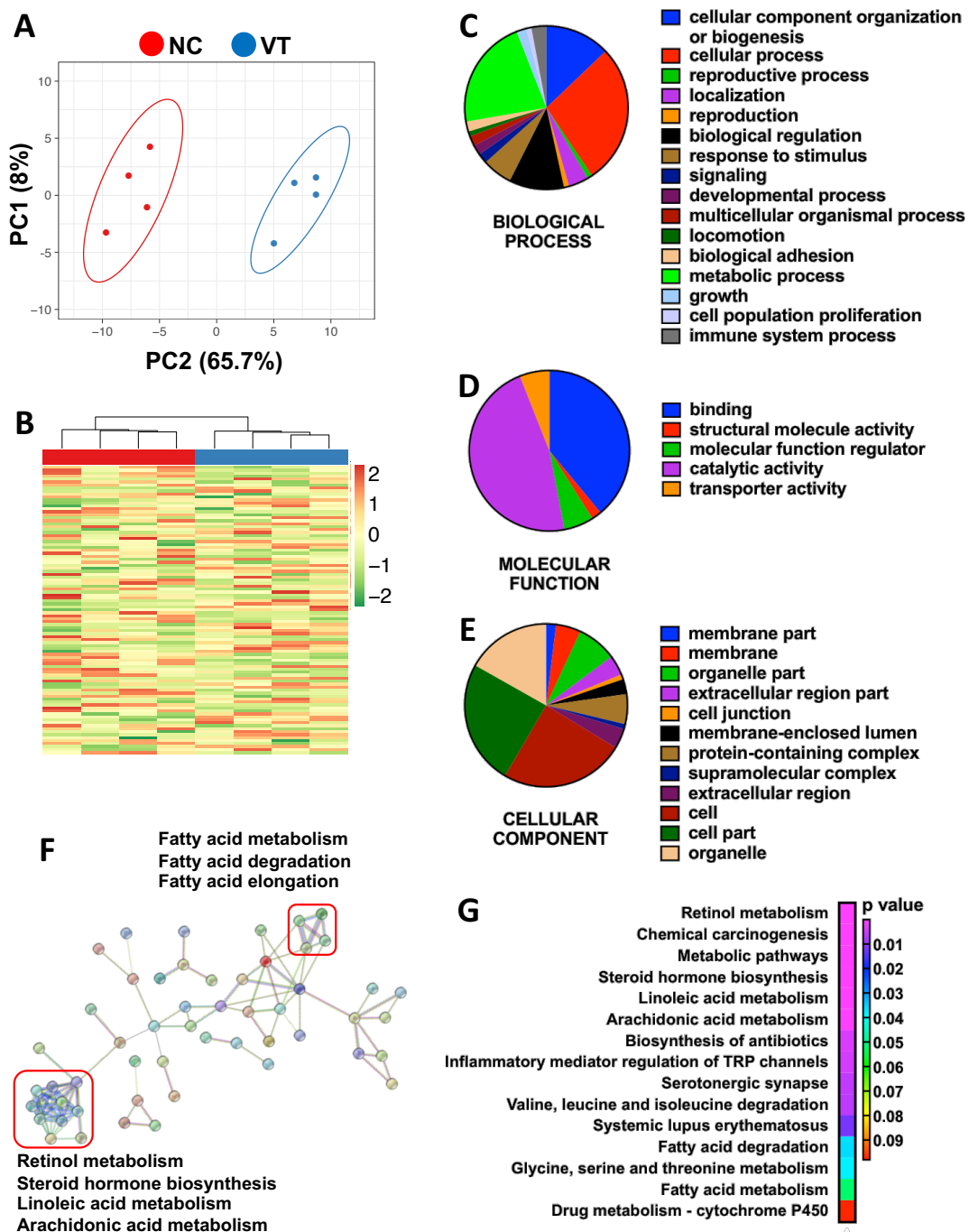


**Figure 7.3.** Protein profile changes in the liver of F3 animals after vitrified embryo transfer procedure. Samples between vitrified-transferred (VT) and naturally-conceived (NC) group were compared. [A] Principal Component Analysis of the differentially expressed proteins (DEPs). [B] Heat Map clustering of the DEPs. [C, D, E] Pie charts representing the DEPs distribution according to their biological process, molecular function, and cellular component. [F] Protein-protein interaction network of DEPs. Not interconnected DEPs were excluded. [G] KEGG analysis for the DEPs.

Thereby, 5 biological process, 9 molecular function and 11 cellular component terms were enriched after functional analysis, suggesting disturbances in the immunological responses, long-chain fatty acid metabolism and cell cycle regulation. KEGG pathway analysis revealed changes in pathways associated with the metabolism of retinoids,

steroid hormones and some long-chain polyunsaturated fatty acids (LCPUFA), such as linoleic and arachidonic acids. In addition, related KEGG terms suggested alterations of the immune system response. Beyond, with DEPs as seed nodes, a protein-protein interaction network was constructed using STRING software (Figure 7.3F). This analysis corroborated most of the terms offered by DAVID software (Figure 7.3G) but, in addition, revealed a tightly interconnected network around two principal clusters. One was related to the fatty acid metabolism, but the other allowed us to highlight that disturbances in the metabolism of retinoids, steroids and LCPUFA kept a strong relationship. Disturbances in the cytochrome P450 were thereby identified as the underlying cause of these changes.

### 7.3.4. Comparative study of the liver epigenome

After quality assessment, 4 NC and 3 VT samples were kept in the final analysis. The mean number of raw reads was  $92.8 \pm 1.6$  million, with a mean CG content (%) of  $52.6 \pm 0.13$ . The percentage of reads having a “Phred quality score” of over 30 (base call accuracy: 99.9%) was  $95.5 \pm 0.22\%$ . Of the 7,303 differentially methylated windows, 2,570 (35.2%) were hypomethylated and 4,733 (64.8%) were hypermethylated. The global mean methylation counts per window was  $12.3 \pm 0.18$  ( $38.9 \pm 0.46\%$ ) and  $15.5 \pm 0.16$  ( $61.1 \pm 0.46\%$ ) for NC and VT samples, respectively. PCA of the differentially methylated windows (Figure 7.4A) and HM clustering of DMGs (Figure 7.4B) revealed a good level of clustering for NC and VT samples, grouping them according to their origin. The MA-plot, scatter plot in a logarithmic scale of fold changes (y-axis) versus the mean expression signal (x-axis), revealed high methylation differences between VT and NC samples (Figure 7.4C). The generally high level of methylation in VT samples suggests that the genome has experienced substantial gain of methylation after VET. However, the landscape of the methylome variation suggests differential patterns of change depending on the genome regions. Thereby, 6 and 10 chromosomes were respectively hypomethylated and hypermethylated in the VT group compared to NC one (Figure 7.4D). Concordantly, the comparative epigenomic analysis revealed 121 DMGs, of which 43 (35.5%) were hypomethylated and 78 (64.5%) were hypermethylated in VT samples compared to the NC ones (Figure 7.4E). From these DMGs, DAVID software recognises 94 genes, whose gene name, associated chromosome/scaffold and methylation difference ( $\Delta\beta$ ) were annotated in Annex III (Supplementary Table S4). Functional analysis showed relevant associations between hypomethylated DMGs with dysregulations of cellular functions, the apoptotic process and the glycerolipid metabolism (Figure 7.4F). Meanwhile, hypermethylated genes were associated with cellular responses to DNA damage, cell ageing, apoptotic signalling, and transcription regulation (Figure 7.4F). DAVID GO term enrichment and KEGG pathway analysis of both hypomethylated and hypermethylated genes are showed in Annex III (Supplementary Table S5). Furthermore, Panther pie charts constructed from DMGs (both hypo- and

hypermethylated) enabled us to identify biological functions sensitive to the transgenerational epigenetic reprogramming process, such as metabolic and immune system processes (Figure 7.4G).

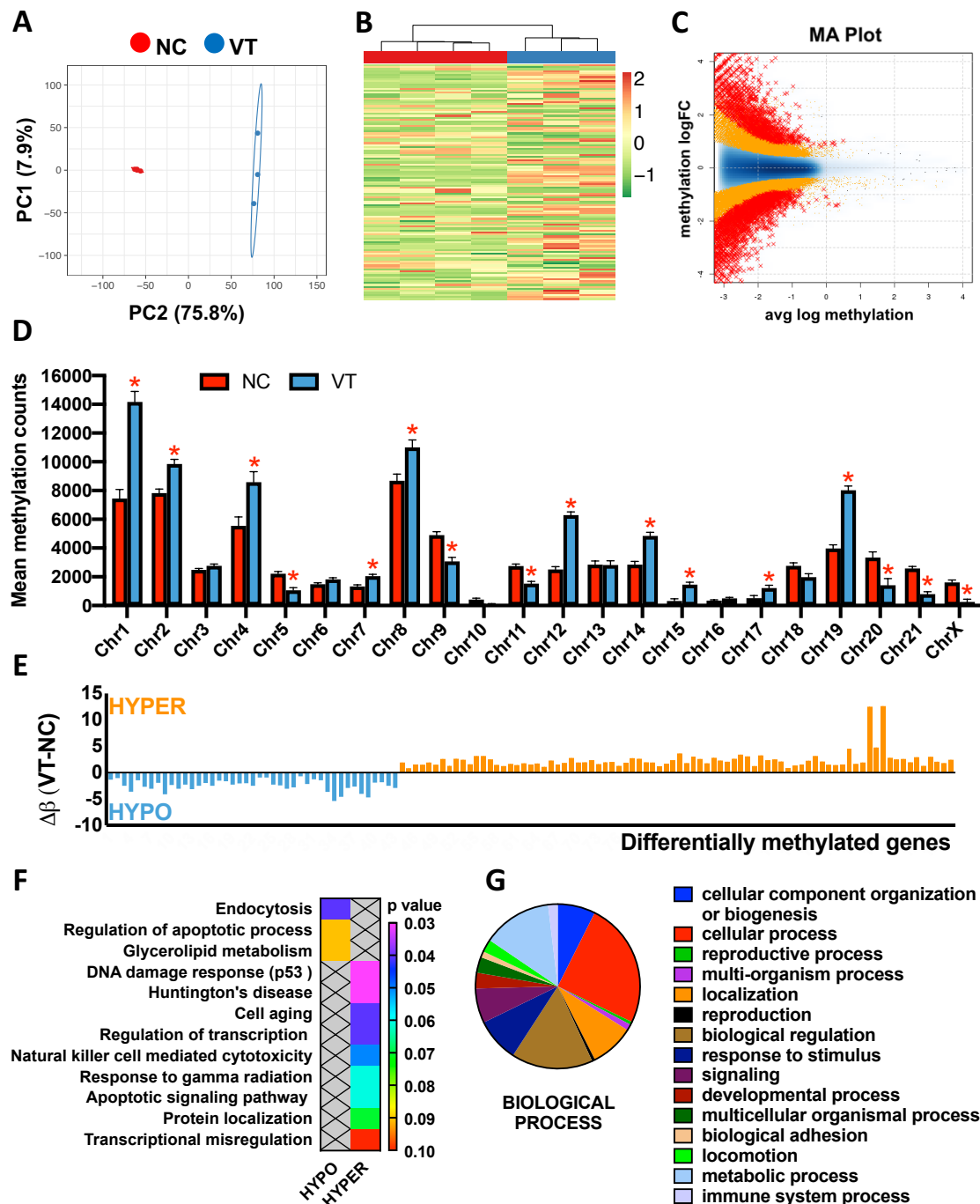


**Figure 7.4.** Genome-wide methylation changes in the liver of F3 animals after vitrified embryo transfer procedure. Samples between vitrified-transferred (VT) and naturally-conceived (NC) group were compared. **[A]** Principal Component Analysis of the differentially methylated windows. **[B]** Heat Map clustering of the differentially methylated genes (DMGs). **[C]** MA plot representing data comparison between VT and NC samples. **[D]** Total number of methylation counts per chromosome. Asterisks denote statistical differences. **[E]** Methylation difference ( $\Delta\beta$ ) of the 121 DMGs calculated as mean VT DNA methylation minus mean NC DNA methylation. **[F]** Gene Ontology (biological process) and KEGG analysis for the hyper- and hypo- DMGs. **[G]** Pie chart representing the total DMGs distribution according to their biological process.

## 7.4. DISCUSSION

Here, our integrative multi-omic approach demonstrated metabolomic, proteomic and epigenomic differences between VT and NC livers, suggesting that ancestor embryos (F1) exposed to VET had undergone a reprogramming event with transgenerational effects (F3). Hence, untargeted metabolomics analyses revealed alterations in both semi-polar and non-polar metabolites in VT animals. In agreement with our findings, several studies described non-polar and semi-polar metabolism alteration after ART (7,40–44). Globally, semi-polar metabolites were up-accumulated in VT animals compared to NC animals, while non-polar metabolites were down-accumulated, suggesting possible compensatory mechanisms (7). Particularly, Feuer et al. observed that conception by IVF reduces growth, impairs glucose tolerance and impacts the serum and liver metabolome, affecting a wide range of compounds such as carbohydrates, amino acids, and, specially, lipids (7,43,44). Concordantly, we have previously demonstrated that VET incurs both direct, intergenerational and transgenerational effects, reducing the growth performance and impacting the hepatic metabolism (18–20). Here, robust information supporting that VET incurs transgenerational metabolic effects was provided. We observed that VET increased the serum glucose levels in F3-VT animals, which also has been reported previously in F1-VT rabbits (19), although it ranged between the normal values (39). However, these findings could suggest that alterations in glucose metabolism, well described in humans after ART and especially after VET (42,45), could be inherited across the generations. Particularly, targeted analysis revealed higher relative affection of the non-polar metabolic pathways compared to the semi-polar ones. In agreement, increasing studies based on ART have described progenies with hepatic disorders in the lipid metabolism in foetal (46) and adult mice (7,41,44,47), as well as serum lipid profile deviations in mice and human (40,43,48,49). Concordantly with our results after VET, Gu et al. (41) observed that ART livers have alterations in the glycerolipid metabolism. Moreover, we studied the unsaturated fatty acids biosynthetic pathway in depth, finding severe alterations, as most of the metabolites involved were significantly downregulated in VT livers compared to those NC. Concordant results were previously described in old mice after ART (47). These compounds merit special attention, as it has been extensively reported that they are crucial for normal development and health in fetuses, newborns, and later stages (50–53). Transgenerational alteration of these metabolites after VET has been proposed as possible mechanisms to explain the phenotypic changes in VT rabbits during three consecutive generations (20). Together with Wang et al. (47), here we found significant downregulation of linoleic and arachidonic acids in the metabolomics analyses, which were also confirmed at the proteomic level. KEGG pathways analysis of DEPs reported alterations in the “linoleic acid metabolism” and “arachidonic acid metabolism”, but also denoted disturbances in the “steroid hormone biosynthesis” and “retinol metabolism”. All these findings are in line with our previous



transcriptomic study carried out on F3-VT rabbits (20). Intriguingly, DEPs involved in these four terms were grouped in the protein-protein interaction network, revealing that they belong to cytochrome P450. The cytochrome P450 proteins catalyse the metabolism of a large number of lipophilic compounds, including linoleic acid, arachidonic acid, retinol and steroid hormones (54,55). All these components have pivotal physiological functions *per se*, but also their derived metabolites, so perturbation of these compounds might have implications for optimal development (51,52,56,57). Particularly, some compounds related to arachidonic acid metabolism (e.g. eicosanoids, phosphatidylcholines...), which are crucial for normal cell function, growth, and immunity (52,58), were down-accumulated in VT animals compared to those NC. In this line, proteomic data also suggested alterations in the immune system. Concordantly, slower development and high risk of infections have been observed in ART offspring (59). Otherwise, it is worth noting that, although it ranged between the normal values (39), lower levels of serum cholesterol were noted in F3-VT animals, which also has been reported in F1-VT rabbits (19). These data are in agreement with previous studies in humans (40,48,49). Here, an impairment of the steroid biosynthesis pathway has been demonstrated in VT animals, as well as downstream alterations in hepatic cholesterol and steroid hormones levels, which are reduced. Steroid hormones are synthesized from cholesterol by members of the P450 and, after interacting with liver receptors, governs pathways related to the lipid and glucose homeostasis, liver growth, body growth, immunity, etc. (55,57,60). This scenario might contribute to explain the lower growth performance, and liver phenotypic changes observed transgenerationally after VET in rabbits (20). Of note, the biosynthesis of active forms of retinoids derivatives from retinol is of crucial importance for many physiological processes, including embryonic development, postnatal growth, and immune responses (56,61). Therefore, future studies studying this metabolic pathway could shed light on the underlying mechanisms causing the VT phenotype.

In this study, we observed that the hepatic epigenome changed significantly between VT and NC animals. More in detail, we identified 121 genes whose pattern of methylation changed in VT animals compared to NC. Of the biological process in which these genes were involved, 82.3% coincided with those attributed to DEPs. Furthermore, after GO term enrichment and KEGG pathway analysis, we found that DMGs were related to lipid metabolism, regulation and signalling of the apoptotic process, cell ageing, DNA damage responses through p53 mediator and immune function. Cell cycle arrest at G1 in response to DNA damage can be induced by p53, promoting senescence or apoptosis, an essential mechanism for embryogenesis, organogenesis, differentiation and reprogramming (62). Concordantly, also at the proteomic level, we detected significant enrichment among the GO terms related to the G1 transition. Further studies on this issue could pave the way to elucidating the underlying mechanisms of the physiological changes exhibited by the VT animals.

Moreover, differential methylation patterns were identified throughout 16 chromosomes, with a marked tendency to hypermethylation. Specifically, some chromosomes such as 1, 12 and 19 showed more significant methylation changes, which might indicate that some genes are altered preferentially than others (63). A high correlation was observed with our previous transcriptomic approach (chapter IV), as differentially methylated chromosomes contained 70.8% of the differentially expressed transcripts, and 81.1% downregulated transcripts belonged to generally hypermethylated (silenced) chromosomes (Annex III, Supplementary Figure S1). The developmental time points at which VT are implemented are precisely the time points at which large-scale reorganisation of the epigenome takes place (10,63). In this sense, the potential effect of ART procedures on the gamete and embryo epigenomes heads the list of mechanistic candidates that might explain the association between ART and its associated outcomes throughout life, including transgenerational ones (2,16,17,63,64). Nevertheless, F3-VT animals were seemingly healthy, supported by the haematological and biochemical blood parameters within the normal physiological range of variability (39). Therefore, rather than a perturbation of the reprogramming process, the VT physiological status could be induced by the intrinsic developmental plasticity of the early mammalian embryo, whereby embryos may respond to environmental cues during ART. Then, this process could change its developmental programme in a manner that can result in a phenotypic variation later in life and in subsequent generations (3,16). Indeed, some of the metabolic disturbances described throughout this study could derive from preimplantation stages, as similar alterations has been observed in early embryos after ART (6,13). There are some limitations affecting this study. First, the number of samples included is relatively small, which may restrict the interpretation of our results. Second, we only tested one tissue. Whether similar differences occur in other tissues, further studies are needed. Third, this work was limited to males, which are less variable, due to their constant hormone status. In females, the effects might likely be different (44), although this hypothesis requires further confirmation. To this end, future research works will be carried out to confirm and validate the biological relevance of these findings. We should keep in mind that ART are constantly evolving and rapidly applied without prior long-term safety evaluation to accommodate the needs of assisted reproduction (5). Therefore, this study must encourage the development of new approaches aimed at ensuring the safest use of ART.

## **7.5. CONCLUSION**

In summary, we conducted a multi-omic strategy that demonstrated the transgenerational inheritance of the molecular reprogramming induced by embryo cryopreservation procedure in ancestors. Our results suggest that alterations in the lipid metabolism and genome methylation patterns were present in the liver tissue of

descendants, unveiling evidences of physiological changes. Further research is needed to validate the biological significance and relevance of these findings, to ensure the proper health and welfare of the progeny with an *in vitro*-life legacy.

## 7.6. REFERENCES

- [1]. Monk D. Germline-derived DNA methylation and early embryo epigenetic reprogramming: The selected survival of imprints. *Int J Biochem Cell Biol* 2015;67:128–38.
- [2]. Ventura-Juncá P, Irrarázaval I, Rolle AJ, Gutiérrez JI, Moreno RD, Santos MJ. In vitro fertilization (IVF) in mammals: Epigenetic and developmental alterations. Scientific and bioethical implications for IVF in humans. *Biol Res* 2015;48:68.
- [3]. Roseboom TJ. Developmental plasticity and its relevance to assisted human reproduction. *Hum Reprod* 2018;33:546–52.
- [4]. Vrooman LA, Bartolomei MS. Can assisted reproductive technologies cause adult-onset disease? Evidence from human and mouse. *Reprod Toxicol* 2017;68:72–84.
- [5]. Zacchini F, Sampino S, Stankiewicz AM, Haaf T, Ptak GE. Assessing the epigenetic risks of assisted reproductive technologies: A way forward. *Int J Dev Biol* 2019;63(3–5):217–22.
- [6]. Ramos-Ibeas P, Heras S, Gómez-Redondo I, Planells B, Fernández-González R, Pericuesta E, et al. Embryo responses to stress induced by assisted reproductive technologies. *Mol Reprod Dev* 2019;86:1292–306.
- [7]. Feuer SK, Rinaudo PF. Physiological, metabolic and transcriptional postnatal phenotypes of in vitro fertilization (IVF) in the mouse. *J Dev Orig Health Dis* 2017;8:403–10.
- [8]. Cohen ME. The ‘brave new baby’ and the law: fashioning remedies for the victims of in vitro fertilization. *Am J Law Med* 1978;4(3):319–36.
- [9]. Uk A, Collardeau-Frachon S, Scavion Q, Michon L, Amar E. Assisted Reproductive Technologies and imprinting disorders: Results of a study from a French congenital malformations registry. *Eur J Med Genet* 2018;61(9):518–23.
- [10]. Novakovic B, Lewis S, Halliday J, Kennedy J, Burgner DP, Czajko A, et al. Assisted reproductive technologies are associated with limited epigenetic variation at birth that largely resolves by adulthood. *Nat Commun* 2019;10(1):3922.
- [11]. Chen M, Heilbronn LK. The health outcomes of human offspring conceived by assisted reproductive technologies (ART). *J Dev Orig Health Dis* 2017;8:388–402.
- [12]. Bergh C, Wennerholm UB. Long-term health of children conceived after assisted reproductive technology. *Ups J Med Sci* 2020;125(2):152–7.
- [13]. Duranthon V, Chavatte-Palmer P. Long term effects of ART: What do animals tell us? *Mol Reprod Dev* 2018;85:348–68.

- [14]. La Rovere M, Franzago M, Stuppia L. Epigenetics and neurological disorders in ART. *Int J Mol Sci* 2019;20(17):4169.
- [15]. Feuer SK, Liu X, Donjacour A, Simbulan R, Maltepe E, Rinaudo PF. Transcriptional signatures throughout development: the effects of mouse embryo manipulation in vitro. *Reproduction* 2017;153(1):107–122.
- [16]. Aiken CE, Ozanne SE. Transgenerational developmental programming. *Hum Reprod Update* 2014;20(1):63–75.
- [17]. Horsthemke B. A critical view on transgenerational epigenetic inheritance in humans. *Nat Commun* 2018;9:2973.
- [18]. Garcia-Dominguez X, Vicente JS, Marco-Jiménez F. Developmental Plasticity in Response to Embryo Cryopreservation: The Importance of the Vitrification Device in Rabbits. *Animals* 2020;10(5):804.
- [19]. Garcia-Dominguez X, Marco-Jiménez F, Peñaranda DS, Vicente JS. Long-Term Phenotypic and Proteomic Changes Following Vitrified Embryo Transfer in the Rabbit Model. *Animals* 2020;10(6):1043.
- [20]. Garcia-Dominguez X, Marco-Jiménez F, Peñaranda DS, Diretto G, García-Carpintero V, Cañizares J, et al. Long-term and transgenerational phenotypic, transcriptional and metabolic effects in rabbit males born following vitrified embryo transfer. *Sci Rep* 2020; In press (see chapter IV).
- [21]. Estany J, Camacho J, Baselga M, Blasco A. Selection response of growth rate in rabbits for meat production. *Genet Sel Evol* 1992;24:527–37.
- [22]. Skinner MK. What is an epigenetic transgenerational phenotype?. F3 or F2. *Reprod Toxicol* 2008;25:2–6.
- [23]. Garcia-Dominguez X, Marco-Jimenez F, Viudes-de-Castro MP, Vicente JS. Minimally invasive embryo transfer and embryo vitrification at the optimal embryo stage in rabbit model. *J Vis Exp* 2019;147:e58055.
- [24]. Zucker I, Beery AK. Males still dominate animal studies. *Nature* 2010;465:690.
- [25]. Ding C, Li Y, Guo F, Jiang Y, Ying W, Li D, et al. A cell-type-resolved liver proteome. *Mol Cell Proteomics* 2016;15(10):3190–202.
- [26]. Diretto G, Rubio-Moraga A, Argando A J, Castillo P, Gómez-Gómez L, Ahrazem O. Tissue-specific accumulation of sulfur compounds and saponins in different parts of garlic cloves from purple and white ecotypes. *Molecules* 2017;22(8):E1359.
- [27]. Cappelli G, Giovannini D, Basso AL, Demurtas OC, Diretto G, Santi C, et al. A *Corylus avellana* L. extract enhances human macrophage bactericidal response against *Staphylococcus aureus* by increasing the expression of anti-inflammatory and iron metabolism genes. *J Funct Foods* 2018;45:499–511.
- [28]. Di Meo F, Aversano R, Diretto G, Demurtas OC, Villano C, Cozzolino S, et al. Anti-cancer activity of grape seed semi-polar extracts in human mesothelioma cell lines. *J Funct Foods* 2019;61:103515.
- [29]. Fiore A, Dall'Osto L, Cazzaniga S, Diretto G, Giuliano G, Bassi R. A quadruple mutant of *Arabidopsis* reveals a  $\beta$ -carotene hydroxylation activity for LUT1/CYP97C1 and

- a regulatory role of xanthophylls on determination of the PSI/PSII ratio. *BMC Plant Biol* 2012;12:50.
- [30]. Rambla JL, Trapero-Mozos A, Diretto G, Moraga AR, Granell A, Gómez LG, et al. Gene-metabolite networks of volatile metabolism in Airen and Tempranillo grape cultivars revealed a distinct mechanism of aroma bouquet production. *Front Plant Sci* 2016;7:1619.
- [31]. Sulli M, Mandolino G, Sturaro M, Onofri C, Diretto G, Parisi B, et al. Molecular and biochemical characterization of a potato collection with contrasting tuber carotenoid content. *PLoS One* 2017;12(9):e0184143.
- [32]. Shilov I V., Seymourt SL, Patel AA, Loboda A, Tang WH, Keating SP, et al. The paragon algorithm, a next generation search engine that uses sequence temperature values sequence temperature values and feature probabilities to identify peptides from tandem mass spectra. *Mol Cell Proteomics* 2007;6(9):1638–55.
- [33]. Perez-Riverol Y, Csordas A, Bai J, Bernal-Llinares M, Hewapathirana S, Kundu DJ, et al. The PRIDE database and related tools and resources in 2019: Improving support for quantification data. *Nucleic Acids Res* 2019;47:D442–50.
- [34]. Peña-Llopis S, Brugarolas J. Simultaneous isolation of high-quality DNA, RNA, miRNA and proteins from tissues for genomic applications. *Nat Protoc* 2013;8(11):2240–55.
- [35]. Li H, Durbin R. Fast and accurate long-read alignment with Burrows-Wheeler transform. *Bioinformatics* 2010;26(5):589–95.
- [36]. Li H, Handsaker B, Wysoker A, Fennell T, Ruan J, Homer N, et al. The Sequence Alignment/Map format and SAMtools. *Bioinformatics* 2009;25(16):2078–9.
- [37]. Lienhard M, Grimm C, Morkel M, Herwig R, Chavez L. MEDIPS: Genome-wide differential coverage analysis of sequencing data derived from DNA enrichment experiments. *Bioinformatics* 2014;30(2):284–6.
- [38]. Quinlan AR, Hall IM. BEDTools: A flexible suite of utilities for comparing genomic features. *Bioinformatics* 2010;26(6):841–2.
- [39]. Fiorello C V, Divers SJ. Rabbits. In: Carpenter JW (James W, editor. *Exotic Animal Formulary*. Elsevier Inc.; 2013. p. 546–95.
- [40]. Miles HL, Hofman PL, Peek J, Harris M, Wilson D, Robinson EM, et al. In vitro fertilization improves childhood growth and metabolism. *J Clin Endocrinol Metab* 2007;92(9):3441–5.
- [41]. Gu L, Zhang J, Zheng M, Dong G, Xu J, Zhang W, et al. A potential high risk for fatty liver disease was found in mice generated after assisted reproductive techniques. *J Cell Biochem* 2018;119(2):1899–910.
- [42]. Chen M, Wu L, Zhao J, Wu F, Davies MJ, Wittert GA, et al. Altered glucose metabolism in mouse and humans conceived by IVF. *Diabetes* 2014;63(10):3189–98.

- [43]. Feuer SK, Liu X, Donjacour A, Lin W, Simbulan RK, Giritharan G, et al. Use of a mouse in vitro fertilization model to understand the developmental origins of health and disease hypothesis. *Endocrinology* 2014;155:1956–69.
- [44]. Feuer SK, Donjacour A, Simbulan RK, Lin W, Liu X, Maltepe E, et al. Sexually dimorphic effect of In Vitro Fertilization (IVF) on adult mouse fat and liver metabolomes. *Endocrinology* 2014;155:4554–67.
- [45]. Norrman E, Petzold M, Clausen TD, Henningsen AK, Opdahl S, Pinborg A, et al. Type 1 diabetes in children born after assisted reproductive technology: A register-based national cohort study. *Hum Reprod* 2020;35(1):221–31.
- [46]. Li B, Xiao X, Chen S, Huang J, Ma Y, Tang N, et al. Changes of Phospholipids in Fetal Liver of Mice Conceived by In Vitro Fertilization1. *Biol Reprod* 2016;94(5):105.
- [47]. Wang LY, Le F, Wang N, Li L, Liu XZ, Zheng YM, et al. Alteration of fatty acid metabolism in the liver, adipose tissue, and testis of male mice conceived through assisted reproductive technologies: Fatty acid metabolism in ART mice. *Lipids Health Dis* 2013;12:5.
- [48]. Guo XY, Liu XM, Jin L, Wang TT, Ullah K, Sheng JZ, et al. Cardiovascular and metabolic profiles of offspring conceived by assisted reproductive technologies: a systematic review and meta-analysis. *Fertil Steril* 2017;107:622–31.
- [49]. Mintjens S, Menting MD, Gemke RJJ, van Poppel MNM, van Wely M, Bendsdorp AJ, et al. The effects of intrauterine insemination and single embryo transfer or modified natural cycle in vitro fertilization on offspring's health—Follow-up of a randomized clinical trial. *Eur J Obstet Gynecol Reprod Biol* 2019;242:131–8.
- [50]. Lee JH. Polyunsaturated fatty acids in children. *Pediatr Gastroenterol Hepatol Nutr* 2013;16(3):153–61.
- [51]. Whelan J, Fritsche K. Linoleic Acid. *Adv Nutr* 2013;4(3):311–2.
- [52]. Hadley KB, Ryan AS, Forsyth S, Gautier S, Salem N. The essentiality of arachidonic acid in infant development. *Nutrients* 2016;8:216.
- [53]. Czumaj A, Śledziński T. Biological role of unsaturated fatty acid desaturases in health and disease. *Nutrients* 2020;12(2):356.
- [54]. Choudhary D, Jansson I, Stoilov I, Sarfarazi M, Schenkman JB. Metabolism of retinoids and arachidonic acid by human and mouse cytochrome P450 1B1. *Drug Metab Dispos* 2004;32(8):840–7.
- [55]. Sewer MB, Li D. Regulation of steroid hormone biosynthesis by the cytoskeleton. *Lipids* 2008;43(12):1109–15.
- [56]. Lidén M, Eriksson U. Understanding retinol metabolism: Structure and function of retinol dehydrogenases. *J Biol Chem* 2006;281(19):13001–4.
- [57]. Fernández-Pérez L, de Mirecki-Garrido M, Guerra B, Díaz M, Díaz-Chico JC. Sex steroids and growth hormone interactions. *Endocrinol y Nutr* 2016;63(4):171–80.
- [58]. Sudano MJ, Rascado TDS, Tata A, Belaz KRA, Santos VG, Valente RS, et al. Lipidome signatures in early bovine embryo development. *Theriogenology* 2016;86(2):472-484.e1.

- [59]. Waynforth D. Effects of conception using assisted reproductive technologies on infant health and development: An evolutionary perspective and analysis using UK millennium cohort data. *Yale J Biol Med* 2018;91:225–35.
- [60]. Bereshchenko O, Bruscoli S, Riccardi C. Glucocorticoids, sex hormones, and immunity. *Front Immunol* 2018;9:1332.
- [61]. Huang Z, Liu Y, Qi G, Brand D, Zheng S. Role of Vitamin A in the Immune System. *J Clin Med* 2018;7(9):258.
- [62]. Cheung H-H, Liu X, Rennert OM. Apoptosis: Reprogramming and the Fate of Mature Cells. *ISRN Cell Biol* 2012;2012:1–8.
- [63]. Mani S, Ghosh J, Coutifaris C, Sapienza C, Mainigi M. Epigenetic changes and assisted reproductive technologies. *Epigenetics* 2020;15:12–25.
- [64]. Calle A, Fernandez-Gonzalez R, Ramos-Ibeas P, Laguna-Barraza R, Perez-Cerezales S, Bermejo-Alvarez P, et al. Long-term and transgenerational effects of in vitro culture on mouse embryos. *Theriogenology* 2012;77:785–93.

### **ACKNOWLEDGEMENTS**

This work was supported by funds from the Ministry of Economy and Competitiveness of Spain (AGL2014-53405-C2-1-P) and Generalitat Valenciana Research Programme (PrometeoII 2014/036). Ximo García-Dominguez was supported by a research grant from the Ministry of Economy and Competitiveness (BES-2015-072429). The authors would like to thank Neil Macowan Language Services for revising the English version of the manuscript.





# **GENERAL DISCUSSION**

X. Garcia-Dominguez

Institute for Animal Science and Technology (ICTA), Laboratory of Reproductive Biotechnology,  
Universitat Politècnica de València, 46022 Valencia, Spain



## 8. GENERAL DISCUSSION

---

### 8.1. DISCUSSION AND FUTURE PROSPECTS

The aim of this thesis is to use the rabbit as animal model to further the characterisation of long-term features of the offspring derived from the transfer of vitrified embryos, both phenotypically and molecularly. First, we show that embryo vitrification procedure affected the long-term phenotype of the derived offspring, with possible cumulative effects over the other techniques that encompass the transfer of cryopreserved embryos. Second, we have identified for the first time profound differences in the molecular physiology of the liver in the vitrified progeny. Third, we demonstrated the transgenerational inheritance of this developmental programming after two generations, accompanied by changes in the genome-wide epigenome. And fourth, we provide evidence proving the healthy status of the vitrified offspring, and their proper reproductive performance.

Today it is well known that preimplantation mammalian embryos are sensitive to their environmental conditions. The embryo's plasticity allows it to develop responses to increase its short-term survival [1]. However, under extreme conditions, developmental reprogramming is usually non-adaptive or the result of a direct perturbation of the epigenetic remodelling that takes place in the preimplantation period, leading to adverse effects and increasing the risk of diseases [2,3,4]. Thereby, suboptimal conditions during ART lead to permanent changes in the postnatal phenotype and metabolism thorough life, which can be inherited by subsequent generations [1,2,5-12]. During cryopreservation and transfer procedures, embryos experience different hostile environments in which they have no intrinsic ability to survive [13]. Throughout this thesis, it has been observed that transfer of vitrified embryos results in a progeny with altered phenotype from birth until adulthood during three consecutive generations. We detected strong evidence of potential changes in the birth weight, growth trajectory, adult body weight and in the lactation performance. Increased birth weight after cryopreservation is a topic extensively reported in humans [14,15]. However, the information beyond birth is still scarce, as for many years embryo cryopreservation has been considered neutral [16]. Paradoxically, more than two decades ago, long-term effects of embryo freezing were unveiled in mice [17]. Our background research supports us, as changes in the body weight after embryo cryopreservation have been reported in rabbit at birth and beyond [18,19]. Particularly, growth kinetics have been studied by other authors in mice, demonstrating that different preimplantation conditions uniquely affect postnatal growth pattern [20-22]. Furthermore, the most dramatic effect of the use of ART in bovine and ovine species is known as large offspring syndrome, characterised by increased birth weight and abnormalities in several organs

[11,23]. In addition, growth deviations in cows and poorer lactation performance have been associated with *in vitro* production of embryos [23].

We also detected changes in the weight of some vital organs (e.g. liver and heart). Abnormalities in the same organs have been reported by other authors after *in vitro* culture, but the liver seemed to be the only organ whose condition presented transgenerational inheritance [6,24]. Authors suggests that in these cases, only a careful *post mortem* histological examination may reveal severely compromised welfare of apparently normal individuals [25]. Otherwise, there is consistent evidence of hepatic metabolism alteration after IVF [8,22,26,27,28]. In agreement, we provide robust information regarding an overall reprogramming of the whole hepatic metabolism after a vitrified embryo transfer procedure. The liver was chosen to be molecularly interrogated in several chapters of this thesis because it seemed to be the tissue most affected after VET, and also plays a pivotal role in growth performance [29,30], another feature highly modified in the VT progeny. Results of high-throughput screenings, based on several omic sciences, revealed high changes in hepatic molecular physiology in the offspring born after VET and across its derived lineage. The most evident change found in all omic studies was related to the metabolism of some polyunsaturated fatty acids, particularly of linoleic and arachidonic acid. Dysregulations in the levels of both acids were found in adult livers after ART [26] and their depletion can result in growth retardation [31,32]. Furthermore, it was known that the bioactive metabolites of ARA (e.g. eicosanoids) modulate the release of somatostatin, a crucial hormone that regulate cell proliferation, growth, and basic metabolic functions and immunity [32]. In addition, our molecular studies provide several findings evidencing immune system alterations. In agreement, high incidence of infections was detected in ART descendants, whose immune problems may result in some sequelae in development due to energetic trade-offs between immunity and growth [33]. Concordantly, direct and transgenerational effects of VET result in lower growth rate and reduced body weight in adulthood. Validating our results, there is robust evidence from epidemiological and animal studies demonstrating that exposure to different environmental conditions during early development affects postnatal growth, metabolism and disease susceptibility in adulthood [5-12,20-22,28]. However, considering that the main goal of ART is to achieve successful pregnancies to term, ensuring healthy and fertile offspring [11], we cannot affirm that this purpose has not been fulfilled. In fact, we highlight that the resultant progeny after VET were fertile and apparently healthy, with normal serum hepatic markers and normal blood count. Therefore, we sustain that changes in postnatal phenotype and metabolism are triggered by early embryo reprogramming under VET conditions.

This phenomenon is broadly referred to as developmental plasticity, whereby diverse phenotypes may arise from a single genotype in response to an organism's early

environment [4]. This concept is closely related to epigenetics, and there is abundant evidence that *in vitro* manipulation affects the epigenetic landscape in embryo cells, which subsequently form tissues and organ systems [6,8,11,34]. These epigenetic changes are thought to be responsible for mediating reprogramming and developmental plasticity, having been linked to aberrant modifications in the epigenome with some ART developmental deviations [6,35-37]. Thus, infants conceived by ART have a 3-fold higher incidence of epigenetic disorders and 2-fold increased risk of birth defects or perinatal mortality compared to infants conceived naturally [35,38]. One study reported a high tendency to be stillborn or die during the first few days of life in calves born after ART [39]. In this sense, after F1 embryos were vitrified and transferred, broad methylation changes were detected in the whole epigenome of an adult tissue in the F3 generation. These results reinforce that heritable epigenetic changes might be the underlying mechanisms of the metabolic and phenotypic changes in the VT progeny. In fact, epigenetic studies point toward differential methylation of genes critical for growth that may be responsible for the increased incidence of larger newborns following transfer of vitrified embryos [40]. Therefore, changes in the gamete and embryo epigenomes after ART head the list of mechanistic candidates that might explain the associated ART outcomes, including transgenerational ones [4,7].

To conceptualise and link early-life experiences with development throughout the lifespan, two theoretical models are systematically applied in epidemiology: “critical period models” and “risk accumulation models” [4]. Generally speaking, critical period models posit that there is a distinct window of responsiveness to environmental information and, after it closes, development is canalised. This means that experiences during sensitive developmental windows early in life lead to permanent changes in phenotype that are not substantially altered by subsequent experiences. Otherwise, risk accumulation models suggest that the window of responsiveness stays open, and late signals can modify responses to the early signal. This means that later exposures accumulate gradually and may exacerbate or mitigate developmental effects of previous exposures. Specifically, manipulations in the preimplantation period during ART seem to fit the risk accumulation models, as changes in postnatal phenotype are increasingly severe as the *in vitro* conditions deviate more extensively from the natural conditions of oviduct and uterus [8,12]. In addition, when different stressors are present, they can act synergistically, inducing more negative effects [11]. Therefore, it is difficult to distinguish the adverse effects of one ART, as current cycles involve several ARTs together. Thus, in most studies, all negative effects are considered as part of the ART protocol, comparing ART-group to the naturally-conceived (control) one [11,41]. This thesis contributes to support this theory, as deviations in the growth trajectory are more pronounced as *in vitro* manipulation increased. However, a particularity was noted when embryo cryopreservation was achieved using different methodologies. We noted that vitrification achieved using cryotop has a positive effect on the *in vitro* and *in vivo*

embryo survival, but incurred higher postnatal deviations than if vitrification was performed in straws. Elsewhere, it is reported that increasing the cooling rate improves survival rates, and thereby a higher survival rate has been demonstrated for minimum volume vitrification devices (e.g. cryotop) compared to conventional plastic straw method [42,43]. In this context, many studies posit that embryo cryopreservation may act as selection pressure (“cryoselection”), in which vitrification and warming processes filter out poor-quality embryos that not sustain the stresses associated with the process, allowing only the stronger ones to survive [44,45,46]. Thereby, slower cooling-warming rates during straw vitrification bring more unfavourable conditions for embryo survival, which could suppose a higher selection pressure that ultimately destroys the most sensitive embryos to ART conditions. Supporting this fact, we noted that straw-vitrified embryos incur high foetal losses at mid-gestation, suggesting that only embryos that are able to overcome the cryopreservation alterations are able to continue their development. In contrast, brittle embryos after ART could ultimately survive after cryotop vitrification and develop into an offspring with more deviant developmental trajectories. In addition, the selection of cryoresistant embryos can favour the inheritance of determinant alleles, which could contribute to the differences shown in some traits by the VT animals [5]. Therefore, with an explosion of vitrification devices appearing in the literature during the last decade [43], here was reported the first evidence to our best knowledge demonstrating that the choice of cryopreservation devices is not trivial, as they influence postnatal long-term phenotypes. In fertility clinics, closed and open vitrification systems have been systematically compared because, while open vitrification carriers reaches high cooling rates allowing higher survival, risks for potential cross-infection through LN2 decrease with closed devices [47]. To date, most embryos are vitrified with open systems worldwide, although closed vitrification has become more popular and widely used in IVF laboratories as a safer option [47]. Probably, our results should encourage the validation of these results in humans favouring the replacement of open devices, as phenotypic deviations obtained for closed devices are lower.

This situation could be also of special importance in the livestock sector, where genomic selection in combination with ARTs, including embryo cryopreservation, are revolutionising the design and implementation of breeding programmes [48,49]. Genomic selection provides estimates of the animal breeding value, but we demonstrated that both embryo cryopreservation and transfer could change the manner in which genes are manifested, leading to changes in growth and lactation performance, both of great interest to the livestock industry. Therefore, if epigenetic information were added to genomic selection, the precision of the selection model could probably be more accurate. Nowadays, ART offspring are currently excluded from genetic evaluation, as some effects inherent to the ART process cannot be estimated in the selection models [50]. Thus, characterisation and implementation of the ART effects

in the selection programme can lead to adjusting the accuracy of the model and better estimating the genetic gains, including ART animals in the analyses.

In this scenario, arguably studying the mechanisms that lead to a reprogrammed epigenetic, transcriptional and/or metabolic state after ART procedures could potentiate our capacity to understand the derived phenotypic changes and determining whether they have biological significance. An interesting approach would be starting by unravelling the molecular changes occurring in a developing embryo secondary to adverse environmental exposures, which later alter the growth and metabolic trajectories across the life course. According with the “quiet range” of metabolic activity theory, embryos with maximum developmental potential will be located in a “Goldilocks zone”, understood as an optimal range of metabolic activity and energetic efficiency [51]. Then, only those embryos able to adapt its metabolism within a homeostatic range during suboptimal ART condition could finally develop until birth, but this adaptation triggers developmental reshapes. In fact, we supported that some of the metabolic alterations here detected in adult animals after VET could be carried over from the preimplantation stage. In favour of these hypotheses, we and others detected transcriptomic evidence in cryopreserved embryos of disturbed lipid and arachidonic acid metabolism, as well as disturbances for steroid biosynthesis [48,52]. In addition, changes in the lipid metabolism have been observed in ART embryos and their stemmed liver in the foetus [10,11,53]. The placenta could be a key organ in this scenario, as it has been proven that embryo cryopreservation disrupted placental lipid metabolism, probably due to a preferential confinement of damaged cells to the trophectoderm [18,54]. However, understanding the molecular physiology sustaining ART phenotypes is complex, because each ART led to a specific and unique blastocyst transcriptional profile, whose fingerprint did not persist throughout development with a clear cohesion [28]. Hence, a tissue-specific impact of each ART was detected in adulthood [8,28]. In addition, there are significant elements that add even more complexity, as several outcomes exhibited after ART are also strain-specific, sexually dimorphic and may not emerge until late adulthood [8]. In this sense, we noted in this thesis that Californian rabbit males resulted more affected after VET than their female counterparts, but we did not observe this dimorphic effect for New Zealand rabbits. We ask ourselves if the dissection of the females and the molecular analysis of their liver would have been the same as in the males. Further omic studies assessing this questions, and studying male and female early embryos separately, might provide considerable insight to decipher how suboptimal *in vitro* conditions result in both short and long term phenotypic defects.

Reproductive sciences have made major contributions to human health, livestock production and environmental management in the past and will continue to do so in future [55]. At present, 1%–6% of children born worldwide are conceived by ART [56].

In the livestock species, >1.5 million embryos are managed each year using ART across the world [57]. Furthermore, > 50 wild species have been successfully reproduced using ART procedures [58]. However, although the main goal of ART is to achieve successful pregnancies to term, ensuring healthy offspring [11], it is obvious that although ART embryos have the ability to implant and reach the end of gestation, alterations that might occur during early life *in vitro* are still present in adulthood. Therefore, ART registries should not only register the success rate of ART cycles, but also the specific ART used to achieve pregnancy and link this information to data on growth, development and health of ART offspring [1]. This can allow us to identify the best ART procedures to obtain competent and healthy embryos, ensuring thus that animal and human assisted reproduction are utilised in the most efficient, but also in the safest possible manner [1,25]. The tendency to ensure this end seems to be aimed at making the *in vitro* conditions as similar as possible to those *in vivo* [34,59,60]. In addition, because epigenetic marks are reversible, we think it is imperative to determine how, when, and whether to use preventive treatments, such as specific diets, drugs or lifestyle changes to reduce the transmission of maladaptative acquired phenotypes [25].

Most of the evidence in the field of ART comes from clinical studies, because whereas most human medical treatments rely on preliminary animal experimentation and modelling, the notable exception to this rule is the practice of ART, as clinical advances have been tested directly in humans [58]. However, in humans, it is difficult to determine real associations between the treatment and outcome, as lifestyle, demographic and clinical factors can act as potential confounders that bias the study results [61]. Therefore, the use of good animal models that avoid these confounding factors is of paramount importance to elucidate ART-related effects *per se* [11,36]. Here, we have demonstrated the potential value of rabbit for studying ART developmental consequences, but further studies reaching the senescence age and involving several species are needed to accumulate robust information on the implications of ART. Although caution is required when extrapolating results from rabbit studies to humans, the rabbit model has been proposed as a better reproductive model for human health than rodents [62]. It is because rabbit genes are apparently more similar to those of the human than are rodent genes [62,63]. In fact, some studies in mice has found a lack of symptoms related to the human disease that they mimicked, meanwhile others reported a low-success rates in the translation of findings from some mouse studies to human diseases, suggesting that other animal models, such as rabbit, may often be more appropriate [63]. Specifically, the renaissance of the laboratory rabbit as a model for human research is closely related to the growing evidence of periconceptual metabolic programming and its determining effects on offspring and adult health [62]. In the present thesis, we have attempted to document our knowledge, as well as ignorance, of the long-term and transgenerational effects of perturbing preimplantation embryos during a vitrified embryo transfer procedure. We suggest that a new



experimental paradigm is required to increase our understanding of the oviduct and uterine environmental stimulus for embryos during their developmental programme configuration, placing this data in the context of the DOHaD phenomenon.

## 8.2. REFERENCES

- [1]. Roseboom TJ. Developmental plasticity and its relevance to assisted human reproduction. *Hum Reprod.* 2018;33:546-552.
- [2]. Fleming TP, Velazquez MA, Eckert JJ. Embryos, DOHaD and David Barker. *J Dev Orig Health Dis.* 2015;6:377-83.
- [3]. Korte SM, Koolhaas JM, Wingfield JC, McEwen BS. The Darwinian concept of stress: benefits of allostasis and costs of allostatic load and the trade-offs in health and disease. *Neurosci Biobehav Rev.* 2005;29:3-38.
- [4]. Laubach ZM, Perng W, Dolinoy DC, Faulk CD, Holekamp KE, Getty T. Epigenetics and the maintenance of developmental plasticity: extending the signalling theory framework. *Biol Rev Camb Philos Soc.* 2018;93:1323-1338.
- [5]. Mahsoudi, B., Li, A., O'Neill, C. Assessment of the long-term and transgenerational consequences of perturbing preimplantation embryo development in mice. *Biol Reprod.* 2007;77:889-96.
- [6]. Calle A, Miranda A, Fernandez-Gonzalez R, Pericuesta E, Laguna R, Gutierrez-Adan A. Male mice produced by in vitro culture have reduced fertility and transmit organomegaly and glucose intolerance to their male offspring. *Biol Reprod.* 2012;87:34.
- [7]. Aiken CE, Ozanne SE. Transgenerational developmental programming. *Hum Reprod Update.* 2014;20:63-75.
- [8]. Feuer SK, Rinaudo PF. Physiological, metabolic and transcriptional postnatal phenotypes of in vitro fertilization (IVF) in the mouse. *J Dev Orig Health Dis.* 2017;8:403-410.
- [9]. Vrooman LA, Bartolomei MS. Can assisted reproductive technologies cause adult-onset disease? Evidence from human and mouse. *Reprod Toxicol.* 2017;68:72-84.
- [10]. Duranthon V, Chavatte-Palmer P. Long term effects of ART: What do animals tell us? *Mol Reprod Dev.* 2018;85:348-368.
- [11]. Ramos-Ibeas P, Heras S, Gómez-Redondo I, Planells B, Fernández-González R, Pericuesta E, *et al.* Embryo responses to stress induced by assisted reproductive technologies. *Mol Reprod Dev.* 2019;86:1292-1306.
- [12]. Feuer S, Rinaudo P. From Embryos to Adults: A DOHaD Perspective on In Vitro Fertilization and Other Assisted Reproductive Technologies. *Healthcare (Basel).* 2016;4:E51.

- [13]. Sparks AE. Human embryo cryopreservation-methods, timing, and other considerations for optimizing an embryo cryopreservation program. *Semin Reprod Med.* 2015;33:128-44.
- [14]. Spijkers S, Lens JW, Schats R, Lambalk CB. Fresh and Frozen-Thawed Embryo Transfer Compared to Natural Conception: Differences in Perinatal Outcome. *Gynecol Obstet Invest* 2017;82:538-546.
- [15]. Hann M, Roberts SA, D'Souza SW, Clayton P, Macklon N, Brison DR. The growth of assisted reproductive treatment-conceived children from birth to 5 years: a national cohort study. *BMC medicine.* 2018;16:224.
- [16]. Auroux M. Long-term effects in progeny of paternal environment and of gamete/embryo cryopreservation. *Hum Reprod Update* 2000;6:550-63.
- [17]. Dulioust E, Toyama K, Busnel MC, Moutier R, Carlier M, Marchaland C, et al. Long-term effects of embryo freezing in mice. *Proceedings of the National Academy of Sciences of the United States of America.* 1995;92:589-93.
- [18]. Saenz-de-Juano MD, Marco-Jimenez F, Schmaltz-Panneau B, Jimenez-Trigos E, Viudes-de-Castro MP, Peñaranda DS, *et al.* Vitrification alters rabbit foetal placenta at transcriptomic and proteomic level. *Reproduction.* 2014;147:789-801.
- [19]. Lavara R, Baselga M, Marco-Jiménez F, Vicente JS. Embryo vitrification in rabbits: Consequences for progeny growth. *Theriogenology.* 2015;84:674-80.
- [20]. Banrezes B, Sainte-Beuve T, Canon E, Schultz RM, Cancela J, Ozil JP. Adult body weight is programmed by a redox-regulated and energy-dependent process during the pronuclear stage in mouse. *PLoS One.* 2011;6:e29388.
- [21]. Donjacour A, Liu X, Lin W, Simbulan R, Rinaudo PF. In vitro fertilization affects growth and glucose metabolism in a sex-specific manner in an outbred mouse model. *Biol Reprod.* 2014;90:80.
- [22]. Feuer SK, Liu X, Donjacour A, Lin W, Simbulan RK, Giritharan G, *et al.* Use of a mouse in vitro fertilization model to understand the developmental origins of health and disease hypothesis. *Endocrinology.* 2014;155:1956-69.
- [23]. Siqueira LGB, Dikmen S, Ortega MS, Hansen PJ. Postnatal phenotype of dairy cows is altered by in vitro embryo production using reverse X-sorted semen. *J Dairy Sci.* 2017;100:5899-5908.
- [24]. Fernández-Gonzalez R, Moreira P, Bilbao A, Jiménez A, Pérez-Crespo M, Ramírez MA, *et al.* Long-term effect of in vitro culture of mouse embryos with serum on mRNA expression of imprinting genes, development, and behavior. *Proc Natl Acad Sci U S A.* 2004;101:5880-5.
- [25]. Calle A, Fernandez-Gonzalez R, Ramos-Ibeas P, Laguna-Barraza R, Perez-Cerezales S, Bermejo-Alvarez P, *et al.* Long-term and transgenerational effects of in vitro culture on mouse embryos. *Theriogenology.* 2012;77:785-93.
- [26]. Wang LY, Le F, Wang N, Li L, Liu XZ, Zheng YM, *et al.* Alteration of fatty acid metabolism in the liver, adipose tissue, and testis of male mice conceived through

- assisted reproductive technologies: fatty acid metabolism in ART mice. *Lipids Health Dis.* 2013;12:5.
- [27]. Feuer SK, Donjacour A, Simbulan RK, Lin W, Liu X, Maltepe E, *et al.* Sexually dimorphic effect of in vitro fertilization (IVF) on adult mouse fat and liver metabolomes. *Endocrinology.* 2014;155:4554-67.
- [28]. Feuer S, Liu X, Donjacour A, Simbulan R, Maltepe E, Rinaudo P. Transcriptional signatures throughout development: the effects of mouse embryo manipulation in vitro *Reproduction.* 2017;153:107-122.
- [29]. Kineman RD, Del Rio-Moreno M, Sarmiento-Cabral A. 40 YEARS of IGF1: Understanding the tissue-specific roles of IGF1/IGF1R in regulating metabolism using the Cre/loxP system. *J Mol Endocrinol.* 2018;61:187-198.
- [30]. Adamek A, Kasprzak A. Insulin-Like Growth Factor (IGF) System in Liver Diseases. *Int J Mol Sci.* 2018;19:E1308.
- [31]. Whelan J, Fritsche K. Linoleic acid. *Adv Nutr.* 2013;4:311-2.
- [32]. Hadley KB, Ryan AS, Forsyth S, Gautier S, Salem N.Jr. The Essentiality of Arachidonic Acid in Infant Development. *Nutrients* 2016;8:216.
- [33]. Waynforth D. Effects of Conception Using Assisted Reproductive Technologies on Infant Health and Development: An Evolutionary Perspective and Analysis Using UK Millennium Cohort Data. *Yale J Biol Med.* 2018;91:225-235.
- [34]. Canovas S, Ivanova E, Romar R, García-Martínez S, Soriano-Úbeda C, García-Vázquez FA, *et al.* DNA methylation and gene expression changes derived from assisted reproductive technologies can be decreased by reproductive fluids. *Elife.* 2017;6:e23670.
- [35]. Novakovic B, Lewis S, Halliday J, Kennedy J, Burgner DP, Czajko A, *et al.* Assisted reproductive technologies are associated with limited epigenetic variation at birth that largely resolves by adulthood. *Nat Commun.* 2019;10:3922.
- [36]. Zacchini F, Sampino S, Stankiewicz AM, Haaf T, Ptak GE. Assessing the epigenetic risks of assisted reproductive technologies: a way forward. *Int J Dev Biol.* 2019;63:217-222.
- [37]. Mani S, Ghosh J, Coutifaris C, Sapienza C, Mainigi M. Epigenetic changes and assisted reproductive technologies. *Epigenetics.* 2020;15:12-25.
- [38]. Uk A, Collardeau-Frachon S, Scavion Q, Michon L, Amar E. Assisted Reproductive Technologies and imprinting disorders: Results of a study from a French congenital malformations registry. *Eur J Med Genet* 2018;61:518-23.
- [39]. Bonilla L, Block J, Denicol AC, Hansen PJ. Consequences of transfer of an in vitro-produced embryo for the dam and resultant calf. *J Dairy Sci.* 2014;97:229–239.
- [40]. Van Heertum K, Weinerman R. Neonatal outcomes following fresh as compared to frozen/thawed embryo transfer in in vitro fertilization. *Birth Defects Res* 2018;110:625-629.

- [41]. Gu L, Zhang J, Zheng M, Dong G, Xu J, Zhang W, *et al.* A potential high risk for fatty liver disease was found in mice generated after assisted reproductive techniques. *J Cell Biochem.* 2018;119:1899-1910.
- [42]. Zhang X, Catalano PN, Gurkan UA, Khimji I, Demirci U. Emerging technologies in medical applications of minimum volume vitrification. *Nanomedicine (Lond).* 2011;6:1115-29.
- [43]. Arav A. Cryopreservation of oocytes and embryos. *Theriogenology.* 2014;81:96-102.
- [44]. Vidal M, Vellvé K, González-Comadran M, Robles A, Prat M, Torné M, *et al.* Perinatal outcomes in children born after fresh or frozen embryo transfer: a Catalan cohort study based on 14,262 newborns. *Fertil Steril.* 2017;107:940-947.
- [45]. Sallem A, Santulli P, Barraud-Lange V, Le Foll N, Ferreux L, Maignien C, *et al.* Extended culture of poor-quality supernumerary embryos improves ART outcomes. *J Assist Reprod Genet.* 2018;35:311-319.
- [46]. Marsico T, Camargo J, Valente RS, Sudano MJ. Embryo competence and cryosurvival: Molecular and cellular features. *Anim. Reprod.* 2019;16:423-439.
- [47]. Cai H, Niringiyumukiza JD, Li Y, Lai Q, Jia Y, Su P, *et al.* Open versus closed vitrification system of human oocytes and embryos: a systematic review and meta-analysis of embryologic and clinical outcomes. *Reprod Biol Endocrinol.* 2018;16:123.
- [48]. Gupta A, Singh J, Dufort I, Robert C, Dias FCF, Anzar M. Transcriptomic difference in bovine blastocysts following vitrification and slow freezing at morula stage. *PLoS One.* 2017;12:e0187268.
- [49]. Kasinathan P, Wei H, Xiang T, Molina JA, Metzger J, Broek D, *et al.* Acceleration of genetic gain in cattle by reduction of generation interval. *Sci Rep.* 2015;5:8674.
- [50]. Mota RR, Lopes PS, Marques LF, da Silva LP, de Resende MD, de Almeida Torres R. The influence of animals from embryo transfer on the genetic evaluation of growth in Simmental beef cattle by using multi-trait models. *Genet Mol Biol.* 2013;36:43-9.
- [51]. Leese HJ, Guerif F, Allgar V, Brison DR, Lundin K, Sturmey RG. Biological optimization, the Goldilocks principle, and how much is lagom in the preimplantation embryo. *Mol Reprod Dev.* 2016;83:748-54.
- [52]. Saenz-de-Juano MD, Marco-Jiménez F, Peñaranda DS, Joly T, Vicente JS. Effects of slow freezing procedure on late blastocyst gene expression and survival rate in rabbit. *Biol Reprod.* 2012;87:91.
- [53]. Li B, Xiao X, Chen S, Huang J, Ma Y, Tang N, *et al.* Changes of Phospholipids in Fetal Liver of Mice Conceived by In Vitro Fertilization. *Biol Reprod.* 2016;94:105.
- [54]. Saenz-de-Juano MD, Vicente JS, Hollung K, Marco-Jiménez F. Effect of Embryo Vitrification on Rabbit Foetal Placenta Proteome during Pregnancy. *PLoS One.* 2015;10:e0125157.

- [55]. Findlay JK, Holland MK, Wong BBM. Reproductive science and the future of the planet. *Reproduction*. 2019;158:91-96.
- [56]. Bi WJ, Cui L, Xiao YJ, Song G, Wang X, Sun L, *et al.* Assessing cardiovascular remodelling in fetuses and infants conceived by assisted reproductive technologies: a prospective observational cohort study protocol. *BMJ Open*. 2019;9:e031452.
- [57]. Sjunnesson Y. In vitro fertilisation in domestic mammals-a brief overview. *Ups J Med Sci*. 2019. doi: 10.1080/03009734.2019.1697911.
- [58]. Paulson RJ, Comizzoli P. Addressing challenges in developing and implementing successful in vitro fertilization in endangered species: an opportunity for humanity to "give back". *Fertil Steril*. 2018;109:418-419.
- [59]. Campo H, García-Domínguez X, López-Martínez S, Faus A, Vicente Antón JS, Marco-Jiménez F, *et al.* Tissue-specific decellularized endometrial substratum mimicking different physiological conditions influences in vitro embryo development in a rabbit model. *Acta Biomater*. 2019;89:126-138.
- [60]. García-Martínez S, Sánchez Hurtado MA, Gutiérrez H, Sánchez Margallo FM, Romar R, Latorre R, *et al.* Mimicking physiological O<sub>2</sub> tension in the female reproductive tract improves assisted reproduction outcomes in pig. *Mol Hum Reprod*. 2018;24:260-270.
- [61]. Skelly AC, Dettori JR, Brodt ED. Assessing bias: the importance of considering confounding. *Evid Based Spine Care J*. 2012;3:9-12.
- [62]. Fischer B, Chavatte-Palmer P, Viebahn C, Navarrete Santos A, Duranthon V. Rabbit as a reproductive model for human health. *Reproduction*. 2012;144:1–10.
- [63]. Esteves PJ, Abrantes J, Baldauf HM, BenMohamed L, Chen Y, Christensen N, *et al.* The wide utility of rabbits as models of human diseases. *Exp Mol Med*. 2018 May 22;50:1-10.



# **CONCLUSIONS**

X. Garcia-Dominguez

Institute for Animal Science and Technology (ICTA), Laboratory of Reproductive Biotechnology,  
Universitat Politècnica de València, 46022 Valencia, Spain





## 9. CONCLUSIONS

---

The conclusions of this thesis are:

- Both embryo transfer and embryo cryopreservation have a long-term effect *per se* on the offspring phenotype, whose effects on the growth rate and body weight are cumulative. Besides, the choice of vitrification device should not be underestimated, as it determines postnatal phenotypes where the growth and lactation performances are differentially affected.
- Vitrified embryo transfer procedures incur transgenerational long-term effects on the resultant progeny, both at phenotypic and molecular level. Across three generations, several omics revealed that alterations in the lipid metabolism, particularly of the unsaturated fatty acids and their derived metabolites, could be the underlying mechanisms leading to a lower growth performance. This developmental reprogramming is thought to be mediated by changes in the epigenome.
- However, neither technique seemed to affect the offspring health status nor their reproductive performance, which are proper. Therefore, developmental reshape exhibited after the transfer of vitrified embryos could be attributed to the intrinsic developmental plasticity of the early mammalian embryo, whereby offspring phenotypes are fine-tuned in the early life in response to the environmental cues.



## **10. ANNEX I**

Supplementary information  
CHAPTER III

### **LONG-TERM PHENOTYPIC AND PROTEOMIC CHANGES FOLLOWING VITRIFIED EMBRYO TRANSFER IN THE RABBIT MODEL**

X. Garcia-Dominguez, F. Marco-Jiménez, D.S. Peñaranda, J.S. Vicente

Institute for Animal Science and Technology, Laboratorio de Biotecnología de la Reproducción,  
Universitat Politècnica de València, 46022 Valencia, Spain



## 10. ANNEX I

**Supplementary Table S1.** Differentially expressed proteins in liver tissue between animals born from vitrified-transferred embryos and those conceived naturally.

Uniprot accession	Gene name	Fold change
G1TQG1	NADH:ubiquinone oxidoreductase subunit B9(NDUFB9)	-2.131
G1TM55	ribosomal protein S6(RPS6)	-1.849
G1TH09	60S ribosomal protein L7a(LOC100341006)	-1.755
G1TT27	ribosomal protein L8(RPL8)	-1.751
G1SVW5	ribosomal protein L4(RPL4)	-1.637
G1TFX2	alpha-1-antitrypsin(LOC100328621)	-1.583
G1T4E7	signal peptidase complex subunit 2(SPCS2)	-1.470
G1TUC2	CCHC-type zinc finger nucleic acid binding protein(CNBP)	-1.402
G1U6B4	ATP synthase subunit e. mitochondrial(LOC108178113)	-1.390
G1SN00	kininogen 1(KNG1)	-1.349
G1T9I4	sorcin(SRI)	-1.237
G1SEH7	NADH:ubiquinone oxidoreductase subunit B8(NDUFB8)	-1.212
G1TKV4	histone H3(LOC103350067)	-1.157
G1SLD5	hypoxia upregulated 1(HYOU1)	-1.092
G1SCT1	prolyl endopeptidase(PREP)	-1.059
U3KMP8	myosin IB(MYO1B)	-0.996
G1TJW1	40S ribosomal protein S8(LOC100352057)	-0.987
G1U9R4	apolipoprotein B(APOB)	-0.968
G1SML9	DnaJ heat shock protein family (Hsp40) member A1(DNAJA1)	-0.938
G1U416	asialoglycoprotein receptor 1(ASGR1)	-0.931
O62648	sulfotransferase family 2A member 1(SULT2A1)	-0.884
G1TZQ6	NADH:ubiquinone oxidoreductase subunit A10(NDUFA10)	-0.868
G1TCW2	osteoclast stimulating factor 1(OSTF1)	-0.846
G1TM29	aldehyde dehydrogenase 16 family member A1(ALDH16A1)	-0.796
G1TSY8	alpha-1-microglobulin/bikunin precursor(AMBP)	-0.780
G1TPL7	dipeptidyl peptidase 3(DPP3)	-0.691
G1SE10	2-hydroxyacyl-CoA lyase 1(HACL1)	-0.686
G1TYY5	LIM and SH3 protein 1(LASP1)	-0.665
G1T7G4	growth arrest specific 2(GAS2)	-0.625
G1SYV9	talin 1(TLN1)	-0.613
G1T6D1	ribosomal protein L23(RPL23)	-0.597
G1U6X6	heterogeneous nuclear ribonucleoprotein H2(LOC100339065)	-0.548
G1SYT7	peptidase. mitochondrial processing beta subunit(PMPCB)	-0.533
G1SHF3	nitrilase 1(NIT1)	-0.517

G1TCE9	hydroxysteroid dehydrogenase like 2(HSDL2)	-0.504
G1T7T6	USO1 vesicle transport factor(USO1)	-0.498
G1SZT8	SEC13 homolog. nuclear pore and COPII coat complex component(SEC13)	-0.492
B2ZDY6	t-complex 1(TCP1)	-0.457
O77768	heterogeneous nuclear ribonucleoprotein C (C1/C2)(HNRNPC)	-0.439
G1SNB1	carboxylesterase 3(CES3)	-0.412
G1U7C5	ribosome binding protein 1(RRBP1)	-0.404
G1T3D7	N-acetylneuraminase synthase(NANS)	-0.396
G1SZ47	ribosomal protein S23(RPS23)	-0.378
AOAOG2JH20	heat shock protein 90 alpha family class A member 1(HSP90AA1)	-0.336
G1SCN8	chaperonin-containing TCP1 subunit 3(CCT3)	-0.297
G1TBS1	Parkinsonism associated deglycase(PARK7)	-0.292
G1U7L4	heat shock protein family A (Hsp70) member 5(HSPA5)	-0.292
G1U032	StAR related lipid transfer domain containing 10(STARD10)	-0.175
G1SKT4	ATP synthase. H+ transporting. mitochondrial F1 complex. alpha subunit 1. cardiac muscle(ATP5A1)	0.193
G1TS42	amylo-alpha-1. 6-glucosidase. 4-alpha-glucanotransferase(AGL)	0.557
G1SP40	amidohydrolase domain containing 1(AMDHD1)	0.687
G1SR29	ATPase H+ transporting V1 subunit A(ATP6V1A)	0.689
G1T3R4	alcohol dehydrogenase class-2 isozyme 1(ADH2-1)	0.705
G1T295	epoxide hydrolase 1(EPHX1)	0.766
G1T8P1	aldehyde dehydrogenase 1 family member L1(ALDH1L1)	0.832
Q75NJ2	aldehyde dehydrogenase 1 family member A1(ALDH1A1)	0.951
G1U0Z4	agmatinase(AGMAT)	0.959
G1TY06	glutathione S-transferase mu 2 (muscle)(GSTM2)	1.249
B7NZF9	nucleophosmin (nucleolar phosphoprotein B23. numatrin)(NPM1)	1.719
G1SZH0	retinol binding protein 4(RBP4)	1.872
G1SMM7	small nuclear ribonucleoprotein D3 polypeptide(SNRPD3)	2.211
G1U1M3	aminoacyl tRNA synthetase complex interacting multifunctional protein 1(AIMP1)	2.351
P04068	epoxide hydrolase 1(EPHX1)	2.648
G1TCQ2	fatty acid binding protein 1(FABP1)	2.754
G1TNI4	glutathione S-transferase Yb-3(LOC100357148)	2.921
G1TMP1	keratin. type I cytoskeletal 18(LOC100008885)	3.948

**Supplementary Table S2.** Functional analysis of differential expressed proteins in liver tissue between animals born from vitrified-transferred embryos and those conceived naturally.

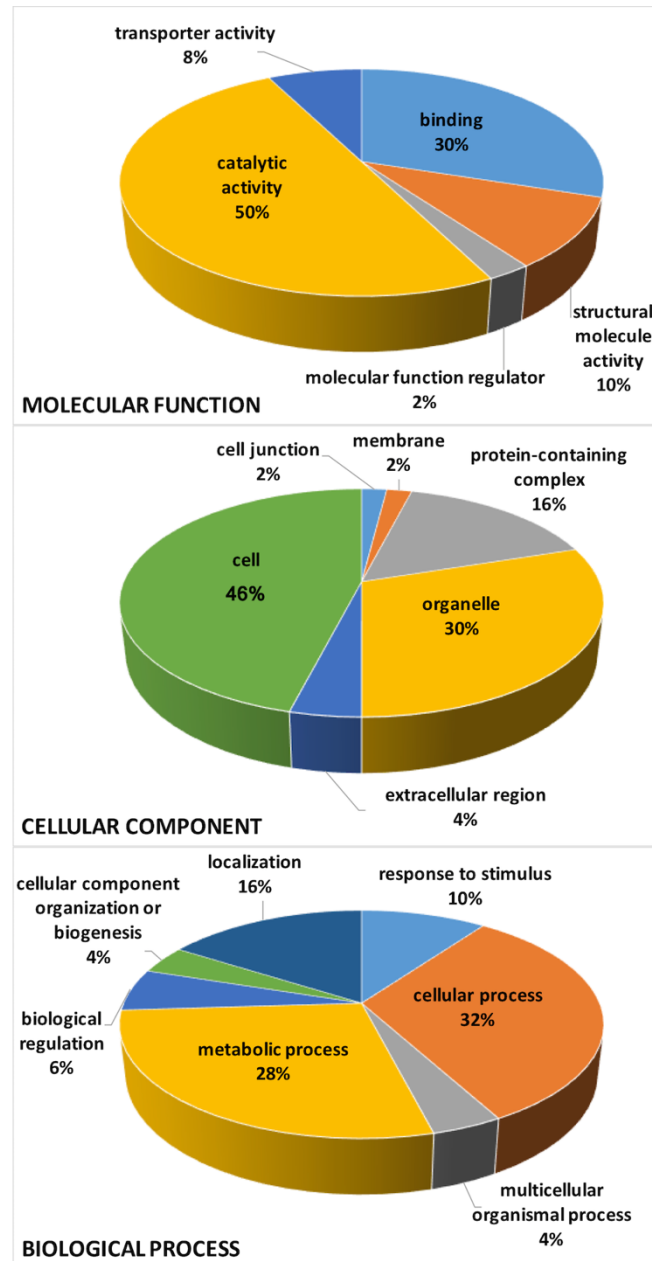
Category*	Term	Count	p-value
BP	toxin transport	4	0.000
BP	mitochondrial electron transport. NADH to ubiquinone	3	0.001
BP	translation	6	0.002
BP	protein folding	4	0.006
BP	10-formyltetrahydrofolate catabolic process	2	0.010
BP	positive regulation of protein localisation to Cajal body	2	0.041
BP	retinol metabolic process	2	0.056
BP	positive regulation of telomerase RNA localisation to Cajal body	2	0.066
BP	protein stabilisation	3	0.071
BP	ATP synthesis coupled proton transport	2	0.080
BP	one-carbon metabolic process	2	0.090
BP	biosynthetic process	2	0.094
BP	binding of sperm to zona pellucida	2	0.099
CC	extracellular exosome	34	0.000
CC	myelin sheath	7	0.000
CC	mitochondrial respiratory chain complex I	4	0.000
CC	cell body	4	0.001
CC	cytosol	10	0.003
CC	membrane	10	0.006
CC	focal adhesion	6	0.010
CC	endoplasmic reticulum chaperone complex	2	0.029
CC	zona pellucida receptor complex	2	0.038
CC	chaperonin-containing T-complex	2	0.043
CC	cytoplasm	15	0.076
MF	aldehyde dehydrogenase (NAD) activity	3	0.000
MF	structural constituent of ribosome	6	0.003
MF	poly(A) RNA binding	11	0.008
MF	hydroxymethyl-, formyl- and related transferase activity	2	0.011
MF	formyltetrahydrofolate dehydrogenase activity	2	0.011
MF	proton-transporting ATPase activity, rotational mechanism	2	0.055
MF	ATPase activity	3	0.060
MF	peptidase activity	2	0.071
MF	glutathione transferase activity	2	0.091
MF	NADH dehydrogenase (ubiquinone) activity	2	0.097

KEGG	Ribosome	7	0.001
KEGG	Metabolism of xenobiotics by cytochrome P450	5	0.001
KEGG	Chemical carcinogenesis	5	0.003
KEGG	Oxidative phosphorylation	5	0.007
KEGG	Parkinson's disease	5	0.010
KEGG	Protein processing in endoplasmic reticulum	5	0.015
KEGG	Drug metabolism - cytochrome P450	3	0.072
KEGG	Alzheimer's disease	4	0.074
KEGG	Huntington's disease	4	0.099

---

\*Functional analysis was referred to the GO term annotation according to the biological process (BP), cellular component (CC) and molecular function (MF) classification, and the KEGG pathways in which they are involved.





**Supplementary Figure S1.** Pie charts showing the distribution of the differentially expressed proteins between animals born from vitrified-transferred embryos and those conceived naturally based on their molecular function, biological process and cellular component.



# 11. ANNEX II

Supplementary information  
CHAPTER IV

## **LONG-TERM AND TRANSGENERATIONAL PHENOTYPIC, TRANSCRIPTIONAL AND METABOLIC EFFECTS IN RABBIT MALES BORN FOLLOWING VITRIFIED EMBRYO TRANSFER**

X. Garcia-Dominguez<sup>1</sup>, F. Marco-Jiménez<sup>1</sup>, D.S. Peñaranda<sup>1</sup>,  
G. Diretto<sup>2</sup>, V. García-Carpintero<sup>3</sup>, J. Cañizares<sup>3</sup>, J.S. Vicente<sup>1</sup>

<sup>1</sup>Institute for Animal Science and Technology (ICTA), Laboratory of Reproductive Biotechnology, Universitat Politècnica de València, 46022 Valencia, Spain

<sup>2</sup>Italian National Agency for New Technologies, Energy and Sustainable Economic Development (ENEA), Casaccia Research Centre, 00123 Rome, Italy

<sup>3</sup>Institute for the Conservation and Breeding of Agricultural Biodiversity (COMAV-UPV), Universitat Politècnica de València, 46022 Valencia, Spain



## 11. ANNEX II

**Supplementary Table S1.** Descriptive analysis of the evaluated quantitative traits.

Traits	n	Mean	SEM	SD
<b>Litter size* (pups)</b>	67	5.8	0.30	2.4
Weaning (4 weeks)	160	650.3	13.88	179.6
<b>Body weight (g)</b> Prepuberty (9 weeks)	154	2302.5	29.72	368.9
Adult (56 weeks)	135	5566.7	56.58	657.4
<b>Growth (g/day)</b> Average weight gain	154	47.0	0.56	6.9
Liver	126	104.4	1.67	18.8
Heart	120	12.7	0.28	3.0
Lungs	127	25.5	0.70	7.9
<b>Organ weight (g)</b> Spleen	127	1.3	0.04	0.4
Kidneys	128	22.8	0.25	2.8
Gonads	128	8.7	0.26	3.0
Adrenal Glands	127	0.6	0.02	0.2
VOL (mL)	633	0.7	0.02	0.4
CON ( $10^6$ )	630	242.1	6.37	159.9
TSE ( $10^6$ spz)	623	145.8	4.34	108.4
MOT (%)	619	68.7	1.03	25.6
PRO (%)	633	39.8	0.77	19.4
VIA (%)	615	75.5	0.45	11.2
NAR (%)	605	90.8	0.26	6.4
ABN (%)	626	20.7	0.36	9.1
<b>Sperm traits</b> VCL ( $\mu\text{m s}^{-1}$ )	636	98.1	0.84	21.1
VSL ( $\mu\text{m s}^{-1}$ )	638	42.2	0.57	14.3
VAP ( $\mu\text{m s}^{-1}$ )	636	60.4	0.67	16.8
LIN (%)	631	43.8	0.63	15.9
STR (%)	627	69.1	0.38	9.6
WOB (%)	634	61.6	0.50	12.6
ALH ( $\mu\text{m}$ )	625	2.9	0.02	0.6
BCF (Hz)	620	11.2	0.08	2.0
Live births <sup>#</sup> (pups)	383	5.5	0.18	3.2

**n** is the number of data in each trait; **SEM**: Standard Error of the Mean; **SD**: Standard deviation; \*Litter size is the number of pups per parity that constituted each generation; **VOL**: Ejaculate volume; **CON**: Spermatic concentration; **TSE**: Total sperm per ejaculate; **spz**: spermatozoa; **MOT**: Percentage of sperm motility; **PRO**: Percentage of progressive motility; **VIA**: Percentage of viable sperm; **NAR**: percentage of normal apical ridge; **ABN**: Percentage of abnormal forms; **VCL**: Curvilinear velocity; **VSL**: straight-line velocity; **VAP**: average path velocity; **LIN**: linearity coefficient ( $\text{VSL}/\text{VCL} \times 100$ ); **STR**: straightness coefficient; **WOB**: wobble coefficient ( $\text{VSL}/\text{VAP} \times 100$ ); **ALH**: amplitude of lateral head displacement; **BCF**: beat cross-frequency; <sup>#</sup>Live births is the number of live pups derived from the male fertility study in each generation.

**Supplementary Table S2.** Bayesian analyses of the phenotypic differences between naturally-conceived animals (NC group) and those derived from vitrified-transferred embryos (VT group) during three generations (F1, F2 and F3), computed as NC-VT.

PHENOTYPIC TRAITS <sup>†</sup>	D <sub>NC-VT</sub>			R	P <sub>0</sub>			HPD <sub>95%</sub>		
	F1	F2	F3		F1	F2	F3	F1	F2	F3
Litter size (pups)	0.2	0.5	-0.3	1	0.58	0.67	0.58	-1.7, 2.1	-1.9, 2.9	-3.2, 2.5
Weaning body weight (g)	62.2*	-26.7	59.4	60	0.94	0.66	0.94	-16.6, 135.6	-152.9, 109.1	-17.9, 134.9
Prepuberty body weight (g)	370.1*	139.3*	287.9*	123	1.00	0.85	1.00	210.1, 524.2	-119.5, 405.2	138.1, 422.5
Average weight gain (g/day)	8.6*	4.7*	6.6*	2	1.00	0.97	1.00	5.9, 11.3	0.18, 10.3	3.7, 9.4
Adult body weight (g)	437.4*	249.5*	247.9*	219	0.99	0.87	0.91	65.5, 801.4	-229.7, 704.3	-129.5, 610.0
Liver (g)	9.3*	12.7*	-16.1*	6	0.99	1.00	1.00	2.2, 16.5	4.3, 20.6	-26.7, -6.0
Heart (g)	1.5*	3.1*	0.3	1	0.98	0.93	0.73	0.1, 2.6	-1.3, 7.6	-0.6, 1.2
Lungs (g)	-1.1	-3.7*	-2.3	3	0.73	0.81	0.90	-4.6, 2.3	-12.9, 4.3	-5.5, 1.3
Spleen (g)	0.1	0.0	-0.2*	0.1	0.65	0.50	0.99	-0.2, 0.3	-0.4, 0.5	-0.4, -0.1
Kidneys (g)	0.4	0.8	-1.0	1	0.71	0.95	0.96	-1.0, 1.7	-0.2, 1.8	-2.2, 0.1
Gonads (g)	-0.7	0.7	-1.0	1	0.93	0.71	0.93	-1.8, 0.2	-1.8, 3.1	-2.4, 0.4
A. Glands (g)	-0.0	0.0	0.1	0.1	0.58	0.52	0.98	-0.1, 0.1	-0.2, 0.18	0.0, 0.2

D<sub>NC-VT</sub> = Mean of the difference NC-VT (median of the marginal posterior distribution of the difference between the NC and the VT groups).

R = Relevant value (proposed as one-third of the SD of the trait), rounded to the first significant number.

P<sub>0</sub> = Probability of the difference (D<sub>NC-VT</sub>) being greater than 0 when D<sub>NC-VT</sub> > 0 or lower than 0 when D<sub>NC-VT</sub> < 0.

HPD<sub>95%</sub> = The highest posterior density region at 95% of probability.

\*Statistical differences were assumed if |D<sub>NC-VT</sub>| surpass R value and its P<sub>0</sub>>0.80.

**Supplementary Table S3.** Bayesian analyses of the sperm/fertility traits differences between naturally-conceived males (NC group) and those derived from vitrified-transferred embryos (VT group) during three generations (F1, F2 and F3), computed as NC-VT.

	$D_{NC-VT}$			R	$P_0$			HPD <sub>95%</sub>		
	F1	F2	F3		F1	F2	F3	F1	F2	F3
<b>SEMEN PARAMETERS</b>										
VOL (ml)	<b>-0.2*</b>	<b>-0.2*</b>	<b>0.1</b>	0.1	1.00	1.00	0.99	-0.3, -0.1	-0.3, -0.1	0.0, 0.1
CON ( $10^6$ )	<b>37.0</b>	<b>8.9</b>	<b>-1.8</b>	53	0.97	0.76	0.53	-0.9, 72.6	-15.6, 33.7	-51.9, 44.6
TSE ( $10^6$ spz)	<b>-22.1</b>	<b>-44.8*</b>	<b>19.3</b>	36	0.89	1.00	0.96	-60.0, 13.8	-64.3, -24.9	-3.0, 40.2
MOT (%)	<b>-5.0</b>	<b>1.5</b>	<b>-1.7</b>	9	0.99	0.94	0.68	-9.3, -0.3	-0.3, 3.5	-9.1, 4.9
PRO (%)	<b>-2.5</b>	<b>-3.9</b>	<b>-2.0</b>	6	0.89	0.98	0.80	-6.5, 1.7	-7.7, -0.2	-6.7, 2.7
VIA (%)	<b>0.4</b>	<b>-0.4</b>	<b>-0.1</b>	4	0.62	0.65	0.53	-2.3, 3.0	-2.4, 1.7	-3.4, 3.1
ABN (%)	<b>-1.1</b>	<b>3.4*</b>	<b>-0.3</b>	3	0.83	1.00	0.58	-3.6, 1.1	1.7, 5.3	-3.1, 2.2
NAR (%)	<b>0.0</b>	<b>0.1</b>	<b>0.7</b>	2	0.52	0.57	0.80	-1.9, 2.0	-1.6, 1.6	-0.8, 2.3
<b>MOTION PARAMETERS</b>										
VCL ( $\mu\text{m s}^{-1}$ )	<b>-13.3*</b>	<b>3.5</b>	<b>8.1*</b>	7	1.00	0.95	1.00	-19.0, -7.8	-0.6, 7.8	2.2, 14.0
VSL ( $\mu\text{m s}^{-1}$ )	<b>-5.5*</b>	<b>0.7</b>	<b>0.6</b>	5	1.00	0.65	0.63	-8.9, -2.1	-2.7, 4.1	-2.8, 3.9
VAP ( $\mu\text{m s}^{-1}$ )	<b>-10.0*</b>	<b>1.2</b>	<b>2.4</b>	6	1.00	0.72	0.88	-14.4, -5.4	-2.7, 4.9	-1.5, 6.3
LIN (%)	<b>-1.7</b>	<b>1.7</b>	<b>-1.9</b>	5	0.74	0.90	0.92	-6.7, 3.2	-0.8, 4.6	-4.7, 0.9
STR (%)	<b>1.8</b>	<b>1.7</b>	<b>-1.5</b>	3	0.92	1.00	0.88	-0.9, 4.3	0.5, 3.0	-4.2, 0.9
WOB (%)	<b>-2.1</b>	<b>-0.9</b>	<b>-1.8</b>	4	0.90	0.73	0.91	-5.2, 1.1	-3.8, 1.9	-4.4, 0.7
ALH ( $\mu\text{m}$ )	<b>-0.1</b>	<b>0.0</b>	<b>0.2</b>	0.2	0.98	0.73	0.99	-0.3, -0.0	-0.1, 0.2	0.0, 0.4
BCF (Hz)	<b>-0.4</b>	<b>0.0</b>	<b>0.4</b>	1	0.96	0.56	0.90	-0.8, 0.1	-0.5, 0.6	-0.2, 0.9
<b>Litter size</b>										
Live births (pups)	<b>-1.1*</b>	<b>-1.1*</b>	<b>-2.8*</b>	1	0.94	0.99	1.00	-2.6, 0.3	-2.1, -0.1	-5.0, -0.8

$D_{NC-VT}$  = Mean of the difference NC-VT (median of the marginal posterior distribution of the difference between the NC and the VT groups).

R = Relevant value (proposed as one-third of the SD of the trait), rounded to the first significant number.

$P_0$  = Probability of the difference ( $D_{NC-VT}$ ) being greater than 0 when  $D_{NC-VT} > 0$  or lower than 0 when  $D_{NC-VT} < 0$ .

HPD<sub>95%</sub> = The highest posterior density region at 95% of probability.

\*Statistical differences were assumed if  $|D_{NC-VT}|$  surpass R value and its  $P_0 > 0.80$ .

**Supplementary Table S4.** Differentially expressed transcripts in liver tissue between animals born from vitrified- transferred embryos and those conceived naturally.

Gene accession	Gene name	Fold Change
ENSOCUG00000025868	gamma-aminobutyric acid type A receptor delta subunit(GABRD)	-7.00
ENSOCUG00000015329	matrix metalloproteinase 7(MMP7)	-5.52
ENSOCUG00000021126	Metallothionein-2A(LOC100343299)	-5.27
ENSOCUG00000003467	prostate stem cell antigen(PSCA)	-5.13
ENSOCUG00000004004	family with sequence similarity 135 member B(FAM135B)	-4.78
ENSOCUG00000011488	Fanconi anaemia complementation group I(FANCI)	-4.34
ENSOCUG00000027388	UDP-GlcNAc:betaGal beta-1.3-N-acetylglucosaminyltransferase 8(B3GNT8)	-4.24
ENSOCUG00000010513	centrosomal protein 55(CEP55)	-4.23
ENSOCUG00000005159	anillin actin binding protein(ANLN)	-4.15
ENSOCUG00000008303	matrix metalloproteinase 12(MMP12)	-4.15
ENSOCUG00000002934	zinc finger protein 280C(ZNF280C)	-4.10
ENSOCUG00000001891	glycerol-3-phosphate acyltransferase 2. mitochondrial(GPAT2)	-4.02
ENSOCUG00000017659	alanyl aminopeptidase. membrane(ANPEP)	-4.00
ENSOCUG00000006444	CD109 molecule(CD109)	-3.99
ENSOCUG00000000374	ADAM metalloproteinase with thrombospondin type 1 motif 15(ADAMTS15)	-3.96
ENSOCUG00000005115	fibroblast activation protein alpha(FAP)	-3.91
ENSOCUG00000002542	solute carrier family 22 member 2(SLC22A2)	-3.84
ENSOCUG00000013111	procollagen C-endopeptidase enhancer 2(PCOLCE2)	-3.82
ENSOCUG00000001726	Wnt family member 11(WNT11)	-3.81
ENSOCUG00000012881	collagen type I alpha 1 chain(COL1A1)	-3.77
ENSOCUG00000024161	potassium voltage-gated channel subfamily J member 15(KCNJ15)	-3.70
ENSOCUG00000013577	family with sequence similarity 171 member A2(FAM171A2)	-3.70
ENSOCUG00000021209	metallothionein-2D(LOC100343557)	-3.69
ENSOCUG00000002945	mesenchyme homeobox 1(MEOX1)	-3.67
ENSOCUG00000015320	collagen type XII alpha 1 chain(COL12A1)	-3.63
ENSOCUG00000021508	chromosome 16 open reading frame. human C1orf106(C16H1orf106)	-3.62
ENSOCUG00000017320	ring finger protein 224(RNF224)	-3.59
ENSOCUG00000000856	E2F transcription factor 1(E2F1)	-3.59
ENSOCUG00000001171	NUF2. NDC80 kinetochore complex component(NUF2)	-3.57
ENSOCUG00000000360	cadherin 6(CDH6)	-3.51
ENSOCUG00000001719	diaphanous related formin 3(DIAPH3)	-3.51
ENSOCUG00000002407	microfibrillar associated protein 5(MFAP5)	-3.48
ENSOCUG00000022280	transmembrane protein 45B(TMEM45B)	-3.47



ENSOCUG00000016157	exonuclease 1(LOC100338764)	-3.46
ENSOCUG00000001376	sodium channel protein type 11 subunit alpha(LOC100349709)	-3.46
ENSOCUG00000029235	metallothionein-1A(LOC100343802)	-3.44
ENSOCUG00000025499	uncharacterised protein CXorf21-like(LOC100345885)	-3.43
ENSOCUG00000010144	tetratricopeptide repeat domain 22(TTC22)	-3.39
ENSOCUG00000001652	cyclin B2(CCNB2)	-3.38
ENSOCUG00000001962	4-hydroxyphenylpyruvate dioxygenase like(HPDL)	-3.37
ENSOCUG00000013140	calmodulin binding transcription activator 1(CAMTA1)	-3.33
ENSOCUG00000004616	myotubularin related protein 11(MTMR11)	-3.32
ENSOCUG00000017111	kinesin family member 4A(KIF4A)	-3.31
ENSOCUG00000013056	zinc finger protein 804B(ZNF804B)	-3.30
ENSOCUG00000002924	galectin 3(LGALS3)	-3.29
ENSOCUG00000000120	ADCYAP receptor type I(ADCYAP1R1)	-3.28
ENSOCUG00000003649	transmembrane and immunoglobulin domain containing 1(TMIGD1)	-3.27
ENSOCUG00000000699	centromere protein E(CENPE)	-3.23
ENSOCUG00000015492	glucagon like peptide 2 receptor(GLP2R)	-3.21
ENSOCUG00000005788	solute carrier family 22 member 7(SLC22A7)	-3.20
ENSOCUG00000022624	solute carrier family 26 member 9(SLC26A9)	-3.18
ENSOCUG00000010814	malic enzyme 1(ME1)	-3.16
ENSOCUG00000006258	WD repeat domain 72(WDR72)	-3.15
ENSOCUG00000017347	leptin receptor(LEPR)	-3.15
ENSOCUG00000029254	family with sequence similarity 159 member A(FAM159A)	-3.14
ENSOCUG00000011025	contactin 4(CNTN4)	-3.13
ENSOCUG00000021051	rippy transcriptional repressor 3(RIPPLY3)	-3.12
ENSOCUG00000023285	trophinin associated protein(TROAP)	-3.12
ENSOCUG00000013412	C-C motif chemokine 7(LOC103351517)	-3.09
ENSOCUG00000007151	cilia and flagella associated protein 70(CFAP70)	-3.07
ENSOCUG00000005507	G protein subunit alpha 14(GNA14)	-3.06
ENSOCUG00000017689	keratin 20(KRT20)	-3.06
ENSOCUG00000008329	ADAM metallopeptidase with thrombospondin type 1 motif 19(ADAMTS19)	-3.06
ENSOCUG00000008179	rhomboid like 3(RHBDL3)	-3.03
ENSOCUG00000015410	NDC80. kinetochore complex component(NDC80)	-3.03
ENSOCUG00000000215	period circadian clock 2(PER2)	-3.03
ENSOCUG00000006186	carboxypeptidase X. M14 family member 1(CPXM1)	-3.01
ENSOCUG00000009880	dual specificity phosphatase 14(DUSP14)	-3.00
ENSOCUG00000006613	spermatogenesis-associated 1(SPATA1)	-2.99
ENSOCUG00000022883	glycerophosphodiester phosphodiesterase domain containing 3(GDPD3)	-2.99
ENSOCUG00000025494	secretogranin III(SCG3)	-2.98
ENSOCUG00000022659	EF-hand and coiled-coil domain containing 1(EFCC1)	-2.98
ENSOCUG00000006673	alpha 1.4-galactosyltransferase(A4GALT)	-2.97

ENSOCUG00000016942	aldehyde dehydrogenase 1 family member A2(ALDH1A2)	-2.95
ENSOCUG00000023005	zinc finger protein 367(ZNF367)	-2.93
ENSOCUG00000013801	SHC binding and spindle associated 1(SHCBP1)	-2.93
ENSOCUG00000026551	lysophosphatidic acid receptor 5(LPAR5)	-2.90
ENSOCUG00000004480	cysteine and glycine rich protein 3(CSRP3)	-2.89
ENSOCUG00000016718	mesenteric oestrogen dependent adipogenesis(MEDAG)	-2.87
ENSOCUG00000026610	transmembrane protein 100(TMEM100)	-2.86
ENSOCUG00000010272	acid phosphatase. prostate(ACPP)	-2.86
ENSOCUG00000012902	glutathione S-transferase Yc(LOC100353428)	-2.85
ENSOCUG00000011042	collagen type VIII alpha 2 chain(COL8A2)	-2.85
ENSOCUG00000024465	collagen type VIII alpha 1 chain(COL8A1)	-2.80
ENSOCUG00000017859	RNA binding motif protein 46(RBM46)	-2.80
ENSOCUG00000017387	claspin(CLSPN)	-2.78
ENSOCUG00000011340	cell division cycle 20(CDC20)	-2.76
ENSOCUG00000015483	fatty acid binding protein 4(FABP4)	-2.75
ENSOCUG00000005747	collagen type XVI alpha 1 chain(COL16A1)	-2.74
ENSOCUG00000006962	aldehyde dehydrogenase 1 family member L2(ALDH1L2)	-2.73
ENSOCUG00000011027	chitinase 1(CHIT1)	-2.70
ENSOCUG00000011350	spondin 1(SPON1)	-2.66
ENSOCUG00000015838	collagen type IX alpha 2 chain(COL9A2)	-2.66
ENSOCUG00000004393	synaptotagmin-15(LOC100351528)	-2.63
ENSOCUG00000001627	solute carrier family 6 member 11(SLC6A11)	-2.62
ENSOCUG00000009332	mucolipin 3(MCOLN3)	-2.62
ENSOCUG00000015214	PSMC3 interacting protein(PSMC3IP)	-2.60
ENSOCUG00000007172	acyl-CoA desaturase(LOC100357419)	-2.59
ENSOCUG00000010941	carboxypeptidase X. M14 family member 2(CPXM2)	-2.58
ENSOCUG00000017197	claudin 6(CLDN6)	-2.57
ENSOCUG00000012176	ubiquitin conjugating enzyme E2 C(UBE2C)	-2.56
ENSOCUG00000017882	anoctamin 3(ANO3)	-2.56
ENSOCUG00000004340	cyclin B1(CCNB1)	-2.56
ENSOCUG00000026482	UDP-glucuronosyltransferase 2B16-like(LOC100340513)	-2.55
ENSOCUG00000000236	repulsive guidance molecule family member a(RGMA)	-2.54
ENSOCUG000000024196	F-box protein 17(FBXO17)	-2.54
ENSOCUG00000001337	prostate androgen-regulated mucin-like protein 1(PARM1)	-2.52
ENSOCUG00000029301	zinc finger and SCAN domain containing 23(ZSCAN23)	-2.52
ENSOCUG00000002173	phosphorylase. glycogen. muscle(PYGM)	-2.50
ENSOCUG00000006527	BUB1 mitotic checkpoint serine/threonine kinase B(BUB1B)	-2.50
ENSOCUG00000012264	collagen type I alpha 2 chain(COL1A2)	-2.49
ENSOCUG00000017043	cell division cycle associated 8(CDCA8)	-2.49
ENSOCUG00000003724	multiple EGF-like domains 10(MEGF10)	-2.48
ENSOCUG00000009932	establishment of sister chromatid cohesion N-acetyltransferase 2(ESCO2)	-2.47
ENSOCUG00000014730	frizzled class receptor 2(FZD2)	-2.47
ENSOCUG00000005709	phosphoglucomutase 2 like 1(PGM2L1)	-2.46

ENSOCUG00000025992	butyrophilin subfamily 1 member A1-like(LOC100344369)	-2.46
ENSOCUG00000025655	G protein-coupled receptor 161(GPR161)	-2.45
ENSOCUG00000003822	family with sequence similarity 83 member B(FAM83B)	-2.44
ENSOCUG00000012683	ADAM metallopeptidase domain 33(ADAM33)	-2.44
ENSOCUG00000012071	glycerol-3-phosphate acyltransferase 3(GPAT3)	-2.44
ENSOCUG00000000094	prostacyclin synthase(LOC103346149)	-2.43
ENSOCUG00000002178	nurim (nuclear envelope membrane protein)(NRM)	-2.42
ENSOCUG00000003876	FH2 domain containing 1(FHDC1)	-2.41
ENSOCUG00000017273	patatin-like phospholipase domain-containing protein 3(LOC100344884)	-2.39
ENSOCUG00000012763	contactin-6(LOC100348097)	-2.37
ENSOCUG00000002878	SLX4 interacting protein(SLX4IP)	-2.36
ENSOCUG00000005592	lumican(LUM)	-2.35
ENSOCUG00000000580	cadherin 16(CDH16)	-2.35
ENSOCUG00000015162	microfibrillar associated protein 4(MFAP4)	-2.34
ENSOCUG00000000547	shugoshin 2(SGO2)	-2.33
ENSOCUG00000004511	heat shock protein family B (small) member 8(HSPB8)	-2.32
ENSOCUG00000002703	forkhead box M1(FOXM1)	-2.32
ENSOCUG00000010198	tropomyosin 2 (beta)(TPM2)	-2.30
ENSOCUG00000016111	ankyrin repeat and EF-hand domain containing 1(ANKEF1)	-2.27
ENSOCUG00000007516	6-phosphofructo-2-kinase/fructose-2,6-biphosphatase 3(PFKFB3)	-2.27
ENSOCUG00000005830	HIG1 hypoxia inducible domain family member 1A(HIGD1A)	-2.27
ENSOCUG00000005324	microtubule associated protein 1A(MAP1A)	-2.25
ENSOCUG00000002337	proline rich 11(PRR11)	-2.25
ENSOCUG00000003165	signal peptide. CUB and EGF-like domain-containing protein 1(LOC100344797)	-2.24
ENSOCUG00000011956	cadherin related family member 2(CDHR2)	-2.22
ENSOCUG00000012232	kin of IRRE like (Drosophila)(KIRREL)	-2.21
ENSOCUG00000016193	osteomodulin(OMD)	-2.21
ENSOCUG00000003030	PARP1 binding protein(PARPBP)	-2.20
ENSOCUG00000014571	SH3 and cysteine-rich domain(STAC)	-2.19
ENSOCUG00000029066	transient receptor potential cation channel subfamily M member 2(LOC103347481)	-2.19
ENSOCUG00000005174	dermatopontin(DPT)	-2.19
ENSOCUG00000003689	nidogen 2(NID2)	-2.17
ENSOCUG00000015893	proprotein convertase subtilisin/kexin type 2(PCSK2)	-2.17
ENSOCUG00000014432	ectonucleotide pyrophosphatase/phosphodiesterase 3(ENPP3)	-2.17
ENSOCUG00000014988	collagen type III alpha 1 chain(COL3A1)	-2.16
ENSOCUG00000012275	testis expressed 9(TEX9)	-2.15
ENSOCUG00000009195	C type lectin domain family 4 member E(CLEC4E)	-2.14
ENSOCUG00000002858	cyclin dependent kinase 1(CDK1)	-2.13
ENSOCUG00000004275	semaphorin 5A(SEMA5A)	-2.12

ENSOCUG00000001375	acyl-CoA desaturase(LOC100346046)	-2.11
ENSOCUG000000012809	solute carrier family 25 member 24(SLC25A24)	-2.11
ENSOCUG000000010936	chromosome unknown open reading frame. human C16orf89(LOC100353142)	-2.11
ENSOCUG00000003903	centromere protein U(CENPU)	-2.10
ENSOCUG00000000092	serpin family F member 1(SERPINF1)	-2.10
ENSOCUG000000009218	phosphodiesterase 10A(PDE10A)	-2.09
ENSOCUG000000029623	ATPase plasma membrane Ca <sup>2+</sup> transporting 3(ATP2B3)	-2.07
ENSOCUG000000017153	transcription factor 19(TCF19)	-2.06
ENSOCUG000000001825	family with sequence similarity 171 member B(FAM171B)	-2.05
ENSOCUG000000011970	transgelin(TAGLN)	-2.04
ENSOCUG000000002707	MID1 interacting protein 1(MID1IP1)	-2.04
ENSOCUG000000013465	TBC1 domain family member 19(TBC1D19)	-2.04
ENSOCUG000000007735	FRAS1 related extracellular matrix protein 2(FREM2)	-2.03
ENSOCUG000000004485	E2F transcription factor 8(E2F8)	-2.02
ENSOCUG000000008953	synaptopodin 2(SYNPO2)	-2.02
ENSOCUG000000003254	cyclin dependent kinase like 2(CDKL2)	-2.02
ENSOCUG000000014056	dedicator of cytokinesis 5(DOCK5)	-2.02
ENSOCUG000000015836	myelin protein zero like 2(MPZL2)	-2.00
ENSOCUG000000022348	zinc finger and BTB domain containing 7C(ZBTB7C)	-2.00
ENSOCUG000000016302	alpha-fetoprotein(AFP)	-2.00
ENSOCUG000000017492	centromere protein F(CENPF)	-1.99
ENSOCUG000000000409	collagen type VI alpha 2 chain(COL6A2)	-1.98
ENSOCUG000000000109	ADAM metallopeptidase with thrombospondin type 1 motif 9(ADAMTS9)	-1.97
ENSOCUG000000015790	kinesin family member 20A(KIF20A)	-1.97
ENSOCUG000000006973	adhesion G protein-coupled receptor E2(ADGRE2)	-1.97
ENSOCUG000000013450	myosin heavy chain 11(MYH11)	-1.97
ENSOCUG000000005503	spindle apparatus coiled-coil protein 1(SPDL1)	-1.96
ENSOCUG000000000847	protein tyrosine phosphatase. receptor type D(PTPRD)	-1.96
ENSOCUG000000000313	ovostatin homolog 2(LOC100348825)	-1.96
ENSOCUG000000013062	acyl-CoA synthetase long-chain family member 6(ACSL6)	-1.95
ENSOCUG000000016236	collagen type XV alpha 1 chain(COL15A1)	-1.94
ENSOCUG000000011244	extra spindle pole bodies like 1. separase(ESPL1)	-1.93
ENSOCUG000000015756	kinetochore scaffold 1(KNL1)	-1.91
ENSOCUG000000013757	solute carrier family 13 member 2(SLC13A2)	-1.90
ENSOCUG000000010184	trehalase(TREH)	-1.90
ENSOCUG000000017620	serum amyloid protein A(LOC100009259)	-1.89
ENSOCUG000000017867	Fraser extracellular matrix complex subunit 1(FRAS1)	-1.88
ENSOCUG000000012148	inositol 1.4.5-trisphosphate receptor type 1(ITPR1)	-1.88
ENSOCUG000000013414	RasGEF domain family member 1C(RASGEF1C)	-1.88
ENSOCUG000000025273	liver carboxylesterase 2(LOC100343300)	-1.87
ENSOCUG000000003277	nucleolar and spindle associated protein 1(NUSAP1)	-1.86
ENSOCUG000000005560	G protein subunit alpha transducin 2(GNAT2)	-1.84

ENSOCUG00000025241	liver carboxylesterase 2-like(LOC100357214)	-1.84
ENSOCUG00000016303	sulfotransferase family. cytosolic. 1C. member 2(SULT1C2)	-1.83
ENSOCUG00000024055	melanoma cell adhesion molecule(MCAM)	-1.83
ENSOCUG00000008571	myomesin 1(MYOM1)	-1.83
ENSOCUG00000008236	lipoprotein lipase(LPL)	-1.82
ENSOCUG00000025132	60S ribosomal protein L23a(LOC108177184)	-1.82
ENSOCUG00000005521	G protein-coupled bile acid receptor 1(GPBAR1)	-1.81
ENSOCUG00000006131	SPARC like 1(SPARCL1)	-1.81
ENSOCUG00000029071	zinc finger protein 81(ZNF81)	-1.80
ENSOCUG00000006714	matrix metalloproteinase 2(MMP2)	-1.80
ENSOCUG00000001785	syntaxin 19(STX19)	-1.78
ENSOCUG00000017585	family with sequence similarity 105 member A(FAM105A)	-1.78
ENSOCUG00000005885	immunoglobulin superfamily member 10(IGSF10)	-1.78
ENSOCUG00000005774	zinc finger protein 521(ZNF521)	-1.77
ENSOCUG00000002468	kinesin family member 20B(KIF20B)	-1.77
ENSOCUG00000002814	topoisomerase (DNA) II alpha(TOP2A)	-1.76
ENSOCUG00000005540	calpain 6(CAPN6)	-1.75
ENSOCUG00000012372	lipin 3(LPIN3)	-1.75
ENSOCUG00000016909	RAD51 recombinase(RAD51)	-1.75
ENSOCUG00000021287	heat shock protein family B (small) member 6(HSPB6)	-1.75
ENSOCUG00000023917	early B cell factor 4(EBF4)	-1.74
ENSOCUG00000007545	EPH receptor B6(EPHB6)	-1.74
ENSOCUG00000005820	ribonucleotide reductase regulatory subunit M2(RRM2)	-1.73
ENSOCUG00000010046	thymidine kinase 1(TK1)	-1.73
ENSOCUG00000003203	TPX2. microtubule nucleation factor(TPX2)	-1.72
ENSOCUG00000001754	formin like 3(FMNL3)	-1.70
ENSOCUG00000013175	fibulin 5(FBLN5)	-1.70
ENSOCUG00000012031	pleckstrin 2(PLEK2)	-1.70
ENSOCUG00000014077	latent transforming growth factor beta binding protein 2(LTBP2)	-1.69
ENSOCUG00000000161	SH3 domain binding protein 2(SH3BP2)	-1.69
ENSOCUG00000017717	grainyhead like transcription factor 1(GRHL1)	-1.68
ENSOCUG00000016964	matrix Gla protein(MGP)	-1.68
ENSOCUG00000002874	protein tyrosine kinase 7 (inactive)(PTK7)	-1.68
ENSOCUG00000015111	glutamate ionotropic receptor NMDA type subunit 2B(GRIN2B)	-1.68
ENSOCUG00000015681	Rac GTPase activating protein 1(RACGAP1)	-1.67
ENSOCUG00000014083	leucine zipper tumour suppressor 1(LZTS1)	-1.67
ENSOCUG00000009017	osteoglycin(OGN)	-1.66
ENSOCUG00000023919	transgelin(LOC100009332)	-1.64
ENSOCUG00000001035	ADAM metalloproteinase with thrombospondin type 1 motif 2(ADAMTS2)	-1.64
ENSOCUG00000022434	cell division cycle associated 3(CDCA3)	-1.63
ENSOCUG00000009143	cyclin E1(CCNE1)	-1.63

ENSOCUG0000001863	vesicle amine transport 1 like(VAT1L)	-1.63
ENSOCUG00000010827	BOC cell adhesion associated. oncogene regulated(BOC)	-1.63
ENSOCUG00000010708	kinesin family member C1(KIFC1)	-1.63
ENSOCUG00000014801	acyl-CoA desaturase(LOC100346561)	-1.63
ENSOCUG00000024282	pleckstrin homology domain containing B2(PLEKHB2)	-1.62
ENSOCUG00000001389	leucine-rich repeat and Ig domain containing 4(LINGO4)	-1.62
ENSOCUG00000022014	notch 3(NOTCH3)	-1.61
ENSOCUG00000006357	ADAM metallopeptidase with thrombospondin type 1 motif 12(ADAMTS12)	-1.61
ENSOCUG00000023213	pro-neuregulin-4. membrane-bound isoform-like(LOC108176558)	-1.61
ENSOCUG00000008491	testin LIM domain protein(TES)	-1.60
ENSOCUG00000010232	anthrax toxin receptor 1(ANTXR1)	-1.60
ENSOCUG00000021663	CUGBP. Elav-like family member 6(CELF6)	-1.60
ENSOCUG00000017377	matrilin 2(MATN2)	-1.60
ENSOCUG00000008818	creatine kinase B(CKB)	-1.60
ENSOCUG00000021411	tsukushi. small leucine-rich proteoglycan(TSKU)	-1.60
ENSOCUG00000001801	forkhead box P2(FOXP2)	-1.59
ENSOCUG00000006490	leucine-rich repeat-containing protein 37A2(LOC103346478)	-1.58
ENSOCUG00000015020	collagen type V alpha 2 chain(COL5A2)	-1.57
ENSOCUG00000004137	protease. serine 23(PRSS23)	-1.55
ENSOCUG00000013868	MMS22 like. DNA repair protein(MMS22L)	-1.55
ENSOCUG00000002424	serum amyloid A-3(SAA3)	-1.54
ENSOCUG00000015443	adenylate cyclase 3(ADCY3)	-1.54
ENSOCUG00000023778	CD300a molecule(CD300A)	-1.53
ENSOCUG00000017136	solute carrier family 27 member 6(SLC27A6)	-1.53
ENSOCUG00000016347	phosphoethanolamine/phosphocholine phosphatase(PHOSPHO1)	-1.53
ENSOCUG00000001921	KIAA0825 ortholog(KIAA0825)	-1.52
ENSOCUG00000024273	sulfatase 2(SULF2)	-1.52
ENSOCUG00000027359	tetraspanin 11(TSPAN11)	-1.52
ENSOCUG00000013478	HtrA serine peptidase 1(HTRA1)	-1.51
ENSOCUG00000003866	fibrillin 1(FBN1)	-1.51
ENSOCUG00000017019	cadherin 11(CDH11)	-1.51
ENSOCUG00000008498	uridine phosphorylase 2(UPP2)	-1.49
ENSOCUG00000008841	glutamate-ammonia ligase(GLUL)	-1.49
ENSOCUG00000027031	zinc finger protein 496(ZNF496)	-1.49
ENSOCUG00000015371	serine peptidase inhibitor. Kunitz type 1(SPINT1)	-1.49
ENSOCUG00000009543	potassium calcium-activated channel subfamily M alpha 1(KCNMA1)	-1.48
ENSOCUG00000010299	cysteine and glycine rich protein 1(CSRP1)	-1.48
ENSOCUG00000015039	fibronectin type III domain containing 1(FNDC1)	-1.47
ENSOCUG00000015853	glutaredoxin(GLRX)	-1.46

ENSOCUG00000012866	TEF. PAR bZIP transcription factor(TEF)	-1.45
ENSOCUG00000003663	actin. gamma 2. smooth muscle. enteric(ACTG2)	-1.44
ENSOCUG00000008855	cerebral endothelial cell adhesion molecule(CERCAM)	-1.44
ENSOCUG00000008012	stathmin(LOC100358241)	-1.43
ENSOCUG00000008476	polo like kinase 1(PLK1)	-1.42
ENSOCUG000000024939	interferon-induced protein with tetratricopeptide repeats 2(IFIT2)	-1.42
ENSOCUG00000022047	MPV17 mitochondrial inner membrane protein like(MPV17L)	-1.42
ENSOCUG00000017494	mannose receptor C type 2(MRC2)	-1.42
ENSOCUG00000026406	butyrophilin subfamily 1 member A1-like(LOC108175832)	-1.41
ENSOCUG00000027184	carbonyl reductase 1(CBR1)	-1.41
ENSOCUG00000016815	islet cell autoantigen 1(ICA1)	-1.40
ENSOCUG00000007759	ubiquitin specific peptidase 2(USP2)	-1.39
ENSOCUG00000005896	inositol polyphosphate-4-phosphatase type II B(INPP4B)	-1.39
ENSOCUG00000005317	calcium release activated channel regulator 2A(CRACR2A)	-1.39
ENSOCUG00000001912	plexin B1(PLXNB1)	-1.38
ENSOCUG00000011626	calcium/calmodulin dependent protein kinase ID(CAMK1D)	-1.38
ENSOCUG00000004590	collagen type XXVII alpha 1 chain(COL27A1)	-1.37
ENSOCUG00000003858	glycine N-methyltransferase(GNMT)	-1.36
ENSOCUG00000026099	peripheral myelin protein 22(PMP22)	-1.36
ENSOCUG00000000637	myosin light chain 9(MYL9)	-1.35
ENSOCUG00000011126	heparanase(HPSE)	-1.35
ENSOCUG00000008478	syntaxin binding protein 4(STXBP4)	-1.35
ENSOCUG00000005900	fibulin 2(FBLN2)	-1.35
ENSOCUG00000006917	ER membrane associated RNA degradation(ERMARD)	-1.35
ENSOCUG00000004505	coiled-coil domain containing 77(CCDC77)	-1.34
ENSOCUG00000014596	lysyl oxidase like 2(LOXL2)	-1.34
ENSOCUG00000016538	minichromosome maintenance complex component 6(MCM6)	-1.33
ENSOCUG00000012971	GLIS family zinc finger 2(GLIS2)	-1.33
ENSOCUG00000010637	minichromosome maintenance complex component 5(MCM5)	-1.33
ENSOCUG00000026731	helicase. lymphoid-specific(HELLS)	-1.33
ENSOCUG00000015372	DEAQ-box RNA dependent ATPase 1(DQX1)	-1.33
ENSOCUG00000004841	dickkopf WNT signalling pathway inhibitor 3(DKK3)	-1.33
ENSOCUG00000002376	HAUS augmin like complex subunit 7(HAUS7)	-1.33
ENSOCUG00000026480	aldehyde oxidase 2(AOX2)	-1.32
ENSOCUG00000015509	non-SMC condensin II complex subunit G2(NCAPG2)	-1.32
ENSOCUG00000010244	matrix metalloproteinase 14(MMP14)	-1.31
ENSOCUG00000013696	BicC family RNA binding protein 1(BICC1)	-1.31
ENSOCUG00000015924	minichromosome maintenance complex component 2(MCM2)	-1.30
ENSOCUG00000016164	cytochrome P450 1B1(LOC100358590)	-1.30

ENSOCUG00000005032	family with sequence similarity 169 member B(FAM169B)	-1.29
ENSOCUG00000006350	solute carrier family 12 member 4(SLC12A4)	-1.29
ENSOCUG00000007526	cystathionine gamma-lyase(CTH)	-1.28
ENSOCUG00000000560	hes related family bHLH transcription factor with YRPW motif-like(HEYL)	-1.27
ENSOCUG00000003212	tumour suppressor candidate 3(TUSC3)	-1.27
ENSOCUG00000006493	stathmin 1(STMN1)	-1.27
ENSOCUG00000006927	Rho GTPase activating protein 42(ARHGAP42)	-1.26
ENSOCUG00000014326	prostaglandin-E(2) 9-reductase-like(LOC100352716)	-1.26
ENSOCUG00000007967	four and a half LIM domains 2(FHL2)	-1.26
ENSOCUG00000024509	butyrophilin subfamily 1 member A1(LOC100343656)	-1.26
ENSOCUG00000016717	INTS3 and NABP interacting protein(INIP)	-1.24
ENSOCUG00000014029	SET domain containing 4(SETD4)	-1.24
ENSOCUG00000013643	PDZ and LIM domain 1(PDLIM1)	-1.24
ENSOCUG00000003091	adenylate cyclase 7(ADCY7)	-1.23
ENSOCUG00000015051	protein phosphatase 1 regulatory subunit 3C(PPP1R3C)	-1.21
ENSOCUG00000005474	sarcoglycan beta(SGCB)	-1.21
ENSOCUG00000001673	triokinase and FMN cyclase(TKFC)	-1.21
ENSOCUG00000006969	decorin(DCN)	-1.21
ENSOCUG00000009260	phospholipase C eta 1(PLCH1)	-1.21
ENSOCUG00000002336	bone marrow stromal cell antigen 1(BST1)	-1.21
ENSOCUG00000013609	lipopolysaccharide binding protein(LBP)	-1.20
ENSOCUG00000014498	solute carrier family 16 member 12(SLC16A12)	-1.19
ENSOCUG00000015234	collagen type XIV alpha 1 chain(COL14A1)	-1.17
ENSOCUG00000000324	proline-serine-threonine phosphatase interacting protein 2(PSTPIP2)	1.39
ENSOCUG00000006009	acyl-coenzyme A thioesterase 1(LOC100344509)	1.43
ENSOCUG00000029130	cytochrome P450 2C1(CYP2C1)	1.46
ENSOCUG00000007555	peptidoglycan recognition protein 2(PGLYRP2)	1.46
ENSOCUG00000007699	kynurenine 3-monooxygenase(KMO)	1.47
ENSOCUG00000022168	serine dehydratase(SDS)	1.51
ENSOCUG00000015313	cytochrome c oxidase protein 20 homolog(LOC100349428)	1.52
ENSOCUG00000014197	macrophage scavenger receptor 1(MSR1)	1.55
ENSOCUG00000016959	absent in melanoma 1-like(AIM1L)	1.56
ENSOCUG00000003246	sulfatase 1(SULF1)	1.58
ENSOCUG00000026526	protein phosphatase. Mg <sup>2+</sup> /Mn <sup>2+</sup> dependent 1E(PPM1E)	1.59
ENSOCUG00000007130	solute carrier family 25 member 25(SLC25A25)	1.60
ENSOCUG00000009725	acyl-CoA wax alcohol acyltransferase 1(AWAT1)	1.61
ENSOCUG00000027233	uncharacterised LOC100346308(LOC100346308)	1.64
ENSOCUG00000006937	coiled-coil domain containing 57(CCDC57)	1.67
ENSOCUG00000004163	solute carrier family 25 member 33(SLC25A33)	1.67
ENSOCUG00000011634	sphingomyelin phosphodiesterase 3(SMPD3)	1.70
ENSOCUG00000001028	major facilitator superfamily domain containing 2A(MFSD2A)	1.75



ENSOCUG00000016068	serpin family E member 1(SERPINE1)	1.75
ENSOCUG00000001185	G protein-coupled receptor 149(GPR149)	1.81
ENSOCUG000000024272	nexilin F-actin binding protein(NEXN)	1.82
ENSOCUG000000011201	CYP4B1-like isozyme short form(CYP4B1)	1.84
ENSOCUG00000007999	dual specificity phosphatase 1(DUSP1)	1.84
ENSOCUG000000021506	Fos proto-oncogene. AP-1 transcription factor subunit(FOS)	1.87
ENSOCUG000000024078	protein GREB1(LOC100345224)	1.89
ENSOCUG000000025236	leukocyte protein(LOC100009166)	1.91
ENSOCUG000000024474	L-gulonolactone oxidase(LOC100341843)	1.91
ENSOCUG000000002702	radical S-adenosyl methionine domain containing 1(RSAD1)	1.92
ENSOCUG000000023743	heat shock 70 kDa protein 1B(LOC100354435)	1.92
ENSOCUG000000002000	sarcoglycan delta(SGCD)	1.93
ENSOCUG000000004662	Tctex1 domain containing 1(TCTEX1D1)	2.02
ENSOCUG000000014749	ATP/GTP-binding protein like 3(AGBL3)	2.06
ENSOCUG000000017424	activating transcription factor 3(ATF3)	2.09
ENSOCUG000000005465	nocturnin(NOCT)	2.10
ENSOCUG000000013296	growth arrest and DNA damage inducible gamma(GADD45G)	2.12
ENSOCUG000000029339	acyl-CoA wax alcohol acyltransferase 2(AWAT2)	2.12
ENSOCUG000000004099	ganglioside induced differentiation associated protein 1 like 1(GDAP1L1)	2.15
ENSOCUG000000004492	potassium voltage-gated channel subfamily Q member 1(KCNQ1)	2.18
ENSOCUG000000009863	protein kinase C theta(PRKCQ)	2.21
ENSOCUG000000002656	trafficking protein particle complex 3 like(TRAPPC3L)	2.26
ENSOCUG000000004269	transient receptor potential cation channel subfamily V member 4(TRPV4)	2.26
ENSOCUG000000006499	mitochondria localised glutamic acid rich protein(MGARP)	2.29
ENSOCUG000000012452	adhesion G protein-coupled receptor F3(ADGRF3)	2.32
ENSOCUG000000012831	insulin like growth factor binding protein 1(IGFBP1)	2.39
ENSOCUG000000008253	tissue factor pathway inhibitor(TFPI)	2.46
ENSOCUG000000025112	heat shock 70 kDa protein 1B(LOC100354037)	2.48
ENSOCUG000000002457	canopy FGF signalling regulator 1(CNPY1)	2.49
ENSOCUG000000015664	tryptophan hydroxylase 2(TPH2)	2.57
ENSOCUG000000005480	TATA-box binding protein associated factor 4b(TAF4B)	2.68
ENSOCUG000000023871	uncharacterised LOC100347087(LOC100347087)	2.78
ENSOCUG000000017102	serpin family A member 7(SERPINA7)	2.81
ENSOCUG000000023547	tubulin alpha-3 chain(LOC100350967)	2.85
ENSOCUG000000007038	urotensin 2B(UTS2B)	2.92
ENSOCUG000000000784	nuclear receptor subfamily 4 group A member 2(NR4A2)	2.99
ENSOCUG000000027771	zymogen granule membrane protein 16- like(LOC100359023)	3.02
ENSOCUG000000023796	lactotransferrin(LTF)	3.03
ENSOCUG000000006597	calmegin(CLGN)	3.14

ENSOCUG00000008182	coiled-coil domain containing 136(CCDC136)	3.24
ENSOCUG00000012939	ectonucleotide pyrophosphatase/phosphodiesterase 5 (putative)(ENPP5)	3.27
ENSOCUG00000002174	testis expressed 12(TEX12)	3.39
ENSOCUG00000029634	arachidonate lipoxygenase 3(ALOXE3)	3.77
ENSOCUG00000022232	zymogen granule membrane protein 16(LOC100345057)	4.89
ENSOCUG00000027212	zymogen granule membrane protein 16-like(LOC100339377)	6.91
ENSOCUG00000017680	family with sequence similarity 212 member B(FAM212B)	< -0.01
ENSOCUG00000008748	5'-nucleotidase domain containing 4(NT5DC4)	< -0.01
ENSOCUG00000010366	transmembrane protease. serine 13(TMPRS13)	< -0.01
ENSOCUG00000016046	potassium voltage-gated channel subfamily A member 6(KCNA6)	< -0.01
ENSOCUG00000001255	RRAD and GEM like GTPase 2(REM2)	< -0.02
ENSOCUG00000002319	PCNA-associated factor-like(LOC100356881)	< -0.02
ENSOCUG00000008557	adenylate cyclase 2(ADCY2)	< -0.02
ENSOCUG00000002283	family with sequence similarity 84 member A(FAM84A)	< -0.03
ENSOCUG00000003999	calcium/calmodulin dependent protein kinase IG(CAMK1G)	< -0.03
ENSOCUG00000005596	gremlin 1. DAN family BMP antagonist(GREM1)	< -0.03
ENSOCUG00000010335	DS cell adhesion molecule like 1(DSCAML1)	< -0.03
ENSOCUG00000015215	homeobox A1(HOXA1)	< -0.03
ENSOCUG00000016650	DEP domain containing 1B(DEPDC1B)	< -0.03
ENSOCUG00000001041	maternal embryonic leucine zipper kinase(MELK)	< -0.04
ENSOCUG00000006091	odd-skipped related transcription factor 1(OSR1)	< -0.04
ENSOCUG00000006437	RUN domain containing 3A(RUNDC3A)	< -0.04
ENSOCUG00000007225	cellular retinoic acid binding protein 2(CRABP2)	< -0.04
ENSOCUG00000002624	Nik related kinase(NRK)	< -0.05
ENSOCUG00000006383	ghrelin and obestatin prepropeptide(GHRL)	< -0.05
ENSOCUG00000006801	minichromosome maintenance 10 replication initiation factor(MCM10)	< -0.05
ENSOCUG00000004047	spindle and kinetochore associated complex subunit 3(SKA3)	< -0.07
ENSOCUG00000006341	calbindin 1(CALB1)	< -0.07
ENSOCUG00000007263	cell surface glycoprotein CD200 receptor 2(LOC100348666)	< -0.08
ENSOCUG00000014335	tripartite motif family like 1(TRIML1)	< -0.08
ENSOCUG00000014421	myelin protein zero(MPZ)	< -0.09
ENSOCUG00000002956	copine 4(CPNE4)	< -0.10
ENSOCUG00000007994	HECT. C2 and WW domain containing E3 ubiquitin protein ligase 1(HECW1)	< -0.11
ENSOCUG00000008418	beta-1.4-N-acetyl-galactosaminyltransferase 3(B4GALNT3)	< -0.11
ENSOCUG00000013934	coiled-coil domain containing 189(CCDC189)	< -0.11
ENSOCUG00000012527	solute carrier family 26 member 7(SLC26A7)	< -0.12
ENSOCUG00000014857	collagen type V alpha 3 chain(COL5A3)	< -0.12
ENSOCUG00000000266	Wnt family member 2B(WNT2B)	< -0.13
ENSOCUG00000001961	RAD51 associated protein 1(RAD51AP1)	< -0.13

ENSOCUG00000008531	hydroxysteroid 17-beta dehydrogenase 3(HSD17B3)	< -0.13
ENSOCUG00000009528	intestinal-type alkaline phosphatase-like(LOC100352107)	< -0.13
ENSOCUG000000027644	translocator protein 2(TSPO2)	< -0.13
ENSOCUG000000017309	5-hydroxytryptamine receptor 4(HTR4)	< -0.15
ENSOCUG000000010677	insulin receptor related receptor(INSRR)	< -0.16
ENSOCUG000000011298	family with sequence similarity 83 member D(FAM83D)	< -0.16
ENSOCUG00000004089	matrix metalloproteinase 28(MMP28)	< -0.17
ENSOCUG000000016277	epiregulin(EREG)	< -0.19
ENSOCUG000000007146	1-aminocyclopropane-1-carboxylate synthase homolog (inactive) like(ACCSL)	< -0.22
ENSOCUG000000029599	killer cell lectin like receptor B1(KLRB1)	< -0.24
ENSOCUG000000006792	non-SMC condensin I complex subunit G(NCAPG)	< -0.32
ENSOCUG000000016390	WNT1 inducible signalling pathway protein 1(WISP1)	< -0.40
ENSOCUG000000029014	chromosome 13 open reading frame. human C1orf105(C13H1orf105)	< -0.41
ENSOCUG000000003120	opioid receptor kappa 1(OPRK1)	< -0.47
ENSOCUG000000014832	STEAP2 metalloredutase(STEAP2)	< -0.56
ENSOCUG000000026203	complement C1q like 1(C1QL1)	< -1.17
ENSOCUG000000002462	solute carrier family 24 member 2(SLC24A2)	< -2.13
ENSOCUG000000026293	leucine-rich repeats and transmembrane domains 1(LRTM1)	< -3.82
ENSOCUG000000000087	TLC domain containing 2(TLCD2)	> 0.02
ENSOCUG000000010077	potassium channel tetramerisation domain containing 19(KCTD19)	> 0.02
ENSOCUG000000007327	contactin associated protein 1(CNTNAP1)	> 0.03
ENSOCUG000000009777	GRB2 associated regulator of MAPK1 subtype 2(GAREM2)	> 0.03
ENSOCUG000000016833	chromosome 13 open reading frame. human C1orf228(C13H1orf228)	> 0.03
ENSOCUG000000022998	tubulin alpha-3 chain(LOC100349209)	> 0.03
ENSOCUG000000004632	carbonic anhydrase 12(CA12)	> 0.04
ENSOCUG000000006025	proopiomelanocortin(POMC)	> 0.04
ENSOCUG000000013544	ATPase H+ transporting V0 subunit a4(ATP6V0A4)	> 0.04
ENSOCUG000000003926	transmembrane protein 89(TMEM89)	> 0.05
ENSOCUG000000004187	paired box 8(PAX8)	> 0.05
ENSOCUG000000007102	tubulin polymerisation promoting protein family member 2(TPPP2)	> 0.05
ENSOCUG000000009532	AF4/FMR2 family member 3(AFF3)	> 0.05
ENSOCUG000000011656	actin like 7A(ACTL7A)	> 0.05
ENSOCUG000000024091	solute carrier family 22 member 8(SLC22A8)	> 0.05
ENSOCUG000000003274	Opa interacting protein 5(OIP5)	> 0.06
ENSOCUG000000015293	porcupine homolog (Drosophila)(PORCN)	> 0.06
ENSOCUG000000016063	CKLF like MARVEL transmembrane domain containing 2(CMTM2)	> 0.06
ENSOCUG000000029056	C type lectin domain family 17 member A(CLEC17A)	> 0.06
ENSOCUG000000000197	hexokinase 2(HK2)	> 0.07

ENSOCUG00000001207	oestrogen related receptor beta(ESRRB)	> 0.07
ENSOCUG000000022774	cation channel sperm associated auxiliary subunit gamma(CATSPERG)	> 0.07
ENSOCUG00000001822	kinesin family member 17(KIF17)	> 0.08
ENSOCUG00000010922	glyceraldehyde-3-phosphate dehydrogenase. spermatogenic(GAPDHS)	> 0.08
ENSOCUG00000013226	BLK proto-oncogene. Src family tyrosine kinase(BLK)	> 0.08
ENSOCUG00000005547	chromosome 19 open reading frame. human C17orf74(C19H17orf74)	> 0.09
ENSOCUG00000013299	heat shock protein family B (small) member 9(HSPB9)	> 0.09
ENSOCUG00000016389	solute carrier family 17 member 6(SLC17A6)	> 0.10
ENSOCUG00000016652	RIB43A domain with coiled-coils 2(RIBC2)	> 0.10
ENSOCUG00000023766	disintegrin and metalloproteinase domain-containing protein 18(LOC100358989)	> 0.10
ENSOCUG00000005270	phosphoglycerate kinase 2(PGK2)	> 0.11
ENSOCUG00000027853	phosphoglycerate mutase 2(PGAM2)	> 0.11
ENSOCUG00000029412	zymogen granule membrane protein 16-like(LOC100352055)	> 0.11
ENSOCUG00000008107	maestro heat like repeat family member 7(MROH7)	> 0.12
ENSOCUG00000015787	beaded filament structural protein 1(BFSP1)	> 0.12
ENSOCUG00000010163	acyl-CoA synthetase bubblegum family member 2(ACSBG2)	> 0.13
ENSOCUG00000022427	myomegalin(LOC103350070)	> 0.14
ENSOCUG00000003737	acrosin binding protein(ACRBP)	> 0.15
ENSOCUG00000027844	solute carrier family 24 member 1(SLC24A1)	> 0.16
ENSOCUG00000000119	solute carrier family 51 alpha subunit(SLC51A)	> 0.17
ENSOCUG00000021920	neuraminidase 4(NEU4)	> 0.18
ENSOCUG00000017222	outer dense fibre of sperm tails 1(ODF1)	> 0.19
ENSOCUG00000015667	SH3 domain containing ring finger 2(SH3RF2)	> 0.20
ENSOCUG00000004280	chromosome 4 open reading frame. human C12orf50(C4H12orf50)	> 0.24
ENSOCUG00000022253	putative spermatogenesis-associated protein 31D3(LOC100341232)	> 0.24
ENSOCUG00000005090	spermatogenic leucine zipper 1(SPZ1)	> 0.26
ENSOCUG00000029604	calcium binding protein. spermatid associated 1(CABS1)	> 0.26
ENSOCUG00000027755	putative spermatogenesis-associated protein 31D3(LOC100355671)	> 0.29
ENSOCUG00000017123	cilia and flagella associated protein 53(CFAP53)	> 0.30
ENSOCUG00000006562	LanC like 3(LANCL3)	> 0.32
ENSOCUG00000001385	ornithine decarboxylase antizyme 3(OAZ3)	> 0.35
ENSOCUG00000010340	arachidonate 15-lipoxygenase. type B(ALOX15B)	> 0.41
ENSOCUG00000015803	tubulointerstitial nephritis antigen(TINAG)	> 0.45
ENSOCUG00000012837	germ cell associated 1(GSG1)	> 0.46
ENSOCUG00000021104	transition protein 2(TNP2)	> 0.47
ENSOCUG00000005537	radial spoke head 9 homolog(RSPH9)	> 0.52
ENSOCUG00000015841	solute carrier family 36 member 3(SLC36A3)	> 0.72

ENSOCUG00000026150	CD19 molecule(CD19)	> 1.04
ENSOCUG00000025309	glycerol kinase 2(GK2)	> 1.60
ENSOCUG00000026777	zymogen granule membrane protein 16(LOC100346433)	> 104.
ENSOCUG00000029690	zymogen granule membrane protein 16(LOC100350057)	> 15.6
ENSOCUG00000027492	zymogen granule membrane protein 16(LOC100346271)	> 18.8
ENSOCUG00000025809	reticulon 4 receptor-like 2(RTN4RL2)	> 2.37
ENSOCUG00000025107	membrane associated ring-CH-type finger 4(MARCH4)	> 4.13
ENSOCUG00000026477	tubulin alpha-3 chain(LOC100350027)	> 7.13

---

**Supplementary Table S5.** Functional analysis of differential expressed transcripts in liver tissue between animals born from vitrified-transferred embryos and those conceived naturally.

Category*	Term	Count	p-value
BP	collagen fibril organisation	9	0.000
BP	mitotic cytokinesis	7	0.000
BP	extracellular fibril organisation	4	0.000
BP	negative regulation of growth	4	0.004
BP	elastic fibre assembly	3	0.007
BP	DNA replication initiation	4	0.007
BP	regulation of cytoskeleton organisation	3	0.011
BP	cellular response to zinc ion	3	0.022
BP	DNA unwinding involved in DNA replication	3	0.022
BP	glomerular filtration	3	0.022
BP	protein localisation to kinetochore	3	0.022
BP	microtubule-based movement	6	0.023
BP	fatty acid biosynthetic process	4	0.027
BP	cell adhesion	9	0.028
BP	response to hormone	3	0.029
BP	positive regulation of vascular endothelial growth factor production	4	0.031
BP	glycolytic process	4	0.035
BP	positive regulation of macrophage derived foam cell differentiation	3	0.037
BP	cellular response to amino acid stimulus	5	0.042
BP	arachidonic acid metabolic process	3	0.045
BP	skin development	4	0.049
BP	endodermal cell differentiation	4	0.054
BP	mitotic metaphase plate congression	4	0.060
BP	positive regulation of branching involved in ureteric bud morphogenesis	3	0.063
BP	heparan sulfate proteoglycan metabolic process	2	0.068
BP	glial cell-derived neurotrophic factor receptor signalling pathway	2	0.068
BP	oesophagus smooth muscle contraction	2	0.068
BP	positive regulation of apoptotic process	8	0.073
BP	collagen catabolic process	3	0.073
BP	artery morphogenesis	3	0.073
BP	acute-phase response	3	0.083
BP	canonical Wnt signalling pathway	5	0.084
BP	cell-matrix adhesion	5	0.084
BP	endothelial cell migration	3	0.094
CC	extracellular matrix	19	0.000

CC	proteinaceous extracellular matrix	20	0.000
CC	extracellular space	47	0.000
CC	zymogen granule membrane	7	0.000
CC	collagen trimer	7	0.000
CC	extracellular exosome	87	0.000
CC	basement membrane	7	0.002
CC	MCM complex	4	0.002
CC	midbody	9	0.005
CC	condensed nuclear chromosome outer kinetochore	3	0.006
CC	spindle microtubule	5	0.010
CC	microfibril	3	0.014
CC	cell surface	17	0.014
CC	microtubule	8	0.039
CC	chromocenter	3	0.046
CC	cytoplasm	75	0.050
CC	fibrillar collagen trimer	2	0.063
CC	Ndc80 complex	2	0.063
CC	elastic fibre	2	0.063
CC	collagen type V trimer	2	0.063
CC	chromatin	5	0.071
<hr/>			
MF	calcium ion binding	30	0.000
MF	extracellular matrix structural constituent	6	0.001
MF	metalloendopeptidase activity	11	0.002
MF	oxidoreductase activity, acting on paired donors, with oxidation of a pair of donors resulting in the reduction of molecular oxygen to two molecules of water	3	0.003
MF	carbohydrate binding	8	0.005
MF	scavenger receptor activity	5	0.021
MF	double-stranded DNA binding	4	0.022
MF	adenylate cyclase activity	3	0.029
MF	long-chain fatty acid-CoA ligase activity	3	0.043
MF	structural constituent of muscle	3	0.058
MF	long-chain-alcohol O-fatty-acyltransferase activity	2	0.060
MF	microtubule motor activity	5	0.066
MF	zinc ion binding	34	0.072
MF	arylsulfatase activity	2	0.089
MF	N-acetylglucosamine-6-sulfatase activity	2	0.089
<hr/>			
KEGG	Protein digestion and absorption	12	0.000
KEGG	Cell cycle	13	0.000
KEGG	PPAR signalling pathway	9	0.000
KEGG	Platelet activation	10	0.005
KEGG	Oocyte meiosis	9	0.005

KEGG	Gap junction	8	0.005
KEGG	Circadian entrainment	8	0.006
KEGG	Starch and sucrose metabolism	5	0.009
KEGG	Oestrogen signalling pathway	8	0.009
KEGG	Glycerolipid metabolism	7	0.010
KEGG	p53 signalling pathway	7	0.010
KEGG	Gastric acid secretion	7	0.010
KEGG	Aldosterone synthesis and secretion	7	0.012
KEGG	Metabolic pathways	45	0.016
KEGG	Salivary secretion	7	0.019
KEGG	Mineral absorption	5	0.020
KEGG	Progesterone-mediated oocyte maturation	7	0.022
KEGG	ECM-receptor interaction	7	0.022
KEGG	Pancreatic secretion	8	0.026
KEGG	Melanogenesis	7	0.032
KEGG	Bile secretion	6	0.032
KEGG	Vascular smooth muscle contraction	8	0.033
KEGG	Oxytocin signalling pathway	9	0.034
KEGG	Biosynthesis of unsaturated fatty acids	4	0.045
KEGG	Fatty acid metabolism	5	0.051
KEGG	Glutamatergic synapse	7	0.052
KEGG	Amoebiasis	7	0.056
KEGG	cAMP signalling pathway	10	0.058
KEGG	GnRH signalling pathway	6	0.059
KEGG	Drug metabolism - other enzymes	5	0.083
KEGG	Retrograde endocannabinoid signalling	6	0.087
KEGG	Dilated cardiomyopathy	6	0.087
KEGG	Adipocytokine signalling pathway	5	0.087
KEGG	Thyroid hormone synthesis	5	0.094
KEGG	Cholinergic synapse	6	0.096

\*Functional analysis was referred to the GO term annotation according to the biological process (BP), cellular component (CC) and molecular function (MF) classification, and the KEGG pathways in which they are involved.



**Supplementary Table S6.** Differentially expressed transcripts of vitrified-transferred animals compared to those naturally-conceived in F1, which are inherited by the vitrified-transferred progeny in the F2 and F3 generations.

DETs inherited by F2	DETs inherited by F3
ENSOCUG0000000109	ENSOCUG0000000092
ENSOCUG0000000197	ENSOCUG0000000215
ENSOCUG0000000215	ENSOCUG0000000266
ENSOCUG0000000313	ENSOCUG0000000580
ENSOCUG0000000580	ENSOCUG0000001185
ENSOCUG0000000856	ENSOCUG0000001754
ENSOCUG0000001171	ENSOCUG0000002462
ENSOCUG0000001375	ENSOCUG0000002542
ENSOCUG0000001376	ENSOCUG0000002624
ENSOCUG0000001627	ENSOCUG0000002702
ENSOCUG0000001652	ENSOCUG0000002956
ENSOCUG0000001673	ENSOCUG0000003030
ENSOCUG0000001863	ENSOCUG0000003091
ENSOCUG0000002000	ENSOCUG0000003246
ENSOCUG0000002703	ENSOCUG0000003724
ENSOCUG0000002707	ENSOCUG0000003858
ENSOCUG0000002814	ENSOCUG0000004004
ENSOCUG0000002858	ENSOCUG0000004047
ENSOCUG0000002878	ENSOCUG0000004275
ENSOCUG0000003203	ENSOCUG0000004343
ENSOCUG0000003217	ENSOCUG0000004480
ENSOCUG0000003246	ENSOCUG0000004632
ENSOCUG0000003467	ENSOCUG0000005159
ENSOCUG0000003649	ENSOCUG0000005521
ENSOCUG0000003876	ENSOCUG0000005830
ENSOCUG0000004393	ENSOCUG0000005885
ENSOCUG0000004485	ENSOCUG0000006350
ENSOCUG0000004492	ENSOCUG0000006597
ENSOCUG0000004632	ENSOCUG0000007151
ENSOCUG0000005032	ENSOCUG0000007327
ENSOCUG0000005159	ENSOCUG0000007759
ENSOCUG0000005465	ENSOCUG0000008236

ENSOCUG00000005540	ENSOCUG00000008303
ENSOCUG00000005820	ENSOCUG00000008329
ENSOCUG00000005900	ENSOCUG00000008571
ENSOCUG00000006009	ENSOCUG00000009195
ENSOCUG00000006357	ENSOCUG00000009332
ENSOCUG00000006490	ENSOCUG00000009528
ENSOCUG00000006801	ENSOCUG00000009532
ENSOCUG00000006962	ENSOCUG00000009543
ENSOCUG00000007172	ENSOCUG00000009725
ENSOCUG00000007516	ENSOCUG00000009932
ENSOCUG00000007555	ENSOCUG00000009993
ENSOCUG00000007759	ENSOCUG00000010144
ENSOCUG00000008179	ENSOCUG00000010184
ENSOCUG00000008329	ENSOCUG00000010637
ENSOCUG00000008478	ENSOCUG00000010814
ENSOCUG00000008841	ENSOCUG00000010941
ENSOCUG00000009260	ENSOCUG00000011025
ENSOCUG00000009725	ENSOCUG00000011195
ENSOCUG00000009880	ENSOCUG00000011350
ENSOCUG00000009993	ENSOCUG00000011488
ENSOCUG00000010299	ENSOCUG00000011956
ENSOCUG00000010708	ENSOCUG00000012148
ENSOCUG00000010814	ENSOCUG00000012372
ENSOCUG00000010975	ENSOCUG00000012902
ENSOCUG00000011025	ENSOCUG00000012939
ENSOCUG00000011201	ENSOCUG00000013140
ENSOCUG00000011298	ENSOCUG00000013226
ENSOCUG00000011340	ENSOCUG00000013412
ENSOCUG00000011488	ENSOCUG00000013609
ENSOCUG00000011634	ENSOCUG00000013757
ENSOCUG00000011656	ENSOCUG00000013934
ENSOCUG00000012071	ENSOCUG00000014077
ENSOCUG00000012148	ENSOCUG00000014204
ENSOCUG00000012452	ENSOCUG00000014498
ENSOCUG00000012831	ENSOCUG00000014857
ENSOCUG00000012902	ENSOCUG00000015111

ENSOCUG00000013074	ENSOCUG00000015313
ENSOCUG00000013111	ENSOCUG00000015329
ENSOCUG00000013160	ENSOCUG00000015483
ENSOCUG00000013414	ENSOCUG00000015664
ENSOCUG00000013478	ENSOCUG00000015787
ENSOCUG00000013544	ENSOCUG00000015803
ENSOCUG00000013643	ENSOCUG00000015893
ENSOCUG00000014077	ENSOCUG00000016193
ENSOCUG00000014801	ENSOCUG00000016347
ENSOCUG00000015483	ENSOCUG00000017347
ENSOCUG00000015664	ENSOCUG00000017620
ENSOCUG00000015667	ENSOCUG00000017803
ENSOCUG00000015681	ENSOCUG00000020947
ENSOCUG00000015803	ENSOCUG00000021508
ENSOCUG00000015924	ENSOCUG00000022280
ENSOCUG00000016303	ENSOCUG00000022308
ENSOCUG00000016347	ENSOCUG00000022392
ENSOCUG00000016496	ENSOCUG00000022543
ENSOCUG00000016718	ENSOCUG00000022883
ENSOCUG00000016815	ENSOCUG00000023285
ENSOCUG00000016909	ENSOCUG00000023455
ENSOCUG00000017043	ENSOCUG00000023547
ENSOCUG00000017102	ENSOCUG00000023778
ENSOCUG00000017136	ENSOCUG00000024091
ENSOCUG00000017197	ENSOCUG00000024196
ENSOCUG00000017516	ENSOCUG00000024492
ENSOCUG00000017689	ENSOCUG00000025107
ENSOCUG00000021126	ENSOCUG00000025241
ENSOCUG00000021209	ENSOCUG00000025501
ENSOCUG00000021411	ENSOCUG00000025698
ENSOCUG00000021423	ENSOCUG00000025809
ENSOCUG00000022047	ENSOCUG00000025901
ENSOCUG00000022434	ENSOCUG00000025992
ENSOCUG00000022543	ENSOCUG00000026203
ENSOCUG00000022659	ENSOCUG00000026303
ENSOCUG00000023005	ENSOCUG00000026482

ENSOCUG00000023455	ENSOCUG00000026551
ENSOCUG00000023796	ENSOCUG00000027492
ENSOCUG00000024019	ENSOCUG00000027755
ENSOCUG00000024465	ENSOCUG00000027771
ENSOCUG00000024506	ENSOCUG00000027844
ENSOCUG00000024939	ENSOCUG00000029029
ENSOCUG00000025107	ENSOCUG00000029066
ENSOCUG00000025132	ENSOCUG00000029235
ENSOCUG00000025236	ENSOCUG00000029412
ENSOCUG00000025273	ENSOCUG00000029465
ENSOCUG00000025494	ENSOCUG00000029599
ENSOCUG00000025657	ENSOCUG00000029634
ENSOCUG00000025868	ENSOCUG00000029690
ENSOCUG00000026783	ENSOCUT00000006764
ENSOCUG00000027184	ENSOCUT00000012795
ENSOCUG00000027359	ENSOCUT00000025404
ENSOCUG00000029056	
ENSOCUG00000029130	
ENSOCUG00000029254	
ENSOCUG00000029301	
ENSOCUG00000029307	
ENSOCUG00000029599	
ENSOCUG00000029623	
ENSOCUT0000002051	
ENSOCUT00000022869	
ENSOCUT00000024066	
ENSOCUT00000025404	
ENSOCUT00000027408	
ENSOCUT00000030408	

---

**Supplementary Table S7.** Functional analysis of differential expressed transcripts inherited by F2 from F1 vitrified-transferred animals, compared to those conceived naturally.

Category*	Term	Count	p-value
BP	fatty acid biosynthetic process	3	0.009
BP	cellular response to DNA damage stimulus	4	0.018
BP	chorionic trophoblast cell differentiation	2	0.038
BP	cell adhesion	4	0.046
BP	cellular response to zinc ion	2	0.053
BP	DNA unwinding involved in DNA replication	2	0.053
BP	cell proliferation	4	0.059
BP	haematopoietic progenitor cell differentiation	3	0.067
BP	mRNA stabilisation	2	0.067
BP	negative regulation of growth	2	0.074
CC	extracellular matrix	4	0.020
CC	perinuclear region of cytoplasm	6	0.066
CC	nuclear chromosome	2	0.073
CC	proteinaceous extracellular matrix	4	0.076
CC	extracellular exosome	21	0.078
MF	oxidoreductase activity, acting on paired donors, with oxidation of a pair of donors resulting in the reduction of molecular oxygen to two molecules of water	3	0.000
MF	zinc ion binding	12	0.045
MF	iron ion binding	4	0.076
KEGG	PPAR signalling pathway	5	0.001
KEGG	Biosynthesis of unsaturated fatty acids	4	0.001
KEGG	Cell cycle	5	0.005
KEGG	AMPK signalling pathway	4	0.028
KEGG	Metabolic pathways	13	0.030
KEGG	Fatty acid metabolism	3	0.035
KEGG	p53 signalling pathway	3	0.057
KEGG	Nitrogen metabolism	2	0.082

\*Functional analysis was referred to the GO term annotation according to the biological process (BP), cellular component (CC) and molecular function (MF) classification, and the KEGG pathways in which they are involved.

**Supplementary Table S8.** Functional analysis of differential expressed transcripts inherited by F3 from F1 vitrified-transferred animals, compared to those conceived naturally.

Category*	Term	Count	p-value
BP	acute-phase response	2	0.087
CC	extracellular matrix	7	0.000
CC	zymogen granule membrane	4	0.000
CC	extracellular exosome	20	0.033
CC	proteinaceous extracellular matrix	4	0.052
CC	anchored component of membrane	2	0.087
MF	carbohydrate binding	4	0.008
MF	glycine binding	2	0.053
KEGG	Circadian entrainment	4	0.007
KEGG	Gap junction	3	0.059
KEGG	Salivary secretion	3	0.059
KEGG	Glutamatergic synapse	3	0.087

\*Functional analysis was referred to the GO term annotation according to the biological process (BP), cellular component (CC) and molecular function (MF) classification, and the KEGG pathways in which they are involved.

**Supplementary Table S9.** Differentially expressed transcripts in liver tissue between vitrified- transferred progeny and that naturally-conceived in F2.

Gene accession	Gene name	Fold Change
ENSOCUG00000012831	insulin like growth factor binding protein 1(IGFBP1)	-6.59
ENSOCUG00000017905	phosphoenolpyruvate carboxykinase 1(PCK1)	-5.47
ENSOCUG00000008474	CD2 molecule(CD2)	-5.19
ENSOCUG00000017694	keratin 23(KRT23)	-4.75
ENSOCUG00000029731	HLA class II histocompatibility antigen. DRB1-4 beta chain(LOC100350168)	-4.56
ENSOCUG00000001327	histamine receptor H4(HRH4)	-4.25
ENSOCUG00000012452	adhesion G protein-coupled receptor F3(ADGRF3)	-4.00
ENSOCUG00000027242	uncharacterised LOC100341342(LOC100341342)	-3.92
ENSOCUG00000012097	Ras and Rab interactor like(RINL)	-3.90
ENSOCUG00000015664	tryptophan hydroxylase 2(TPH2)	-3.68
ENSOCUG00000008210	C-C motif chemokine receptor 9(CCR9)	-3.58
ENSOCUG00000004897	fms related tyrosine kinase 3(FLT3)	-3.57
ENSOCUG00000015667	SH3 domain containing ring finger 2(SH3RF2)	-3.54
ENSOCUG00000029056	C type lectin domain family 17 member A(CLEC17A)	-3.53
ENSOCUG00000029546	lipase family member J(LIPJ)	-3.52
ENSOCUG00000013618	phosphorylase kinase catalytic subunit gamma 1(PHKG1)	-3.49
ENSOCUG00000012752	signal regulatory protein beta 2(SIRPB2)	-3.47
ENSOCUG00000026984	tigger transposable element derived 3(TIGD3)	-3.46
ENSOCUG00000029347	neural retina leucine zipper(NRL)	-3.43
ENSOCUG00000013315	Cbp/p300 interacting transactivator with Glu/Asp rich carboxy-terminal domain 1(CITED1)	-3.37
ENSOCUG00000025132	60S ribosomal protein L23a(LOC108177184)	-3.30
ENSOCUG00000007555	peptidoglycan recognition protein 2(PGLYRP2)	-3.29
ENSOCUG00000008285	neuronal growth regulator 1(NEGR1)	-3.24
ENSOCUG00000024754	G protein subunit alpha transducin 3(GNAT3)	-3.16
ENSOCUG00000006954	perforin 1(PRF1)	-3.12
ENSOCUG00000017113	ankyrin repeat and SOCS box containing 4(ASB4)	-3.08
ENSOCUG00000026162	inhibitor of carbonic anhydrase(LOC100345698)	-3.02
ENSOCUG00000003715	lymphocyte transmembrane adaptor 1(LAX1)	-3.01
ENSOCUG00000008378	dipeptidyl peptidase like 10(DPP10)	-2.99
ENSOCUG00000011825	zinc finger DHHC-type containing 1(ZDHHC1)	-2.99
ENSOCUG00000027044	TNF receptor superfamily member 25(TNFRSF25)	-2.98
ENSOCUG00000011428	coiled-coil domain containing 30(CCDC30)	-2.95
ENSOCUG00000017102	serpin family A member 7(SERPINA7)	-2.94
ENSOCUG00000003403	high affinity immunoglobulin gamma Fc receptor I(LOC100358696)	-2.88
ENSOCUG00000028182	carbonyl reductase [NADPH] 1(LOC100345459)	-2.85
ENSOCUG00000017136	solute carrier family 27 member 6(SLC27A6)	-2.84

ENSOCUG0000000580	cadherin 16(CDH16)	-2.83
ENSOCUG0000000585	aspartoacylase(ASPA)	-2.80
ENSOCUG00000008419	solute carrier family 25 member 30(SLC25A30)	-2.73
ENSOCUG00000029599	killer cell lectin like receptor B1(KLRB1)	-2.70
ENSOCUG00000005940	aryl hydrocarbon receptor nuclear translocator like(ARNTL)	-2.66
ENSOCUG00000026619	myosin VIIB(MYO7B)	-2.65
ENSOCUG00000021209	metallothionein-2D(LOC100343557)	-2.61
ENSOCUG00000007196	chromosome unknown open reading frame. human C1orf127(LOC108176210)	-2.54
ENSOCUG00000013552	potassium calcium-activated channel subfamily N member 3(KCNN3)	-2.54
ENSOCUG00000002000	sarcoglycan delta(SGCD)	-2.51
ENSOCUG00000024883	permeability factor 2(LOC100354804)	-2.49
ENSOCUG00000014365	amyloid P component. serum(APCS)	-2.48
ENSOCUG00000010231	cholinergic receptor nicotinic epsilon subunit(CHRNE)	-2.46
ENSOCUG00000012464	CD6 molecule(CD6)	-2.43
ENSOCUG00000003246	sulfatase 1(SULF1)	-2.36
ENSOCUG00000017821	GATA binding protein 3(GATA3)	-2.36
ENSOCUG00000016751	receptor activity modifying protein 1(RAMP1)	-2.33
ENSOCUG00000015778	solute carrier family 25 member 47(SLC25A47)	-2.32
ENSOCUG00000025273	liver carboxylesterase 2(LOC100343300)	-2.32
ENSOCUG00000015483	fatty acid binding protein 4(FABP4)	-2.29
ENSOCUG00000022630	major intrinsic protein of lens fibre(MIP)	-2.28
ENSOCUG00000004936	neuron navigator 3(NAV3)	-2.27
ENSOCUG00000025663	carnitine O-palmitoyltransferase 1. liver isoform(LOC100350311)	-2.26
ENSOCUG00000005985	clusterin(CLU)	-2.25
ENSOCUG00000006009	acyl-coenzyme A thioesterase 1(LOC100344509)	-2.20
ENSOCUG00000027980	60S ribosomal protein L23a(LOC108176709)	-2.19
ENSOCUG00000005819	tyrosine-protein kinase ZAP-70(LOC100342021)	-2.17
ENSOCUG00000025236	leukocyte protein(LOC100009166)	-2.17
ENSOCUG00000014227	SEC14 like lipid binding 3(SEC14L3)	-2.15
ENSOCUG00000022646	S100 calcium binding protein A12(S100A12)	-2.12
ENSOCUG00000029573	carbonyl reductase [NADPH] 1(LOC100344692)	-2.10
ENSOCUG00000007434	peptidoglycan recognition protein 1(PGLYRP1)	-2.06
ENSOCUG00000021476	S-acyl fatty acid synthase thioesterase. medium chain(LOC100349940)	-2.04
ENSOCUG00000000901	seizure related 6 homolog like 2(SEZ6L2)	-2.04
ENSOCUG00000025590	linker for activation of T-cells(LAT)	-2.04
ENSOCUG000000009725	acyl-CoA wax alcohol acyltransferase 1(AWAT1)	-2.02
ENSOCUG00000004492	potassium voltage-gated channel subfamily Q member 1(KCNQ1)	-2.00
ENSOCUG00000029130	cytochrome P450 2C1(CYP2C1)	-1.95
ENSOCUG00000000313	ovostatin homolog 2(LOC100348825)	-1.93



ENSOCUG00000021126	Metallothionein-2A(LOC100343299)	-1.93
ENSOCUG00000004345	CD79b molecule(CD79B)	-1.92
ENSOCUG00000008793	FK506 binding protein 1B(FKBP1B)	-1.87
ENSOCUG00000008329	ADAM metallopeptidase with thrombospondin type 1 motif 19(ADAMTS19)	-1.84
ENSOCUG00000016772	DNA damage inducible transcript 4(DDIT4)	-1.82
ENSOCUG00000024174	potassium voltage-gated channel subfamily B member 1(KCNB1)	-1.81
ENSOCUG00000024529	solute carrier family 7 member 13(LOC100348219)	-1.81
ENSOCUG00000004307	ephrin A1(EFNA1)	-1.80
ENSOCUG00000015352	energy homeostasis associated(ENHO)	-1.76
ENSOCUG00000017009	junction adhesion molecule like(JAML)	-1.75
ENSOCUG00000011634	sphingomyelin phosphodiesterase 3(SMPD3)	-1.73
ENSOCUG00000005924	solute carrier family 2 member 1(SLC2A1)	-1.71
ENSOCUG00000011201	CYP4B1-like isozyme short form(CYP4B1)	-1.68
ENSOCUG00000009566	S100 calcium binding protein A8(S100A8)	-1.68
ENSOCUG00000024108	potassium voltage-gated channel subfamily C member 3(LOC100338015)	-1.64
ENSOCUG00000014352	glycine amidinotransferase(GATM)	-1.60
ENSOCUG00000005177	flavin containing monooxygenase 2(FMO2)	1.64
ENSOCUG00000001594	solute carrier family 16 member 6(SLC16A6)	1.64
ENSOCUG00000017033	transferrin receptor(TFRC)	1.65
ENSOCUG00000003477	protein phosphatase 1 regulatory subunit 3B(PPP1R3B)	1.65
ENSOCUG00000017852	aquaporin 3 (Gill blood group)(AQP3)	1.67
ENSOCUG00000002965	zinc finger protein 652(ZNF652)	1.67
ENSOCUG00000010715	tubulin gamma complex associated protein 5(TUBGCP5)	1.68
ENSOCUG00000026333	period circadian clock 1(PER1)	1.68
ENSOCUG00000005579	integrin subunit beta 3(ITGB3)	1.68
ENSOCUG00000029430	carbonyl reductase [NADPH] 1(LOC100345202)	1.68
ENSOCUG00000008551	5'-aminolevulinate synthase 1(ALAS1)	1.68
ENSOCUG00000015053	mitogen-activated protein kinase kinase kinase MLT(LOC100351826)	1.70
ENSOCUG00000013478	HtrA serine peptidase 1(HTRA1)	1.70
ENSOCUG00000017924	membrane metalloendopeptidase(MME)	1.71
ENSOCUG00000007955	TEA domain transcription factor 1(TEAD1)	1.72
ENSOCUG00000017626	integrin subunit alpha V(ITGAV)	1.72
ENSOCUG00000014907	WNT inhibitory factor 1(WIF1)	1.73
ENSOCUG00000009279	ATP-binding cassette subfamily A member 1(ABCA1)	1.74
ENSOCUG00000000957	thyroid hormone responsive(THRSP)	1.75
ENSOCUG00000011526	aminoadipate aminotransferase(AADAT)	1.76
ENSOCUG00000017745	DNA polymerase epsilon. catalytic subunit(POLE)	1.76
ENSOCUG00000015924	minichromosome maintenance complex component 2(MCM2)	1.77
ENSOCUG00000002707	MID1 interacting protein 1(MID1IP1)	1.77
ENSOCUG00000029364	inositol hexakisphosphate kinase 3(IP6K3)	1.77

ENSOCUG00000016303	sulfotransferase family. cytosolic. 1C. member 2(SULT1C2)	1.78
ENSOCUG00000013643	PDZ and LIM domain 1(PDLIM1)	1.81
ENSOCUG00000000030	solute carrier family 17 member 5(SLC17A5)	1.81
ENSOCUG00000010299	cysteine and glycine rich protein 1(CSRP1)	1.81
ENSOCUG00000005032	family with sequence similarity 169 member B(FAM169B)	1.81
ENSOCUG00000027187	proteoglycan 4(PRG4)	1.83
ENSOCUG00000003696	pecanex homolog 1 (Drosophila)(PCNX1)	1.83
ENSOCUG00000012344	KH RNA binding domain containing. signal transduction associated 2(KHDRBS2)	1.84
ENSOCUG00000007890	SCO-spondin(SSPO)	1.84
ENSOCUG00000012735	coenzyme Q10B(COQ10B)	1.86
ENSOCUG00000015939	lactate dehydrogenase A(LDHA)	1.88
ENSOCUG00000017197	claudin 6(CLDN6)	1.89
ENSOCUG00000027184	carbonyl reductase 1(CBR1)	1.90
ENSOCUG00000000483	calpain 9(CAPN9)	1.90
ENSOCUG00000004393	synaptotagmin-15(LOC100351528)	1.90
ENSOCUG00000013550	upstream transcription factor family member 3(USF3)	1.90
ENSOCUG00000011308	microtubule associated serine/threonine kinase like(MASTL)	1.90
ENSOCUG00000014944	aldolase. fructose-bisphosphate B(ALDOB)	1.90
ENSOCUG00000014983	PPFIA binding protein 2(PPFIBP2)	1.91
ENSOCUG00000007109	diaphanous related formin 2(DIAPH2)	1.93
ENSOCUG00000010708	kinesin family member C1(KIFC1)	1.93
ENSOCUG00000007887	ATP-binding cassette subfamily C member 5(ABCC5)	1.93
ENSOCUG00000004543	apoptosis inducing factor. mitochondria associated 2(AIFM2)	1.94
ENSOCUG00000010916	sacsin molecular chaperone(SACS)	1.94
ENSOCUG00000005927	acyl-CoA synthetase medium chain family member 5(ACSM5)	1.95
ENSOCUG00000027823	amine sulfotransferase-like(LOC100338493)	1.96
ENSOCUG00000006490	leucine-rich repeat-containing protein 37A2(LOC103346478)	1.96
ENSOCUG00000005415	peroxisomal membrane protein 4(PXMP4)	1.97
ENSOCUG00000024939	interferon-induced protein with tetratricopeptide repeats 2(IFIT2)	1.97
ENSOCUG00000011340	cell division cycle 20(CDC20)	1.97
ENSOCUG00000007432	acetyl-CoA carboxylase beta(ACACB)	1.98
ENSOCUG00000021923	cut like homeobox 2(CUX2)	1.98
ENSOCUG00000001335	myosin IA(MYO1A)	1.98
ENSOCUG00000006357	ADAM metallopeptidase with thrombospondin type 1 motif 12(ADAMTS12)	1.99
ENSOCUG00000007844	SOS Ras/Rac guanine nucleotide exchange factor 1(SOS1)	1.99
ENSOCUG00000008478	syntaxin binding protein 4(STXBP4)	2.00
ENSOCUG00000004231	BTB domain and CNC homolog 2(BACH2)	2.01
ENSOCUG00000005912	1.4-alpha-glucan branching enzyme 1(GBE1)	2.01
ENSOCUG00000027006	UDP-glucuronosyltransferase 2B16-like(LOC100340258)	2.03
ENSOCUG00000024065	nuclear prelamin A recognition factor(NARF)	2.04
ENSOCUG00000017689	keratin 20(KRT20)	2.04

ENSOCUG00000017427	3-hydroxy-3-methylglutaryl-CoA reductase(HMGCR)	2.04
ENSOCUG00000002814	topoisomerase (DNA) II alpha(TOP2A)	2.04
ENSOCUG00000006386	ATPase phospholipid transporting 10A (putative)(ATP10A)	2.05
ENSOCUG00000007382	inhibin beta E subunit(INHBE)	2.06
ENSOCUG00000003203	TPX2. microtubule nucleation factor(TPX2)	2.06
ENSOCUG00000016909	RAD51 recombinase(RAD51)	2.07
ENSOCUG00000013212	ATP citrate lyase(ACLY)	2.08
ENSOCUG00000003071	lipin 1(LPIN1)	2.08
ENSOCUG00000008872	alanyl-tRNA synthetase(AARS)	2.09
ENSOCUG00000014077	latent transforming growth factor beta binding protein 2(LTBP2)	2.09
ENSOCUG00000022715	zinc finger homeobox 2(ZFHX2)	2.12
ENSOCUG00000022885	cytochrome c oxidase subunit 6C(LOC100352363)	2.12
ENSOCUG00000002297	uncoupling protein 1(UCP1)	2.12
ENSOCUG00000014801	acyl-CoA desaturase(LOC100346561)	2.13
ENSOCUG00000000109	ADAM metallopeptidase with thrombospondin type 1 motif 9(ADAMTS9)	2.14
ENSOCUG00000009367	SET domain containing lysine methyltransferase 7(SETD7)	2.14
ENSOCUG00000017118	adiponectin receptor 2(ADIPOR2)	2.14
ENSOCUG00000007182	growth arrest specific 2 like 3(GAS2L3)	2.15
ENSOCUG00000005820	ribonucleotide reductase regulatory subunit M2(RRM2)	2.17
ENSOCUG00000006877	transcription factor CP2 like 1(TFCP2L1)	2.21
ENSOCUG00000001375	acyl-CoA desaturase(LOC100346046)	2.21
ENSOCUG00000013772	tubulin delta 1(TUBD1)	2.23
ENSOCUG00000013111	procollagen C-endopeptidase enhancer 2(PCOLCE2)	2.26
ENSOCUG00000007516	6-phosphofructo-2-kinase/fructose-2,6-biphosphatase 3(PFKFB3)	2.29
ENSOCUG00000013474	calcium voltage-gated channel subunit alpha1 D(CACNA1D)	2.29
ENSOCUG00000012071	glycerol-3-phosphate acyltransferase 3(GPAT3)	2.30
ENSOCUG00000012148	inositol 1,4,5-trisphosphate receptor type 1(ITPR1)	2.30
ENSOCUG00000016347	phosphoethanolamine/phosphocholine phosphatase(PHOSPHO1)	2.31
ENSOCUG00000007172	acyl-CoA desaturase(LOC100357419)	2.32
ENSOCUG00000001171	NUF2. NDC80 kinetochore complex component(NUF2)	2.32
ENSOCUG00000007690	zinc finger CCCH-type containing 12D(ZC3H12D)	2.32
ENSOCUG00000012902	glutathione S-transferase Yc(LOC100353428)	2.33
ENSOCUG00000013740	phosphoglucomutase 2(PGM2)	2.34
ENSOCUG00000024465	collagen type VIII alpha 1 chain(COL8A1)	2.35
ENSOCUG00000011953	centromere protein I(CENPI)	2.35
ENSOCUG00000026935	GULP. engulfment adaptor PTB domain containing 1(GULP1)	2.35
ENSOCUG00000007701	KN motif and ankyrin repeat domains 4(KANK4)	2.36
ENSOCUG00000013414	RasGEF domain family member 1C(RASGEF1C)	2.37
ENSOCUG00000005208	methylenetetrahydrofolate dehydrogenase (NADP+ dependent) 2. methenyltetrahydrofolate cyclohydrolase(MTHFD2)	2.37

ENSOCUG00000015780	transcobalamin 1(TCN1)	2.38
ENSOCUG00000003467	prostate stem cell antigen(PSCA)	2.38
ENSOCUG00000017133	glycerophosphodiester phosphodiesterase domain containing 2(GDPD2)	2.40
ENSOCUG00000013807	sperm associated antigen 5(SPAG5)	2.42
ENSOCUG00000008316	striatin interacting protein 2(STRIP2)	2.42
ENSOCUG00000008179	rhomboid like 3(RHBDL3)	2.42
ENSOCUG00000007893	glycerol-3-phosphate acyltransferase. mitochondrial(GPAM)	2.43
ENSOCUG00000005956	aldehyde dehydrogenase 18 family member A1(ALDH18A1)	2.44
ENSOCUG00000015681	Rac GTPase activating protein 1(RACGAP1)	2.44
ENSOCUG00000027359	tetraspanin 11(TSPAN11)	2.45
ENSOCUG00000012480	bestrophin 4(BEST4)	2.50
ENSOCUG00000005900	fibulin 2(FBLN2)	2.54
ENSOCUG00000010012	adenylate kinase 4(AK4)	2.57
ENSOCUG00000003768	leukaemia inhibitory factor(LIF)	2.59
ENSOCUG00000011000	growth arrest specific 7(GAS7)	2.61
ENSOCUG00000022434	cell division cycle associated 3(CDCA3)	2.62
ENSOCUG00000006777	family with sequence similarity 102 member B(FAM102B)	2.62
ENSOCUG00000014453	acetyl-CoA carboxylase alpha(ACACA)	2.68
ENSOCUG00000009379	MIS18 kinetochore protein A(MIS18A)	2.70
ENSOCUG00000011957	aurora kinase B(AURKB)	2.71
ENSOCUG00000013069	ELOVL fatty acid elongase 6(ELOVL6)	2.72
ENSOCUG00000014969	pyruvate kinase. liver and RBC(PKLR)	2.72
ENSOCUG00000008841	glutamate-ammonia ligase(GLUL)	2.72
ENSOCUG00000004106	glycine decarboxylase(GLDC)	2.74
ENSOCUG00000010776	Fanconi anaemia complementation group B(FANCB)	2.77
ENSOCUG00000000215	period circadian clock 2(PER2)	2.77
ENSOCUG00000022945	asparagine synthetase (glutamine-hydrolysing)(ASNS)	2.80
ENSOCUG00000022659	EF-hand and coiled-coil domain containing 1(EFCC1)	2.80
ENSOCUG00000013819	ribosomal protein S6 kinase like 1(RPS6KL1)	2.87
ENSOCUG00000023520	fibronectin leucine-rich transmembrane protein 1(FLRT1)	2.91
ENSOCUG00000029751	transmembrane 9 superfamily member 2(LOC100353059)	2.92
ENSOCUG00000002703	forkhead box M1(FOXM1)	2.96
ENSOCUG00000007124	TTK protein kinase(TTK)	3.03
ENSOCUG00000029228	leucine-rich repeat containing 19(LRRC19)	3.04
ENSOCUG00000009736	neurotrophic receptor tyrosine kinase 2(NTRK2)	3.04
ENSOCUG00000007213	high mobility group box 4(HMGB4)	3.05
ENSOCUG00000006288	ninein like(NINL)	3.07
ENSOCUG00000004232	zinc finger and BTB domain containing 20(ZBTB20)	3.08
ENSOCUG00000003048	tubulin polymerisation promoting protein(TPPP)	3.09
ENSOCUG00000013321	retinoic acid early transcript 1E(RAET1E)	3.14
ENSOCUG00000006801	minichromosome maintenance 10 replication initiation factor(MCM10)	3.16
ENSOCUG00000000856	E2F transcription factor 1(E2F1)	3.23

ENSOCUG00000011488	Fanconi anaemia complementation group I(FANCI)	3.23
ENSOCUG00000003876	FH2 domain containing 1(FHDC1)	3.23
ENSOCUG00000007759	ubiquitin specific peptidase 2(USP2)	3.23
ENSOCUG00000002858	cyclin dependent kinase 1(CDK1)	3.24
ENSOCUG00000015803	tubulointerstitial nephritis antigen(TINAG)	3.30
ENSOCUG00000016718	mesenteric oestrogen dependent adipogenesis(MEDAG)	3.32
ENSOCUG00000013508	interleukin 17 receptor B(IL17RB)	3.32
ENSOCUG00000029623	ATPase plasma membrane Ca <sup>2+</sup> transporting 3(ATP2B3)	3.37
ENSOCUG00000026022	derlin 3(DERL3)	3.40
ENSOCUG00000022047	MPV17 mitochondrial inner membrane protein like(MPV17L)	3.40
ENSOCUG00000025868	gamma-aminobutyric acid type A receptor delta subunit(GABRD)	3.41
ENSOCUG00000005465	nocturnin(NOCT)	3.45
ENSOCUG00000029254	family with sequence similarity 159 member A(FAM159A)	3.45
ENSOCUG00000011025	contactin 4(CNTN4)	3.48
ENSOCUG00000016815	islet cell autoantigen 1(ICA1)	3.53
ENSOCUG00000004932	E2F transcription factor 7(E2F7)	3.61
ENSOCUG00000001673	triokinase and FMN cyclase(TKFC)	3.68
ENSOCUG00000009260	phospholipase C eta 1(PLCH1)	3.73
ENSOCUG00000001652	cyclin B2(CCNB2)	3.74
ENSOCUG00000011124	fibroblast growth factor 18(FGF18)	3.78
ENSOCUG00000009071	kinesin family member 24(KIF24)	3.79
ENSOCUG00000011656	actin like 7A(ACTL7A)	3.94
ENSOCUG00000001129	solute carrier family 26 member 3(SLC26A3)	3.98
ENSOCUG00000004485	E2F transcription factor 8(E2F8)	4.17
ENSOCUG00000003649	transmembrane and immunoglobulin domain containing 1(TMIGD1)	4.21
ENSOCUG00000006962	aldehyde dehydrogenase 1 family member L2(ALDH1L2)	4.25
ENSOCUG00000021411	tsukushi. small leucine-rich proteoglycan(TSKU)	4.28
ENSOCUG00000007427	FAT atypical cadherin 3(FAT3)	4.39
ENSOCUG00000013792	kinetochore associated 1(KNTC1)	4.40
ENSOCUG00000001627	solute carrier family 6 member 11(SLC6A11)	4.45
ENSOCUG00000000144	calcium voltage-gated channel auxiliary subunit beta 4(CACNB4)	4.50
ENSOCUG00000025494	secretogranin III(SCG3)	4.81
ENSOCUG00000009557	polypeptide N-acetylgalactosaminyltransferase 8(GALNT8)	4.82
ENSOCUG00000009880	dual specificity phosphatase 14(DUSP14)	4.95
ENSOCUG00000027371	kinesin family member 2C(KIF2C)	4.98
ENSOCUG00000010814	malic enzyme 1(ME1)	5.02
ENSOCUG00000017054	testis expressed 33(TEX33)	5.19
ENSOCUG00000017043	cell division cycle associated 8(CDCA8)	5.19
ENSOCUG00000013544	ATPase H <sup>+</sup> transporting V0 subunit a4(ATP6V0A4)	6.00
ENSOCUG00000001376	sodium channel protein type 11 subunit alpha(LOC100349709)	7.15
ENSOCUG00000006498	desmoglein 1(DSG1)	< -0.01

ENSOCUG00000015925	TNF receptor superfamily member 8(TNFRSF8)	< -0.02
ENSOCUG00000016573	carboxypeptidase. vitellogenic like(CPVL)	< -0.02
ENSOCUG00000029301	zinc finger and SCAN domain containing 23(ZSCAN23)	< -0.02
ENSOCUG00000004632	carbonic anhydrase 12(CA12)	< -0.03
ENSOCUG00000005540	calpain 6(CAPN6)	< -0.03
ENSOCUG00000010540	cyclic nucleotide gated channel beta 1(CNGB1)	< -0.03
ENSOCUG00000012845	SERTA domain containing 4(SERTAD4)	< -0.03
ENSOCUG00000016508	solute carrier family 12 member 1(SLC12A1)	< -0.03
ENSOCUG00000023218	left-right determination factor 2(LOC100101568)	< -0.03
ENSOCUG00000012514	X-ray radiation resistance associated 1(XRRA1)	< -0.04
ENSOCUG00000001190	GDNF family receptor alpha 2(GFRA2)	< -0.05
ENSOCUG00000002522	prostaglandin F receptor(PTGFR)	< -0.05
ENSOCUG00000003021	ceramide kinase like(CERKL)	< -0.05
ENSOCUG00000026570	zinc finger protein 296(ZNF296)	< -0.06
ENSOCUG00000014051	interleukin 17 receptor D(IL17RD)	< -0.07
ENSOCUG00000000771	C-C motif chemokine 3-like 1(LOC100348776)	< -0.08
ENSOCUG00000023796	lactotransferrin(LTF)	< -0.08
ENSOCUG00000013086	cytotoxic and regulatory T cell molecule(CRTAM)	< -0.09
ENSOCUG00000004825	dopamine receptor D1(DRD1)	< -0.10
ENSOCUG00000023342	reticulon 2(RTN2)	< -0.10
ENSOCUG00000005968	purinergic receptor P2Y8(P2RY8)	< -0.11
ENSOCUG00000022151	doublecortin domain containing 2B(DCDC2B)	< -0.11
ENSOCUG00000006864	T cell surface glycoprotein CD3 epsilon chain(LOC100339529)	< -0.12
ENSOCUG00000015699	acid sensing ion channel subunit 1(ASIC1)	< -0.13
ENSOCUG00000014788	tudor domain containing 9(TDRD9)	< -0.17
ENSOCUG00000009994	transmembrane 6 superfamily member 1(TM6SF1)	< -0.19
ENSOCUG00000015805	NADPH oxidase 5(NOX5)	< -0.19
ENSOCUG00000025107	membrane associated ring-CH-type finger 4(MARCH4)	< -0.19
ENSOCUG00000021259	coiled-coil domain containing 74B(CCDC74B)	< -0.20
ENSOCUG00000001717	src kinase associated phosphoprotein 1(SKAP1)	< -0.21
ENSOCUG00000027509	C-X3-C motif chemokine receptor 1(CX3CR1)	< -0.21
ENSOCUG00000001863	vesicle amine transport 1 like(VAT1L)	< -0.22
ENSOCUG00000002937	ankyrin repeat and death domain containing 1B(ANKDD1B)	< -0.25
ENSOCUG00000027321	proline-serine-threonine phosphatase interacting protein 1(PSTPIP1)	< -0.31
ENSOCUG00000022335	defensin NP-3a(LOC100009134)	< -0.60
ENSOCUG00000016243	metallothionein 3(MT3)	< -0.97
ENSOCUG00000004688	polycystic kidney and hepatic disease 1 (autosomal recessive)-like 1(PKHD1L1)	> 0.00
ENSOCUG00000011128	GLI family zinc finger 1(GLI1)	> 0.02
ENSOCUG00000000953	RecQ mediated genome instability 2(RMI2)	> 0.04
ENSOCUG00000005159	anillin actin binding protein(ANLN)	> 0.04
ENSOCUG00000006290	leucine-rich repeat and fibronectin type III domain-containing protein 5(LOC100349270)	> 0.04

ENSOCUG00000001617	myotubularin related protein 8(MTMR8)	> 0.05
ENSOCUG00000004633	prostaglandin-E receptor 3(PTGER3)	> 0.07
ENSOCUG00000011298	family with sequence similarity 83 member D(FAM83D)	> 0.07
ENSOCUG00000004978	cartilage acidic protein 1(CRTAC1)	> 0.08
ENSOCUG00000022194	family with sequence similarity 72 member A(FAM72A)	> 0.08
ENSOCUG00000029469	phosphatidylinositol 3.4.5-trisphosphate 3-phosphatase TPTE2(LOC100346342)	> 0.08
ENSOCUG00000015149	thrombospondin type laminin G domain and EAR repeats(TSPEAR)	> 0.09
ENSOCUG00000015368	family with sequence similarity 83 member A(FAM83A)	> 0.09
ENSOCUG00000016102	allantoicase(ALLC)	> 0.09
ENSOCUG00000001278	inturned planar cell polarity protein(INTU)	> 0.11
ENSOCUG00000015283	chromosome 9 open reading frame. human C18orf54(C9H18orf54)	> 0.11
ENSOCUG00000006484	kinesin family member 27(KIF27)	> 0.12
ENSOCUG00000002926	DLG associated protein 5(DLGAP5)	> 0.13
ENSOCUG00000000197	hexokinase 2(HK2)	> 0.15
ENSOCUG00000010181	Rho guanine nucleotide exchange factor 39(ARHGEF39)	> 0.16
ENSOCUG00000010249	ubiquitin conjugating enzyme E2 T(UBE2T)	> 0.17
ENSOCUG00000029613	zymogen granule membrane protein 16-like(LOC100358477)	> 0.22
ENSOCUG00000002878	SLX4 interacting protein(SLX4IP)	> 0.23
ENSOCUG00000009066	sterile alpha motif domain containing 12(SAMD12)	> 0.25
ENSOCUG00000009652	family with sequence similarity 229 member B(FAM229B)	> 0.28
ENSOCUG00000023005	zinc finger protein 367(ZNF367)	> 0.46
ENSOCUG00000010723	solute carrier family 51 beta subunit(SLC51B)	> 0.53
ENSOCUG00000010762	ChaC glutathione specific gamma-glutamylcyclotransferase 1(CHAC1)	> 0.58

---

**Supplementary Table S10.** Functional analysis of the differentially expressed transcripts in liver tissue between vitrified- transferred progeny and that naturally-conceived in F2.

Category*	Term	Count	p-value
BP	fatty acid biosynthetic process	5	0.00099
BP	chorionic trophoblast cell differentiation	3	0.0056
BP	biosynthetic process	4	0.01
BP	phagocytosis. engulfment	3	0.015
BP	triglyceride biosynthetic process	3	0.015
BP	trophoblast giant cell differentiation	3	0.023
BP	positive regulation of inflammatory response	4	0.027
BP	positive regulation of osteoblast proliferation	3	0.028
BP	positive regulation of tumour necrosis factor production	4	0.03
BP	astrocyte development	3	0.039
BP	positive regulation of DNA endoreduplication	2	0.048
BP	negative regulation of natural killer cell differentiation involved in immune response	2	0.048
BP	growth of symbiont in host	2	0.048
BP	immune response	8	0.05
BP	negative regulation of interferon gamma production	3	0.057
BP	circadian regulation of gene expression	4	0.064
BP	acetyl-CoA metabolic process	2	0.071
BP	negative regulation of transcription involved in G1/S transition of mitotic cell cycle	2	0.071
BP	aortic valve morphogenesis	2	0.071
BP	regulation of glucose import	2	0.071
BP	positive regulation of interleukin-5 secretion	2	0.094
BP	regulation of hair cycle	2	0.094
BP	hepatocyte differentiation	2	0.094
BP	peptidoglycan catabolic process	2	0.094
BP	mitotic spindle midzone assembly	2	0.094
BP	detection of bacterium	2	0.094
BP	signalling	2	0.094
BP	positive regulation of interleukin-13 secretion	2	0.094
BP	cellular response to DNA damage stimulus	5	0.098
CC	cell-cell junction	7	0.018
CC	T cell receptor complex	3	0.019
CC	extracellular matrix	6	0.026
CC	extracellular exosome	54	0.043
CC	chromosome passenger complex	2	0.065
CC	external side of plasma membrane	7	0.093
CC	mitochondrial membrane	3	0.098
MF	oxidoreductase activity. acting on paired donors. with oxidation of a pair of donors resulting in the reduction of molecular oxygen to two molecules of water	3	0.0014
MF	drug binding	4	0.029
MF	ATP-binding	33	0.041



MF	N-acetylmuramoyl-L-alanine amidase activity	2	0.043
MF	acetyl-CoA carboxylase activity	2	0.043
MF	peptidoglycan receptor activity	2	0.043
MF	hydrolase activity. acting on ester bonds	3	0.046
MF	calcium ion binding	16	0.066
MF	E-box binding	3	0.082
MF	glycerol-3-phosphate O-acyltransferase activity	2	0.084
MF	biotin carboxylase activity	2	0.084
MF	microtubule motor activity	4	0.095
<hr/>			
KEGG	Metabolic pathways	45	0.00016
KEGG	PPAR signalling pathway	8	0.00058
KEGG	Pyruvate metabolism	6	0.0022
KEGG	Glucagon signalling pathway	8	0.0033
KEGG	AMPK signalling pathway	9	0.0035
KEGG	Biosynthesis of unsaturated fatty acids	5	0.0037
KEGG	Fatty acid metabolism	6	0.0052
KEGG	Glycolysis / Gluconeogenesis	6	0.012
KEGG	Biosynthesis of antibiotics	11	0.018
KEGG	Insulin signalling pathway	8	0.018
KEGG	Haematopoietic cell lineage	6	0.02
KEGG	Fanconi anaemia pathway	5	0.02
KEGG	Fatty acid biosynthesis	3	0.023
KEGG	Metabolism of xenobiotics by cytochrome P450	6	0.036
KEGG	Adipocytokine signalling pathway	5	0.046
KEGG	Arrhythmogenic right ventricular cardiomyopathy (ARVC)	5	0.05
KEGG	Mineral absorption	4	0.052
KEGG	Insulin resistance	6	0.063
KEGG	Chemical carcinogenesis	6	0.063
KEGG	Carbon metabolism	6	0.1

\*Functional analysis was referred to the GO term annotation according to the biological process (BP), cellular component (CC) and molecular function (MF) classification, and the KEGG pathways in which they are involved.

**Supplementary Table S11.** Differentially expressed transcripts in liver tissue between vitrified-transferred progeny and that naturally-conceived in F3.

Gene accession	Gene name	Fold change
ENSOCUG00000014290	dual oxidase maturation factor 2(LOC100355642)	-5.06
ENSOCUG00000001277	N-terminal EF-hand calcium binding protein 1(NECAB1)	-4.70
ENSOCUG00000009306	La ribonucleoprotein domain family member 6(LARP6)	-4.48
ENSOCUG00000007726	ST6 beta-galactoside alpha-2.6-sialyltransferase 2(ST6GAL2)	-4.29
ENSOCUG00000000144	calcium voltage-gated channel auxiliary subunit beta 4(CACNB4)	-4.26
ENSOCUG00000000658	bone morphogenetic protein 3(BMP3)	-4.23
ENSOCUG00000009399	carbonic anhydrase 4(CA4)	-4.22
ENSOCUG00000009494	casein beta(CSN2)	-4.19
ENSOCUG00000017347	leptin receptor(LEPR)	-4.08
ENSOCUG00000000706	formin homology 2 domain containing 3(FHOD3)	-4.07
ENSOCUG00000015552	plexin A4(PLXNA4)	-4.06
ENSOCUG00000015764	cyclin dependent kinase like 3(CDKL3)	-3.97
ENSOCUG00000013140	calmodulin binding transcription activator 1(CAMTA1)	-3.93
ENSOCUG00000000370	ADAM metallopeptidase with thrombospondin type 1 motif 8(ADAMTS8)	-3.87
ENSOCUG00000001033	opioid receptor delta 1(OPRD1)	-3.86
ENSOCUG00000012661	protein tyrosine phosphatase. receptor type U(PTPRU)	-3.83
ENSOCUG00000016712	delta/notch like EGF repeat containing(DNER)	-3.79
ENSOCUG00000012685	paired like homeodomain 2(PITX2)	-3.77
ENSOCUG00000006833	dynein axonemal heavy chain 12(DNAH12)	-3.76
ENSOCUG00000023975	butyrophilin subfamily 1 member A1-like(LOC100351205)	-3.71
ENSOCUG00000000948	gamma-aminobutyric acid type A receptor rho1 subunit(GABRR1)	-3.70
ENSOCUG00000017171	fibroblast growth factor 21(FGF21)	-3.65
ENSOCUG00000008297	proteoglycan 2. pro eosinophil major basic protein(PRG2)	-3.59
ENSOCUG00000014727	actin like 6B(ACTL6B)	-3.56
ENSOCUG00000024982	butyrophilin-like protein 1(LOC100009510)	-3.53
ENSOCUG00000009285	chromosome 1 open reading frame. human C11orf53(C1H11orf53)	-3.52
ENSOCUG00000015664	tryptophan hydroxylase 2(TPH2)	-3.51
ENSOCUG00000027714	solute carrier family 23 member 1(LOC100342535)	-3.50
ENSOCUG00000014660	connector enhancer of kinase suppressor of Ras 2(CNKSR2)	-3.49
ENSOCUG00000023263	NDUFA4. mitochondrial complex associated like 2(NDUFA4L2)	-3.42
ENSOCUG00000004632	carbonic anhydrase 12(CA12)	-3.40
ENSOCUG00000005134	kinocilin(KNCN)	-3.34
ENSOCUG00000008047	von Willebrand factor A domain containing 3A(VWA3A)	-3.34
ENSOCUG00000010733	cystic fibrosis transmembrane conductance regulator(CFTR)	-3.28
ENSOCUG00000000612	CD101 molecule(CD101)	-3.22

ENSOCUG00000014767	phosphoprotein membrane anchor with glycosphingolipid microdomains 1(PAG1)	-3.21
ENSOCUG00000009532	AF4/FMR2 family member 3(AFF3)	-3.20
ENSOCUG00000001788	RAS guanyl releasing protein 1(RASGRP1)	-3.18
ENSOCUG00000003735	hydroxycarboxylic acid receptor 1(HCAR1)	-3.16
ENSOCUG00000006107	GRAM domain containing 2(GRAMD2)	-3.16
ENSOCUG000000010199	oncostatin M(OSM)	-3.15
ENSOCUG000000008771	interleukin 1 alpha(IL1A)	-3.13
ENSOCUG00000007124	TTK protein kinase(TTK)	-3.11
ENSOCUG00000003013	ADP ribosylation factor like GTPase 11(ARL11)	-3.11
ENSOCUG000000017852	aquaporin 3 (Gill blood group)(AQP3)	-3.06
ENSOCUG000000026551	lysophosphatidic acid receptor 5(LPAR5)	-3.05
ENSOCUG000000029634	arachidonate lipoxygenase 3(ALOXE3)	-3.01
ENSOCUG000000000092	serpin family F member 1(SERPINF1)	-2.97
ENSOCUG000000015893	proprotein convertase subtilisin/kexin type 2(PCSK2)	-2.95
ENSOCUG000000025837	NFAT activating protein with ITAM motif 1(NFAM1)	-2.93
ENSOCUG000000015699	acid sensing ion channel subunit 1(ASIC1)	-2.91
ENSOCUG000000011279	membrane associated ring-CH-type finger 1(MARCH1)	-2.90
ENSOCUG000000008082	GTPase activating Rap/RanGAP domain like 3(GARNL3)	-2.90
ENSOCUG000000025842	chromosome 19 open reading frame. human C17orf97(C19H17orf97)	-2.88
ENSOCUG000000012963	suppressor of cancer cell invasion(SCAI)	-2.87
ENSOCUG000000000877	mast cell expressed membrane protein 1(MCEMP1)	-2.85
ENSOCUG000000005959	arachidonate 12-lipoxygenase. 12R type(ALOX12B)	-2.85
ENSOCUG000000016029	IQ motif containing D(IQCD)	-2.83
ENSOCUG000000025779	C-C motif chemokine receptor 6(CCR6)	-2.82
ENSOCUG000000024244	C-C motif chemokine receptor 4(CCR4)	-2.80
ENSOCUG000000001355	IKAROS family zinc finger 3(IKZF3)	-2.78
ENSOCUG000000001103	caspase 1(CASP1)	-2.77
ENSOCUG000000008303	matrix metalloproteinase 12(MMP12)	-2.77
ENSOCUG000000021508	chromosome 16 open reading frame. human C1orf106(C16H1orf106)	-2.75
ENSOCUG000000026482	UDP-glucuronosyltransferase 2B16-like(LOC100340513)	-2.75
ENSOCUG000000007438	complement C3a receptor 1(C3AR1)	-2.74
ENSOCUG000000013226	BLK proto-oncogene. Src family tyrosine kinase(BLK)	-2.74
ENSOCUG000000015787	beaded filament structural protein 1(BFSP1)	-2.73
ENSOCUG000000006204	ubiquitin associated and SH3 domain containing A(UBASH3A)	-2.73
ENSOCUG000000005159	anillin actin binding protein(ANLN)	-2.72
ENSOCUG000000010247	ATPase H+ transporting V0 subunit d2(ATP6V0D2)	-2.72
ENSOCUG000000014255	dual oxidase 2(DUOX2)	-2.71
ENSOCUG000000003578	anterior gradient 2. protein disulphide isomerase family member(AGR2)	-2.65
ENSOCUG000000028024	immunity related GTPase M(IRGM)	-2.65
ENSOCUG000000013081	angiopoietin like 7(ANGPTL7)	-2.65

ENSOCUG00000016948	solute carrier organic anion transporter family member 4C1(SLCO4C1)	-2.64
ENSOCUG00000007151	cilia and flagella associated protein 70(CFAP70)	-2.63
ENSOCUG000000027925	leukocyte immunoglobulin-like receptor subfamily A member 2(LOC100347041)	-2.63
ENSOCUG000000025839	retinol dehydrogenase 5(RDH5)	-2.61
ENSOCUG00000008131	tripartite motif containing 62(TRIM62)	-2.59
ENSOCUG00000004961	CUGBP. Elav-like family member 2(CELF2)	-2.57
ENSOCUG00000002622	keratin 75(KRT75)	-2.56
ENSOCUG000000027244	uncharacterised LOC100347962(LOC100347962)	-2.56
ENSOCUG000000003970	transgelin 3(TAGLN3)	-2.55
ENSOCUG000000002486	collagen type VI alpha 6 chain(COL6A6)	-2.55
ENSOCUG000000016613	ring finger protein 222(RNF222)	-2.54
ENSOCUG000000009113	phosphodiesterase 1C(PDE1C)	-2.53
ENSOCUG000000004874	BTB/POZ domain-containing protein KCTD12(LOC100347604)	-2.50
ENSOCUG000000013273	membrane spanning 4-domains A15(MS4A15)	-2.50
ENSOCUG000000005107	HOP homeobox(HOPX)	-2.48
ENSOCUG000000003156	chromosome 1 open reading frame. human C11orf16(C1H11orf16)	-2.47
ENSOCUG000000006958	transmembrane protein 173(TMEM173)	-2.46
ENSOCUG000000009528	intestinal-type alkaline phosphatase-like(LOC100352107)	-2.46
ENSOCUG000000022422	colorectal cancer associated 2(COLCA2)	-2.45
ENSOCUG000000022151	doublecortin domain containing 2B(DCDC2B)	-2.44
ENSOCUG000000021559	alkaline ceramidase 3(ACER3)	-2.42
ENSOCUG000000007566	actin. alpha 1. skeletal muscle(ACTA1)	-2.41
ENSOCUG000000016789	DENN domain containing 2C(DENND2C)	-2.41
ENSOCUG000000016508	solute carrier family 12 member 1(SLC12A1)	-2.40
ENSOCUG000000024433	Fc fragment of IgE receptor II(FCER2)	-2.40
ENSOCUG000000009077	membrane spanning 4-domains A2(MS4A2)	-2.38
ENSOCUG000000000962	origin recognition complex subunit 1(ORC1)	-2.38
ENSOCUG000000003665	C-C motif chemokine receptor 5(CCR5)	-2.36
ENSOCUG000000017547	calcium voltage-gated channel subunit alpha1 E(CACNA1E)	-2.36
ENSOCUG000000017805	caprin family member 2(CAPRIN2)	-2.36
ENSOCUG000000025413	cytohesin 4(CYTH4)	-2.35
ENSOCUG000000008543	tenascin N(TNN)	-2.34
ENSOCUG000000007053	steroid 21-hydroxylase(LOC100342636)	-2.33
ENSOCUG000000027044	TNF receptor superfamily member 25(TNFRSF25)	-2.33
ENSOCUG000000021441	natural killer cell granule protein 7(NKG7)	-2.31
ENSOCUG000000010618	ankyrin 2(ANK2)	-2.31
ENSOCUG000000015057	macrophage expressed 1(MPEG1)	-2.31
ENSOCUG000000010753	G protein-coupled receptor 84(GPR84)	-2.30
ENSOCUG000000011023	nebulin related anchoring protein(NRAP)	-2.30
ENSOCUG000000023473	guanylate-binding protein 5(LOC100346209)	-2.30
ENSOCUG000000010544	carnitine O-octanoyltransferase(CROT)	-2.29

ENSOCUG00000008553	prune homolog 2(PRUNE2)	-2.28
ENSOCUG00000008666	Ras-related GTP-binding B(RRAGB)	-2.28
ENSOCUG00000000804	secernin 1(SCRN1)	-2.27
ENSOCUG00000001824	toll-like receptor 1(TLR1)	-2.27
ENSOCUG00000017422	integrin subunit alpha X(ITGAX)	-2.27
ENSOCUG00000013948	Rho GTPase activating protein 20(ARHGAP20)	-2.24
ENSOCUG00000009313	chromosome 4 open reading frame. human C20orf196(C4H20orf196)	-2.24
ENSOCUG00000002805	adenosine monophosphate deaminase 3(AMPD3)	-2.24
ENSOCUG00000009395	contactin 1(CNTN1)	-2.24
ENSOCUG00000013757	solute carrier family 13 member 2(SLC13A2)	-2.23
ENSOCUG00000029253	guanylate-binding protein 4(LOC100346726)	-2.22
ENSOCUG00000002966	transcriptional repressor GATA binding 1(TRPS1)	-2.22
ENSOCUG00000015673	zona pellucida glycoprotein 1(ZP1)	-2.22
ENSOCUG00000010984	HLA class I histocompatibility antigen. A-36 alpha chain(LOC100355380)	-2.20
ENSOCUG00000022093	aggrecan(ACAN)	-2.20
ENSOCUG00000003215	sprouty RTK signalling antagonist 4(SPRY4)	-2.20
ENSOCUG00000007196	chromosome unknown open reading frame. human C1orf127(LOC108176210)	-2.20
ENSOCUG00000002956	copine 4(CPNE4)	-2.18
ENSOCUG00000008294	uropodin 1B(UPK1B)	-2.18
ENSOCUG00000001617	myotubularin related protein 8(MTMR8)	-2.17
ENSOCUG00000017568	pyrimidinergic receptor P2Y6(P2RY6)	-2.16
ENSOCUG00000022761	interleukin 3 receptor subunit alpha(IL3RA)	-2.16
ENSOCUG00000007669	myosin VA(MYO5A)	-2.15
ENSOCUG00000023342	reticulon 2(RTN2)	-2.14
ENSOCUG00000014857	collagen type V alpha 3 chain(COL5A3)	-2.13
ENSOCUG00000029066	transient receptor potential cation channel subfamily M member 2(LOC103347481)	-2.13
ENSOCUG00000004317	C-X-C motif chemokine receptor 6(CXCR6)	-2.13
ENSOCUG00000015956	lymphoid restricted membrane protein(LRMP)	-2.12
ENSOCUG00000012244	perilipin 2(PLIN2)	-2.12
ENSOCUG00000006003	endoplasmic reticulum protein 27(ERP27)	-2.11
ENSOCUG00000017559	KIAA1147 ortholog(KIAA1147)	-2.11
ENSOCUG00000021037	interferon-induced GTP-binding protein Mx2(LOC100009451)	-2.10
ENSOCUG00000011452	coagulation factor XIII A chain(LOC103352261)	-2.09
ENSOCUG00000025033	KIAA0895 like(KIAA0895L)	-2.08
ENSOCUG00000012014	solute carrier family 15 member 1(SLC15A1)	-2.08
ENSOCUG00000004314	transient receptor potential cation channel subfamily M member 1(TRPM1)	-2.07
ENSOCUG00000014109	cell division cycle associated 2(CDCA2)	-2.07
ENSOCUG00000027844	solute carrier family 24 member 1(SLC24A1)	-2.07
ENSOCUG00000008677	neuritin 1(NRN1)	-2.05

ENSOCUG00000005845	amyloid beta precursor protein binding family B member 1 interacting protein(APBB1IP)	-2.02
ENSOCUG00000007153	copine 6(CPNE6)	-2.00
ENSOCUG00000008086	leucine-rich repeat containing 15(LRRC15)	-1.99
ENSOCUG00000006002	amyloid beta precursor like protein 1(APLP1)	-1.98
ENSOCUG00000014189	annexin A8(ANXA8)	-1.96
ENSOCUG00000009317	minichromosome maintenance 8 homologous recombination repair factor(MCM8)	-1.95
ENSOCUG00000012337	collagen type XXI alpha 1 chain(COL21A1)	-1.95
ENSOCUG00000004750	grainyhead like transcription factor 2(GRHL2)	-1.95
ENSOCUG000000027509	C-X3-C motif chemokine receptor 1(CX3CR1)	-1.94
ENSOCUG00000006243	WDFY family member 4(WDFY4)	-1.94
ENSOCUG00000006248	interleukin 15 receptor subunit alpha(IL15RA)	-1.94
ENSOCUG00000001241	major facilitator superfamily domain containing 4A(MFSD4A)	-1.94
ENSOCUG00000005775	MYB proto-oncogene like 2(MYBL2)	-1.94
ENSOCUG00000012157	radical S-adenosyl methionine domain containing 2(RSAD2)	-1.93
ENSOCUG00000012433	malic enzyme 2(ME2)	-1.93
ENSOCUG00000002661	protein FAM26F(LOC100353536)	-1.93
ENSOCUG00000000624	solute carrier family 26 member 6(SLC26A6)	-1.93
ENSOCUG00000000001	alcohol dehydrogenase 6(LOC100343992)	-1.92
ENSOCUG00000000580	cadherin 16(CDH16)	-1.91
ENSOCUG000000026640	sestrin 3(SESN3)	-1.91
ENSOCUG00000015222	ankyrin repeat domain 45(ANKRD45)	-1.91
ENSOCUG00000005830	HIG1 hypoxia inducible domain family member 1A(HIGD1A)	-1.91
ENSOCUG000000025013	solute carrier family 45 member 3(SLC45A3)	-1.90
ENSOCUG000000023957	mucin 1. cell surface associated(MUC1)	-1.90
ENSOCUG000000022280	transmembrane protein 45B(TMEM45B)	-1.89
ENSOCUG00000017198	tubby bipartite transcription factor(TUB)	-1.89
ENSOCUG00000013618	phosphorylase kinase catalytic subunit gamma 1(PHKG1)	-1.88
ENSOCUG00000016143	polypeptide N-acetylgalactosaminyltransferase 6(GALNT6)	-1.88
ENSOCUG00000014077	latent transforming growth factor beta binding protein 2(LTBP2)	-1.88
ENSOCUG00000008175	phosphodiesterase 7A(PDE7A)	-1.88
ENSOCUG00000009360	macrophage stimulating 1 receptor(MST1R)	-1.87
ENSOCUG00000005766	inositol 1.4.5-trisphosphate receptor type 3(LOC100008939)	-1.87
ENSOCUG00000013609	lipopolysaccharide binding protein(LBP)	-1.86
ENSOCUG00000000383	phospholipase A2 group IVE(PLA2G4E)	-1.86
ENSOCUG000000026233	HRAS-like suppressor 2(LOC100344012)	-1.85
ENSOCUG00000006001	PLAG1 zinc finger(PLAG1)	-1.85
ENSOCUG00000001029	cadherin 17(CDH17)	-1.84
ENSOCUG00000016405	EvC ciliary complex subunit 2(EVC2)	-1.84
ENSOCUG000000025809	reticulon 4 receptor-like 2(RTN4RL2)	-1.82
ENSOCUG00000000418	purinergic receptor P2Y13(P2RY13)	-1.81
ENSOCUG00000003362	laeverin(LVRN)	-1.81

ENSOCUG00000027626	CD247 molecule(CD247)	-1.81
ENSOCUG00000000386	RCAN family member 3(RCAN3)	-1.80
ENSOCUG00000010687	potassium voltage-gated channel subfamily A regulatory beta subunit 2(KCNAB2)	-1.80
ENSOCUG00000005455	NLR family pyrin domain containing 3(NLRP3)	-1.79
ENSOCUG00000012783	diacylglycerol lipase alpha(DAGLA)	-1.78
ENSOCUG00000011985	calcium voltage-gated channel subunit alpha1 A(CACNA1A)	-1.78
ENSOCUG00000000266	Wnt family member 2B(WNT2B)	-1.77
ENSOCUG00000017943	lymphocyte cytosolic protein 1(LCP1)	-1.77
ENSOCUG000000009012	Fc receptor-like 5(FCRL5)	-1.77
ENSOCUG00000007382	inhibin beta E subunit(INHBE)	-1.76
ENSOCUG00000013808	G protein-coupled receptor 68(GPR68)	-1.76
ENSOCUG00000001554	tetratricopeptide repeat. ankyrin repeat and coiled-coil containing 2(TANC2)	-1.75
ENSOCUG00000006188	peripherin(PRPH)	-1.75
ENSOCUG00000003091	adenylate cyclase 7(ADCY7)	-1.75
ENSOCUG00000004172	V-set and immunoglobulin domain containing 4(VSIG4)	-1.75
ENSOCUG00000001239	sidekick cell adhesion molecule 1(SDK1)	-1.74
ENSOCUG00000007896	mast cell immunoglobulin like receptor 1(MILR1)	-1.74
ENSOCUG00000010184	trehalase(TREH)	-1.74
ENSOCUG00000013684	transmembrane protein 54(TMEM54)	-1.72
ENSOCUG00000003246	sulfatase 1(SULF1)	-1.71
ENSOCUG00000005839	immunoglobulin like domain containing receptor 2(ILDR2)	-1.71
ENSOCUG00000001150	GTPase. IMAP family member 8(GIMAP8)	-1.70
ENSOCUG00000022477	arachidonate 15-lipoxygenase(ALOX15)	-1.70
ENSOCUG00000009869	laminin subunit alpha 3(LAMA3)	-1.70
ENSOCUG00000016877	protocadherin 20(PCDH20)	-1.70
ENSOCUG00000029313	B cell scaffold protein with ankyrin repeats 1(BANK1)	-1.69
ENSOCUG00000005931	paired immunoglobulin like type 2 receptor alpha(PILRA)	-1.69
ENSOCUG00000024196	F-box protein 17(FBXO17)	-1.68
ENSOCUG00000010144	tetratricopeptide repeat domain 22(TTC22)	-1.68
ENSOCUG00000002090	Ras association domain family member 2(RASSF2)	-1.68
ENSOCUG00000002085	solute carrier family 25 member 36(SLC25A36)	-1.67
ENSOCUG00000002781	methylenetetrahydrofolate dehydrogenase (NADP+ dependent) 1-like(MTHFD1L)	-1.66
ENSOCUG00000016771	prostaglandin-endoperoxide synthase 2(PTGS2)	-1.66
ENSOCUG00000008776	F-box protein 43(FBXO43)	-1.66
ENSOCUG00000021564	toll-like receptor 12(LOC100338778)	-1.66
ENSOCUG00000009557	polypeptide N-acetylgalactosaminyltransferase 8(GALNT8)	-1.66
ENSOCUG00000001616	proprotein convertase subtilisin/kexin type 5(PCSK5)	-1.66
ENSOCUG00000026162	inhibitor of carbonic anhydrase(LOC100345698)	-1.66
ENSOCUG00000016556	G protein-coupled receptor class C group 5 member A(GPRC5A)	-1.65
ENSOCUG00000014051	interleukin 17 receptor D(IL17RD)	-1.64

ENSOCUG00000016985	membrane-bound O-acyltransferase domain containing 2(MBOAT2)	-1.64
ENSOCUG00000006725	lamin tail domain containing 1(LMNTD1)	-1.63
ENSOCUG00000002052	LDL receptor related protein 4(LRP4)	-1.63
ENSOCUG00000009332	mucolipin 3(MCOLN3)	-1.63
ENSOCUG00000009932	establishment of sister chromatid cohesion N-acetyltransferase 2(ESCO2)	-1.62
ENSOCUG00000000558	myosin IF(MYO1F)	-1.62
ENSOCUG00000007857	leucine-rich repeat kinase 2(LRRK2)	-1.61
ENSOCUG00000016179	thymocyte selection associated family member 2(THEMIS2)	-1.61
ENSOCUG00000012271	tumour necrosis factor superfamily member 13b(TNFSF13B)	-1.61
ENSOCUG00000001910	adhesion G protein-coupled receptor L3(ADGRL3)	-1.61
ENSOCUG00000016193	osteomodulin(OMD)	-1.61
ENSOCUG00000003763	protein tyrosine phosphatase. non-receptor type 22(PTPN22)	-1.60
ENSOCUG00000012654	phosphatidylinositol-3,4,5-trisphosphate dependent Rac exchange factor 1(PREX1)	-1.60
ENSOCUG00000013596	solute carrier family 4 member 7(SLC4A7)	-1.59
ENSOCUG00000015363	neurofascin(NFASC)	-1.58
ENSOCUG00000005208	methylenetetrahydrofolate dehydrogenase (NADP+ dependent) 2. methenyltetrahydrofolate cyclohydrolase(MTHFD2)	-1.58
ENSOCUG00000025702	cytochrome P450 4A5-like(LOC100341018)	-1.58
ENSOCUG00000003403	high affinity immunoglobulin gamma Fc receptor I(LOC100358696)	-1.58
ENSOCUG00000001235	ADAM metallopeptidase domain 19(ADAM19)	-1.57
ENSOCUG00000022873	transmembrane protein 178B(LOC100357183)	-1.57
ENSOCUG00000004392	forkhead box N3(FOXP3)	-1.56
ENSOCUG00000001426	integrin subunit beta 7(ITGB7)	-1.56
ENSOCUG00000017539	spleen associated tyrosine kinase(SYK)	-1.56
ENSOCUG00000014498	solute carrier family 16 member 12(SLC16A12)	-1.56
ENSOCUG00000026334	glycoprotein nmb(GPNMB)	-1.56
ENSOCUG00000010297	signal induced proliferation associated 1 like 2(SIPA1L2)	-1.55
ENSOCUG00000017831	platelet activating factor receptor(PTAFR)	-1.54
ENSOCUG00000028059	NLR family CARD domain containing 3(NLRC3)	-1.54
ENSOCUG00000011824	RIO kinase 1(RIOK1)	-1.54
ENSOCUG00000023225	colony stimulating factor 2 receptor alpha subunit(CSF2RA)	-1.54
ENSOCUG00000012238	NACHT and WD repeat domain containing 2(NWD2)	-1.53
ENSOCUG00000011488	Fanconi anaemia complementation group I(FANCI)	-1.53
ENSOCUG00000004426	suppressor of glucose. autophagy associated 1(SOGA1)	-1.53
ENSOCUG00000005521	G protein-coupled bile acid receptor 1(GPBAR1)	-1.53
ENSOCUG00000010782	leucine-rich repeat containing 8 family member C(LRRC8C)	-1.52
ENSOCUG00000000256	protein tyrosine phosphatase domain containing 1(PTPDC1)	-1.52
ENSOCUG00000009368	dual specificity phosphatase 22(DUSP22)	-1.52
ENSOCUG00000017694	keratin 23(KRT23)	-1.52
ENSOCUG00000006116	F-box protein 48(FBXO48)	-1.52



ENSOCUG00000026714	CD5 molecule like(CD5L)	-1.51
ENSOCUG00000012016	semaphorin 3D(SEMA3D)	-1.51
ENSOCUG00000002211	solute carrier family 16 member 14(SLC16A14)	-1.51
ENSOCUG00000016775	NFKB inhibitor delta(NFKBID)	-1.51
ENSOCUG00000010231	cholinergic receptor nicotinic epsilon subunit(CHRNE)	-1.51
ENSOCUG00000012566	POU class 2 associating factor 1(POU2AF1)	-1.51
ENSOCUG00000009543	potassium calcium-activated channel subfamily M alpha 1(KCNMA1)	-1.50
ENSOCUG00000001754	formin like 3(FMNL3)	-1.50
ENSOCUG00000004014	leucine-rich repeat transmembrane neuronal 3(LRRTM3)	-1.50
ENSOCUG00000011397	triggering receptor expressed on myeloid cells 1(LOC100349504)	-1.50
ENSOCUG00000000215	period circadian clock 2(PER2)	-1.49
ENSOCUG00000011550	CD86 molecule(CD86)	-1.49
ENSOCUG00000015721	CD180 molecule(CD180)	-1.49
ENSOCUG00000010719	WD repeat domain 76(WDR76)	-1.49
ENSOCUG00000009751	HCK proto-oncogene. Src family tyrosine kinase(HCK)	-1.48
ENSOCUG00000006540	phospholipase C beta 2(PLCB2)	-1.48
ENSOCUG00000015778	solute carrier family 25 member 47(SLC25A47)	-1.48
ENSOCUG00000003030	PARP1 binding protein(PARPBP)	-1.48
ENSOCUG00000002338	SLAM family member 8(SLAMF8)	-1.47
ENSOCUG00000007865	T cell surface glycoprotein CD3 gamma chain(LOC100355340)	-1.47
ENSOCUG00000029605	odorant-binding protein(LOC103347146)	-1.47
ENSOCUG00000017018	ring finger protein 152(RNF152)	-1.46
ENSOCUG00000001185	G protein-coupled receptor 149(GPR149)	-1.46
ENSOCUG00000022836	aconitate decarboxylase 1(ACOD1)	-1.46
ENSOCUG00000009070	semaphorin 3C(SEMA3C)	-1.46
ENSOCUG00000004712	GA binding protein transcription factor beta subunit 2(GABPB2)	-1.46
ENSOCUG00000029399	SH2 domain containing 1B(SH2D1B)	-1.44
ENSOCUG00000015870	centrosomal protein 89(CEP89)	-1.44
ENSOCUG00000010547	HLF. PAR bZIP transcription factor(HLF)	-1.44
ENSOCUG00000005728	G protein regulated inducer of neurite outgrowth 2(GPRIN2)	-1.43
ENSOCUG00000002192	post-GPI attachment to proteins 1(PGAP1)	-1.43
ENSOCUG00000017147	CDP-diacylglycerol synthase 1(CDS1)	-1.43
ENSOCUG00000005167	angiopoietin like 1(ANGPTL1)	-1.43
ENSOCUG00000004033	chromosome 16 open reading frame. human C1orf74(C16H1orf74)	-1.43
ENSOCUG00000025681	leucine-rich repeat neuronal 4(LRRN4)	-1.43
ENSOCUG00000009651	DnaJ heat shock protein family (Hsp40) member B7(DNAJB7)	-1.42
ENSOCUG00000010621	Bruton tyrosine kinase(BTK)	-1.42
ENSOCUG00000002197	integrin subunit beta 8(ITGB8)	-1.42
ENSOCUG00000024091	solute carrier family 22 member 8(SLC22A8)	-1.42

ENSOCUG00000002480	SLA class II histocompatibility antigen. DQ haplotype D alpha chain(LOC100343144)	-1.42
ENSOCUG00000014953	spectrin repeat containing nuclear envelope family member 3(SYNE3)	-1.42
ENSOCUG00000016192	cysteinyl leukotriene receptor 1(CYSLTR1)	-1.42
ENSOCUG00000010728	apolipoprotein A1(APOA1)	-1.42
ENSOCUG00000002231	very low density lipoprotein receptor(VLDLR)	-1.42
ENSOCUG00000006043	ubiquitin specific peptidase 13 (isopeptidase T-3)(USP13)	-1.42
ENSOCUG00000006029	alpha-2-macroglobulin(LOC100349077)	-1.41
ENSOCUG00000010941	carboxypeptidase X. M14 family member 2(CPXM2)	-1.41
ENSOCUG00000009801	cysteine-rich hydrophobic domain 1(CHIC1)	-1.41
ENSOCUG00000015479	POU class 2 homeobox 1(POU2F1)	-1.41
ENSOCUG00000022385	nidogen-1(LOC103347221)	-1.40
ENSOCUG00000024216	myosin IG(MYO1G)	-1.40
ENSOCUG00000000830	dedicator of cytokinesis 2(DOCK2)	-1.40
ENSOCUG00000027586	EPM2A interacting protein 1(EPM2AIP1)	-1.39
ENSOCUG00000008236	lipoprotein lipase(LPL)	-1.39
ENSOCUG00000023075	plectin(LOC100349129)	-1.39
ENSOCUG00000011752	pygopus family PHD finger 1(PYGO1)	-1.39
ENSOCUG00000011054	phosphatidylinositol-4,5-bisphosphate 3-kinase catalytic subunit delta(PIK3CD)	-1.39
ENSOCUG00000006708	actin filament associated protein 1(AFAP1)	-1.39
ENSOCUG00000005885	immunoglobulin superfamily member 10(IGSF10)	-1.38
ENSOCUG00000010659	ADAM metallopeptidase domain 23(ADAM23)	-1.38
ENSOCUG00000009276	myosin binding protein C. slow type(MYBPC1)	-1.37
ENSOCUG00000001587	integrin alpha-M(LOC100351865)	-1.37
ENSOCUG00000017504	synaptotagmin 9(SYT9)	-1.37
ENSOCUG00000015877	secreted frizzled related protein 4(SFRP4)	-1.37
ENSOCUG00000014633	PBX/knotted 1 homeobox 2(PKNOX2)	-1.37
ENSOCUG00000015623	plexin A3(PLXNA3)	-1.37
ENSOCUG00000007763	calcium voltage-gated channel auxiliary subunit alpha2delta 1(CACNA2D1)	-1.37
ENSOCUG00000002018	UHRF1 binding protein 1(UHRF1BP1)	-1.37
ENSOCUG00000014786	INO80 complex subunit D(INO80D)	-1.36
ENSOCUG00000000960	sidekick cell adhesion molecule 2(SDK2)	-1.36
ENSOCUG00000004804	feline leukaemia virus subgroup C cellular receptor 1(FLVCR1)	-1.35
ENSOCUG00000003405	major facilitator superfamily domain containing 6(MFSD6)	-1.35
ENSOCUG00000029469	phosphatidylinositol 3,4,5-trisphosphate 3-phosphatase TPTE2(LOC100346342)	-1.35
ENSOCUG00000006445	frizzled class receptor 4(FZD4)	-1.35
ENSOCUG00000016347	phosphoethanolamine/phosphocholine phosphatase(PHOSPHO1)	-1.35
ENSOCUG00000000534	lymphocyte cytosolic protein 2(LCP2)	-1.34
ENSOCUG00000000136	basonuclin 1(BNC1)	-1.34
ENSOCUG00000003720	dual specificity phosphatase 4(DUSP4)	-1.34

ENSOCUG00000009774	lysosomal protein transmembrane 5(LAPTM5)	-1.34
ENSOCUG00000002530	prostaglandin-endoperoxide synthase 1(PTGS1)	-1.34
ENSOCUG00000014567	acyloxyacyl hydrolase(AOAH)	-1.33
ENSOCUG00000004988	lysyl oxidase like 4(LOXL4)	-1.33
ENSOCUG00000004275	semaphorin 5A(SEMA5A)	-1.32
ENSOCUG00000017204	DAB1. reelin adaptor protein(DAB1)	-1.32
ENSOCUG00000007759	ubiquitin specific peptidase 2(USP2)	-1.31
ENSOCUG00000022167	complement C5a receptor 1(C5AR1)	-1.31
ENSOCUG00000029622	SLAM family member 9(LOC103350037)	-1.30
ENSOCUG00000000718	solute carrier family 1 member 2(SLC1A2)	-1.30
ENSOCUG00000015570	FRY microtubule binding protein(FRY)	-1.30
ENSOCUG00000003701	toll-like receptor 10(TLR10)	-1.30
ENSOCUG00000024364	MIER family member 2(MIER2)	-1.30
ENSOCUG00000009379	MIS18 kinetochore protein A(MIS18A)	-1.29
ENSOCUG00000013916	protein kinase C beta(PRKCB)	-1.29
ENSOCUG00000001920	G protein-coupled receptor class C group 5 member B(GPRC5B)	-1.29
ENSOCUG00000002071	glycerol-3-phosphate acyltransferase 4(GPAT4)	-1.29
ENSOCUG00000029457	hamartin(LOC103346667)	-1.29
ENSOCUG00000007916	glucosaminyl (N-acetyl) transferase 1. core 2(GCNT1)	-1.28
ENSOCUG00000012990	LON peptidase N-terminal domain and ring finger 3(LONRF3)	-1.28
ENSOCUG00000011956	cadherin related family member 2(CDHR2)	-1.28
ENSOCUG00000006113	pleckstrin(PLEK)	-1.28
ENSOCUG00000010101	interferon regulatory factor 5(IRF5)	-1.28
ENSOCUG00000013467	ring finger protein 150(RNF150)	-1.28
ENSOCUG00000012402	uropodin-3b(LOC100355286)	-1.28
ENSOCUG00000023355	myosin VIIA(MYO7A)	-1.27
ENSOCUG00000002553	elastin microfibril interfacer 2(EMILIN2)	-1.27
ENSOCUG00000026567	histocompatibility antigen DM heterodimer light chain-like(RLA-DMB)	-1.27
ENSOCUG00000013517	NCK associated protein 1 like(NCKAP1L)	-1.27
ENSOCUG00000024108	potassium voltage-gated channel subfamily C member 3(LOC100338015)	-1.27
ENSOCUG00000025513	insulin like growth factor binding protein 5(IGFBP5)	-1.27
ENSOCUG00000014740	solute carrier family 37 member 2(SLC37A2)	-1.26
ENSOCUG00000029435	ligand-dependent corepressor(LOC100343926)	-1.26
ENSOCUG00000026260	solute carrier family 6 member 8(SLC6A8)	-1.26
ENSOCUG00000013550	upstream transcription factor family member 3(USF3)	-1.26
ENSOCUG00000009436	cyclic nucleotide gated channel alpha 2(CNGA2)	-1.26
ENSOCUG00000012620	Werner syndrome RecQ like helicase(WRN)	-1.26
ENSOCUG00000010987	transmembrane protein 26(TMEM26)	-1.26
ENSOCUG00000009050	reelin(RELN)	-1.26
ENSOCUG00000000401	hexokinase 3(HK3)	-1.26
ENSOCUG00000000763	phospholipase A2 group VII(PLA2G7)	-1.26

ENSOCUG00000027817	protein phosphatase 1 regulatory subunit 16B(PPP1R16B)	-1.25
ENSOCUG00000013120	polyhomeotic homolog 3(PHC3)	-1.25
ENSOCUG00000011691	serine/threonine kinase 17b(STK17B)	-1.25
ENSOCUG00000009478	Rho GTPase activating protein 31(ARHGAP31)	-1.25
ENSOCUG00000000007	GLI pathogenesis related 2(GLIPR2)	-1.25
ENSOCUG00000006803	ectonucleoside triphosphate diphosphohydrolase 5(ENTPD5)	-1.25
ENSOCUG00000016651	AXL receptor tyrosine kinase(AXL)	-1.25
ENSOCUG00000003221	lysine demethylase 7A(KDM7A)	-1.25
ENSOCUG00000014964	ATP-binding cassette subfamily B member 4(ABCB4)	-1.25
ENSOCUG00000014482	plexin domain containing 2(PLXDC2)	-1.24
ENSOCUG00000017793	CD38 molecule(CD38)	-1.24
ENSOCUG00000028137	indian hedgehog(IHH)	-1.24
ENSOCUG00000008922	FGR proto-oncogene. Src family tyrosine kinase(FGR)	-1.24
ENSOCUG00000014795	insulin like growth factor 1 receptor(IGF1R)	-1.24
ENSOCUG00000008600	formyl peptide receptor 1(FPR1)	-1.24
ENSOCUG00000021438	adhesion G protein-coupled receptor E5(ADGRE5)	-1.23
ENSOCUG00000015483	fatty acid binding protein 4(FABP4)	-1.23
ENSOCUG00000001711	trophinin(TRO)	-1.23
ENSOCUG00000024991	alpha kinase 1(ALPK1)	-1.23
ENSOCUG00000009447	oxysterol binding protein like 7(OSBPL7)	-1.23
ENSOCUG00000002306	protease. serine. 8(PRSS8)	-1.22
ENSOCUG00000006497	peroxidasin(PXDN)	-1.22
ENSOCUG00000010918	FER tyrosine kinase(FER)	-1.22
ENSOCUG00000009042	CNKSR family member 3(CNKSR3)	-1.22
ENSOCUG00000012372	lipin 3(LPIN3)	-1.21
ENSOCUG00000015909	heparin binding EGF-like growth factor(HBEGF)	-1.21
ENSOCUG00000002566	sex hormone binding globulin(SHBG)	-1.21
ENSOCUG00000011309	plexin domain containing 1(PLXDC1)	-1.21
ENSOCUG00000008291	bridging integrator 2(BIN2)	-1.21
ENSOCUG00000022214	acyl-coenzyme A thioesterase 4(LOC100343752)	-1.21
ENSOCUG00000011981	protein tyrosine phosphatase. receptor type C(PTPRC)	-1.21
ENSOCUG00000023778	CD300a molecule(CD300A)	-1.21
ENSOCUG00000001006	tachykinin receptor 1(TACR1)	-1.21
ENSOCUG00000013642	dedicator of cytokinesis 11(DOCK11)	-1.21
ENSOCUG00000016755	UDP-glucuronosyltransferase 2A3(LOC100359229)	-1.20
ENSOCUG00000008757	myoferlin(MYOF)	-1.20
ENSOCUG00000003924	apolipoprotein L3(LOC100350735)	-1.20
ENSOCUG00000010012	adenylate kinase 4(AK4)	-1.20
ENSOCUG00000010637	minichromosome maintenance complex component 5(MCM5)	-1.20
ENSOCUG00000016343	regulator of telomere elongation helicase 1(RTEL1)	-1.19
ENSOCUG00000002613	versican(VCAN)	-1.19
ENSOCUG00000024739	zinc finger BED-type containing 6(ZBED6)	-1.19

ENSOCUG00000025736	apolipoprotein B mRNA editing enzyme catalytic subunit 1(APOBEC1)	-1.19
ENSOCUG00000016115	ras-related C3 botulinum toxin substrate 2 (rho family, small GTP-binding protein Rac2)(RAC2)	-1.19
ENSOCUG00000023116	protein argonaute-1(LOC100347349)	-1.19
ENSOCUG00000006571	OTU deubiquitinase 3(OTUD3)	-1.19
ENSOCUG00000008656	guanylate-binding protein 5(LOC100349257)	-1.19
ENSOCUG00000011935	PTC7 protein phosphatase homolog(PPTC7)	-1.19
ENSOCUG00000026383	aldo-keto reductase family 1 member B10(AKR1B10)	-1.19
ENSOCUG00000000786	EPH receptor A2(EPHA2)	-1.19
ENSOCUG00000007922	ST8 alpha-N-acetyl-neuraminide alpha-2.8-sialyltransferase 4(ST8SIA4)	-1.19
ENSOCUG00000004618	CKLF like MARVEL transmembrane domain containing 4(CMTM4)	-1.19
ENSOCUG00000016280	C-X-C motif chemokine ligand 10(CXCL10)	-1.18
ENSOCUG00000017892	zinc finger CCCH-type containing, antiviral 1(ZC3HAV1)	-1.18
ENSOCUG00000024065	nuclear prelamin A recognition factor(NARF)	-1.18
ENSOCUG00000005237	protocadherin 17(PCDH17)	-1.18
ENSOCUG00000001289	septin 11(SEPT11)	-1.18
ENSOCUG00000029190	placenta specific 8(PLAC8)	-1.18
ENSOCUG00000028062	GTPase, IMAP family member 1(GIMAP1)	-1.18
ENSOCUG00000022216	collectin subfamily member 12(COLEC12)	-1.18
ENSOCUG00000013760	neuralised E3 ubiquitin protein ligase 1(NEURL1)	-1.18
ENSOCUG00000014820	cytochrome b reductase 1(LOC100346448)	-1.18
ENSOCUG00000010563	TAP binding protein(TAPBP)	-1.17
ENSOCUG00000002485	HLA class II histocompatibility antigen, DQ beta 1 chain(LOC100351163)	-1.17
ENSOCUG00000001594	solute carrier family 16 member 6(SLC16A6)	-1.17
ENSOCUG00000000575	hepatitis A virus cellular receptor 1(HAVCR1)	-1.17
ENSOCUG00000012814	TROVE domain family member 2(TROVE2)	-1.16
ENSOCUG00000012148	inositol 1.4.5-trisphosphate receptor type 1(ITPR1)	-1.16
ENSOCUG00000000715	CD44 molecule (Indian blood group)(CD44)	-1.16
ENSOCUG00000007286	collagen type IV alpha 4 chain(COL4A4)	-1.15
ENSOCUG00000004436	insulin receptor(INSR)	-1.15
ENSOCUG00000011764	LIM domain containing preferred translocation partner in lipoma(LPP)	-1.15
ENSOCUG00000014976	ERCC excision repair 4, endonuclease catalytic subunit(ERCC4)	-1.15
ENSOCUG00000014646	fasciculation and elongation protein zeta 1(FEZ1)	-1.15
ENSOCUG00000001481	family with sequence similarity 65 member B(FAM65B)	-1.14
ENSOCUG00000004942	protein kinase AMP-activated catalytic subunit alpha 2(PRKAA2)	-1.14
ENSOCUG00000025241	liver carboxylesterase 2-like(LOC100357214)	-1.14
ENSOCUG000000009311	CD84 molecule(CD84)	-1.14
ENSOCUG00000006719	lysophosphatidylcholine acyltransferase 2(LPCAT2)	-1.14

ENSOCUG00000002281	cytochrome P450 2U1(LOC100353947)	-1.13
ENSOCUG00000015138	complement component 1. q subcomponent. C chain(C1QC)	-1.13
ENSOCUG00000012906	SPARC related modular calcium binding 2(SMOC2)	-1.13
ENSOCUG00000008688	cilia and flagella associated protein 43(CFAP43)	-1.13
ENSOCUG00000007380	inhibin beta C subunit(INHBC)	-1.13
ENSOCUG00000004808	Cbl proto-oncogene(CBL)	-1.13
ENSOCUG00000011350	spondin 1(SPON1)	-1.13
ENSOCUG0000001060	ankyrin repeat domain 13A(ANKRD13A)	-1.13
ENSOCUG00000002935	family with sequence similarity 46 member C(FAM46C)	-1.13
ENSOCUG00000012779	G protein-coupled receptor 137B(GPR137B)	-1.12
ENSOCUG00000000142	coagulation factor VIII(F8)	-1.12
ENSOCUG00000023891	DNA damage inducible 1 homolog 2(DDI2)	-1.12
ENSOCUG00000026291	arrestin beta 1(ARRB1)	-1.11
ENSOCUG00000003729	nuclear factor related to kappaB binding protein(NFRKB)	-1.11
ENSOCUG00000006350	solute carrier family 12 member 4(SLC12A4)	-1.11
ENSOCUG00000013527	abhydrolase domain containing 2(ABHD2)	-1.10
ENSOCUG00000005112	F-box protein 32(FBXO32)	-1.10
ENSOCUG00000000427	peptidase M20 domain containing 1(PM20D1)	-1.09
ENSOCUG00000027006	UDP-glucuronosyltransferase 2B16-like(LOC100340258)	-1.08
ENSOCUG00000006566	X-linked Kx blood group(XK)	-1.08
ENSOCUG00000026015	liver carboxylesterase 2-like(LOC100358248)	-1.07
ENSOCUG00000011544	integrin subunit beta 2(ITGB2)	-1.07
ENSOCUG00000001497	fatty acid binding protein 7(FABP7)	1.08
ENSOCUG00000015313	cytochrome c oxidase protein 20 homolog(LOC100349428)	1.10
ENSOCUG00000014585	zinc finger DHHC-type containing 2(ZDHC2)	1.12
ENSOCUG00000000688	F-box protein 27(FBXO27)	1.13
ENSOCUG00000004733	prostaglandin-E(2) 9-reductase-like(PGER2)	1.13
ENSOCUG00000005985	clusterin(CLU)	1.13
ENSOCUG00000024462	60S ribosomal protein L27(LOC100356974)	1.14
ENSOCUG00000014776	solute carrier family 26 member 8(SLC26A8)	1.17
ENSOCUG00000017350	glycosyltransferase 1 domain containing 1(GLT1D1)	1.17
ENSOCUG00000002702	radical S-adenosyl methionine domain containing 1(RSAD1)	1.18
ENSOCUG00000024412	serum amyloid A-4 protein(LOC100342244)	1.20
ENSOCUG00000003858	glycine N-methyltransferase(GNMT)	1.21
ENSOCUG00000029478	fragile X mental retardation 1 neighbour(FMR1NB)	1.23
ENSOCUG00000006681	ATP synthase. H+ transporting. mitochondrial Fo complex subunit F6(ATP5J)	1.24
ENSOCUG00000008329	ADAM metallopeptidase with thrombospondin type 1 motif 19(ADAMTS19)	1.24
ENSOCUG00000007493	isopentenyl-diphosphate Delta-isomerase 1(LOC100343510)	1.25
ENSOCUG00000016551	C1q and tumour necrosis factor related protein 7(C1QTNF7)	1.28
ENSOCUG00000009195	C type lectin domain family 4 member E(CLEC4E)	1.30
ENSOCUG00000029235	metallothionein-1A(LOC100343802)	1.31
ENSOCUG00000004160	family with sequence similarity 107 member A(FAM107A)	1.34

ENSOCUG00000012902	glutathione S-transferase Yc(LOC100353428)	1.34
ENSOCUG00000015329	matrix metalloproteinase 7(MMP7)	1.36
ENSOCUG00000008193	actin. alpha 2. smooth muscle. aorta(ACTA2)	1.37
ENSOCUG00000023425	alpha-fetoprotein(LOC103350776)	1.37
ENSOCUG00000014505	tribbles pseudokinase 3(TRIB3)	1.37
ENSOCUG00000009825	biphenyl hydrolase like(BPHL)	1.40
ENSOCUG00000009769	immunoglobulin superfamily member 1(IGSF1)	1.40
ENSOCUG00000007890	SCO-spondin(SSPO)	1.41
ENSOCUG00000016210	RAB15 effector protein(REP15)	1.41
ENSOCUG00000010814	malic enzyme 1(ME1)	1.41
ENSOCUG00000006139	semaphorin 5B(SEMA5B)	1.45
ENSOCUG00000015111	glutamate ionotropic receptor NMDA type subunit 2B(GRIN2B)	1.50
ENSOCUG00000008104	growth differentiation factor 6(GDF6)	1.52
ENSOCUG00000008571	myomesin 1(MYOM1)	1.52
ENSOCUG00000016772	DNA damage inducible transcript 4(DDIT4)	1.53
ENSOCUG00000009725	acyl-CoA wax alcohol acyltransferase 1(AWAT1)	1.54
ENSOCUG00000002542	solute carrier family 22 member 2(SLC22A2)	1.62
ENSOCUG00000015619	calbindin 2(CALB2)	1.64
ENSOCUG00000015771	squalene epoxidase(SQLE)	1.70
ENSOCUG00000008109	chromosome 3 open reading frame. human C8orf34(C3H8orf34)	1.70
ENSOCUG00000024372	trace amine-associated receptor 4(TAAR4)	1.71
ENSOCUG00000007266	sodium channel protein type 1 subunit alpha(LOC100009591)	1.75
ENSOCUG00000017620	serum amyloid protein A(LOC100009259)	1.79
ENSOCUG00000013412	C-C motif chemokine 7(LOC103351517)	1.81
ENSOCUG00000004297	otoancorin(OTOA)	1.81
ENSOCUG00000010549	monocyte to macrophage differentiation associated(MMD)	1.85
ENSOCUG00000013324	hypocretin neuropeptide precursor(HCRT)	1.86
ENSOCUG00000015777	potassium voltage-gated channel subfamily D member 1(KCND1)	1.96
ENSOCUG00000012939	ectonucleotide pyrophosphatase/phosphodiesterase 5 (putative)(ENPP5)	2.03
ENSOCUG00000013934	coiled-coil domain containing 189(CCDC189)	2.07
ENSOCUG00000025992	butyrophilin subfamily 1 member A1-like(LOC100344369)	2.09
ENSOCUG00000007327	contactin associated protein 1(CNTNAP1)	2.10
ENSOCUG00000027125	ATP-binding cassette subfamily A member 3(LOC100353012)	2.31
ENSOCUG00000029754	TSSK6 activating cochaperone(TSACC)	2.32
ENSOCUG00000021120	mucin 15. cell surface associated(MUC15)	2.32
ENSOCUG00000025107	membrane associated ring-CH-type finger 4(MARCH4)	2.33
ENSOCUG00000027492	zymogen granule membrane protein 16(LOC100346271)	2.36
ENSOCUG00000005346	tudor domain containing 15(TDRD15)	2.41
ENSOCUG00000006124	leukaemia NUP98 fusion partner 1(LNP1)	2.47
ENSOCUG00000026936	delta like non-canonical Notch ligand 1(DLK1)	2.51

ENSOCUG00000001309	isthmin 1(ISM1)	2.52
ENSOCUG00000002462	solute carrier family 24 member 2(SLC24A2)	2.55
ENSOCUG000000013373	sperm tail PG-rich repeat containing 1(STPG1)	2.64
ENSOCUG000000011025	contactin 4(CNTN4)	2.67
ENSOCUG000000009438	claudin 10(CLDN10)	2.80
ENSOCUG000000026267	aldo-keto reductase family 1. member C1 (dihydrodiol dehydrogenase 1; 20-alpha (3-alpha)-hydroxysteroid dehydrogenase)(AKR1C5)	2.83
ENSOCUG000000003017	glutamate rich 3(ERICH3)	2.98
ENSOCUG000000008391	GDNF family receptor alpha 3(GFRA3)	2.99
ENSOCUG000000029690	zymogen granule membrane protein 16(LOC100350057)	3.03
ENSOCUG000000021940	putative alpha-1-antitrypsin-related protein(LOC100358746)	3.08
ENSOCUG000000003953	chromosome 13 open reading frame. human C1orf146(C13H1orf146)	3.17
ENSOCUG000000015301	sodium voltage-gated channel beta subunit 1(SCN1B)	3.27
ENSOCUG000000029599	killer cell lectin like receptor B1(KLRB1)	3.32
ENSOCUG000000016764	myelin transcription factor 1 like(MYT1L)	3.51
ENSOCUG000000027771	zymogen granule membrane protein 16-like(LOC100359023)	3.52
ENSOCUG000000017790	steroid 17-alpha-hydroxylase/17.20 lyase(LOC100346394)	3.58
ENSOCUG000000008181	carboxypeptidase E(CPE)	3.60
ENSOCUG000000012592	ankyrin repeat and SOCS box containing 5(ASB5)	3.65
ENSOCUG000000005979	chromosome 15 open reading frame. human C4orf17(C15H4orf17)	3.66
ENSOCUG000000022883	glycerophosphodiester phosphodiesterase domain containing 3(GDPD3)	3.66
ENSOCUG000000004205	protease. serine 35(PRSS35)	3.95
ENSOCUG000000029412	zymogen granule membrane protein 16-like(LOC100352055)	4.02
ENSOCUG000000003021	ceramide kinase like(CERKL)	4.59
ENSOCUG000000027755	putative spermatogenesis-associated protein 31D3(LOC100355671)	4.81
ENSOCUG000000017941	platelet microbicidal protein 1(LOC100008921)	5.67
ENSOCUG000000000901	seizure related 6 homolog like 2(SEZ6L2)	6.23
ENSOCUG000000029318	zymogen granule membrane protein 16-like(LOC100351054)	6.75
ENSOCUG000000015803	tubulointerstitial nephritis antigen(TINAG)	7.38
ENSOCUG000000029735	carboxypeptidase E(LOC100343425)	10.72
ENSOCUG000000000199	deuterosome assembly protein 1(DEUP1)	< -0.01
ENSOCUG000000000315	glutamate ionotropic receptor AMPA type subunit 3(GRIA3)	< -0.01
ENSOCUG000000000341	regulator of G protein signalling 6(RGS6)	< -0.01
ENSOCUG000000000774	protocadherin 9(PCDH9)	< -0.01
ENSOCUG000000001022	solute carrier family 13 member 1(SLC13A1)	< -0.01
ENSOCUG000000001703	cation channel sperm associated 3(CATSPER3)	< -0.01
ENSOCUG000000002830	tensin 4(TNS4)	< -0.01
ENSOCUG000000003724	multiple EGF-like domains 10(MEGF10)	< -0.01
ENSOCUG000000004480	cysteine and glycine rich protein 3(CSRP3)	< -0.01
ENSOCUG000000006146	paired box 7(PAX7)	< -0.01



ENSOCUG00000006307	translin associated factor X interacting protein 1(TSNAXIP1)	< -0.01
ENSOCUG00000006728	myomesin 3(MYOM3)	< -0.01
ENSOCUG00000011270	CD1b molecule(CD1B)	< -0.01
ENSOCUG00000014011	glutamate receptor interacting protein 1(GRIP1)	< -0.01
ENSOCUG00000014187	KIAA1024 ortholog(KIAA1024)	< -0.01
ENSOCUG00000015507	sushi domain containing 5(SUSD5)	< -0.01
ENSOCUG00000016053	RAB44. member RAS oncogene family(RAB44)	< -0.01
ENSOCUG00000016787	serpin family B member 5(SERPINB5)	< -0.01
ENSOCUG00000016970	dynein heavy chain domain 1(DNHD1)	< -0.01
ENSOCUG00000022989	ring finger protein 32(RNF32)	< -0.01
ENSOCUG00000027297	EF-hand calcium binding domain 8(EFCAB8)	< -0.01
ENSOCUG00000027575	potassium voltage-gated channel subfamily H member 2(KCNH2)	< -0.01
ENSOCUG00000001040	nei like DNA glycosylase 3(NEIL3)	< -0.02
ENSOCUG00000001986	phospholipase C delta 4(PLCD4)	< -0.02
ENSOCUG00000005563	lysosomal associated membrane protein 3(LAMP3)	< -0.02
ENSOCUG00000006290	leucine-rich repeat and fibronectin type III domain-containing protein 5(LOC100349270)	< -0.02
ENSOCUG00000009933	germinal centre associated signalling and motility(GCSAM)	< -0.02
ENSOCUG00000011975	zinc finger and BTB domain containing 8B(ZBTB8B)	< -0.02
ENSOCUG00000015565	potassium voltage-gated channel subfamily J member 5(KCNJ5)	< -0.02
ENSOCUG00000021520	RASD family member 2(RASD2)	< -0.02
ENSOCUG00000021659	arachidonate 12-lipoxygenase. 12S type(ALOX12)	< -0.02
ENSOCUG00000023547	tubulin alpha-3 chain(LOC100350967)	< -0.02
ENSOCUG00000026674	granzyme A(LOC100346200)	< -0.02
ENSOCUG00000027210	Fc fragment of IgG binding protein(FCGBP)	< -0.02
ENSOCUG00000027997	tescalcin(TESC)	< -0.02
ENSOCUG00000000883	transketolase-like 1(TKTL1)	< -0.03
ENSOCUG00000006061	thymocyte selection associated(THEMIS)	< -0.03
ENSOCUG00000010009	eosinophil peroxidase(EPX)	< -0.03
ENSOCUG00000012981	tropomodulin 2(TM0D2)	< -0.03
ENSOCUG00000023285	trophinin associated protein(TROAP)	< -0.03
ENSOCUG00000029569	keratin 17(KRT17)	< -0.03
ENSOCUG00000006579	sphingosine kinase 1(SPHK1)	< -0.04
ENSOCUG00000007567	solute carrier family 38 member 11(SLC38A11)	< -0.04
ENSOCUG00000011561	olfactory receptor 1J1(LOC100345888)	< -0.04
ENSOCUG00000016659	embigin(EMB)	< -0.04
ENSOCUG00000026537	membrane spanning 4-domains A18(MS4A18)	< -0.04
ENSOCUG00000000194	early growth response 3(EGR3)	< -0.05
ENSOCUG00000000793	calcineurin like EF-hand protein 2(CHP2)	< -0.05
ENSOCUG00000001178	family with sequence similarity 78 member B(FAM78B)	< -0.05
ENSOCUG00000011516	adenylate kinase 7(AK7)	< -0.05
ENSOCUG00000014829	synaptotagmin 1(SYT1)	< -0.05

ENSOCUG00000023952	netrin G1(NTNG1)	< -0.05
ENSOCUG00000004004	family with sequence similarity 135 member B(FAM135B)	< -0.06
ENSOCUG00000004369	chromosome 3 open reading frame. human C5orf46(C3H5orf46)	< -0.06
ENSOCUG00000008657	cell growth regulator with EF-hand domain 1(CGREF1)	< -0.06
ENSOCUG00000027283	solute carrier family 25 member 45(SLC25A45)	< -0.06
ENSOCUG00000009843	SPARC/osteonectin. cwcv and kazal like domains proteoglycan 1(SPOCK1)	< -0.07
ENSOCUG00000014008	chromatin assembly factor 1 subunit B(CHAF1B)	< -0.07
ENSOCUG00000004603	retinal degeneration 3(RD3)	< -0.08
ENSOCUG00000013829	potassium channel tetramerisation domain containing 4(KCTD4)	< -0.08
ENSOCUG00000009695	EPS8 like 3(EPS8L3)	< -0.09
ENSOCUG00000017737	purinergic receptor P2X 2(P2RX2)	< -0.11
ENSOCUG00000006014	phosphodiesterase 6H(PDE6H)	< -0.14
ENSOCUG00000003089	proteoglycan 3. pro eosinophil major basic protein 2(PRG3)	< -0.32
ENSOCUG00000003984	solute carrier family 8 member A3(SLC8A3)	> 0.01
ENSOCUG00000006597	calmegin(CLGN)	> 0.01
ENSOCUG00000014837	solute carrier family 39 member 12(SLC39A12)	> 0.01
ENSOCUG00000017128	neuromedin U(NMU)	> 0.01
ENSOCUG00000017476	epoxide hydrolase 4(EPHX4)	> 0.01
ENSOCUG00000021711	protein phosphatase 1 regulatory inhibitor subunit 1B(PPP1R1B)	> 0.01
ENSOCUG00000027106	hyaluronan synthase 2(HAS2)	> 0.01
ENSOCUG00000004691	prominin 2(PROM2)	> 0.02
ENSOCUG00000004847	growth associated protein 43(GAP43)	> 0.02
ENSOCUG00000011440	glutamate ionotropic receptor delta type subunit 2(GRID2)	> 0.02
ENSOCUG00000012760	zinc finger and BTB domain containing 32(ZBTB32)	> 0.02
ENSOCUG00000015813	neuromedin U receptor 1(NMUR1)	> 0.02
ENSOCUG00000024593	aldehyde oxidase 4(AOX4)	> 0.02
ENSOCUG00000028202	family with sequence similarity 178 member B(FAM178B)	> 0.02
ENSOCUG00000001290	synaptotagmin 12(SYT12)	> 0.03
ENSOCUG00000004746	spermatogenesis-associated 16(SPATA16)	> 0.03
ENSOCUG00000002301	cyclin B1 interacting protein 1(CCNB1IP1)	> 0.04
ENSOCUG00000002624	Nik related kinase(NRK)	> 0.07
ENSOCUG00000004047	spindle and kinetochore associated complex subunit 3(SKA3)	> 0.08
ENSOCUG00000029446	tripartite motif containing 60(TRIM60)	> 0.12
ENSOCUG00000003481	REGG like(RERGL)	> 0.14
ENSOCUG00000026203	complement C1q like 1(C1QL1)	> 0.14

**Supplementary Table S12.** Functional analysis of the differentially expressed transcripts in liver tissue between vitrified-transferred progeny and that naturally-conceived in F3.

Category	Term	Count	p-value
BP	chemotaxis	13	0.000
BP	immune response	18	0.000
BP	inflammatory response	16	0.000
BP	arachidonic acid metabolic process	5	0.001
BP	integrin-mediated signalling pathway	9	0.002
BP	cell adhesion	13	0.002
BP	linoleic acid metabolic process	4	0.003
BP	lipoygenase pathway	4	0.003
BP	haematopoietic progenitor cell differentiation	9	0.003
BP	regulation of autophagy	5	0.009
BP	sperm capacitation	4	0.011
BP	regulation of ventricular cardiac muscle cell membrane repolarisation	4	0.015
BP	T cell receptor signalling pathway	6	0.015
BP	B cell receptor signalling pathway	5	0.018
BP	ventral spinal cord development	3	0.018
BP	lipid transport	5	0.024
BP	negative regulation of tumour necrosis factor production	5	0.024
BP	positive regulation of defence response to virus by host	9	0.025
BP	locomotion involved in locomotory behaviour	3	0.027
BP	glial cell differentiation	3	0.027
BP	regulation of calcium ion-dependent exocytosis	3	0.027
BP	neuronal action potential propagation	3	0.027
BP	positive regulation of neutrophil chemotaxis	4	0.027
BP	neutrophil chemotaxis	5	0.027
BP	phagocytosis. recognition	3	0.036
BP	GTP metabolic process	3	0.036
BP	transmembrane transport	8	0.037
BP	positive regulation of cytokine secretion	4	0.038
BP	positive regulation of type I interferon production	3	0.047
BP	skeletal muscle fibre development	4	0.051
BP	positive regulation of gene expression	11	0.052
BP	signal transduction	14	0.053
BP	positive regulation of vascular endothelial growth factor production	4	0.058
BP	receptor clustering	3	0.059
BP	cellular response to exogenous dsRNA	3	0.059
BP	behavioural response to pain	3	0.059
BP	response to oxidative stress	6	0.063
BP	defence response to virus	7	0.070

BP	homophilic cell adhesion via plasma membrane adhesion molecules	7	0.070
BP	negative regulation of T cell activation	3	0.071
BP	peripheral nervous system development	3	0.071
BP	regulation of signal transduction	3	0.071
BP	calcium-mediated signalling	4	0.082
BP	sodium ion transport	4	0.082
BP	secretory granule localisation	2	0.088
BP	positive regulation of hydrolase activity	2	0.088
BP	positive regulation of toll-like receptor 7 signalling pathway	2	0.088
BP	Fc epsilon receptor signalling pathway	2	0.088
BP	enzyme linked receptor protein signalling pathway	2	0.088
BP	positive regulation of toll-like receptor 9 signalling pathway	2	0.088
BP	cyclooxygenase pathway	2	0.088
BP	regulation of NADP metabolic process	2	0.088
BP	cell-cell adhesion mediated by cadherin	2	0.088
BP	positive regulation of protein kinase activity	4	0.090
BP	positive regulation of cell migration	8	0.091
BP	xenophagy	7	0.093
BP	innate immune response	8	0.095
BP	transmission of nerve impulse	3	0.098
BP	neuromuscular synaptic transmission	3	0.098
BP	heterotypic cell-cell adhesion	3	0.098
BP	long-term synaptic potentiation	4	0.099
BP	regulation of heart rate by cardiac conduction	4	0.099
CC	integral component of membrane	212	0.000
CC	extracellular matrix	13	0.000
CC	cell surface	26	0.000
CC	zymogen granule membrane	5	0.005
CC	receptor complex	10	0.008
CC	intracellular membrane-bounded organelle	8	0.020
CC	extracellular space	38	0.033
CC	apical plasma membrane	12	0.034
CC	brush border membrane	4	0.039
CC	proteinaceous extracellular matrix	11	0.050
CC	extracellular exosome	96	0.051
CC	node of Ranvier	3	0.053
CC	voltage-gated potassium channel complex	6	0.056
CC	neuronal cell body	9	0.056
CC	MHC class II protein complex	3	0.077
CC	phagocytic cup	3	0.077

MF	calcium ion binding	39	0.000
MF	peroxidase activity	5	0.000
MF	carbohydrate binding	9	0.006
MF	non-membrane spanning protein tyrosine kinase activity	6	0.006
MF	arachidonate 12-lipoxygenase activity	3	0.009
MF	glycoprotein binding	6	0.026
MF	hyaluronic acid binding	4	0.027
MF	3'.5'-cyclic-nucleotide phosphodiesterase activity	3	0.029
MF	protein tyrosine phosphatase activity	8	0.036
MF	transmembrane signalling receptor activity	5	0.036
MF	phospholipid binding	5	0.040
MF	phosphatidylserine binding	4	0.048
MF	transporter activity	8	0.050
MF	heparin binding	7	0.064
MF	voltage-gated calcium channel activity	4	0.067
MF	C-C chemokine receptor activity	3	0.067
MF	secondary active sulfate transmembrane transporter activity	3	0.067
MF	voltage-gated potassium channel activity	5	0.077
MF	iron ion binding	10	0.077
MF	prostaglandin-endoperoxide synthase activity	2	0.077
MF	proton-dependent oligopeptide secondary active transmembrane transporter activity	2	0.077
MF	dioxygenase activity	2	0.077
<hr/>			
KEGG	Staphylococcus aureus infection	11	0.000
KEGG	Cell adhesion molecules (CAMs)	16	0.000
KEGG	Serotonergic synapse	13	0.000
KEGG	Calcium signalling pathway	17	0.001
KEGG	Chemokine signalling pathway	16	0.001
KEGG	Long-term depression	9	0.001
KEGG	Platelet activation	13	0.002
KEGG	Retrograde endocannabinoid signalling	11	0.002
KEGG	Asthma	6	0.003
KEGG	Rap1 signalling pathway	17	0.005
KEGG	Neuroactive ligand-receptor interaction	19	0.005
KEGG	Haematopoietic cell lineage	9	0.005
KEGG	Oxytocin signalling pathway	13	0.006
KEGG	Type I diabetes mellitus	7	0.007
KEGG	Fc gamma R-mediated phagocytosis	9	0.007
KEGG	Graft-versus-host disease	6	0.010
KEGG	Regulation of lipolysis in adipocytes	7	0.010
KEGG	Circadian entrainment	9	0.010
KEGG	ECM-receptor interaction	9	0.010

KEGG	Glutamatergic synapse	10	0.012
KEGG	Tuberculosis	14	0.012
KEGG	PI3K-Akt signalling pathway	20	0.016
KEGG	Leishmaniasis	8	0.016
KEGG	Fc epsilon RI signalling pathway	7	0.017
KEGG	Dopaminergic synapse	10	0.021
KEGG	Inflammatory mediator regulation of TRP channels	9	0.025
KEGG	Cytokine-cytokine receptor interaction	14	0.025
KEGG	Morphine addiction	8	0.029
KEGG	VEGF signalling pathway	6	0.033
KEGG	Ovarian steroidogenesis	6	0.036
KEGG	Viral myocarditis	7	0.036
KEGG	Intestinal immune network for IgA production	6	0.039
KEGG	Arachidonic acid metabolism	8	0.040
KEGG	Glycerophospholipid metabolism	8	0.042
KEGG	Rheumatoid arthritis	8	0.042
KEGG	Phosphatidylinositol signalling system	8	0.044
KEGG	Aldosterone synthesis and secretion	7	0.048
KEGG	mTOR signalling pathway	6	0.053
KEGG	Allograft rejection	5	0.061
KEGG	Natural killer cell mediated cytotoxicity	8	0.061
KEGG	Axon guidance	9	0.069
KEGG	Salivary secretion	7	0.074
KEGG	Phagosome	10	0.082
KEGG	Type II diabetes mellitus	5	0.084
KEGG	Amoebiasis	8	0.084
KEGG	Thyroid hormone synthesis	6	0.091

\*Functional analysis was referred to the GO term annotation according to the biological process (BP), cellular component (CC) and molecular function (MF) classification, and the KEGG pathways in which they are involved.

**Supplementary Table S13.** Targeted identification of differentially accumulated metabolites in liver tissue between vitrified- transferred progeny and that naturally-conceived in F1, F2 and F3 generations.

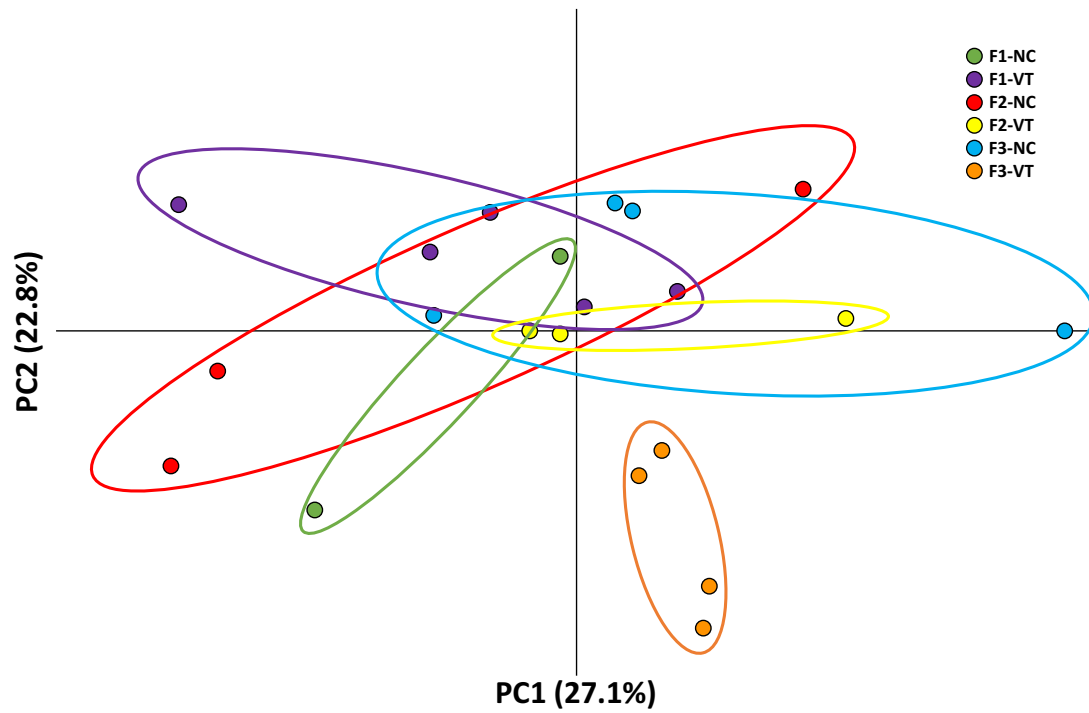
Metabolic pathway	Metabolite name	Fold change F1	Fold change F2	Fold change F3
Glycolysis Gluconeogenesis	glycerate-3P	0.70	<b>3.47</b>	<b>2.55</b>
	ThPP	2.56	<b>1.44</b>	<b>1.64</b>
	2-hydroxy-ethyl-ThPP	0.93	0.04	<b>0.86</b>
	β-D-Glucose-6P	-0.22	-0.07	0.21
	glycerate-1.3P2	-0.41	<b>-0.64</b>	0.19
	glyceraldehyde-3P	<b>-1.58</b>	-1.15	-0.18
	S-Acetyl-Dihydrolipoamide-E	<b>0.61</b>	-0.07	<b>0.34</b>
	Lipoamide-E	<b>-0.54</b>	<b>-0.23</b>	-0.37
	β-D-Fructose-1.6P2	<b>-0.98</b>	0.55	-0.53
Citrate cycle (TCA cycle)	cAMP	<b>-0.61</b>	0.34	0.51
	oxalosuccinate	<b>3.59</b>	<b>2.52</b>	<b>2.12</b>
	ThPP	2.56	<b>1.44</b>	<b>1.64</b>
	2-hydroxy-ethyl-ThPP	0.93	0.04	<b>0.86</b>
	succinate	<b>-0.64</b>	<b>-0.40</b>	0.15
	cis-aconitate	0.00	0.10	0.13
	S-Acetyl-Dihydrolipoamide-E	<b>0.61</b>	-0.07	<b>0.34</b>
	citrate	<b>-0.62</b>	<b>-0.82</b>	-0.18
	Lipoamide-E	<b>-0.54</b>	<b>-0.23</b>	-0.37
	3-carboxy-1-hydroxypropyl-ThPP	<b>2.65</b>	0.41	-1.06
Biosynthesis of amino acids	arginine	-0.07	-0.03	0.17
	asparagine	0.05	-0.04	0.30
	aspartate	-0.04	-0.04	0.31
	cysteine	<b>-2.38</b>	<b>-2.32</b>	-2.11
	glutamic_acid	0.12	0.05	0.35
	glutamine	-0.44	-0.69	-0.05
	histidine	-0.12	-0.03	0.25
	isoleucine-leucine	0.31	-0.15	0.50
	lysine	0.09	0.19	-0.01
	methionine	0.19	<b>-0.27</b>	0.39
	phenylalanine	0.03	-0.08	0.29
	proline	0.20	-0.25	0.38
	serine	0.17	<b>-0.66</b>	-1.85
	threonine	0.24	0.09	0.34
	tryptophan	<b>-5.51</b>	<b>-2.04</b>	<b>-1.25</b>
tyrosine	0.44	-0.10	0.51	
valine	0.36	0.01	0.92	
Oxidative phosphorylation	NADH	<b>-2.99</b>	<b>-1.33</b>	1.31
	fumarate	-0.22	-0.18	0.30
	gluconate	-0.73	-0.69	0.00

	succinate	<b>-0.64</b>	<b>-0.40</b>	0.15
	adenosine_diphosphate	0.47	-0.07	0.09
	FAD2+	0.03	-0.03	-0.17
	glucose	<b>0.95</b>	0.21	-0.51
Biosynthesis of unsaturated fatty acids	Adrenic_acid	<b>-0.65</b>	<b>0.74</b>	<b>-0.85</b>
	Arachidic_acid	0.32	<b>-0.96</b>	<b>-0.64</b>
	Arachidonic_acid	<b>-0.13</b>	<b>0.78</b>	<b>-0.59</b>
	Behenic_acid	0.85	0.34	-0.55
	Docosadienoic_acid	-0.39	<b>0.37</b>	-0.44
	Docosahexaenoic_acid	-0.09	0.26	-0.37
	Docosapentaenoic_acid	<b>-0.40</b>	<b>0.50</b>	<b>-0.78</b>
	Erucic_acid	-0.09	<b>-0.07</b>	<b>-0.27</b>
	Icosadienoic_acid	-0.10	<b>0.39</b>	-0.23
	Icosapentaenoic_acid	<b>0.10</b>	<b>0.42</b>	-0.34
	Icosatrienoic_acid	-0.09	<b>0.53</b>	-0.41
	Icosenoic_acid	0.00	-0.01	-0.15
	Lignoceric_acid	0.99	0.05	-0.29
	Linoleic_acid	-0.07	<b>0.50</b>	<b>-0.72</b>
	Nervonic_acid	<b>0.24</b>	<b>0.24</b>	<b>-0.59</b>
	Oleic_acid	-0.07	0.04	<b>-0.55</b>
	$\alpha$ -Linolenic_acid	<b>0.29</b>	0.20	<b>-0.62</b>
	Palmitic_acid	0.06	<b>-0.15</b>	<b>-0.36</b>
	Stearic_acid	<b>0.50</b>	<b>0.32</b>	<b>-0.24</b>
	Arachidonic acid metabolism	11.14.15-theta	<b>1.16</b>	<b>-1.14</b>
hepoxilin_A3		0.32	0.21	0.36
leukotriene_F4		0.64	-0.03	0.27
11-dehydro_Thromboxane_B2		0.53	0.15	0.23
6-Ketoprostaglandin_E1		-0.08	-0.16	0.18
Trioxilin_A3		0.05	0.12	0.20
5,6-Dihydroxy-8Z,11Z,14Z- eicosatrienoic_acid		<b>1.18</b>	<b>-1.08</b>	0.06
6-Ketoprostaglandin_E1		<b>0.78</b>	<b>-0.47</b>	-0.08
Tetrahydro-3.4-furandiol		0.13	0.09	-0.29
prostaglandin_B2		<b>-0.80</b>	<b>-0.84</b>	-0.33
11.14.15-theta		<b>1.16</b>	<b>-1.14</b>	-0.50
15-Keto-prostaglandin_F2alpha		<b>-0.74</b>	<b>-1.03</b>	-0.37
5-Oxo-ETE		<b>0.66</b>	-0.38	-0.47
5-HETE		<b>0.36</b>	-0.07	<b>-0.50</b>
11(12)oxido-5.8.14- eicosatrienoic_acid		<b>0.43</b>	-0.12	<b>-0.52</b>
14.15-dihydroxy-5.-8.11- eicosatrienoic_acid		0.35	0.01	<b>-0.72</b>
5(6)oxido-8.11.14- eicosatrienoic_acid		0.16	0.38	<b>-0.96</b>
Lecithins		0.18	-0.68	<b>-1.25</b>



	11.12.19-/11.12.20-trihydroxy-5.8.14-eicosatrienoic	<b>1.24</b>	<b>-1.21</b>	<b>-0.66</b>
	14.15.19-/14.15.20-trihydroxy-5.8.11-eicosatrienoic	<b>1.05</b>	<b>-0.55</b>	-0.36
	Prostacyclin	<b>0.87</b>	<b>-1.11</b>	-0.50
	PC_(36:5)	<b>-0.57</b>	0.31	<b>-1.00</b>
	PC_(38:7)	0.22	0.04	-0.26
	PC_(34:4)	<b>-0.76</b>	0.61	<b>-0.81</b>
	PC_(30:3)	-0.27	0.02	<b>-0.77</b>
	PC_(40:6)	<b>0.58</b>	<b>-0.64</b>	-0.27
	PC_(38:6)	-0.25	0.25	-0.47
	PC_(36:4)	<b>-0.58</b>	0.38	<b>-0.83</b>
	PC_(30:0)	<b>-0.49</b>	-0.02	<b>-0.96</b>
	PC_(34:1)	-0.45	0.01	-0.51
Phosphatidylcholines	PC_(34:2)	<b>-0.43</b>	0.03	<b>-0.70</b>
	PC_(38:5)	<b>-0.42</b>	0.33	<b>-0.69</b>
	PC_(36:3)	<b>-0.46</b>	0.27	<b>-0.71</b>
	PC_(38:4)	<b>-0.49</b>	0.58	<b>-0.74</b>
	PC_(34:0)	-0.32	-0.54	-0.61
	PC_(32:1)	-0.46	0.08	<b>-0.79</b>
	PC_(36:1)	-0.13	-0.11	<b>-0.86</b>
	PC_(32:0)	<b>-0.54</b>	-0.37	-0.43
	PC_(34:6)	-0.55	-0.63	<b>-0.87</b>
	PC_(36:2)	-0.10	-0.13	<b>-0.92</b>
	SM_(18:0)	-0.21	0.21	<b>-0.80</b>
Sphingolipid metabolism	SM_(d34:0)	0.05	-0.24	-0.54
	SM_(16:0)	-0.19	-0.32	<b>-0.71</b>
	cholesterol	<b>-0.20</b>	-0.07	-0.17
Cholesterol metabolism	cholesterol_alpha-epoxide	0.04	-0.03	<b>-0.48</b>
	TAG_(50:1)	<b>1.71</b>	<b>0.46</b>	<b>-1.84</b>
	TAG_(50:4)	<b>1.40</b>	-0.58	<b>-1.95</b>
	TAG_(54:5)	<b>0.28</b>	<b>1.57</b>	<b>-1.02</b>
	TAG_(54:8)	<b>0.81</b>	<b>1.38</b>	<b>-1.56</b>
Glycerolipid metabolism	TAG_(52:1)	<b>1.59</b>	<b>0.43</b>	<b>-1.13</b>
	TAG_(52:2)	<b>1.10</b>	<b>0.68</b>	<b>-1.07</b>
	TAG_(54:9)	<b>2.01</b>	<b>-0.70</b>	<b>-1.34</b>
	TAG_(50:0)	<b>1.83</b>	<b>1.07</b>	<b>-1.35</b>

Red denotes statistical differences at  $p < 0.05$ .



**Supplementary Figure S1.** Principal component analysis, assessing the expression profile variability of each sample in each generation. Adjusted ellipses indicate the dispersion of the samples by experimental group (NC: naturally-conceived; VT: vitrified-transferred) and generation (F1, F2 and F3).

## **12. ANNEX III**

Supplementary information  
CHAPTER V

### **TRANSGENERATIONAL EFFECTS FOLLOWING VITRIFIED EMBRYO TRANSFER IN RABBITS: A MULTI-OMIC APPROACH**

X. Garcia-Dominguez<sup>1</sup>, G. Diretto<sup>2</sup>, D.S. Peñaranda<sup>1</sup>, S. Frusciante<sup>2</sup>  
V. García-Carpintero<sup>3</sup>, J. Cañizares<sup>3</sup>, F. Marco-Jiménez<sup>1</sup>, J.S. Vicente<sup>1</sup>

<sup>1</sup>Institute for Animal Science and Technology (ICTA), Laboratory of Reproductive Biotechnology, Universitat Politècnica de València, 46022 Valencia, Spain

<sup>2</sup>Italian National Agency for New Technologies, Energy and Sustainable Development (ENEA), Casaccia Research Centre, 00123 Rome, Italy.

<sup>3</sup>Institute for the Conservation and Breeding of Agricultural Biodiversity (COMAV-UPV), Universitat Politècnica de València, 46022 Valencia, Spain



## 12. ANNEX III

**Supplementary Table S1.** Targeted identification of differentially accumulated metabolites in liver tissue due to a transgenerational effect of the vitrified embryo transfer procedure.

Metabolic pathway	Metabolite name	Fold change
Biosynthesis of amino acids	Arginine	0,13
	Asparagine	0,26
	Aspartate	0,28
	Cysteine	<b>-2,00</b>
	Glutamic_acid	0,29
	Glutamine	-0,15
	Histidine	<b>0,23</b>
	Isoleucine-leucine	0,46
	Lysine	0,05
	Methionine	0,27
	Phenylalanine	0,24
	Proline	0,28
	Serine	-1,65
	Threonine	0,31
	Tryptophan	<b>-1,07</b>
Tyrosine	0,35	
Valine	0,72	
Arachidonic acid metabolism	11-dehydro_Thromboxane_B2	0,12
	Hepoxilin_A3	0,32
	Leukotriene_F4	0,17
	Prostaglandin_B2	<b>-0,38</b>
	Prostacyclin	0,08
	11,14,15-theta	0,39
	15-Keto-prostaglandin_f2alpha	<b>-0,52</b>
	6-ketoprostaglandin_e1	0,17
	Trioxilin_A3	0,18
	11,14,15-theta	-0,34
Linoleic acid metabolism	5,6-Dihydroxy-8Z,11Z,14Z-eicosatrienoic_acid	0,24
	5-hete	<b>-0,47</b>
	5-oxo-ete	<b>-0,38</b>
	6-ketoprostaglandin_e1	-0,16
	Lecithins	<b>-1,15</b>
	Tetrahydro-3,4-furandiol	-0,10
	Prostacyclin	-0,38

	14,15,19-/14,15,20-trihydroxy-5,8,11-eicosatri	<b>-0,42</b>
	11(12)oxido-5,8,14-eicosatrienoic_acid	<b>-0,52</b>
	14,15-dihydroxy-5,-8,11-eicosatrienoic_acid	<b>-0,60</b>
	11,12,19-/11,12,20-trihydroxy-5,8,14-eicosatri	<b>-0,53</b>
	5(6)oxido-8,11,14-eicosatrienoic_acid	<b>-0,86</b>
	PC_(36:5)	<b>-0,93</b>
	PC_(38:7)	-0,15
	PC_(34:4)	<b>-0,75</b>
	PC_(30:3)	<b>-0,65</b>
	PC_(40:6)	-0,15
	PC_(38:6)	-0,39
	PC_(36:4)	<b>-0,76</b>
	PC_(30:0)	<b>-0,82</b>
	PC_(34:1)	-0,36
	PC_(34:2)	<b>-0,61</b>
	PC_(38:5)	<b>-0,61</b>
	PC_(36:3)	<b>-0,61</b>
	PC_(38:4)	<b>-0,62</b>
	PC_(34:0)	<b>-0,45</b>
	PC_(32:1)	<b>-0,65</b>
	PC_(36:1)	<b>-0,73</b>
	PC_(32:0)	-0,30
	PC_(36:2)	<b>-0,81</b>
	PC_(40:5)	<b>-0,91</b>
	PC_(34:6)	<b>-0,82</b>
<hr/>		
	2-hydroxy-ethyl-thpp	0,65
	Camp	0,47
	Glucose	-0,41
	Glyceraldehyde-3P	0,14
Glycolysis	Glycerate-1,3P2	-0,21
	Glycerate-3P	<b>2,57</b>
Gluconeogenesis	$\beta$ -D-Fructose-1,6P2	<b>-0,44</b>
	$\beta$ -D-Glucose-6P	0,15
	Thpp	<b>1,65</b>
	S-acetyl-dihydrolipoamide-e	<b>0,34</b>
	Lipoamide-E	-0,34
<hr/>		
	Adenosine_diphosphate	0,05
	Fad2+	-0,13
Oxidative phosphorylation	Fumarate	0,41
	Gluconate	-0,15
	Glucose	-0,41
	Nadh	1,05

	Succinate	0,02
Biosynthesis of unsaturated fatty acids	Adrenic_acid	<b>-0,77</b>
	Arachidic_acid	<b>-0,48</b>
	Arachidonic_acid	<b>-0,58</b>
	Behenic_acid	-0,61
	Docosadienoic_acid	<b>-0,49</b>
	Docosahexaenoic_acid	<b>-0,36</b>
	Docosapentaenoic_acid	<b>-0,71</b>
	Erucic_acid	<b>-0,17</b>
	Icosadienoic_acid	<b>-0,18</b>
	Icosapentaenoic_acid	<b>-0,35</b>
	Icosatrienoic_acid	<b>-0,32</b>
	Icosenoic_acid	-0,10
	Lignoceric_acid	-0,42
	Linoleic_acid	<b>-0,67</b>
	Nervonic_acid	<b>-0,63</b>
	Oleic_acid	<b>-0,48</b>
A-Linolenic_acid	<b>-0,58</b>	
Palmitic_acid	<b>-0,28</b>	
Stearic_acid	<b>-0,20</b>	
Steroid biosynthesis	24-epi-Campesterol	<b>-0,70</b>
	24-methylenecholesterol	2,87
	5-dehydroavenasterol	0,18
	7-dehydrocholesterol	-0,16
	7alpha,24-Dihydroxy-4-cholesten-3-one	<b>-0,44</b>
	Episterol	<b>-0,34</b>
	Lathosterol	-0,26
	Secalciferol	-0,79
	3alpha,7alpha-Dihydroxy-5beta-cholestanate	-0,04
	S-squalene_2,3-epoxide	<b>-0,56</b>
	22(r)-hydroxycholesterol	<b>-0,98</b>
	3alpha,7alpha,26-Trihydroxy-5beta-cholestan	-0,10
	Calcidiol	-0,06
	14-demethyllanosterol	0,01
	4alpha-Methylzymosterol-4-carboxylate	0,92
	Squalene	<b>-0,54</b>
	3alpha,7alpha,12alpha,26-Tetrahydroxy-5beta	0,80
	Calcitriol	-0,62
	Cholesterol	<b>-0,14</b>
7-dehydrodesmosterol	<b>-0,99</b>	
Campesterol	-0,10	
3alpha,7alpha-Dihydroxy-5beta-cholestane	<b>-0,29</b>	

	Pregnenolone	-0,66
	Calcitriol	0,90
	4alpha-Methylzymosterol	-0,52
	Cortisol	-0,30
	6 $\beta$ hydroxy testosterone	0,07
	Aldosterone	<b>-0,52</b>
	Androsterone	-0,14
	B-Estradiol	-0,20
	Corticosterone	0,35
	Cortol	-0,37
Steroid hormone biosynthesis	Cortolone	-0,45
	Estriol	<b>-0,19</b>
	Methoxyestrone	0,01
	Pregnenolone	0,28
	Progesterone	-0,13
	Testosterone	<b>-0,43</b>
	Cortol	-0,42
	Pregnanediol	-0,49
	TAG_(50:1)	<b>-1,86</b>
	TAG_(50:4)	<b>-1,98</b>
	TAG_(54:5)	<b>-1,06</b>
Glycerolipid metabolism	TAG_(54:9)	<b>-1,36</b>
	TAG_(54:8)	<b>-1,59</b>
	TAG_(52:1)	<b>-1,17</b>
	TAG_(52:2)	<b>-1,11</b>
	TAG_(50:0)	<b>-1,38</b>
	2-hydroxy-ethyl-thpp	0,65
	3-carboxy-1-hydroxypropyl-thpp	-0,85
	Cis-aconitate	0,10
Citrate cycle (TCA cycle)	Citrate	<b>-0,30</b>
	Oxalosuccinate	<b>2,09</b>
	Succinate	0,02
	Thpp	<b>1,65</b>
	S-acetyl-dihydrolipoamide-e	<b>0,34</b>
	Lipoamide-E	-0,34



**Supplementary Table S2.** Differentially expressed proteins in liver tissue due to a transgenerational effect of the vitrified embryo transfer procedure.

Uniprot accession	Gene name	Fold change
U3KPP4	Cytochrome P450 2C30	-3.78
G1T1G8	Periplakin	-3.60
G1SRH7	Serine and arginine rich splicing factor 3	-2.08
G1TYL5	2'-deoxynucleoside 5'-phosphate N-hydrolase 1	-1.95
A0A0A0MQQ2	S100 calcium binding protein A12	-1.95
G1TN25	Alpha-2-glycoprotein 1, zinc-binding	-1.91
G1T7F1	Histone H1.4	-1.66
G1TIS5	Annexin A1	-1.62
P12345	Glutamic-oxaloacetic transaminase 2	-1.55
G1SJS1	Histone H2B type 2-E	-1.37
G1U522	Protein kinase camp-dependent type II regulatory subunit alpha	-1.27
G1SMM7	Small nuclear ribonucleoprotein D3 polypeptide	-1.21
G1TC61	Putative RNA-binding protein Luc7-like 2	-1.07
G1T7S1	Aflatoxin B1 aldehyde reductase member 3	-1.04
G1TUX5	Protein HP-25 homolog 2	-1.01
G1T5K6	Translocase of outer mitochondrial membrane 40 like	-0.97
G1TP83	Histone H2B type 1	-0.94
B7NZF9	Nucleophosmin	-0.93
G1TN62	40S ribosomal protein S19	-0.89
G1TWP4	Valyl-trna synthetase	-0.84
G1T726	Hydroxyacyl-coa dehydrogenase	-0.83
G1TFX2	Alpha-1-antitrypsin	-0.83
G1SHI0	Acetyl-coa acyltransferase 1	-0.81
G1SSN2	Sirtuin 5	-0.71
G1SN67	Serpin family B member 1	-0.67
G1U7L4	Heat shock protein family A	-0.59
G1T9I4	Sorcin	-0.57
G1TBU9	Acetyl-coa acyltransferase 2	-0.51
G1SU01	Nipsnap homolog 3A	-0.43
G1TES6	Hydroxysteroid 17-beta dehydrogenase 10	-0.40
G1T3Y8	Heat shock protein family D	-0.27
G1TU13	40S ribosomal protein S17	-0.23
G1T0L9	Ribophorin I	-0.13
G1TPR2	Glucosamine-phosphate N-acetyltransferase 1	0.30
G1SVP7	Glutathione S-transferase omega 1	0.30
G1TE35	Nudix hydrolase 12	0.35
G1T3Z1	Mannose binding lectin 2	0.40
G1SVJ1	Dihydropyrimidine dehydrogenase	0.42

G1TS42	Amylo-alpha-1, 6-glucosidase, 4-alpha-glucanotransferase	0.45
G1SV60	Transmembrane and coiled-coil domains 1	0.46
G1SN14	Cullin associated and neddylation dissociated 1	0.48
G1TAH7	Transketolase	0.49
G1U2K8	Cytochrome P450-like	0.51
G1TCT8	Major facilitator superfamily domain containing 9	0.53
G1T6X2	Cytochrome P450 2C15-like	0.54
G1U7D9	Solute carrier family 27 member 5	0.57
U3KLZ1	Flavin containing monooxygenase 3	0.66
G1SMY3	2-acylglycerol O-acyltransferase 2-B	0.67
G1TBR1	NAD	0.68
G1T3H9	Desmocollin 2	0.71
G1U4I6	Fatty acid amide hydrolase	0.80
G1SKJ7	Glycine N-methyltransferase	0.80
G1TUC2	CCHC-type zinc finger nucleic acid binding protein	0.82
G1TZE5	Chromosome 13 open reading frame, human c1orf50	0.96
G1TYM3	Cytochrome P450. family 2, subfamily b, polypeptide 4	0.96
G1TLX2	Cytochrome P450 2C16	0.98
G1T9T6	Ethanolamine-phosphate phospho-lyase	1.01
G1T932	Pipecolic acid and sarcosine oxidase	1.03
G1TI39	Radixin	1.03
G1SL36	Glycine decarboxylase	1.04
G1TR70	Cytochrome P450 2C4	1.07
U3KM06	UDP-glucuronosyltransferase 2A3	1.14
G1U9S0	Cytochrome P450 2C2	1.20
G1T0Z2	Histone H2A type 1-A	1.51
G1SUM7	ATP-binding cassette subfamily C member 2	1.66
G1SEE9	Thyroid hormone responsive	1.76
G1TGH4	Retinol saturase	1.77
G1TPC5	Tumour protein D52	1.79
G1ST24	Acetyl-coa carboxylase beta	2.05
G1TTZ8	Formimidoyltransferase cyclodeaminase	2.13
G1SZ66	Mannose-P-dolichol utilisation defect 1	5.80

---

**Supplementary Table S3.** Functional analysis of differentially expressed proteins in liver tissue due to a transgenerational effect of the vitrified embryo transfer procedure.

Category*	Term	Count	p-value
BP	Defence response to Gram-positive bacterium	3	0.01
BP	Negative regulation of ryanodine-sensitive calcium release channel activity	2	0.02
BP	Very long-chain fatty acid metabolic process	2	0.03
BP	Negative regulation of catalytic activity	2	0.04
BP	Positive regulation of G1/S transition of mitotic cell cycle	2	0.05
BP	Innate immune response in mucosa	2	0.07
BP	Antibacterial humoral response	2	0.07
CC	Organelle membrane	7	0.00
CC	Endoplasmic reticulum membrane	10	0.00
CC	Extracellular exosome	23	0.00
CC	Nucleosome	4	0.00
CC	Myelin sheath	5	0.00
CC	Mitochondrial inner membrane	5	0.00
CC	Extracellular space	9	0.01
CC	Integral component of endoplasmic reticulum membrane	3	0.02
CC	Peroxisome	3	0.02
CC	Cytosol	8	0.04
CC	U1 snrnp	2	0.04
MF	Aromatase activity	6	0.00
MF	Heme binding	7	0.00
MF	Iron ion binding	7	0.00
MF	Monooxygenase activity	4	0.00
MF	Oxidoreductase activity, acting on paired donors, with incorporation or reduction of molecular oxygen	4	0.00
MF	Transferase activity, transferring acyl groups other than amino-acyl groups	3	0.00
MF	Oxidoreductase activity, acting on paired donors, with incorporation or reduction of molecular oxygen, reduced flavin or flavoprotein as one donor, and incorporation of one atom of oxygen	3	0.00
MF	Folic acid binding	2	0.03
MF	3-hydroxyacyl-coa dehydrogenase activity	2	0.04
MF	NAD <sup>+</sup> binding	2	0.06
MF	Poly(A) RNA binding	9	0.07
KEGG	Retinol metabolism	8	0.00
KEGG	Chemical carcinogenesis	8	0.00

KEGG	Metabolic pathways	22	0.00
KEGG	Steroid hormone biosynthesis	7	0.00
KEGG	Linoleic acid metabolism	5	0.00
KEGG	Arachidonic acid metabolism	6	0.00
KEGG	Biosynthesis of antibiotics	7	0.00
KEGG	Inflammatory mediator regulation of TRP channels	5	0.00
KEGG	Serotonergic synapse	5	0.01
KEGG	Valine, leucine and isoleucine degradation	4	0.01
KEGG	Systemic lupus erythematosus	5	0.01
KEGG	Fatty acid degradation	3	0.04
KEGG	Glycine, serine and threonine metabolism	3	0.04
KEGG	Fatty acid metabolism	3	0.05
KEGG	Drug metabolism - cytochrome P450	3	0.10

---

\*Functional analysis was referred to the GO term annotation according to the biological process (BP), cellular component (CC) and molecular function (MF) classification, and the KEGG pathways in which they are involved.

**Supplementary Table S4.** Differentially methylated genes in liver tissue due to a transgenerational effect of the vitrified embryo transfer procedure.

Type	Gene accession	Gene name	Chromosome /scaffold	$\Delta\beta$
Hypo	ENSOCUG00000023366	WD repeat domain 4	GL019261	-4.70
Hypo	ENSOCUG00000017543	Acylglycerol kinase, mitochondrial	GL019263	-3.67
Hypo	ENSOCUG00000003231	TBC1 domain family member 14	GL019275	-3.61
Hypo	ENSOCUG00000007282	SVOP like	GL018853	-3.14
Hypo	ENSOCUG00000004404	Multiple C2 and transmembrane domain containing 2	GL018708	-3.05
Hypo	ENSOCUG00000006366	S100 calcium binding protein P	GL019770	-3.05
Hypo	ENSOCUG00000026584	Ras association domain-containing protein 3	GL018886	-2.91
Hypo	ENSOCUG00000015993	Par-6 family cell polarity regulator beta	GL018822	-2.81
Hypo	ENSOCUG00000004266	Family with sequence similarity 222 member A	GL019210	-2.68
Hypo	ENSOCUG00000023160	Olfactory receptor 6B3		-2.65
Hypo	ENSOCUG00000007918	NOP2/Sun RNA methyltransferase family member 2	GL018756	-2.51
Hypo	ENSOCUG00000007288	Lon peptidase 2, peroxisomal	GL018732	-2.51
Hypo	ENSOCUG00000002796	DDB1- and CUL4-associated factor 12-like protein 2		-2.50
Hypo	ENSOCUG00000013731	Runt related transcription factor 1	GL018729	-2.48
Hypo	ENSOCUG00000014651	Dexh-box helicase 9	GL019071	-2.42
Hypo	ENSOCUG00000004927	Breast carcinoma amplified sequence 1	GL018712	-2.33
Hypo	ENSOCUG00000007274	Tripartite motif containing 24	GL018853	-2.28
Hypo	ENSOCUG00000014336	Multivesicular body subunit 12B	GL018699	-2.27
Hypo	ENSOCUG00000009223	Docking protein 5	GL018712	-2.26
Hypo	ENSOCUG00000016405	Evc ciliary complex subunit 2	GL018874	-2.18
Hypo	ENSOCUG00000009429	1-acylglycerol-3-phosphate O-acyltransferase 5	GL018713	-2.03
Hypo	ENSOCUG00000010151	WD repeat and FYVE domain containing 2	GL018705	-2.01
Hypo	ENSOCUG00000007803	Disco interacting protein 2 homolog C	GL018778	-1.98
Hypo	ENSOCUG00000004466	WD repeat domain 37	GL018707	-1.93
Hypo	ENSOCUG00000023551	Dnaj homolog subfamily C member 8	GL018701	-1.91
Hypo	ENSOCUG00000008722	KIAA2022 ortholog	GL018757	-1.63
Hypo	ENSOCUG00000003497	SHC binding and spindle associated 1 like	GL019071	-1.45
Hypo	ENSOCUG00000000876	Integrator complex subunit 6	GL018705	-1.33
Hypo	ENSOCUG00000016847	ATP-binding cassette subfamily B member 7	GL018757	-1.25
Hypo	ENSOCUG00000013902	Sperm acrosome associated 4	GL019039	-0.94

Hypo	ENSOCUG00000016120	Nucleolar GTP-binding protein 1	GL018778	-0.70
Hypo	ENSOCUG00000005446	ADP ribosylation factor guanine nucleotide exchange factor 2	GL018725	-0.61
Hypo	ENSOCUG00000017426	Glutamate metabotropic receptor 7	GL018703	-0.60
Hyper	ENSOCUG00000001208	Relaxin/insulin like family peptide receptor 1	GL018701	0.84
Hyper	ENSOCUG00000005566	G protein-coupled receptor 50	GL018731	1.11
Hyper	ENSOCUG00000012148	Inositol 1,4,5-trisphosphate receptor type 1	GL018703	1.21
Hyper	ENSOCUG00000015945	Mutated in colorectal cancers	GL018744	1.25
Hyper	ENSOCUG00000003938	Deleted in lymphocytic leukaemia, 7	GL018705	1.26
Hyper	ENSOCUG00000001660	Von Willebrand factor C and EGF domains	GL018717	1.29
Hyper	ENSOCUG00000017773	Tankyrase	GL018709	1.35
Hyper	ENSOCUG00000021608	Pyridoxal	GL019091	1.43
Hyper	ENSOCUG00000004645	Whirlin	GL018699	1.44
Hyper	ENSOCUG00000003760	Kelch-like family member 2	GL018701	1.46
Hyper	ENSOCUG00000001573	Protein tyrosine phosphatase, receptor type T	GL018718	1.50
Hyper	ENSOCUG00000001518	LCA5L, lebercilin like	GL018907	1.51
Hyper	ENSOCUG00000005132	Williams-Beuren syndrome chromosome region 28	GL018765	1.53
Hyper	ENSOCUG00000021767	Hydroxylysine kinase	GL018746	1.53
Hyper	ENSOCUG00000001499	Pleckstrin homology domain containing A4	GL019028	1.55
Hyper	ENSOCUG00000006423	BCL2 associated X. apoptosis regulator	GL019028	1.55
Hyper	ENSOCUG00000002815	Interferon gamma receptor 2	GL018729	1.60
Hyper	ENSOCUG00000009375	Protein phosphatase 6 catalytic subunit	GL018699	1.62
Hyper	ENSOCUG00000004344	Forkhead box K1	GL018871	1.65
Hyper	ENSOCUG00000012302	PBX homeobox 3	GL018699	1.69
Hyper	ENSOCUG00000014169	Ankyrin repeat and SOCS box containing 7	GL018753	1.76
Hyper	ENSOCUG00000029446	Tripartite motif containing 60	GL018701	1.79
Hyper	ENSOCUG00000012963	Suppressor of cancer cell invasion	GL018699	1.81
Hyper	ENSOCUG00000006503	TBC1 domain family member 2B	GL018746	1.86
Hyper	ENSOCUG00000023002	Kelch-like protein 20	GL018825	1.90
Hyper	ENSOCUG00000001522	SH3 domain binding glutamate rich protein	GL018907	1.91
Hyper	ENSOCUG00000000146	IQ motif containing gtpase activating protein 1	GL018738	1.92
Hyper	ENSOCUG00000007308	Zinc finger and SCAN domain containing 2	GL018738	1.92
Hyper	ENSOCUG00000011791	Receptor interacting serine/threonine kinase 1	GL018715	1.93
Hyper	ENSOCUG00000025866	Adenylate kinase 8	GL018764	1.97

Hyper	ENSOCUG00000007599	Nuclear receptor subfamily 6 group A member 1	GL018699	1.98
Hyper	ENSOCUG00000009825	Biphenyl hydrolase like	GL018715	2.03
Hyper	ENSOCUG00000014888	Interferon alpha and beta receptor subunit 1	GL018729	2.08
Hyper	ENSOCUG00000016878	BRCA2. DNA repair associated	GL018702	2.11
Hyper	ENSOCUG00000021019	Ras protein specific guanine nucleotide releasing factor 1	GL018746	2.27
Hyper	ENSOCUG00000014818	Potassium calcium-activated channel subfamily N member 2	GL019132	2.28
Hyper	ENSOCUG00000005747	Collagen type XVI alpha 1 chain	GL018704	2.28
Hyper	ENSOCUG00000012670	Arf-GAP with gtpase. ANK repeat and PH domain-containing protein 1	GL018948	2.37
Hyper	ENSOCUG00000016499	Nad	GL018715	2.38
Hyper	ENSOCUG00000008082	Gtpase activating Rap/rangap domain like 3	GL018699	2.39
Hyper	ENSOCUG00000029680	Putative alpha-1-antitrypsin-related protein	GL018883	2.46
Hyper	ENSOCUG00000016865	Zinc finger protein 831	GL018755	2.52
Hyper	ENSOCUG00000003587	Zinc finger MIZ-type containing 1	GL018836	2.52
Hyper	ENSOCUG00000013908	Lysine acetyltransferase 5	GL019220	2.59
Hyper	ENSOCUG00000001607	Putative serine protease 41	GL018828	2.61
Hyper	ENSOCUG00000002047	Transient receptor potential cation channel subfamily M member 8	GL018736	2.62
Hyper	ENSOCUG00000011025	Contactin 4	GL018703	2.63
Hyper	ENSOCUG00000015227	ADAM metallopeptidase with thrombospondin type 1 motif 17	GL018753	2.64
Hyper	ENSOCUG00000010830	Proline rich coiled-coil 2B	GL018764	2.76
Hyper	ENSOCUG00000006729	G protein-coupled receptor kinase 3	GL018766	2.78
Hyper	ENSOCUG00000024741	Transmembrane protease. serine 2	GL019053	2.80
Hyper	ENSOCUG00000014362	Integrin subunit alpha L	GL018752	2.83
Hyper	ENSOCUG00000026490	Arylacetamide deacetylase-like 4	GL018739	2.92
Hyper	ENSOCUG00000013433	Slingshot protein phosphatase 1	GL018777	3.05
Hyper	ENSOCUG00000015765	Isocitrate dehydrogenase 3	GL018746	3.09
Hyper	ENSOCUG00000003258	Cytochrome c oxidase subunit 5A. mitochondrial	GL018768	3.15
Hyper	ENSOCUG00000003266	SIN3 transcription regulator family member A	GL018768	3.15
Hyper	ENSOCUG00000016234	SV2 related protein	GL018777	3.25
Hyper	ENSOCUG00000015510	C2 calcium dependent domain containing 2	GL019181	3.40
Hyper	ENSOCUG00000012944	Ubiquitin conjugating enzyme E2 G2	GL019021	3.66
Hyper	ENSOCUG00000023837	PR domain zinc finger protein 15		4.75

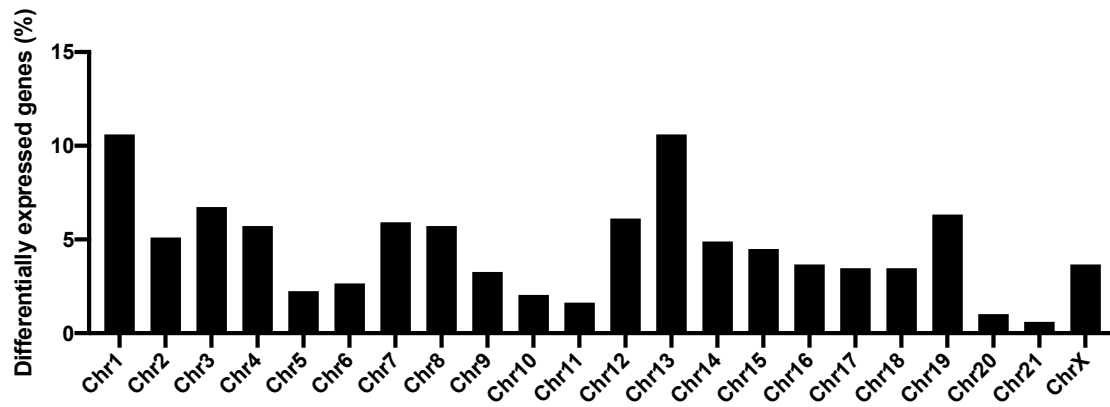
$\Delta\beta$ : Methylation difference calculated as mean VT DNA methylation minus mean NC DNA methylation.

**Supplementary Table S5.** Functional analysis of differentially methylated genes in liver tissue due to a transgenerational effect of the vitrified embryo transfer procedure.

Type <sup>+</sup>	Category*	Term	Count	p-value
Hypo	BP	Regulation of apoptotic process	2	0.09
Hypo	CC	Cell cortex	2	0.08
Hypo	CC	Recycling endosome	2	0.09
Hypo	KEGG	Endocytosis	3	0.04
Hypo	KEGG	Glycerolipid metabolism	2	0.09
Hyper	BP	DNA damage response, signal transduction by p53 class mediator resulting in transcription of p21 class mediator	2	0.03
Hyper	BP	Cell ageing	2	0.04
Hyper	BP	Positive regulation of transcription from RNA polymerase II promoter	5	0.04
Hyper	BP	Response to gamma radiation	2	0.06
Hyper	BP	Intrinsic apoptotic signalling pathway in response to endoplasmic reticulum stress	2	0.06
Hyper	BP	Establishment of protein localisation	2	0.07
Hyper	CC	Transcription factor complex	4	0.01
Hyper	CC	Cytosol	7	0.01
Hyper	CC	Growth cone	2	0.08
Hyper	KEGG	Huntington's disease	4	0.03
Hyper	KEGG	Natural killer cell mediated cytotoxicity	3	0.05
Hyper	KEGG	Transcriptional misregulation in cancer	3	0.10

+ Type is referred to the epigenetic status of the gene: hypomethylated (hypo) or hypermethylated (hyper). \*Functional analysis was referred to the GO term annotation according to the biological process (BP), cellular component (CC) and molecular function (MF) classification, and the KEGG pathways in which they are involved.





**Supplementary Figure S1.** Percentage of differentially expressed genes of our previous transcriptomic study that belong from each chromosome.





